RECOMMENDATIONS FOR LONGITUDINAL POST-TENSIONING IN FULL-DEPTH PRECAST CONCRETE BRIDGE DECK PANELS

by

Susan E. Bowers

Thesis submitted to the faculty of the
Virginia Polytechnic Institute and State University
in partial fulfillment of the requirements for the degree of

MASTER OF SCIENCE

in

CIVIL ENGINEERING

Dr. Carin L. Roberts-Wollmann, Chairperson
Dr. Thomas E. Cousins
Dr. Rodney T. Davis

May 8, 2007
Blacksburg, Virginia

Keywords: Precast Panels, Longitudinal Post-Tensioning, Age-Adjusted Effective Modulus, Prestress Losses

RECOMMENDATIONS FOR LONGITUDINAL POST-TENSIONING IN FULL-DEPTH PRECAST CONCRETE BRIDGE DECK PANELS

by

Susan E. Bowers

ABSTRACT

Full-depth precast concrete panels offer an efficient alternative to traditional cast-in-place concrete for replacement or new construction of bridge decks. Research has shown that longitudinal post-tensioning helps keep the precast bridge deck in compression and avoid problems such as leaking, cracking, spalling, and subsequent rusting on the beams at the transverse panel joints. Current design recommendations suggest levels of initial compression for precast concrete decks in a very limited number of bridge configurations. The time-dependent effects of creep and shrinkage in concrete and relaxation of prestressing steel complicate bridge behavior, making the existing recommendations for post-tensioning in precast deck panels invalid for all bridges with differing girder types, sizes, spacings, and span lengths. Therefore, the development of guidelines for levels of post-tensioning applicable to a variety of bridge types is necessary so designers may easily implement precast concrete panels in bridge deck construction or rehabilitation.

To fulfill the needs described, the primary objective of this research was to determine the initial level of post-tensioning required in various precast concrete bridge deck panel systems in order to maintain compression in the transverse panel joints until the end of each bridge's service life. These recommendations were determined by the results of parametric studies which investigated the behavior of bridges with precast concrete decks supported by both steel and prestressed concrete girders in single spans as well as two and three continuous spans. The three primary variables in each parametric study included girder type, girder spacing, and span length. The age-adjusted effective modulus method was used to account for the ongoing effects of creep and shrinkage in concrete. Results from the Mathcad models used in the parametric studies were confirmed through comparison with results obtained from finite element models generated in DIANA.

Initial levels of post-tensioning for various bridge systems are proposed based on the trends observed in the parametric studies. The precast decks of the simple span bridges with

steel girders and the one, two, and three span bridges with prestressed concrete girders needed only 200 psi of initial post-tensioning to remain in compression under permanent and time-dependent loads throughout each bridge's service life. The precast decks of the two and three span continuous bridges with steel girders, however, needed a significantly higher level of initial compression due to the negative moments created by live loads.

ACKNOWLEDGEMENTS

I am very grateful to Dr. Carin Roberts-Wollmann, whose ongoing guidance, support, and patience made my completion of this research possible. It has been an honor to work with Dr. Wollmann, who has inspired me through her many roles as a gifted female engineer, an enthusiastic and motivating professor, a loving mother, and a cheerful friend. I also thank Dr. Tommy Cousins and Dr. Rodney Davis for the time they dedicated and the insight they provided as my committee members.

I genuinely appreciate the opportunity provided by the Charles E. Via, Jr. Department of Civil and Environmental Engineering to pursue a Master's degree at Virginia Tech. I would like to thank the Via family in particular for their contributions to the generous fellowship and financial support I received to attend graduate school. I am also grateful to the Virginia Transportation Research Council for funding precast concrete panel research.

The knowledge and assistance provided by my deck panel groupies, Sean Sullivan and Matt Swenty, have been an invaluable part of this research experience. I would especially like to thank Sean for involving me in so much of his experimental work at the structures lab and for his willingness to help with my many questions. I am also grateful to Eric Crispino for the use of his girder design spreadsheets.

I am especially thankful for David Finkenbinder and Chris Carroll, two fellow Shear Studs and incredible friends who always made time to listen, help, or take a break for chocolate. I am not sure how I would have made it through the past two years without both of them, as well as the support and Christian love of the remarkable women in my bible study. I have certainly been rewarded for following the advice of my friends Andrew Burkholder and Kirsten Baldwin-Metzger who encouraged me to come to Virginia Tech. I would also like to thank all of the other graduate students with whom I have become friends along the way.

I would not have made it this far without the love and encouragement of my parents, Robert and Nancy Bowers. By teaching me the value of education and perseverance, they have helped me to succeed in many ways. I am also forever grateful to Stephen Kelley who has never stopped believing in me and who will always have a special place in my heart.

Finally, I thank God for all of the blessings in my life. I am deeply saddened by the loss of my friend Dan O'Neil and all of the others in the tragic events of April 16, 2007. I believe

that the Hokies will now unite more strongly than ever before, and I pray that God will reveal His plans for each of us to invent the future here at Virginia Tech and throughout the rest of our lives.

TABLE OF CONTENTS

LIST OF FIGURES

LIST OF TABLES

CHAPTER 1: INTRODUCTION

1.1 Full-Depth Precast Concrete Bridge Deck Panels

The rapid pace of life in today's society demands transportation infrastructure which is reliable, efficient, and safe. As traffic volumes continue to increase, the performance and durability of existing roads and bridges are challenged and scrutinized on a daily basis. When problems arise, it is important that the responsible transportation agency have the ability to perform the necessary maintenance or construction in a timely and effective manner. For the rehabilitation of bridge decks, full-depth precast concrete panels provide a solution which is quick and easy to implement.

Many advantages to using a precast panel system for bridge decks exist. First, all of the deck panels can be manufactured at a concrete precasting facility prior to the start of construction at the bridge site. This prefabrication eliminates the time it would otherwise take to cast and cure a concrete deck in place at a bridge site, leaving only a minimal amount of cast-in-place material to be required for securing connections at the site. Along with simplifying the construction process, the precast panels allow for a much faster bridge deck replacement or repair, which significantly reduces the duration of bridge closure and the corresponding disruptions of traffic. In most cases, the flow of traffic can be maintained on a portion of the bridge while precast panels are used to fix segments of the bridge deck in other locations. The precast system is an economical option due to the savings in required field labor and the reduced inconvenience of delays for bridge users. Finally, the precast system can be a practical solution for a variety of transportation infrastructure needs, including new bridge construction as well as bridge deck rehabilitation or replacement (Issa, 1995b).

Although prefabrication of the concrete panels makes the process of constructing the precast system fairly easy, the design of the panels and the other components present in the system are all important to ensure a properly functioning bridge deck. The panels themselves usually have thicknesses ranging from 6 to 10 in., while their lengths and widths may vary from several feet to much longer lengths depending on the bridge deck layout and the requirements of the project. The connection between the precast panel components and the supporting girders is typically provided by shear studs, which resist the horizontal shear forces created between the bottom of the precast deck and the top of the girders. The gap between the bottom of the deck

panels and the top of the girders is generally 1-2 in. thick and is referred to as the haunch. A specific number of open blockouts are formed through the thickness in each precast panel to provide space for the shear studs which extend up from the top flanges of the girders. The joints between the precast panels typically have either a male-female or female-female configuration. The precast panels commonly contain prestressing strands, regular steel reinforcement, bonded post-tensioning tendons, or some combination of these three in the transverse direction to resist bending moments across the width of the bridge. In addition, the panels should contain ducts for longitudinal post-tensioning of the bridge deck, which helps keep the transverse panel joints in compression and resist bending moments along the length of the bridge (Issa, 1995a).

Given this information about the components of the precast bridge deck system, the procedure for construction of the system can be described in a few easy steps. First, the bridge girders are erected on their supports. Next, groups of precast concrete panels are arranged on top of the girders along the bridge, and leveling bolts are used to adjust the panels to their final elevations. After the panels are in place, the transverse panel joints are filled with grout or coated with epoxy, and the entire bridge deck is longitudinally post-tensioned to seal and compress the joints. If shear connectors are installed after the precast deck is in place, this step is completed next. Formwork to contain the haunch is assembled, and a non-shrink, high strength grout is used to fill the haunch and the open blockouts in the panels. Most of the grouts used to fill the haunch and blockouts set very rapidly and obtain the strength required to allow traffic on the bridge within a few hours or days. Following the grouting process, waterproofing membranes and overlays may be added to the deck surface to enhance its appearance, rideability, and durability. Figure 1.1 illustrates the components involved in this construction process for a bridge containing precast concrete deck panels and prestressed concrete girders.

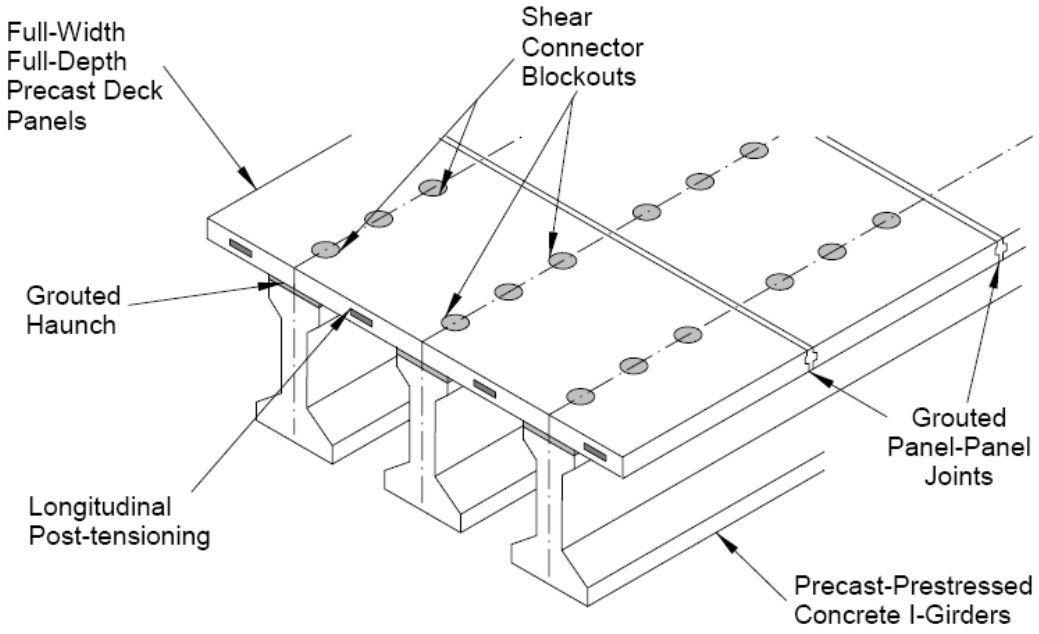

Figure 1.1: Precast Concrete Bridge Deck Panel System (Scholz, 2004)

1.2 Prestressing Methods

Some elaboration on the concepts of prestressing is necessary for a complete understanding of this research. Pretensioning and post-tensioning are the two methods used to produce an initial state of compression in concrete members. While concrete has a significant amount of strength in compression, its tensile strength is very low and is often considered to be zero in design. The initial compressive load applied to a concrete member during the process of prestressing is therefore intended to lessen or eliminate the tensile stresses that would otherwise develop in the concrete under service loads.

The primary difference between the methods of pretensioning and post-tensioning involves the time at which the compressive force is applied to the concrete member. In a pretensioned member, the steel strands are tensioned and anchored outside the beam area before the placement of the concrete. After the concrete is cast and it attains sufficient strength, the prestressing strands are cut; this releases the jacking force, which is transferred from the steel strands into the concrete through the bond between the two materials. In a post-tensioned member, on the other hand, the steel strands are stressed and the compressive force is applied to the concrete after it has set and has gained adequate strength. Post-tensioned members typically

contain hollow ducts around which the concrete for the member is cast. The steel strands are threaded through these open ducts, anchored at one end, and then stressed at the other end. The stressing mechanism reacts against the concrete member itself. Once the desired jacking force is reached, additional anchors are used to secure the tendons at the stressing end, and the stressing jack is detached. The strand elongation and the jacking pressure are both monitored throughout the stressing process to calculate the amount of tension in the strand at any time.

Following the post-tensioning process, the ducts containing the tendons are usually filled with grout, which is pressurized and pumped into the ducts at one end until it emerges at the other end. Once the grout hardens, the bonds created allow forces to be transferred from the steel strands through the grout to the walls of the ducts. While the primary compression force is still applied to the concrete through the anchorages which stay in place, grouting increases the member's flexural strength and enhances its performance in the case of overload (Nilson, 1987). The post-tensioning operations described herein apply to the precast concrete bridge deck panels investigated in this research.

1.3 Time Dependent Effects in Concrete

In concrete structures, creep and shrinkage cause strains to gradually develop. Usually the concrete contains prestressed and/or non-prestressed steel, so the development of strains in the cross section over time causes stresses to be induced in every element of the cross section, including the concrete itself as well as any steel that is present (Dilger, 1982). In many cases, the stresses and deformations resulting from this continuous redistribution of forces can influence the structure as much as the dead and live loads which are applied to it. Therefore, it is very important to consider the long-term effects of creep and shrinkage in concrete, as well as relaxation of prestressing steel, in the design and analysis of concrete elements. In this research, the effects which these ongoing changes have on the post-tensioning and the corresponding level of compression it applies to the precast concrete bridge deck panels are of particular interest and importance.

1.4 Research Objectives

The primary objective of this research is to recommend the initial level of post-tensioning required in various precast concrete bridge deck panel systems in order to maintain compression

in the transverse panel joints until the end of each bridge's service life. The predictions of stress changes over time are made by performing time-dependent analyses which consider the redistribution of forces in bridge systems caused by creep and shrinkage in concrete and relaxation of prestressing steel. The age-adjusted effective modulus method is used to account for the ongoing effects of creep and shrinkage in concrete.

In order to recommend initial post-tensioning levels for precast concrete deck panels in a wide variety of bridge systems, another goal of this research is to conduct parametric studies using numerous models which, as a whole, allow for the evaluation of both steel and prestressed concrete girders in simple spans as well as two and three span continuous bridges. All of these models were created using Mathcad. Finally, results from both simple and continuous span models are compared to analytical results obtained from finite element models generated in DIANA. These finite element models were verified separately by experimental results obtained from a full-scale bridge mockup constructed and tested in the Virginia Tech Structures and Materials Laboratory.

1.5 Thesis Organization

This document includes five chapters which present different aspects of the research performed. Chapter 2 provides a summary of the applicable literature regarding full-depth precast concrete panels used for bridge decks, including prior recommendations made concerning levels of post-tensioning required to keep the deck panel joints in compression. This literature review also explains the major time-dependent effects which occur in prestressed concrete structures, and presents several models which have been developed and used to predict these long-term effects. Chapter 3 summarizes the methods used to develop the models containing steel and prestressed concrete girders in one, two and three spans, and then explains the process of conducting parametric studies to investigate the initial amount of post-tensioning needed for each different bridge system. Chapter 4 describes the results of the parametric studies and provides an analysis of these results for each different type of bridge system. In Chapter 5, the research is summarized and conclusions are drawn. The recommended levels of initial longitudinal post-tensioning for each type of bridge system investigated in this research are also provided.

CHAPTER 2: LITERATURE REVIEW

2.1 Precast Concrete Bridge Deck Panel Systems

2.1.1 History

The first attempts at implementing precast concrete slabs for use in bridge decks were made by New York, Alabama, and Indiana in the early 1970's. These first precast panels were more frequently applied in the construction of new bridge decks rather than in deck rehabilitation projects, and non-composite deck-girder systems were more common than composite systems. In 1982, a PCI Bridge Committee survey concluded that precast, prestressed concrete bridge deck panels were being used regularly in 21 states and were starting to be integrated in another seven states. Later, in 1986, a PCI Bridge Producers Committee survey led to the development of design specifications for precast panel systems and the subsequent publication of suggested practice for implementing such systems (Issa, 1995b).

2.1.2 Implementation

In order to gain a better understanding of the ways in which precast bridge deck panels were being implemented, Issa et al. (1995b) conducted a survey of the methods being used by different transportation agencies throughout the United States and Canada. The researchers requested information regarding construction methods, structural component dimensions and details, material specifications, connection types, and performance ratings of the various elements of precast bridge deck panels systems. After compiling this information, it was clear that each department of transportation had used unique techniques to design and construct its own precast panel bridge decks, and the paper describes some of these applications in selected states. Examination of these different procedures allowed the researchers to identify the most important parts of a precast bridge deck system and conclude the essential functions of these parts in such a system. The critical parts of a well functioning precast deck panel system include an efficient construction sequence, an appropriate grouting material, transverse prestressing, longitudinal post-tensioning, and particular types of panel-to-panel joints and panel-to-girder shear connectors (Issa, 1995b).

2.1.3 Field Performance

In addition to gathering details on the vital components of a precast deck panel system, Issa et al. also wished to use the information collected throughout their surveys to "evaluate the stability, durability, and performance of the proposed bridge deck system exposed to harsh conditions" (1995b). As a result, the survey responses pertaining to the difficulties encountered with the panel-to-panel joints and the possible reasons associated with these issues were of particular interest. Of the small number of transportation agencies that did respond to this part of the survey, the most common reasons for problems with the precast panel joints were construction procedures, material quality, and maintenance. These conclusions directly lead to the first goal for future research presented at the end of the paper, which involves finding "the best jointing system between the panels that can provide high flexural and shear resistance, full bond, and complete tightness" (Issa, 1995b). The initial level of post-tensioning across the precast concrete panels is a key factor in maintaining the desired compression across the panel joints.

As a follow-up to the aforementioned studies, Issa et al. performed field inspections of bridges in several different states to assess the structural performance of full-depth precast, prestressed concrete deck panels in service (1995a). The results of these visual field surveys supported the findings of the previous study, further clarifying the best methods for implementing precast panels in future bridge deck construction or replacement, along with highlighting the advantages and disadvantages of different precast panel systems. The primary conclusion drawn from this follow-up study was that precast concrete panels can provide a cost-effective and efficient replacement for deteriorated bridge decks. In most situations, the researchers rated the performance of the precast panels as excellent. Alternatively, the cases where inadequate performance was observed were attributed to several possible factors, including the absence of longitudinal post-tensioning, the horizontal shear connection type, the panel-to-panel joint configuration, and the construction methods and materials used.

Of the above possible contributors to poor precast deck panel performance, the most important variable in relation to this research is the level of longitudinal post-tensioning in the deck. One way to avoid malfunction in a bridge deck made up of precast concrete panels is to ensure that the transverse joints between adjacent panels remain in compression to prevent problems such as leaking, cracking, spalling, and subsequent rusting on the beams below. In the

field inspection performed by Issa et al. (1995a), some of the same bridges which showed evidence of these problems occurring at the transverse joints also lacked longitudinal post-tensioning in their precast decks. The New York State Thruway Authority bridges at Krumkill Road and the Amsterdam Interchange, for example, both exhibited major cracking, spalling, leaking, and rusting at the transverse joints; these conditions were all mainly credited to the lack of any longitudinal post-tensioning to keep the precast panel joints tight. The Route 235 Bridge over Dogue Creek in Fairfax, Virginia also showed evidence of leakage, cracking, rusting, and efflorescence at the precast panel joints in a deck with no longitudinal post-tensioning. Similarly, the 18 Alaska DOT bridges over the Dalton Highway displayed cracking at nearly all of the transverse joints, with particularly severe cracking and some material loss over the supports. As in the aforementioned bridge examples, these faulty conditions were primarily attributed to an absence of longitudinal post-tensioning to tighten the transverse joints and keep the deck in compression. As a result, one of the researchers' major recommendations was to longitudinally post-tension precast concrete bridge deck panels "to secure the tightness of the joints, to keep the joint in compression, and to guard against leakage" (Issa, 1995a).

2.1.4 Finite Element Modeling

Following their literature review, questionnaire surveys, and field investigations on precast concrete panels used in bridge deck construction and rehabilitation (1995), Issa et al. presented a third study in 1998 regarding the finite element modeling and analysis of such a system. While several different bridges were modeled, two of these models were selected to be presented in detail in the third paper. These two bridges were the Route 229 Bridge over Big Indian Run in Culpeper, Virginia and the Welland River Bridge near Niagara Falls in Canada: a simply supported bridge and a three-span continuous structure, respectively. Both bridges consisted of precast concrete decks supported by rolled steel beams, and were modeled and analyzed using the finite element software ALGOR.

The primary objective of this third study by Issa et al. was to use the results obtained from the finite element analyses to establish the stresses in the systems under service loads, and to recommend the corresponding levels of post-tensioning necessary to maintain compression in the transverse joints (1998). Since the entire deck should remain in compression, the key areas of concern were the transverse joints with the highest tension stresses. For the Culpeper Bridge

model, separate analyses considering the individual effects of live load due to maximum moment and shear as well as several post-tensioning levels were all superimposed to investigate the resulting bridge deck stresses. As expected in a simple span case, the highest levels of tension occurred at the bottom of the transverse joints. While the largest tension stresses were found to be around 100 psi, Issa et al. suggested a minimum initial deck post-tensioning level of 200 psi to keep the transverse joints in compression and also account for the time-dependent effects of creep and shrinkage in the concrete (1998).

The Welland River Bridge model, on the other hand, exemplified more complicated behavior due to the negative moment regions induced over the interior supports of the three-span continuous structure. Therefore, in this model, tension values were high both at the bottom of the midspan joints and at the top of the joints over the interior supports. After modeling this structure and plotting the stresses at the top and bottom of the bridge deck along its length, it was confirmed that the most critical tensile stresses were situated at the interior supports on the top surface of the bridge deck. Following several additional analyses, Issa et al. recommended a minimum initial deck post-tensioning level of 450 psi to ensure compression in the deck at the critical interior support locations of such continuous bridge structures (1998).

2.1.5 Experimental Testing

In 2000, Issa, et al. performed an additional study, this time to investigate the behavior of full-depth precast concrete panels used in bridge decks experimentally. As in previous studies, one of their main goals was to examine the amount of longitudinal post-tensioning needed to keep the transverse panel joints in compression and maintain continuity in the deck. To accomplish this, they tested three different two-span continuous bridge models with precast concrete deck panels supported by steel girders, all scaled down by a factor of ¼ from the design of a four-span continuous bridge prototype. The first bridge model contained a bridge deck with no longitudinal post-tensioning, whereas the second and third models incorporated initial post-tensioning levels of 208 and 380 psi, respectively, into their deck systems.

Results of the experimental testing confirmed the need for longitudinal post-tensioning in an efficiently functioning precast deck panel system. The first loading for the bridge with the non-post-tensioned deck was a static test, which caused the first crack to form in the transverse joint near the interior support of the two-span continuous structure at a load of 11 kips. The

authors credited this early cracking to the absence of longitudinal post-tensioning to keep the transverse deck panel joints in compression. Later loading initiated a crack in the transverse joint at the other end of the same panel near the interior support. This second crack led to complete splitting in the transverse joints at both ends of the panel, which then became separated from the rest of the panels and caused failure of the deck. It was also determined that the steel stringers had been over designed, so smaller sections were used in the last two bridge models to reduce the structure's overall stiffness by a factor of 0.4.

The second bridge model, which contained 208 psi of post-tensioning in the deck, showed no cracking following an initial static loading identical to that applied to the nonpost-tensioned model discussed above. Issa et al. again credited this result to the longitudinal post-tensioning added to the deck. The additional fact that the steel stringer size had been decreased between the first and second tests made the absence of cracking after initial loading in the second test even more significant. The researchers claimed these results as proof that the added longitudinal post-tensioning "significantly enhances the structural behavior of the bridge deck model as well as reduces the tensile stresses in the transverse joints, hence rendering them in compression" (Issa et al., 2000). When the first crack in the second test did form, its corresponding load was about three times greater than the load for first cracking in the first model. In addition, this crack formed right over the interior support, not at a transverse joint. The absence of cracking in the transverse joints upon additional loading further confirms the value of the longitudinal post-tensioning in the bridge deck.

The only difference between the second and third bridge models was that the third model contained a higher level of post-tensioning, 380 psi, in the deck. Due to this larger amount of post-tensioning, initial cracking occurred in the third model at a load of 5 kips higher than that for the second. During further testing of the third bridge model, the most important event observed was that the post-tensioning helped to close the crack resulting from the addition of a substantial amount of loading. The most important overall conclusion from the experimental research was that "the longitudinal post-tensioning was effective in delaying crack initiation" (Issa et al., 2000).

2.2 Time-Dependent Effects in Concrete

The behavior of a concrete structure over an extended period of time depends on two main criteria. These two factors include the loads which are applied to the structure, and the long-term effects of creep and shrinkage in the concrete and relaxation in the prestressing steel. While the applied service loads will be unique for every different structure, the time-dependent effects of creep, shrinkage, and steel relaxation can be defined and accounted for in the same way for all concrete structures.

2.2.1 Creep

Creep is defined as deformation of concrete under constant load over a long period of time. The basic principles of creep can be described using Figure 2.1.

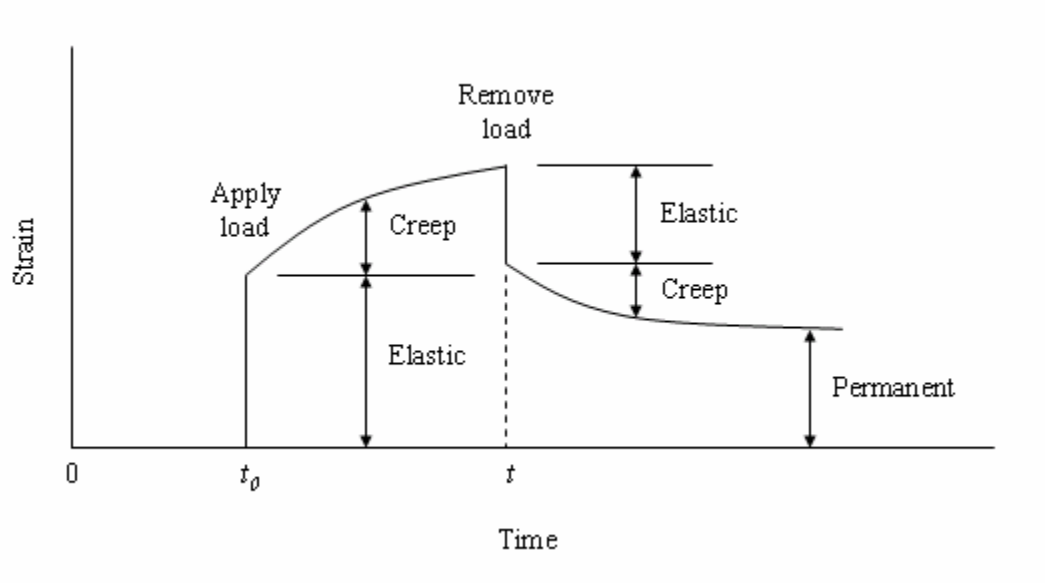

Figure 2.1: Elastic and creep strains due to loading and unloading (after MacGregor, 2005)

When the first load is applied, an initial elastic strain, ε_i, immediately develops in the concrete. Additional creep strains, ε_c, develop over time as long as the load remains on the structure. As indicated by the slope of the graph between times t_o and t in Figure 2.1, the rate of creep is highest upon initial loading, and then decreases with time after that. Removal of the load at time t results in the recovery of some of the elastic and creep strains, but the remaining amount of residual strain results in permanent deformation and deflection of the structure. Other

consequences of creep may include loss of prestressing force and redistribution of stresses within a given cross section (MacGregor, 2005).

In order to analyze the effects of creep on the behavior of structures, a term called the creep coefficient is defined as the ratio of the creep strain after some duration of load (from time t_o to time t in Figure 2.1) to the initial elastic strain:

$$\phi(t,t_o) = \frac{\varepsilon_c}{\varepsilon_i} \tag{2.1}$$

The value of the creep coefficient depends on several quantities, including the compressive strength of the concrete and its age at loading, the dimensions of the component, and the relative humidity and temperature of the environment in which the component is located. Numerous methods for calculating the creep coefficient exist (MacGregor, 2005), and the two different procedures applied in this research are presented here.

2.2.1.1 AASHTO LRFD Creep Model

The method applied for calculating the creep coefficients in all of the parametric studies performed in this research was that presented by the 2006 Interim AASHTO LRFD Bridge Design Specifications, where the creep coefficient is computed as:

$$\psi(t,t_i) = 1.9 k_{vs} k_{hc} k_f k_{td} t_i^{-0.118} \tag{2.2}$$

in which:

$$k_{vs} = 1.45 - 0.13(V/S) \geq 1.0 \tag{2.3}$$

$$k_{hc} = 1.56 - 0.008H \tag{2.4}$$

$$k_f = \frac{5}{1 + f_{ci}^{'}} \tag{2.5}$$

$$k_{td} = \frac{t}{61 - 4 f_{ci}^{'} + t} \tag{2.6}$$

where:

k_{vs} = factor for the effect of the volume-to-surface ratio of the component

k_{hc} = humidity factor for creep

k_f = factor for the effect of concrete strength

k_{td} = time development factor

V/S = volume-to-surface ratio

H = relative humidity (%)

$f_{ci}^{'}$ = specified compressive strength of concrete at time of prestressing for pretensioned members

t = maturity of concrete (days), defined as age of concrete between time of loading and time being considered for analysis of creep effects

t_i = age of concrete when load is initially applied (days)

2.2.1.2 CEB-FIP Creep Model

The method implemented in selected Mathcad models to allow direct comparison with finite element results from DIANA was that presented by the CEB-FIP Model Code 1990 equations, where the creep coefficient is calculated from

$$\phi(t,t_0) = \phi_o \beta_c (t - t_0) \tag{2.7}$$

in which:

$$\phi_o = \phi_{RH} \beta(f_{cm}) \beta(t_0) \tag{2.8}$$

$$\phi_{RH} = 1 + \frac{1 - RH / RH_o}{0.46(h/h_o)^{1/3}} \tag{2.9}$$

$$\beta(f_{cm}) = \frac{5.3}{(f_{cm} / f_{cmo})^{0.5}} \tag{2.10}$$

$$\beta(t_0) = \frac{1}{0.1 + (t_0 / t_1)^{0.2}} \tag{2.11}$$

$$h = \frac{2A_c}{u} \tag{2.12}$$

$$\beta_c(t - t_0) = \left[\frac{(t - t_0)/t_1}{\beta_H + (t - t_0)/t_1} \right]^{0.3} \tag{2.13}$$

$$\beta_H = 150 \left\{ 1 + \left(1.2 \frac{RH}{RH_o} \right)^{18} \right\} \frac{h}{h_o} + 250 \le 1500 \tag{2.14}$$

where:

ϕ_o = notional creep coefficient

β_c = coefficient to describe the development of creep with time after loading

t = age of concrete (days)

f_{cm} = mean compressive strength of concrete at age 28 days (MPa), obtained by adding 8 MPa to the compressive strength of the concrete

f_{cmo} = 10 MPa

RH = relative humidity of the ambient environment (%)

RH_o = 100%

h = notational size of member (mm)

A_c = cross-section of member (mm^2)

u = perimeter of the member in contact with the atmosphere (mm)

h_o = 100 mm

t_1 = 1 day

t_0 = age of concrete at loading (days), adjusted according to

$$t_0 = t_{0,T}\left[\frac{9}{2+(t_{0,T}/t_{1,T})^{1.2}}+1\right]^{\alpha} \geq 0.5\,days \tag{2.15}$$

where:

α = 0 for normal or rapid hardening cements (as assumed in this research)

$t_{1,T}$ = 1 day

$t_{0,T}$ = the age of concrete at loading (days) adjusted according to

$$t_T = \sum_{i=1}^{n} \Delta t_i \exp\left[13.65 - \frac{4000}{273+T(\Delta t_i)/T_0}\right] \tag{2.16}$$

where:

t_T = the temperature adjusted concrete age which replaces t in the corresponding equations

Δt_i = number of days where a temperature T prevails

$T(\Delta t_i)$ = temperature (°C) during the time period Δt_i

T_0 = 1°C

Equation F.10 was not used in the implementation of the CEB-FIP Model equations in this research. The quantity $t_{0,T}$ was simply taken as the age of concrete at loading (in days) and then adjusted by equation F.9 to obtain t_0.

2.2.2 Shrinkage

Shrinkage is defined as a decrease in the volume of concrete due to loss of water. The basic principles of shrinkage can be described using Figure 2.2.

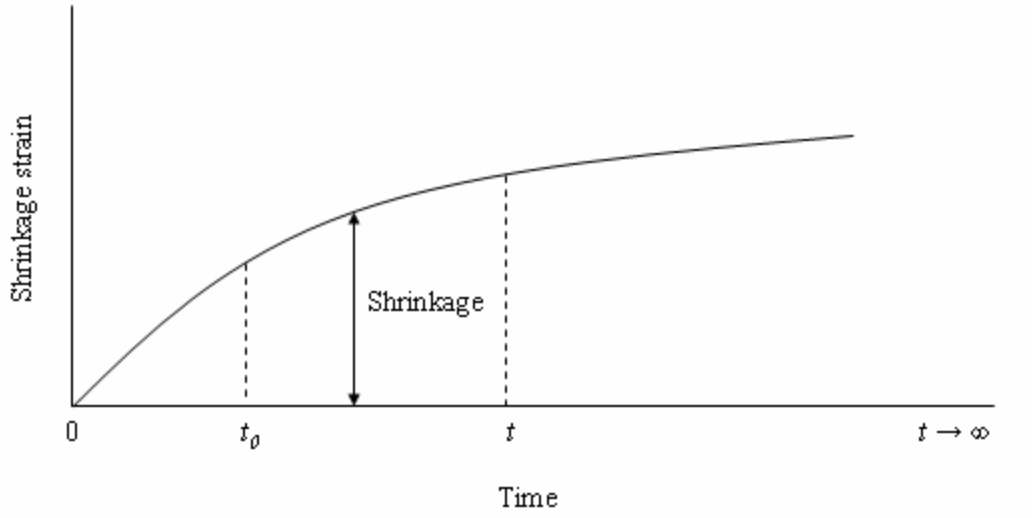

Figure 2.2: Shrinkage of an unloaded specimen (after MacGregor, 2005)

As illustrated in Figure 2.2, this shrinkage begins as soon as the concrete begins to cure, and occurs most rapidly at this initial time. Like creep, the rate of shrinkage decreases over time, and the shrinkage strain approaches some maximum value as time approaches infinity.

The main type of shrinkage is referred to most simply as shrinkage, or more descriptively as drying shrinkage. Since moisture must diffuse out of the concrete for this type of shrinkage to take place, the magnitude of shrinkage strains is largely dependent on the relative humidity of the concrete element's environment, with larger shrinkage strains occurring in less humid environments. Other factors which affect shrinkage strains include the concrete's composition and the ratio of volume to surface area of the concrete member.

Similar to creep, there are numerous methods for calculating shrinkage strains in concrete, and the two different procedures applied in this research are presented here.

2.2.2.1 AASHTO LRFD Shrinkage Model

The method applied for calculating the shrinkage strains in all of the parametric studies performed in this research was that presented by the 2006 Interim AASHTO LRFD Bridge Design Specifications, where the strain due to shrinkage at time *t* is computed as

$$\varepsilon_{sh} = -k_{vs} k_{hs} k_f k_{td} * 0.48 \times 10^{-3} \tag{2.17}$$

in which:

$$k_{hs} = 2.00 - 0.014H \tag{2.18}$$

where:

k_{hs} = humidity factor for shrinkage

t = maturity of concrete (days), defined as age of concrete between end of curing for shrinkage calculations and time being considered for analysis of shrinkage effects

and all other factors and variables are as defined in the previous section for creep, 2.2.1.

2.2.2.2 CEB-FIP Shrinkage Model

Again, the method implemented in selected Mathcad models to allow direct comparison with finite element results from DIANA was that presented by the CEB-FIP Model Code 1990 equations, where the shrinkage strain is calculated from

$$\varepsilon_{cs}(t, t_s) = \varepsilon_{cso} \beta_s (t - t_s) \tag{2.19}$$

in which:

$$\varepsilon_{cso} = \varepsilon_s(f_{cm}) \beta_{RH} \tag{2.20}$$

$$\varepsilon_s(f_{cm}) = \left[160 + 10\beta_{sc}(9 - f_{cm} / f_{cmo})\right] \times 10^{-6} \tag{2.21}$$

$$\beta_{RH} = -1.55\beta_{sRH} \quad \text{for } 40\% \leq \text{RH} < 99\% \tag{2.22}$$

$$\beta_{RH} = +0.25 \quad \text{for RH} \geq 99\% \tag{2.23}$$

$$\beta_{sRH} = 1 - \left(\frac{RH}{RH_o}\right)^3 \tag{2.24}$$

$$\beta_s(t - t_s) = \left[\frac{(t - t_s)/t_1}{350(h/h_o)^2 + (t - t_s)/t_1}\right]^{0.5} \tag{2.25}$$

where:

ε_{cso} = notional shrinkage coefficient

β_s = coefficient to describe the development of shrinkage with time

t = age of concrete (days)

t_s = age of concrete (days) at the beginning of shrinkage

f_{cm} = mean compressive strength of concrete at age 28 days (MPa), obtained by adding 8 MPa to the compressive strength of the concrete

f_{cmo} = 10 MPa

β_{sc} = coefficient which depends on the type of cement: β_{sc} = 5 for normal or rapid hardening cements (as assumed in this research)

RH = relative humidity of the ambient environment (%)

RH_o = 100%

h is defined in equation F.6

h_o = 100 mm

t_1 = 1 day

2.2.3 Steel Relaxation

Unlike the time-dependent effects of creep and shrinkage which are inherent in the behavior of concrete as a material, relaxation occurs in the steel strands used for prestressing operations, and therefore only becomes a concern in pretensioned or post-tensioned concrete members. Because this research focuses on post-tensioning of precast concrete bridge deck panels, the long-term effects of steel relaxation are certainly an applicable concern.

Relaxation can be described as "the loss of stress in a stressed material held at constant length" (Nilson, 1987). Although changes in applied loads along with concrete creep and shrinkage produce variations in strand length in prestressed concrete elements, tendon length is assumed to remain constant for the purposes of calculating loss of force due to steel relaxation. Like creep and shrinkage, relaxation of prestressing steel may continue for a very long time, and must therefore be considered in design as a notable contributor to long-term loss of prestress force.

Factors which affect the amount of relaxation that will occur include the magnitude and duration of the initial force, as well as the grade and type of steel strands being used. The two main types of prestressing tendons are low-relaxation and stress-relieved strand. The method used for calculating steel relaxation values in this research was that given by the 2006 Interim AASHTO LRFD Bridge Design Specifications, where the relaxation over a certain time interval is given by:

$$\Delta f_{pR1} = \left[\frac{f_{pt}}{K_L'} \frac{\log(24t)}{\log(24t_i)} \left(\frac{f_{pt}}{f_{py}} - 0.55 \right) \right] \left[1 - \frac{3(\Delta f_{pSR} + \Delta f_{pCR})}{f_{pt}} \right] K_{id} \quad (2.26)$$

where:

f_{pt} = stress in prestressing strands immediately after transfer (ksi)

K_L' = factor accounting for type of steel, equal to 45 for low relaxation steel and 10 for stress relieved steel

f_{py} = yield strength of prestressing steel (ksi)

t = time being considered for analysis of relaxation effects (days)

t_i = age of prestressing steel at beginning of the time being considered for analysis of relaxation effects (days)

Δf_{pSR} = prestress loss due to shrinkage of concrete over a given time interval (ksi)

Δf_{pCR} = prestress loss due to creep of concrete over a given time interval (ksi)

K_{id} = factor that accounts for the restraint of the concrete member caused by bonded reinforcement

The AASHTO LRFD Commentary notes that in equation 2.26 above, "the term in the first square brackets is the intrinsic relaxation without accounting for strand shortening due to creep and shrinkage of concrete," while "the second term in square brackets accounts for relaxation reduction due to creep and shrinkage of concrete" (AASHTO, 2006). Therefore, only the term in the first square brackets in equation 2.26 was used to calculate steel relaxation losses in this research, since creep and shrinkage were accounted for separately using the models presented in the previous sections.

2.3 Time-Dependent Analysis Methods for Concrete Structures

The theories regarding creep and shrinkage in concrete are reasonably straightforward and understandable. The behavior of concrete becomes much more complex, however, once it is placed in a structural system in which the effects of creep and shrinkage are combined with other materials and loads. Stresses and deformations induced by creep and shrinkage of concrete and other applied loads are also affected by the presence of reinforcing or prestressing steel within the concrete and/or the pairing of concrete elements with steel sections in composite

construction. The effects of creep and shrinkage over time produce constant force redistributions in each element of a cross section, and must be considered in the design and analysis of concrete structures.

Several procedures for describing and modeling these time-dependent effects in concrete have been formulated and discussed. The fundamentals of some of these models along with the reasons for the one chosen for use in this research are described in the following.

2.3.1 Effective Modulus (EM) Method

The Effective Modulus method, proposed by McMillan (1916) and Faber (1927), is suggested by Dilger (2005) to be "the oldest and simplest method to analyze time dependent effects in concrete structures." This method involves a reduction of the modulus of elasticity to account for creep in concrete. To obtain the effective modulus, the elastic modulus $E(t_o)$ is reduced by a factor which incorporates the creep coefficient $\phi(t,t_o)$ defined in equation 2.1:

$$E_{ef} = \frac{E(t_o)}{1+\phi(t,t_o)} \tag{2.27}$$

The effective modulus given in equation 2.27 may be employed in any elastic analysis. However, this implies that the strain due to creep at age *t* is governed by the magnitude of the stress at that time, and the stress history is disregarded. Therefore, there are only two circumstances under which the EM method produces reliable results. These two situations occur when there are no major variations in the concrete stress throughout the time interval being examined, and when the concrete is old enough that the effects of aging are negligible. The EM method underestimates strains when the stress in the concrete is decreasing, and it overestimates strains when the stress is increasing (Dilger, 2005).

2.3.2 Rate of Creep (RC) Method

A second method for predicting time-dependent effects in concrete was inspired by the results of experiments performed by Glanville (1930) on early-age concrete. Glanville concluded that the rate at which concrete creeps is unrelated to the concrete's age when it is loaded; in other words, this means that "all creep curves are parallel" (Dilger, 2005). While creep curves for fairly young concrete may be approximately parallel, this assumption is definitely inaccurate for older concrete. Therefore, overestimations are produced for both

deformations due to creep during increasing stress and relaxation of stress during constant strain. The following two methods include efforts made to remedy the faults of the RC method.

2.3.3 Rate of Flow (RF) Method

Proposed by England and Illston (1965), the rate of flow method was the first attempted improvement on the RC method. They suggested that the creep compliance be defined as the sum of "(1) elastic strain, (2) delayed elastic strain (which is recoverable), and (3) (irrecoverable) flow" (Dilger, 2005). Their experiments showed that the recoverable elastic strain component was not influenced by the age of concrete at loading and approached a final value more quickly than the irrecoverable flow component. Although this method was considerably better than the RC method, the delayed elastic strain and the irrecoverable flow still had to be individual components in the formulation of the creep function.

2.3.4 Improved Dischinger (ID) Method

Further attempts to enhance the RC and RF methods resulted in the improved Dischinger method, which was a mixture of the RC and RF methods and was suggested by Nielsen in 1970. Nielsen's approach was to include the delayed elastic strain as part of the elastic deformation, and then take the irrecoverable flow component to be identical to the total creep from the RC method. Nielsen's method was later modified by Rusch, Jungwirth and Hilsdorf (1973) and presented in the 1978 CEB-FIP Model Code.

2.3.5 Age-Adjusted Effective Modulus (AAEM) Method

The age-adjusted effective modulus method is simply an improved version of the effective modulus method described above. The AAEM method enhances the EM method by including a quantity called the aging coefficient, χ, which was first presented by Trost in 1967, and further refined by Bazant (1972). The age-adjusted effective modulus is given by Dilger (1982) as:

$$E_c^* = \frac{E_c(t_o)}{1+\chi\phi(t,t_o)} \tag{2.28}$$

where:

$E_c(t_o)$ = modulus of elasticity of concrete loaded at age t_o

$\phi(t,t_o)$ = creep coefficient at time t for concrete loaded at age t_o

χ = aging coefficient

Recall that the EM method was unable to account for two frequently occurring instances: large variations in the concrete stress as well as aging of the concrete throughout the time interval being examined. Bazant presents the theoretical formulation of the AAEM method, and then defends its superiority over the EM method with several examples. He includes computations of the aging coefficient for creep functions both with and without provision for a fluctuating elastic modulus. The aging coefficients which result from the two different creep models are very different, illustrating the significance of considering a time-varying elastic modulus, which was neglected in prior work. In addition, Bazant points out that the inclusion of the aging coefficient in the effective modulus equation is needed to adjust the quantity for aging of the material, whereas the previous effective modulus could only provide accurate results for an unchanging material.

Dilger implements the principles of the age-adjusted effective modulus method in the calculation of what he refers to as "creep-transformed" section properties in his paper on the topic (1982). Dilger introduces and explains these properties in an attempt to simplify the analysis of concrete members either (1) with one or more combined layers of prestressed and non-prestressed reinforcement, or (2) as part of a larger composite cross section. He relates a creep-transformed section analysis to an examination of elastic stresses in a member made up of two different materials, where the temperature of one material (concrete) changes, while the other material (reinforcement) maintains the same temperature. The final stresses generated in each of the two different materials may then be determined by applying the forces created by the free temperature strain in one component to the transformed cross section which accounts for the two different materials in the original cross section. Relating this concept to the method Dilger presents, the free temperature strain is analogous to the strains produced by free shrinkage and creep, while the time-dependent effects of creep in concrete are handled by the creep-transformed section properties. Dilger's creep-transformed section properties are only applicable to uncracked concrete cross sections (Dilger, 1982).

Because of its use of the aging coefficient, the age-adjusted effective modulus method is ideal for calculating gradual changes in concrete stress due to the long-term effects described previously. The aging coefficient describes the effect which concrete aging has on the final value of creep associated with gradual changes in stress following the initial application of load at age t_o. Similarly, the magnitude of the aging coefficient is influenced by three factors: the concrete's age when it is first loaded, the length of time it is loaded, and the value of the creep coefficient. The argument (t, t_o) is typically omitted from the notation of the aging coefficient since it is identical to the argument of the creep coefficient to which it is related (Dilger, 1982).

The concept of the aging coefficient may be better understood by investigating its physical meaning using two different approaches. First, consider a stress of ultimate magnitude σ_o which is (1) gradually applied to a structure beginning at time t_o, and (2) applied in full, immediately at age t_o. In this case, the creep resulting from the gradually applied stress is smaller than that due to the instantly applied stress by a factor equal to the aging coefficient χ. The alternative explanation is that the creep produced by the stress σ_o applied over time is equivalent to the creep resulting from the immediate application of the reduced stress $\chi\sigma_o$ at time t_o (Dilger, 2005).

The magnitude of the aging coefficient ranges from 0.5 to 1.0. The minimum value of 0.5 is associated with concrete loaded very early in its life and subjected to a long duration of creep. The maximum value of 1.0, on the other hand, distinguishes a material which is aged at loading and exposed to only a short time interval of creep. When there is no aging and χ is 1.0, the age-adjusted effective modulus from equation 2.28 simplifies to the effective modulus given in equation 2.27. When Trost first presented the aging coefficient (1967), he gave it a value of 0.75, the average of the two bounds (Dilger, 2005).

After elaborating on the age-adjusted effective modulus concept first introduced by Trost and Bazant, Dilger explains how this method may be applied to the time-dependent analysis of non-composite and composite concrete members (1982). For both types of members, Dilger presents equations which satisfy equilibrium, compatibility, and constitutive requirements for modeling and calculating the long-term changes occurring in a concrete cross section. He applies these equations in examples, noting the need for additional consideration of two important elements in a composite cross-section: the inclusion of the concrete deck in the creep-transformed section, and the force and moment resulting from the unequal free strains which

develop between the deck and the girder. The equations used for time-dependent analysis in this research are based on the same principles as those presented by Dilger (1982).

2.4 Summary of Need for Research

This chapter has described the progress made regarding the development, application, and behavior of precast concrete panels used for rehabilitation or new construction of bridge decks. Since the long-term effects of creep and shrinkage in concrete and relaxation of prestressing steel significantly impact the behavior of precast concrete panels, these phenomena have also been explained. Further details concerning the various methods available for predicting the behavior of concrete as a result of these time-dependent effects are included.

When describing the need for the research presented in this thesis, it is first important to note the reasons for which longitudinal post-tensioning in precast concrete bridge deck panels should be required. From their survey of various transportation agencies, Issa et al. determined that the quality of the panel-to-panel joint performance was a key element pertaining to the success of a fully precast bridge deck (1995). In their follow-up field inspections of bridges containing precast concrete decks, Issa et al. described the performance of the precast panels in many cases as excellent (1995). The problems observed in the cases of inferior performance, however, were partially attributed to the absence of longitudinal post-tensioning in the precast deck. As illustrated by the example bridges mentioned above, some of the same bridges which experienced leaking, cracking, spalling, and subsequent rusting on the beams at the transverse panel joints also lacked longitudinal post-tensioning in their precast decks. These examples prove that the precast panels should be longitudinally post-tensioned in order to tighten the transverse joints and keep the deck in compression, thereby eliminating potential problems with the panel joints.

After justifying the need for post-tensioning of precast concrete bridge deck panels, it is necessary to determine the corresponding amount of compressive force which should be applied to the panels. Further studies conducted by Issa, et al. included finite element modeling (1998) and experimental testing (2000) of different bridge systems with decks made out of full-depth precast concrete panels. While the finite element studies produced recommended initial levels of post-tensioning for both simple and continuous span bridges, each of these two recommendations was based on only one bridge configuration. The two configurations analyzed were a simple

span bridge and a three-span continuous bridge, both with precast deck panels supported by rolled steel girders. Furthermore, while the later experimental studies again indicated the need for longitudinal post-tensioning in a precast bridge deck, these experiments included only two-span continuous bridge models of precast concrete panels on steel girders with three different levels of longitudinal post-tensioning.

While Issa et al. has provided some recommendations regarding levels of longitudinal post-tensioning for precast bridge decks, these suggestions have been limited to systems with (1) only steel girders and (2) only the specific configurations of span length, girder size, girder spacing, and so on used in each finite element model or experimental mockup. Due to the time-dependent effects in concrete discussed earlier, a precast concrete bridge deck supported by prestressed concrete girders is likely to behave very differently than a precast deck supported by steel girders. Clearly, there is a need for simple, straightforward design recommendations which provide appropriate levels of post-tensioning for a variety of bridge systems, including those with steel and prestressed concrete girders at different spacings, as well as single or multiple continuous spans of assorted lengths. By simplifying the design of a fully precast concrete bridge deck, the recommendations presented in this thesis should motivate the use of more precast construction, thereby alleviating more of today's transportation problems.

CHAPTER 3: METHODS, MODELING, AND TESTING

3.1 Introduction

To investigate trends in the amount of longitudinal post-tensioning needed to keep the joints between precast concrete bridge deck panels in compression, numerous models of different bridge systems were developed using the software Mathcad. Each model bridge cross-section consisted of either steel or prestressed concrete girders, a 1 in. haunch, and a deck made out of full-depth precast concrete panels. The level of post-tensioning applied to the precast concrete bridge deck in each model was varied until the transverse panel joints were observed to be in compression at the assumed end of each bridge's service life. This chapter describes the procedures used to develop the models in Mathcad, the determination of the girder types and other bridge details used for the parametric studies, and the implementation of the models in the parametric studies themselves.

3.2 Material Properties

3.2.1 Steel and Prestressed Concrete Girders

The bridge models containing steel girders included either rolled shapes or plate girders, each with a modulus of elasticity of 29,000 ksi. The cross-sections with prestressed concrete girders included either Virginia PCBT girders or AASHTO standard girders, each with a minimum 28 day compressive strength of 7000 psi and an aging coefficient of 0.7. The value of 0.7 was selected as a typical aging coefficient based on past applications of the quantity and its range of values from 0.5 to 1 established by Trost (Dilger, 2005). The prestressing strands were all ½ in. diameter, Grade 270 low relaxation strands, with a cross-sectional area of 0.153 in^2 and a modulus of elasticity of 28,500 ksi.

3.2.2 Precast Concrete Panels and Haunch

The precast concrete panels making up the bridge deck in each model had a minimum 28 day compressive strength of 5000 psi. The steel girder bridges had 8.5 in. thick precast decks, while the prestressed concrete girder bridges had 8 in. thick precast decks. Each bridge model also contained a 1 in. thick haunch separating the top of each girder from the bottom of the precast deck. The minimum 28 day compressive strength of the haunch was assumed to be equal

to that of the precast deck. As for the prestressed concrete girders, the deck and the haunch were both assigned an aging coefficient of 0.7. Like the strands used in the prestressed concrete girders, the deck post-tensioning strands were all ½ in. diameter, Grade 270 low relaxation strands, with a cross-sectional area of 0.153 in^2 and a modulus of elasticity of 28,500 ksi.

3.3 Model Development

The primary steps in the development of the Mathcad models included denoting the time intervals to be analyzed for each type of bridge, and determining the equations to calculate the redistribution of stresses due to long-term creep, shrinkage, and steel relaxation corresponding to each of these time intervals. For the multiple span bridges, it was also necessary to consider the effects of continuity and live loads, particularly at the interior supports. The procedures used to develop each type of bridge model are discussed in this section.

3.3.1 Construction Time Intervals

The time-dependent analyses performed in each Mathcad model were separated into the major time intervals existing throughout the construction and service life of a bridge with a deck composed of precast concrete panels. For the bridges with precast concrete deck panels supported by steel girders, the two time intervals containing stress redistributions were denoted as:

1. D/SG 1 – Time of post-tensioning the deck to the start of composite action between the deck and girders
2. D/SG 2 – Start of composite action between deck and girders to the end of the bridge's service life, which was estimated as 10,000 days.

While these two phases also applied to the bridges with precast concrete deck panels supported by prestressed concrete girders, an additional phase was necessary to account for the time-dependent effects occurring in the prestressed concrete girder. The three time intervals for the precast deck panel/prestressed concrete girder system were denoted as:

1. D/CG 1 – Time of transfer of prestress to the concrete girder to the start of composite action between the girders and deck
2. D/CG 2 – Time of post-tensioning the deck to the start of composite action between the deck and girders

3. D/CG 3 – Start of composite action between deck and girders to the end of the bridge's service life, which was estimated as 10,000 days.

Table 3.1 indicates the construction time intervals on which the time-dependent analyses performed in the various bridge models were based. The times in days indicated for the two steel girder bridge phases are relative to the time at which the precast concrete panels for that system were cast. For the prestressed concrete girder bridges, it was assumed that the concrete girders and deck panels were both cast at the same time, so the three concrete girder bridge intervals are relative to this particular time of girder and panel casting. Composite action was assumed to occur instantaneously at 60 days in both the steel and prestressed concrete girder bridges.

Table 3.1: Construction Time Intervals for Bridge Models

Time Interval	Start Time (days)	End Time (days)
D/SG 1	55	60
D/SG 2	60	10000
D/CG 1	1	60
D/CG 2	55	60
D/CG 3	60	10000

3.3.2 Equations for Time-Dependent Analysis

Once the appropriate time intervals were established, it was necessary to write systems of equations to model the behavior and solve for the changes occurring in a given bridge in each of the time intervals listed above. Whereas long-term prestress losses only had to be considered in the decks of the bridges with steel girders, the bridges containing prestressed concrete girders presented a more complicated situation, with time-dependent effects occurring in both the concrete girders and the concrete deck. Maintaining a consistent sign convention throughout the development of these equations was essential. Tensile stresses and lengthening strains were defined as positive, while compressive stresses and shortening strains were considered negative. In addition, compression or shortening at the top of a member indicated positive moment and positive curvature. The systems of equations used to solve for the changes occurring in each bridge system over time are presented in this section. Since many of the variables used in each

type of model appear multiple times in different equations, all quantities are defined in Appendix A.

3.3.2.1 Bridges with Steel Girders

The first time interval for the steel girder bridges, D/SG 1, includes the changes in forces and strains occurring from the time that the deck is post-tensioned to the start of composite action between the concrete deck and the steel girders. During this time, creep, shrinkage, and steel relaxation simultaneously cause the force in the post-tensioning to become less tensile, and the corresponding force in the deck concrete to become less compressive. In addition, compressive shrinkage strains occur in the deck concrete, which results in shortening of the post-tensioning steel as well. These changes are modeled by the following four equations:

Equilibrium

$$\Delta N_d + \Delta N_{ptd} = 0 \tag{3.1}$$

Compatibility

$$\Delta \varepsilon_d = \Delta \varepsilon_{ptd} \tag{3.2}$$

Constitutive

$$\Delta \varepsilon_d = \frac{N_{do}}{A_d E_d}\phi_d + \frac{\Delta N_d}{A_d E_d}(1+\mu_d \phi_d) + \varepsilon_{shd} \tag{3.3}$$

$$\Delta \varepsilon_{ptd} = \frac{\Delta N_{ptd} - \Delta f_{pR} A_{ptd}}{A_{ptd} E_{ptd}} \tag{3.4}$$

where all variables are defined in Appendix A.

Equation 3.1 defines the equilibrium requirement that the change in the compressive axial force in the deck concrete must be equal and opposite of the corresponding change in the tensile axial force in the post-tensioning strands. Equation 3.2 establishes compatibility between the changes in strain in the deck concrete and the post-tensioning steel. Equations 3.3 and 3.4 identify the constituents of the changes in strain in the deck concrete and the post-tensioning tendons. The three terms in equation 3.3 represent the creep associated with the initial strain in the deck, the elastic strain and creep strain components of the change in strain in the deck during D/SG 1, and the shrinkage strain in the deck concrete during D/SG 1. The two quantities in the numerator of equation 3.4 represent the change in axial force which contributes to the change in strain in the deck post-tensioning strands, and the change in force due to relaxation of the post-

tensioning steel which is subtracted out since it has no corresponding change in strain. The quantities ϕ_d, ε_{shd}, and Δf_{pR} in equations 3.3 and 3.4 represent the deck creep coefficient, deck shrinkage strain, and post-tensioning strand relaxation corresponding to the D/SG 1 time interval only. Figure 3.1 illustrates the initial axial compressive force and the changes occurring in the D/SG 1 phase defined by equations 3.1-3.4. While all of the varying quantities are represented as positive in the figure, the appropriate sign conventions were accounted for in the corresponding equations.

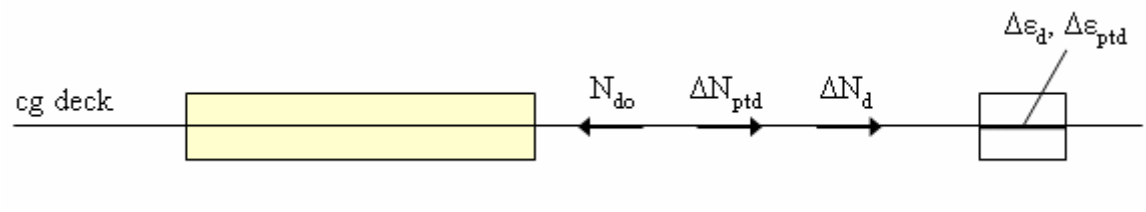

Figure 3.1: Initial Force and Changes Occurring in the D/SG 1 Phase

The second time interval for the steel girder bridges, D/SG 2, includes the changes in forces, moments, strains, and curvature from the start of composite action between deck and girders to the end of the bridge's service life, which was estimated as 10,000 days. In the composite cross-sections of the steel girder bridges, the concrete deck and haunch undergo creep and shrinkage while the steel girder resists these forces. The corresponding changes in forces, moments, strains and curvature for the D/SG 2 time interval in the steel girder bridges are modeled by the following equations:

Equilibrium

$$\Delta N_d + \Delta N_h + \Delta N_g + \Delta N_{ptd} = 0 \tag{3.5}$$

$$\Delta M_d + \Delta M_h + \Delta M_g + \Delta N_h * a + \Delta N_g * b = 0 \tag{3.6}$$

Compatibility

$$\Delta \varepsilon_d = \Delta \varepsilon_{ptd} \tag{3.7}$$

$$\Delta \varepsilon_d = \Delta \varepsilon_h - \Delta \chi * a \tag{3.8}$$

$$\Delta \varepsilon_d = \Delta \varepsilon_g - \Delta \chi * b \tag{3.9}$$

Constitutive

$$\Delta \varepsilon_d = \frac{N_{doc}}{A_d E_d} \phi_d + \frac{\Delta N_d}{A_d E_d}(1 + \mu_d \phi_d) + \varepsilon_{shd} \tag{3.10}$$

$$\Delta\varepsilon_g = \frac{\Delta N_g}{A_g E_g} \tag{3.11}$$

$$\Delta\varepsilon_h = \frac{\Delta N_h}{A_h E_h}(1+\mu_h\phi_h) + \varepsilon_{shh} \tag{3.12}$$

$$\Delta\varepsilon_{ptd} = \frac{\Delta N_{ptd} - \Delta f_{pR} A_{ptd}}{A_{ptd} E_{ptd}} \tag{3.13}$$

$$\Delta\chi = \frac{\Delta M_d}{I_d E_d}(1+\mu_d\phi_d) \tag{3.14}$$

$$\Delta\chi = \frac{\Delta M_h}{I_h E_h}(1+\mu_h\phi_h) \tag{3.15}$$

$$\Delta\chi = \frac{\Delta M_g}{I_g E_g} \tag{3.16}$$

where all variables are defined in Appendix A.

Equations 3.5 and 3.6 define the equilibrium requirements for the changes in forces and moments in the composite system. Equation 3.7 was discussed previously, and equations 3.8 and 3.9 establish additional strain compatibility relationships present based on the assumption that plane sections remain plane throughout the composite cross section. The terms in equations 3.10, 3.12, and 3.13 are similar to those discussed for the D/SG 1 time interval, and the quantity N_{doc} in equation 3.10 is the force in the deck at the beginning of the composite phase. Equation 3.11 represents the change in strain in the steel girder which undergoes no creep or shrinkage. Equations 3.14 and 3.15 each describe the change in curvature based on the elastic and creep-producing changes in moment in the concrete deck and haunch, respectively. Equation 3.16 also represents the change in curvature, but in terms of the elastic change in moment in the steel girder. The quantities ϕ_d, ϕ_h, ε_{shd}, ε_{shh}, and Δf_{pR} in the above equations represent the creep coefficients, shrinkage strains, and steel strand relaxation corresponding to the D/SG 2 time interval only. Figure 3.2 illustrates the initial force present and the changes occurring throughout the D/SG 2 phase defined by equations 3.5-3.16. While all of the varying quantities are represented as positive in the figure, the appropriate sign conventions were accounted for in the corresponding equations.

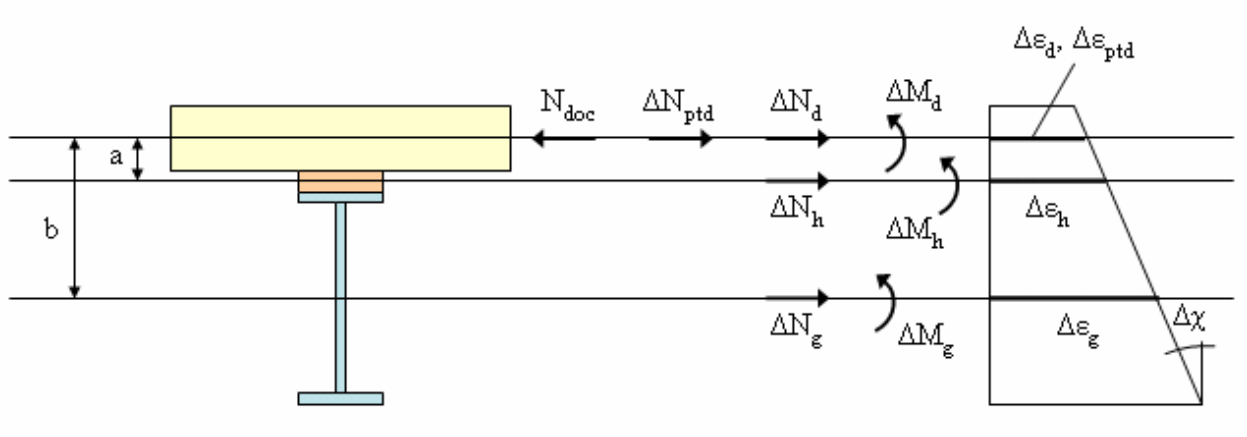

Figure 3.2: Initial Force and Changes Occurring in the D/SG 2 Phase

3.3.2.2 Bridges with Prestressed Concrete Girders

The first phase listed above for the prestressed concrete girder bridges, D/CG 1, includes the changes in forces, moments, strains, and curvature occurring from the time that prestress is transferred to the girder to the time that the girder becomes composite with the deck. Since steel girders alone are not affected by long-term prestress losses, this phase was not needed in the analysis of the steel girder bridges. The changes occurring in the prestressed concrete girder from transfer of prestress to composite action with the deck are modeled by the following equations:

Equilibrium

$$\Delta N_g + \Delta N_{psg} = 0 \tag{3.17}$$

$$\Delta M_g + \Delta N_{psg} * e_g = 0 \tag{3.18}$$

Compatibility

$$\Delta\varepsilon_g = \Delta\varepsilon_{psg} - \Delta\chi * e_g \tag{3.19}$$

Constitutive

$$\Delta\varepsilon_g = \frac{N_{go}}{A_{gn}E_g}\phi_g + \frac{\Delta N_g}{A_{gn}E_g}(1+\mu_g\phi_g) + \varepsilon_{shg} \tag{3.20}$$

$$\Delta\chi = \frac{M_{go}}{E_g I_{gn}}\phi_g + \frac{\Delta M_g}{E_g I_{gn}}(1+\mu_g\phi_g) \tag{3.21}$$

$$\Delta\varepsilon_{psg} = \frac{\Delta N_{psg} - \Delta f_{pR}A_{psg}}{A_{psg}E_{psg}} \tag{3.22}$$

where all variables are defined in Appendix A.

While the format and purpose of equations 3.17 through 3.22 are similar to that explained for the steel girder time intervals above, these equations now account for the prestressing force and time-dependent effects occurring in the concrete girder. The quantities N_{go} and M_{go} indicate the initial force and moment due to the prestress in the girder, and the variables ϕ_g, ε_{shg}, and Δf_{pR} represent the girder creep coefficient, girder shrinkage strain, and prestressing strand relaxation corresponding to the D/CG 1 time interval only. Figure 3.3 illustrates the initial force and moment as well as the changes occurring in the D/CG 1 phase defined by equations 3.17-3.22. While all of the varying quantities are represented as positive in the figure, the appropriate sign conventions were accounted for in the corresponding equations.

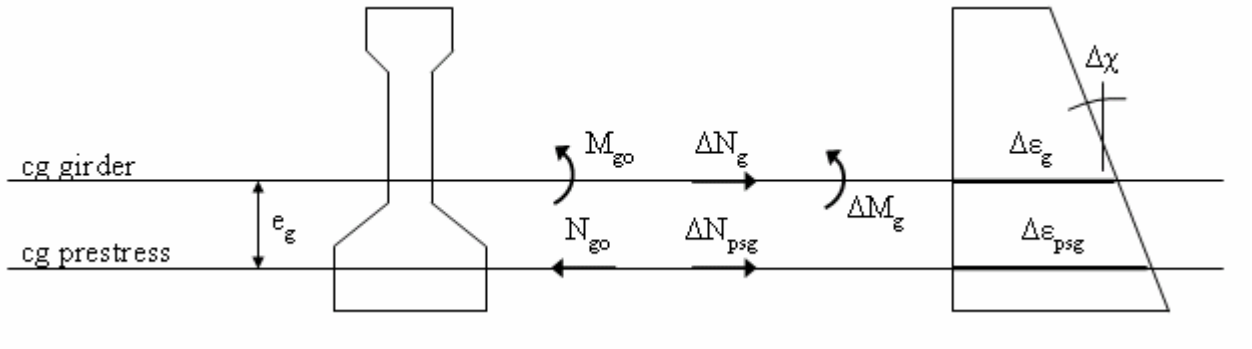

Figure 3.3: Initial Effects and Changes Occurring in the D/CG 1 Phase

The second phase listed above for the prestressed concrete girder bridges, D/CG 2, is identical to the first time interval for the steel girder bridges (D/SG 1). This is true because only the concrete deck panels are affected by the changes occurring during this time interval, which spans from the time of deck post-tensioning to the beginning of composite action between the deck and girders. Therefore, the same equations (3.1 to 3.4) presented for calculating changes during the D/SG 1 phase apply for calculating changes during the D/CG 2 phase, and Figure 3.1 again illustrates these quantities.

The third time interval for the prestressed concrete girder bridge models, D/CG 3, is similar to the second time interval for the steel girder bridges (D/SG 2). For both types of girders, this phase begins with the start of composite action between the deck and girders and concludes at the end of the bridge's service life. In the composite cross-sections of the prestressed concrete girder bridges, however, the concrete deck, haunch, and girder each

experience the effects of creep and shrinkage at different rates, making the time-dependent redistribution of forces and moments much more complex than in the steel girder bridges. The changes in forces, moments, strains and curvature for the D/CG 3 time interval in the prestressed concrete girder bridges are modeled by the following equations:

Equilibrium

$$\Delta N_d + \Delta N_h + \Delta N_g + \Delta N_{psg} + \Delta N_{ptd} = 0 \tag{3.23}$$

$$\Delta M_d + \Delta M_h + \Delta M_g + \Delta N_h * a + \Delta N_g * b + \Delta N_{psg} * c = 0 \tag{3.24}$$

Compatibility

$$\Delta \varepsilon_d = \Delta \varepsilon_{ptd} \tag{3.25}$$

$$\Delta \varepsilon_d = \Delta \varepsilon_h - \Delta \chi * a \tag{3.26}$$

$$\Delta \varepsilon_d = \Delta \varepsilon_g - \Delta \chi * b \tag{3.27}$$

$$\Delta \varepsilon_d = \Delta \varepsilon_{psg} - \Delta \chi * c \tag{3.28}$$

Constitutive

$$\Delta \varepsilon_d = \frac{N_{doc}}{A_d E_d} \phi_d + \frac{\Delta N_d}{A_d E_d}(1 + \mu_d \phi_d) + \varepsilon_{shd} \tag{3.29}$$

$$\Delta \varepsilon_g = \frac{N_{goc}}{A_g E_g} \phi_g + \frac{\Delta N_g}{A_g E_g}(1 + \mu_g \phi_g) + \varepsilon_{shg} \tag{3.30}$$

$$\Delta \varepsilon_h = \frac{\Delta N_h}{A_h E_h}(1 + \mu_h \phi_h) + \varepsilon_{shh} \tag{3.31}$$

$$\Delta \varepsilon_{ptd} = \frac{\Delta N_{ptd} - \Delta f_{pR} A_{ptd}}{A_{ptd} E_{ptd}} \tag{3.32}$$

$$\Delta \varepsilon_{psg} = \frac{\Delta N_{psg} - \Delta f_{pR} A_{psg}}{A_{psg} E_{psg}} \tag{3.33}$$

$$\Delta \chi = \frac{\Delta M_d}{I_d E_d}(1 + \mu_d \phi_d) \tag{3.34}$$

$$\Delta \chi = \frac{\Delta M_h}{I_h E_h}(1 + \mu_h \phi_h) \tag{3.35}$$

$$\Delta \chi = \frac{M_{goc}}{I_g E_g} \phi_g + \frac{\Delta M_g}{I_g E_g}(1 + \mu_g \phi_g) \tag{3.36}$$

where all variables are defined in Appendix A.

Equations 3.23 through 3.36 represent the same kind of changes that were discussed for the composite steel girder bridge phase (D/SG 2), except now the equations are further complicated by the prestressing and time-dependent effects in the concrete girder as well as the deck. The quantities N_{doc} and N_{goc} are the initial forces in the deck and girder at the beginning of the composite phase, while M_{goc} is the initial moment in the girder at the beginning of the composite phase. The creep coefficients, shrinkage strains, and steel strand relaxation quantities correspond to the D/CG 3 time interval only. Figure 3.4 illustrates the initial forces and moment as well as the changes occurring in the D/CG 3 phase defined by equations 3.23-3.36. While all of the varying quantities are represented as positive in the figure, the appropriate sign conventions were accounted for in the corresponding equations.

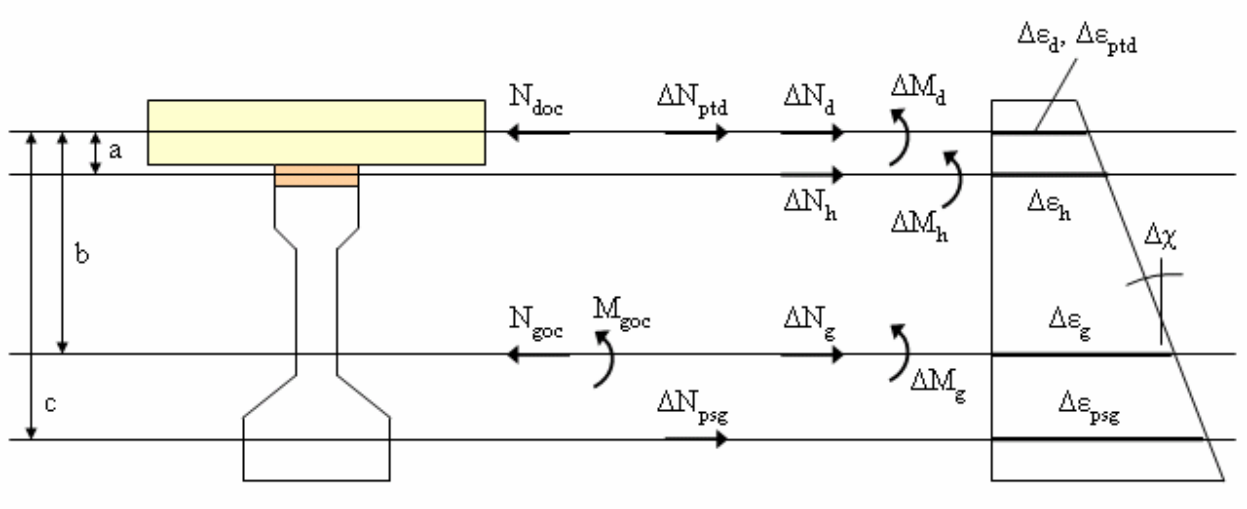

Figure 3.4: Initial Effects and Changes Occurring in the D/CG 3 Phase

3.3.3 Simple Span Models

This section summarizes the step-by-step approach taken to formulate each of the simple span bridge models in Mathcad. All variables used in the Mathcad models are presented in Appendix A. Examples of a simple span steel girder model and a simple span prestressed concrete girder model are given in Appendix B. It is important to note that any section properties or stresses calculated in the following procedures are located at midspan. In the simple span prestressed concrete girder models, midspan was the critical location for potential tensile stresses in the deck if upward camber of the girder dominated the curvature of the span.

In the simple span steel girder models, midspan was then also used as the location for calculating the stresses throughout the deck, which are constant along a span under uniform curvature.

3.3.3.1 Bridges with Steel Girders

The basic steps to formulate the simple span steel girder bridge models included:

1. Define and/or calculate all material properties, section properties, and time intervals.
2. Program Mathcad routines to calculate creep coefficients and shrinkage values based on the AASHTO 2006 Interim equations provided in Chapter 2.
3. Perform calculations for phase D/SG 1, deck post-tensioning to composite action:
    a. Compute the average stress in the post-tensioning tendons immediately after jacking, considering instantaneous losses due to anchor seating.
    b. Apply equation 2.9 to find the relaxation in the tendons over the time interval.
    c. Apply the creep and shrinkage routines programmed in step 2 to calculate the creep coefficient and shrinkage strain in the concrete deck during the time interval.
    d. Insert equations 3.1-3.4 into matrices and use matrix algebra to solve for the unknown changes in forces and strains.
4. Perform calculations for phase D/SG 2, composite action to end of bridge service life:
    a. Apply the creep and shrinkage routines programmed in step 2 to calculate the creep coefficient and shrinkage strain in the concrete deck during the time interval.
    b. Update the initial axial force N_{do} in the deck to account for the change in force in the deck from D/SG 1, and use the new quantity N_{doc} for the calculations in the interval D/SG 2.
    c. Apply equation 2.9 to find the relaxation in the post-tensioning strands over the time interval.
    d. Insert equations 3.5-3.16 into matrices and use matrix algebra to solve for the unknown changes in forces, moments, strains, and curvature.
    e. Calculate and plot the final stresses throughout the composite cross section.

3.3.3.2 Bridges with Prestressed Concrete Girders

The basic steps to formulate the simple span prestressed concrete girder bridge models were very similar to those used for the steel girder bridge models, except for the addition of the D/CG 1 time interval to account for the concrete in the girder. The approach for formulating these models is described in the following:

1. Define and/or calculate all material properties, section properties, and time intervals. Include the net section properties and the transformed section properties for the prestressed concrete girder alone.
2. Include the programmed Mathcad routines to calculate creep coefficients and shrinkage values based on the AASHTO 2006 Interim equations provided in Chapter 2.
3. Perform calculations for phase D/CG 1, transfer of girder prestress to the start of composite action between the girders and deck:
    a. Calculate the jacking force in the prestressing strand, and subtract the elastic shortening losses to obtain the initial force in the net concrete cross-section.
    b. Calculate the initial moment at midspan, considering the girder self weight and the initial prestressing force.
    c. Apply equation 2.9 to find the relaxation in the prestressing strands over the time interval.
    d. Apply the Mathcad routines to calculate the creep coefficient and shrinkage strain in the concrete girder during the time interval.
    e. Insert equations 3.17-3.22 into matrices and use matrix algebra to solve for the unknown changes in forces, moments, strains, and curvature.
4. Perform calculations for phase D/CG 2, post-tensioning of the deck to the start of composite action between the deck and prestressed concrete girders:
    a. These computations are identical to those described for phase D/SG 1.
5. Perform calculations for phase D/CG 3, start of composite action to the end of the bridge's service life:
    a. These computations are similar to those described for phase D/SG 2, except that the time-dependent equations for the concrete girder composite section (3.23-3.36) are implemented.

3.3.4 Continuous Span Models

All of the two and three span continuous bridge models begin with the simple span procedures described above. Once this process is used to find the stresses in the concrete deck in a simple span case, each Mathcad model continues with additional calculations to account for the time-dependent effects in either two or three continuous spans. Although somewhat conservative, the continuous spans were created by duplicating the previously designed simple spans and assuming continuity at the interior supports to maintain simplicity in the models. It is also important to note that the most critical location in the continuous models was assumed to be at the interior support(s), where the highest values of tension in the concrete should occur at the top of the deck due to negative bending caused by live loads and stress redistributions.

The first new step introduced in the two and three-span continuous bridge models involved using the force method to calculate the stresses induced by the time-dependent effects and continuity at the interior support(s). This procedure was very similar for the two and three-span continuous models, and is illustrated in Figures 3.5 and 3.6, respectively. The force method equations are also presented along with the figures. Refer to Appendix A for variable definitions.

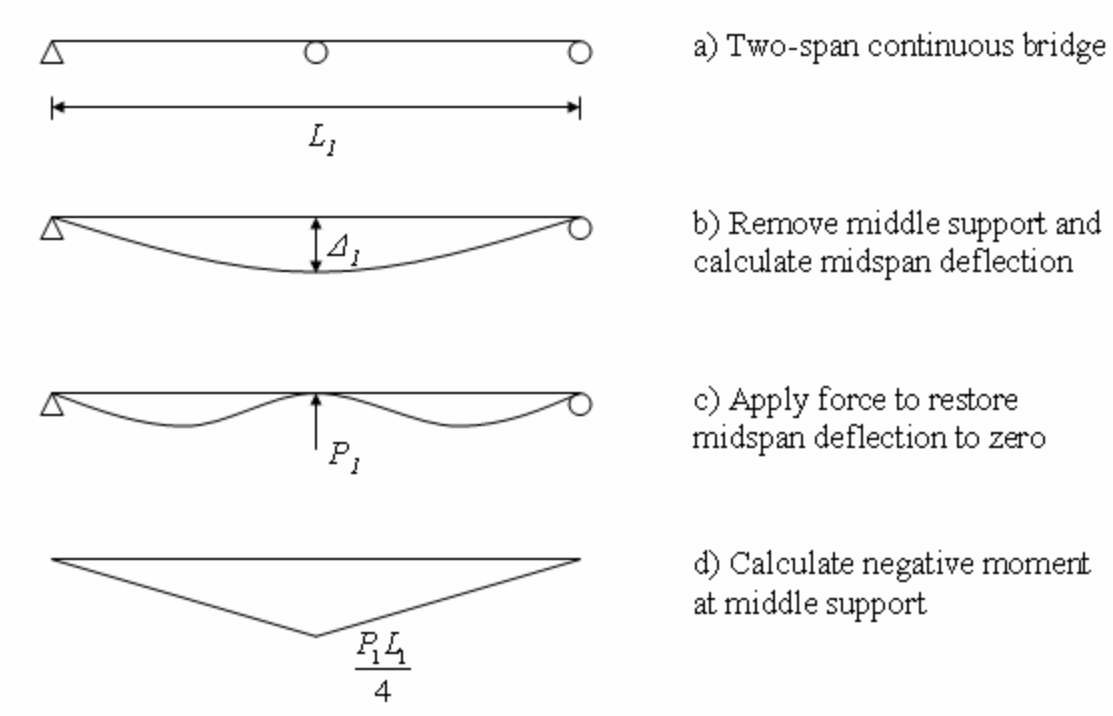

Figure 3.5: Force Method Approach for Two-Span Continuous Bridges

In Figure 3.5(b), the midspan deflection is

$$\Delta_1 = \chi \frac{L_1^2}{8} \tag{3.37}$$

where the curvature χ is calculated from the age-adjusted effective modulus method.

The deflection restored by the force P_1 is

$$\Delta_{P_1} = \frac{P_1 L_1^3}{48 E_{gaatr} I_{atr}} \tag{3.38}$$

where

E_{gaatr} = age-adjusted transformed modulus of elasticity of the girder, ksi

I_{atr} = age-adjusted transformed moment of inertia of the composite cross section, in^4

Since Δ_1 must equal Δ_{P1}, setting equations 3.37 and 3.38 equal and solving for P_1 results in

$$P_1 = \frac{6 E_{gaatr} I_{atr} \chi}{L_1} \tag{3.39}$$

After solving for P_1, the maximum negative moment at the interior support was calculated using the equation in Figure 3.5(d), and the corresponding stress in the deck concrete was determined by

$$\sigma = \frac{M_{\max}(depth_t - c_{atr})}{I_{atr}} n_{dga} \tag{3.40}$$

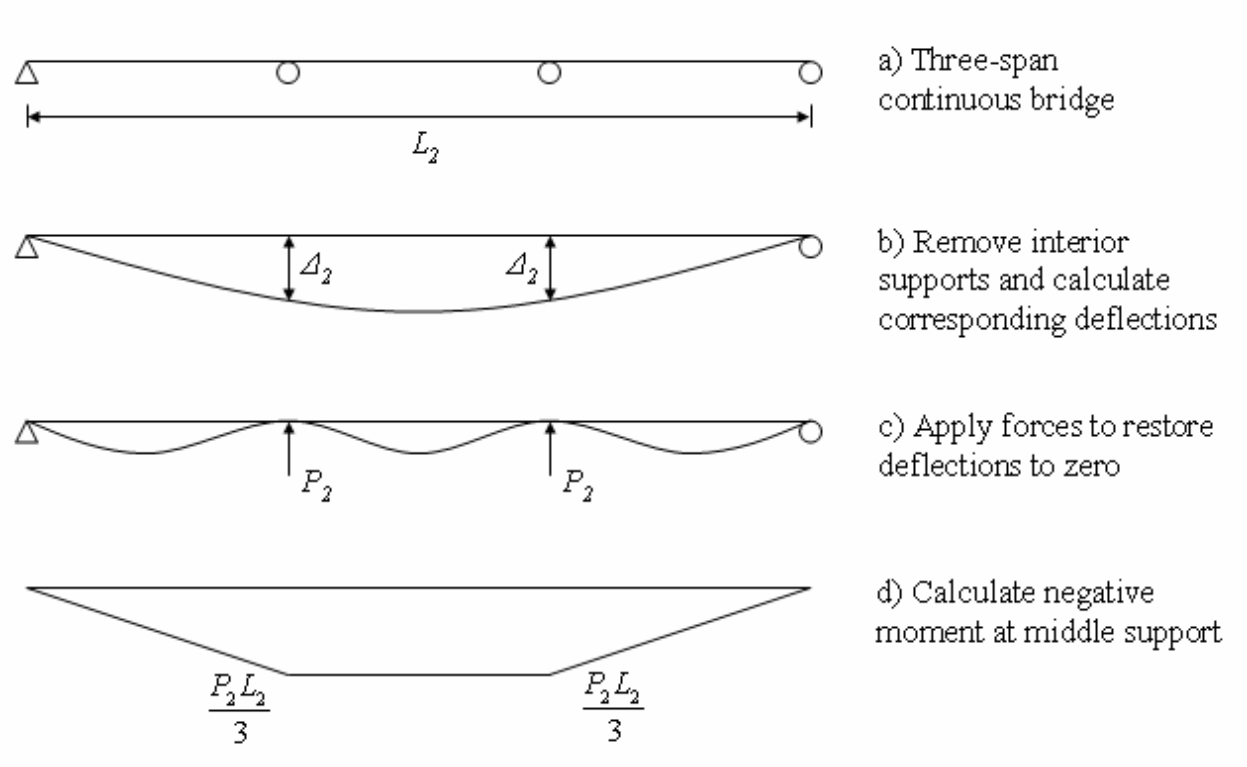

Figure 3.6: Force Method Approach for Three-Span Continuous Bridges

In Figure 3.6(b), the midspan deflection is

$$\Delta_2 = \chi \frac{L_2^{\,2}}{9} \tag{3.41}$$

The deflection restored by the force P_2 is

$$\Delta_{P_2} = \frac{P_2 L_2^{\,3}}{28 E_{gaatr} I_{atr}} \tag{3.42}$$

where

E_{gaatr} = age-adjusted transformed modulus of elasticity of the girder, ksi

I_{atr} = age-adjusted transformed moment of inertia of the composite cross section, in^4

Since Δ_2 must equal Δ_{P2}, setting equations 3.41 and 3.42 equal and solving for P_2 results in

$$P_2 = \frac{28 E_{gaatr} I_{atr} \chi}{9 L_2} \tag{3.43}$$

After solving for P_2, the maximum negative moment at the interior support was calculated using the equation in Figure 3.6(d), and the corresponding stress in the deck concrete was determined by equation 3.40.

After finding the critical deck stress due to time-dependent effects, the next new requirement for a continuous system was to account for the component of stress in the deck due to live loads. The live loads on each bridge created negative moments and subsequent tensile stresses at the interior support(s). These negative moments were found using QConBridge, a software package created by the Washington State Department of Transportation (Brice, 2005). The QConBridge software allows the user to input the bridge specifications, from which it calculates the shear and moment envelopes for the loading combination(s) selected by the user. The available live load categories were Design Tandem + Lane, Design Truck + Lane, Dual Truck Train + Lane, Dual Tandem Train + Lane, and Fatigue Truck. The Live Load Envelope option determined the worst case of each of these combinations, so that envelope was plotted for each bridge to find the maximum negative moment at the interior support(s). Since QConBridge included impact but not distribution factors in its analyses, the live load distribution factor for moment in an interior girder had to be calculated for each bridge model. The equations for computing these distribution factors are provided in Appendix C.

3.3.4.1 Bridges with Steel Girders

After the simple span analysis, the additional steps necessary to analyze two or three continuous spans with steel girders follow. Refer to Appendix C for an example continuous steel girder bridge model in Mathcad.

1. Calculate the regular and age-adjusted transformed section properties for the composite section including the haunch.
2. Calculate the stresses induced by continuity at the interior support(s) using the appropriate force method described above.
3. Use QConBridge to determine the negative moment at the interior support(s) due to live loads on the bridge, and calculate the corresponding tensile stress.
4. Multiply the stress due to live loads by the appropriate distribution factor calculated from the equations in Appendix C. The stress due to live loads was also multiplied by a factor of 0.8, which is for the Service III "load combination relating only to tension in

prestressed concrete superstructures with the objective of crack control" (AASHTO, 2004). Although the original intention of this factor was for controlling cracking in the tensile region at the bottom of prestressed concrete girders in positive bending, for this research it was similarly assumed to apply to tension at the top of the concrete in a negative moment region of a bridge deck.

5. Find the final stress in the deck by summing three quantities: the stress at the top of the deck after the simple span analysis, the stress generated at the interior support(s) due to continuity and time-dependent effects, and the factored stress due to live loads.

3.3.4.2 Bridges with Prestressed Concrete Girders

The procedure for analysis of the continuous spans with prestressed concrete girders was significantly more complicated than that for the steel girders. Unlike the uniform change in curvature assumed to exist along the full length of a composite span with steel beams, a span with composite concrete girders does not exhibit a constant change in curvature along its length because of the varying centroid of prestress in the girders and the time-dependent effects involved in the system. In this case, the time-dependent behavior is complicated by the typically unequal ages of the girder and deck concretes as well as the effects of continuity. Therefore, a sectional analysis was performed for these models, and the change in curvature during the composite time interval (D/CG 3) was calculated at several locations along each span. These locations included the ends (Section A), the ¼ and ¾ points (Section B) and midspan (Section C) in each span. The change in curvature at each location during the interval D/CG 3 was then used to calculate the component of stress at the continuous supports due to continuity using the force method described above.

With reference to the simple span analysis described above, the additional steps necessary to evaluate two or three continuous spans with prestressed concrete girders include the following. Refer to Appendix C for additional details regarding the calculations indicated, as well as two examples of continuous prestressed concrete girder bridge models in Mathcad.

1. Design the harped strand layout for each girder using allowable stress limits. This task was not necessary in the concrete girder simple span models because midspan was the only location considered. For the continuous span models, however, section properties at the supports had to be calculated and used to find the corresponding stresses.

2. At each section considered along the beam, calculate the centroid and eccentricity of the prestressing strands in the girder alone, along with the net section and transformed section properties for the prestressed concrete girder.
3. Perform calculations for the D/CG 1 time interval as in the simple span models, except repeat these calculations at each section (A, B, and C) to be analyzed along the span.
4. Perform calculations for the D/CG 2 phase as in the simple span models.
5. Perform calculations for the D/CG 3 time interval as in the simple span models, again repeating these calculations at each location to be analyzed along the span.
6. Plot the change in curvature from phase D/CG 3 at each location along the span.
7. Using the change in curvature vs. length graph, apply the moment-area method to compute the resulting deflection at the interior support(s), assuming removal of the support(s).
8. Calculate the regular and age-adjusted transformed section properties for the composite section including the haunch at the cross-section located at the end of each span.
9. Use the force method described above to restore the previously computed deflection and find the corresponding stress at the top of the deck at the same support location. Use the age-adjusted transformed section properties in this step since the stress is produced by a slowly developing force.
10. Determine the negative moment and the corresponding tensile stress at the interior support(s) due to live loads on the bridge. QConBridge was implemented again for assistance with this task.
11. As in the continuous steel girder bridges, multiply the live load stress by the appropriate distribution factor and the 0.8 Service III load factor.
12. Compute the final stress in the bridge deck.

3.4 Parametric Studies

After developing each type of bridge model in Mathcad, these models were employed to investigate the response of different bridge layouts to various amounts of post-tensioning in their precast concrete decks. The primary goal was to look for trends in the behavior of similar bridges so that simple design recommendations regarding levels of post-tensioning for bridge decks could be made. Several design aids were accessed to establish the characteristics of the

bridges used in these parametric studies. Once the bridge layouts were determined, executing the parametric studies was fairly straightforward.

3.4.1 Selection of Steel Girders

Span lengths of 60 ft, 90 ft, and 120 ft with girder spacings of 6 ft and 9 ft were selected for evaluation in the steel girder bridge parametric studies. To easily determine appropriate girder sizes corresponding to these dimensions, suggestions from the Structural Steel Designer's Handbook (Brockenbrough, 2006) were incorporated. The girder depth to be used in each span length was determined by the Handbook's recommendation that the depth of the steel girder alone should be at least 1/30 of the span for composite highway girders (2006). This guideline determined the use of W24 and W36 rolled sections for the 60 and 90 ft spans, respectively, as well as the use of 48 in. deep plate girders for the 120 ft spans, since W48 rolled sections are not available. An Excel worksheet created by the author for the design of simple span steel girder bridges was then used to perform the additional checks necessary to determine the specific dimensions of each girder. The following checks typical of any steel girder bridge design were completed:

- Strength limit states, including nominal flexural resistance, compact section, ductility, flange and web proportions, shear of unstiffened webs, web local yielding, and web crippling
- Fatigue and fracture
- Service limit states
- Constructability, including yielding, lateral-torsional buckling, flange local buckling, and web bend-buckling

Tables 3.2 and 3.3 provide the details of the different steel girders used in the simple and continuous span parametric studies.

Table 3.2: Steel Girders used in Parametric Studies

Girder Spacing (ft)	Span Length (ft)	Steel Girder Depth (in)	W or Plate Girder Section
6	60	24	W24x103
6	90	36	W36x160
6	120	48	PL 1, d=48
9	60	24	W24x146
9	90	36	W36x232
9	120	48	PL 2, d=50

Table 3.3: Plate Girder Dimensions

Plate Girder	Total Depth (in)	t_f (in)	b_f (in)	t_w (in)	d_w (in)
PL 1	48	1.125	14	0.75	45.75
PL 2	50	1.375	16	0.875	47.25

3.4.2 Selection of Prestressed Concrete Girders

Due to the larger availability of PCBT and AASHTO girder design aids and the additional complexity inherent in the time-dependent analysis of bridges with prestressed concrete girders, a greater number of cross sections with concrete girders were analyzed in the parametric studies. Three different sizes of each type of concrete girder were selected, and a 'short' and a 'long' span length for both 6 and 9 ft girder spacings were designed for each type of girder. An attempt was made to maintain consistent span length to girder depth ratios for each set of similar span lengths and girder spacings for each girder type.

The bridges with PCBT, or Prestressed Concrete Bulb-T, girders were designed using the Virginia standard bulb-T details and preliminary design tables. The PCBT-37, PCBT-61, and PCBT-85 girders (with respective depths of 37, 61, and 85 in.) were chosen, and the required number of prestressing strands for each combination of span length and girder spacing was determined using the preliminary design tables. The bridges with AASHTO girders were designed using the AASHTO I-Beam details and design charts provided in the PCI Bridge Design Manual (2005). The AASHTO Type II, Type IV, and Type VI girders with respective depths of 36, 54, and 72 in. were selected, and the required number of prestressing strands for each combination of span length and girder spacing was determined using the preliminary design

charts. Table 3.4 shows the details of the different prestressed concrete girders used in the simple and continuous span parametric studies.

Table 3.4: Prestressed Concrete Girders used in Parametric Studies

Girder Type	Girder Spacing (ft)	Span Length (ft)	L/d	No. of ½ in. Dia. Strands
PCBT-37	6	40 75	13.0 24.3	14 28
	9	40 -	13.0 -	14 -
PCBT-61	6	65 125	12.8 24.6	16 50
	9	50 85	9.8 16.7	18 28
PCBT-85	6	85 150	12.0 21.2	20 50
	9	70 125	9.9 17.6	22 44
AASHTO Type II (d = 36 in.)	6	45 70	15.0 23.3	8 28
	9	35 55	11.7 18.3	8 24
AASHTO Type IV (d = 54 in.)	6	75 120	16.7 26.7	16 54
	9	65 100	14.4 22.2	18 50
AASHTO Type VI (d = 72 in.)	6	100 160	16.7 26.7	22 76
	9	100 140	16.7 23.3	30 76

3.4.3 Method for Conducting Parametric Studies

After all of the models were created and the steel and prestressed concrete girder bridges were designed, the amount of initial compression in the deck of each bridge model was varied by changing the number of post-tensioning strands. This process was started at an initial compression stress of about 100 or 200 psi in the deck, and as the stress was increased by increments of either 100 or 200 psi, the resulting stress in the deck panel joints at the end of each time-dependent analysis was recorded. The number of post-tensioning strands in the deck was

increased until the results showed that the deck panel joints remained in compression at the end of the bridge service life.

CHAPTER 4: RESULTS AND ANALYSIS

4.1 Overview

Parametric studies were performed to investigate the amount of post-tensioning required in precast concrete bridge decks to keep the panel joints in compression throughout the service life of a bridge. These studies included bridges with many different configurations. Once the results were obtained, they were examined for relationships between the required level of compression in the deck and the three main variables of girder type, girder spacing, and individual span length. The results of the parametric studies and the trends recognized in these findings are discussed in this chapter. Before any of these parametric studies were performed, however, the results of selected Mathcad models were verified with finite element model results.

4.2 Comparison with Finite Element Modeling Results

In order to verify the modeling procedures used in this research, results from selected Mathcad models were compared with results from finite element models created using the software DIANA. While the Mathcad models divided the analysis of each bridge into only the two or three major time intervals throughout its construction and life, the finite element models incorporated a much more rigorous time-step approach for considering the time-dependent effects in concrete and the corresponding redistributions of forces and moments in the bridge cross sections. To properly compare results from the two types of models, the AASHTO LRFD creep and shrinkage equations incorporated in the Mathcad models and parametric studies were changed to the CEB-FIP Model Code 1990 equations which were used to account for creep and shrinkage in the DIANA software. The CEB-FIP Model Code 1990 equations were presented in Chapter 2.

The first comparison between the two types of models was performed for the 125 ft long simple span bridge with PCBT-61 girders spaced at 6 ft. The precast deck panels were initially post-tensioned to 309 psi, and the self weight of the panels was neglected in the calculations for the composite phase in each model. The differences in results between the two models are given in Table 4.1.

Table 4.1: Comparison between Mathcad and DIANA Finite Element Models

Time Interval	Quantity	Mathcad Results		DIANA Results		% Difference
Phase 1: Day 1 - Day 55	ΔN_g =	159.18	k	152.62	k	4.30%
	ΔN_{ps} =	-159.18	k	-152.62	k	4.30%
	$\Delta\kappa$ =	7.2	με/in	6.59	με/in	9.26%
	$\Delta\varepsilon_g$ =	-0.000552		-0.000549		0.55%
	$\Delta\varepsilon_{ps}$ =	-0.00073		-0.0007		4.29%
Phase 2: Day 55 - Day 60	ΔN_d =	1.36	k	1.31	k	3.82%
	ΔN_{pt} =	-1.36	k	-1.31	k	3.82%
	$\Delta\varepsilon_d$ =	-0.0000521		-0.00005		4.20%
	$\Delta\varepsilon_{pt}$ =	-0.0000521		-0.00005		4.20%
Phase 3: Day 60 - Day 10000	ΔN_d =	2.52	k	2.75	k	8.36%
	ΔN_{pt} =	-12.96	k	-11.54	k	12.31%
	ΔN_h =	-21.32	k	-22.6	k	5.66%
	ΔN_{ps} =	-168.86	k	-165.7	k	1.91%
	$\Delta\varepsilon_d$ =	-0.00049549		-0.000441		12.36%
	$\Delta\varepsilon_{pt}$ =	-0.00049549		-0.000441		12.36%
	$\Delta\varepsilon_h$ =	-0.00051721		-0.000471		9.81%
	$\Delta\varepsilon_g$ =	-0.00066635		-0.00065		2.52%
	$\Delta\varepsilon_{ps}$ =	-0.0007745		-0.00076		1.91%
	$\Delta\kappa$ =	4.57	με/in	5.295	με/in	13.69%
Total Stresses at Day 10000	σ_{d_top} =	-0.266	ksi	-0.254	ksi	4.72%
	σ_{d_bot} =	-0.340	ksi	-0.351	ksi	3.13%
	σ_{h_top} =	-0.451	ksi	-0.479	ksi	5.85%
	σ_{h_bot} =	-0.457	ksi	-0.482	ksi	5.19%
	σ_{g_top} =	-0.696	ksi	-0.752	ksi	7.45%
	σ_{g_bot} =	-1.81	ksi	-1.77	ksi	2.26%

The differences in results between the two models shown in Table 4.1 are all less than 15%, so the results produced from the parametric studies conducted using the Mathcad models were considered valid.

The second comparison between the Mathcad and finite element models was drawn using the bridge model with two continuous 60 ft spans of W24x103 rolled steel girders spaced at 6 ft. Table 4.2 shows the results obtained from performing both Mathcad and DIANA analyses to determine the final stress at the top of the deck over the interior support in this two span continuous steel girder bridge model. The stresses reported in Table 4.2 are only due to the

initial post-tensioning, member self weight, creep, and shrinkage; relaxation losses and live loads were neglected in both models to obtain these results. Figure 4.1 graphically illustrates the results given in Table 4.2.

Table 4.2: Final Stresses at Top of Deck over Int. Supp. for Two Span Cont. W24x103 Girders

No. of Strands in Deck	Initial Comp. in Deck (psi)	Mathcad Result (psi)	DIANA Result (psi)
6	-300	302	328
12	-600	153	33.9
16	-799	54	-196

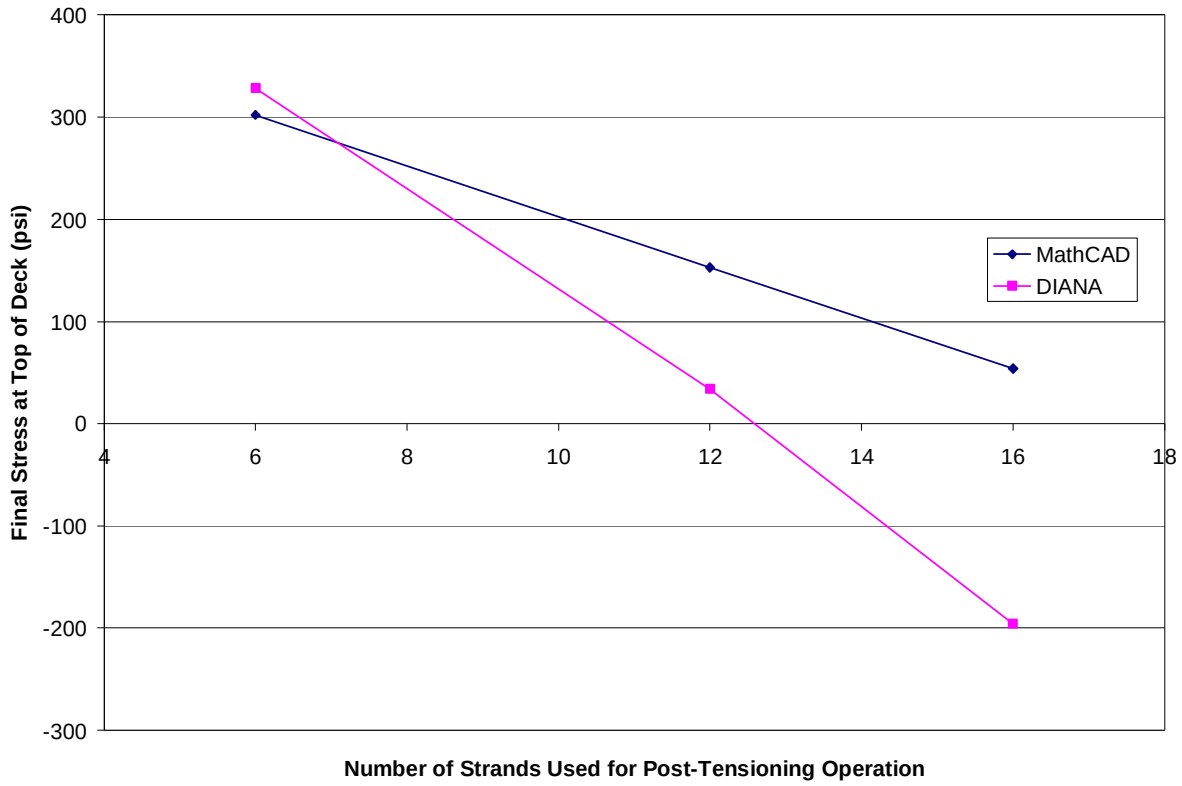

Figure 4.1: Comparison of Final Stresses at Top of Deck over Interior Support

Figure 4.1 confirms that the results obtained from Mathcad and DIANA exhibit similar trends. The Mathcad results become more conservative with increasing amounts of initial compression by predicting larger overall losses of compression in the precast concrete bridge deck.

4.3 Simple Span Models

4.3.1 Bridges with Steel Girders

The first set of parametric studies was performed for simple span bridges with steel girders and a precast concrete deck. The precast concrete decks in each of the six different steel girder bridges were post-tensioned to stresses ranging from 100 to 400 psi in increments of approximately 100 psi. The results are given in Table 4.3. Because the initial compression in the deck was altered by changing the number of post-tensioning strands, the initial compressive stresses vary slightly from 100 to 103 psi in the first set of parametric studies, 200 to 206 psi in the second set, and so on. This explanation applies to the slight variation in initial deck compressive stress for each set of parametric studies in all of the tables that follow. In addition, Figure 4.2 illustrates typical distributions of stress and strain obtained throughout the steel girder bridge cross sections at the end of service. The values shown in Figure 4.2 correspond with the results for the simple span W24x103 model initially post-tensioned to -200 psi in Table 4.3, which is also provided as an example Mathcad model in Appendix B.

Table 4.3: Parametric Studies for Simple Span Steel Girder Models

Girder Type	Girder Spacing (ft)	Span Length (ft)	No. of Strands in Deck	Initial Comp. in Deck (psi)	Final Stress in Deck		
					Top (psi)	Middle (psi)	Bottom (psi)
W24x103	6	60	2	-100	-112	-47	19
W36x160	6	90	2	-102	-63	-19	26
PL 1, d=48	6	120	2	-103	-23	9	41
W24x146	9	60	3	-100	-109	-45	19
W36x232	9	90	3	-102	-62	-19	24
PL 2, d=50	9	120	3	-103	-29	2	34
W24x103	6	60	4	-200	-209	-136	-62
W36x160	6	90	4	-204	-156	-106	-56
PL 1, d=48	6	120	4	-206	-111	-75	-39
W24x146	9	60	6	-200	-205	-133	-62
W36x232	9	90	6	-204	-154	-105	-57
PL 2, d=50	9	120	6	-206	-117	-82	-47
W24x103	6	60	6	-300	-303	-222	-142
W36x160	6	90	6	-306	-246	-191	-136
PL 1, d=48	6	120	6	-309	-197	-158	-118
W24x146	9	60	9	-300	-294	-216	-137
W36x232	9	90	9	-306	-240	-187	-134
PL 2, d=50	9	120	9	-309	-200	-162	-124
W24x103	6	60	8	-400	-393	-305	-218
W36x160	6	90	8	-408	-332	-273	-213
PL 1, d=48	6	120	8	-412	-280	-237	-194
W24x146	9	60	12	-400	-373	-289	-206
W36x232	9	90	12	-408	-316	-260	-203
PL 2, d=50	9	120	12	-412	-274	-234	-193

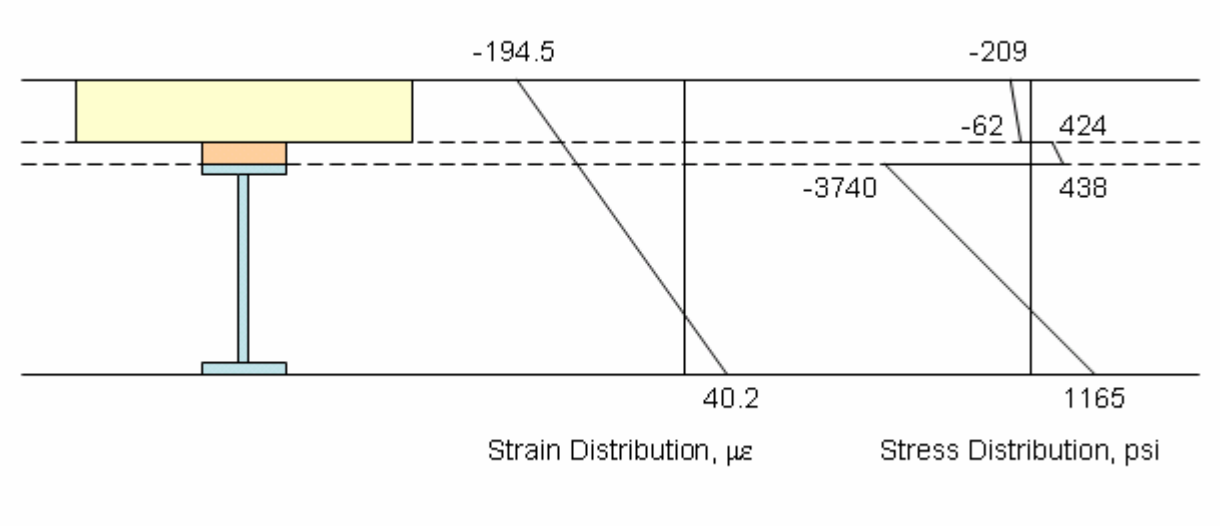

Figure 4.2: Typical Distributions of Stress and Strain for Steel Girder Bridge Models at End of Service Life

For each bridge model and different amount of initial post-tensioning in the deck, Table 4.3 shows the final stresses at the top, middle, and bottom of the concrete deck at midspan after accounting for the time-dependent effects in the concrete. Although these calculations were performed at midspan, the changes in stress throughout the depth of the concrete deck are constant along the length of the simple span which experiences uniform changes in curvature. For the simple span steel girder bridges, it was expected that the worst location for potential tensile stresses in the concrete would be along the bottom of the deck throughout the span, since this is where the steel girder provides the greatest restraint of creep and shrinkage in the concrete deck. These predictions were verified by the results, which showed that in each of the 24 parametric studies, the compressive stresses were highest at the top of the bridge deck, and the stresses became less compressive or even somewhat tensile from the top of the deck to the bottom of the deck.

In order to maintain compression throughout the depth of the concrete deck at midspan, at least 200 psi of initial post-tensioning in the precast panels was required. The initial compressive stress of 200 psi resulted in a minimum of 39-62 psi residual compression in the precast panel joints in each of the six models. Larger amounts of initial post-tensioning were needed to obtain greater amounts of residual compression in the concrete deck. Figure 4.3 illustrates the relationship between the most tensile final stress (located at the bottom of the

concrete deck in each case) and the span length at each of the four levels of initial post-tensioning.

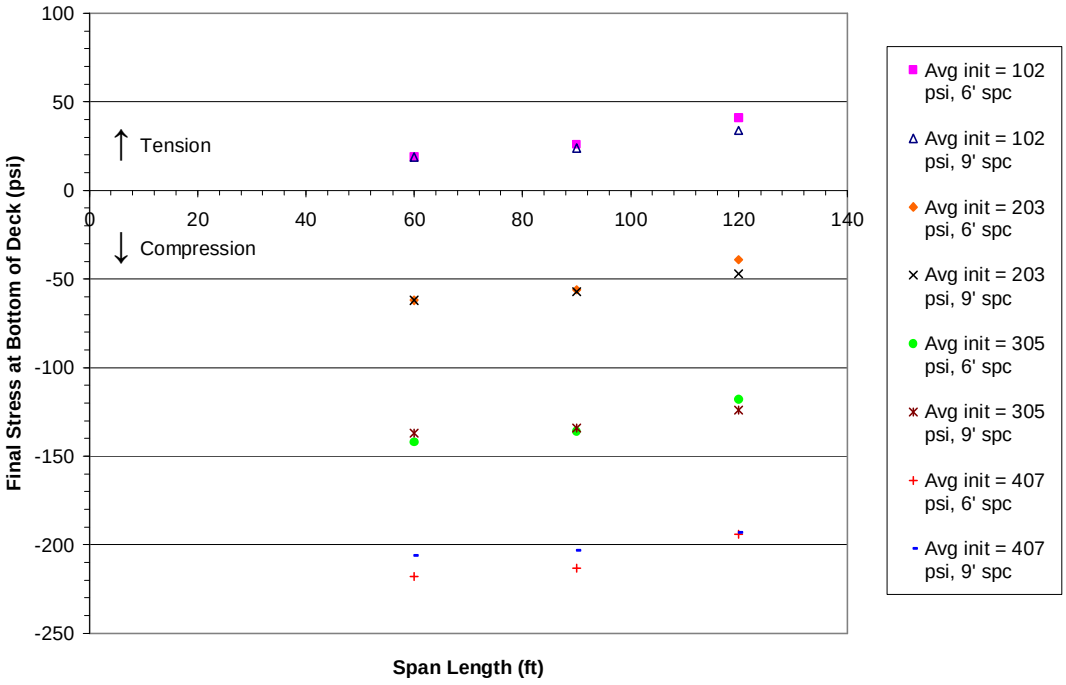

Figure 4.3: Final Deck Stress vs. Span Length for Simple Span Steel Girder Models

Figure 4.3 indicates a linear relationship between the span length and the critical deck stress at the end of service for the simple span steel girder bridges. The final stresses were not significantly affected by the girder spacing (6 ft or 9 ft). The figure also shows that at each different level of initial post-tensioning, the net loss of compression in the deck increases with span length. These losses are better identified in Figure 4.4.

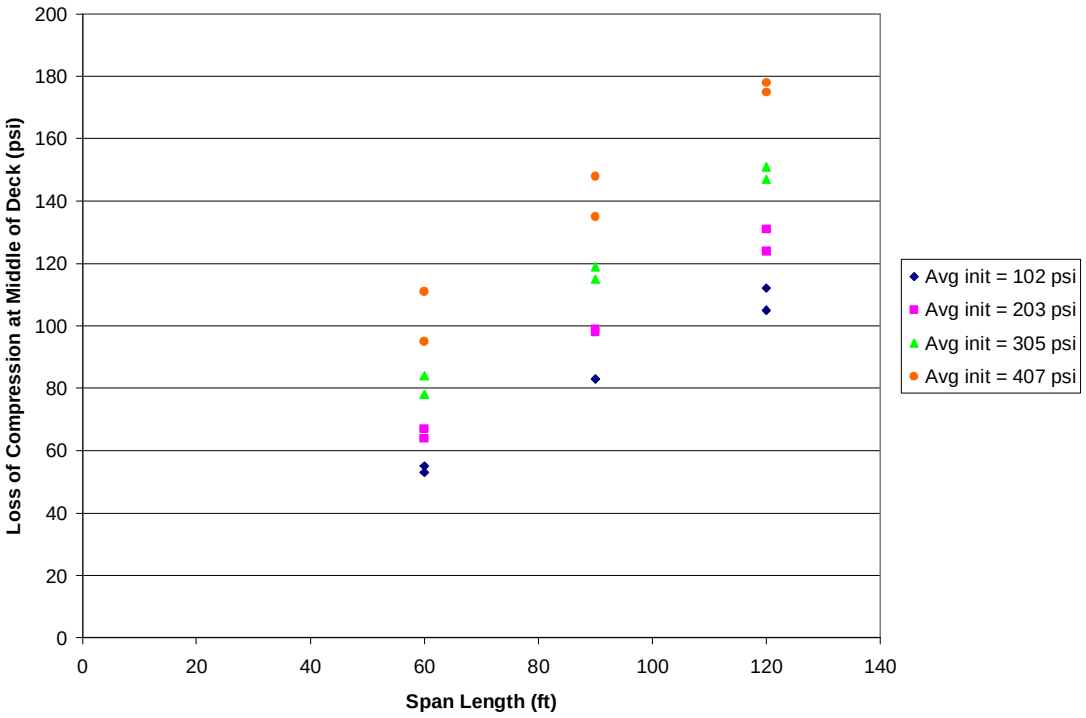

Figure 4.4: Net Loss of Compression at Middle of Deck for Simple Span Steel Girder Models

The behavior indicated in Figures 4.3 and 4.4 for the simple span steel girder bridges is logical. While the steel girder sizes increase proportionally with span length, the size of the effective deck cross sections at 6 ft. and 9 ft. girder spacings stay the same. Therefore, as the deck becomes less stiff relative to the girder with increasing girder sizes, the steel girder restrains the creep and shrinkage of the deck concrete more, causing it to experience greater losses of compression. The deck to girder stiffness ratios are shown in Table 4.4.

Table 4.4: Comparison of Deck and Girder Stiffnesses for Each Steel Girder Model

Girder	Spacing (ft)	Span (ft)	Ag (in^2)	Ad (in^2)	Eg*Ag	Ed*Ad	Larger EA	(Ed*Ad)/(Eg*Ag)
W24x103	6	60	30.30	612	878700	2466671	deck	2.81
W36x160	6	90	47.00	612	1363000	2466671	deck	1.81
PL 1, d=48	6	120	65.81	612	1908490	2466671	deck	1.29
W24x146	9	60	43.00	918	1247000	3700007	deck	2.97
W36x232	9	90	68.10	918	1974900	3700007	deck	1.87
PL 2, d=50	9	120	85.34	918	2474860	3700007	deck	1.50

4.3.2 Bridges with Prestressed Concrete Girders

The second set of parametric studies was performed for simple span bridges with prestressed concrete girders and a precast concrete deck. The precast decks in each of the 23 different prestressed concrete girder bridges were post-tensioned to stresses ranging from 100-330 psi in increments of approximately 100 psi. The results for PCBT and AASHTO girders are given in Tables 4.5 and 4.6, respectively. For each bridge model and different amount of initial post-tensioning in the deck, these tables show the final stresses at the top, middle, and bottom of the concrete deck at midspan after accounting for the time-dependent effects in the concrete.

Table 4.5: Parametric Studies for Simple Span PCBT Girder Models

Girder Type	Girder Spacing (ft)	Span Length (ft)	No. of Strands in Deck	Initial Comp. in Deck (psi)	Final Stress in Deck		
					Top (psi)	Middle (psi)	Bottom (psi)
PCBT-37	6	40	2	-102	-7	-27	-47
PCBT-37	6	40	4	-205	-92	-108	-123
PCBT-37	6	40	6	-307	-177	-188	-199
PCBT-37	6	75	2	-108	-118	-137	-157
PCBT-37	6	75	4	-215	-207	-222	-237
PCBT-37	6	75	6	-323	-295	-305	-316
PCBT-37	9	40	3	-102	-40	-55	-70
PCBT-37	9	40	6	-205	-130	-140	-150
PCBT-37	9	40	9	-307	-220	-224	-229
PCBT-61	6	65	2	-107	-52	-58	-65
PCBT-61	6	65	4	-213	-135	-139	-143
PCBT-61	6	65	6	-320	-217	-218	-220
PCBT-61	6	125	2	-110	-234	-246	-257
PCBT-61	6	125	4	-219	-319	-327	-336
PCBT-61	6	125	6	-329	-403	-409	-415
PCBT-61	9	50	3	-105	-29	-42	-55
PCBT-61	9	50	6	-209	-116	-126	-135
PCBT-61	9	50	9	-314	-202	-209	-216
PCBT-61	9	85	3	-108	-114	-123	-132
PCBT-61	9	85	6	-216	-203	-209	-215
PCBT-61	9	85	9	-325	-292	-294	-297
PCBT-85	6	85	2	-108	-66	-71	-75
PCBT-85	6	85	4	-216	-147	-149	-152
PCBT-85	6	85	6	-325	-227	-228	-228
PCBT-85	6	150	2	-110	-260	-262	-265
PCBT-85	6	150	4	-220	-341	-342	-342
PCBT-85	6	150	6	-330	-422	-421	-420
PCBT-85	9	70	3	-107	-46	-54	-62
PCBT-85	9	70	6	-214	-131	-137	-143
PCBT-85	9	70	9	-322	-216	-220	-224
PCBT-85	9	125	3	-110	-177	-183	-189
PCBT-85	9	125	6	-219	-264	-268	-272
PCBT-85	9	125	9	-329	-350	-352	-354

Table 4.6: Parametric Studies for Simple Span AASHTO Girder Models

Girder Type	Girder Spacing (ft)	Span Length (ft)	No. of Strands in Deck	Initial Comp. in Deck (psi)	Final Stress in Deck		
					Top (psi)	Middle (psi)	Bottom (psi)
Type II	6	45	2	-104	-110	-114	-118
Type II	6	45	4	-207	-206	-205	-203
Type II	6	45	6	-311	-302	-295	-288
Type II	6	70	2	-107	-129	-177	-226
Type II	6	70	4	-214	-229	-271	-314
Type II	6	70	6	-322	-327	-364	-401
Type II	9	35	3	-101	-88	-97	-106
Type II	9	35	6	-202	-184	-187	-191
Type II	9	35	9	-302	-280	-277	-275
Type II	9	55	3	-106	-85	-133	-180
Type II	9	55	6	-211	-186	-227	-269
Type II	9	55	9	-317	-285	-321	-357
Type IV	6	75	2	-108	-122	-115	-107
Type IV	6	75	4	-215	-210	-200	-189
Type IV	6	75	6	-323	-298	-284	-270
Type IV	6	120	2	-109	-246	-253	-260
Type IV	6	120	4	-219	-335	-339	-342
Type IV	6	120	6	-328	-424	-424	-425
Type IV	9	65	3	-107	-100	-98	-95
Type IV	9	65	6	-213	-192	-186	-180
Type IV	9	65	9	-320	-284	-275	-265
Type IV	9	100	3	-109	-165	-178	-191
Type IV	9	100	6	-218	-259	-268	-278
Type IV	9	100	9	-327	-352	-358	-364
Type VI	6	100	2	-109	-124	-119	-113
Type VI	6	100	4	-218	-205	-197	-189
Type VI	6	100	6	-327	-285	-275	-265
Type VI	6	160	2	-110	-321	-322	-324
Type VI	6	160	4	-220	-401	-401	-401
Type VI	6	160	6	-330	-482	-479	-477
Type VI	9	100	3	-109	-128	-126	-125
Type VI	9	100	6	-218	-214	-210	-206
Type VI	9	100	9	-327	-300	-293	-287
Type VI	9	140	3	-110	-231	-240	-249
Type VI	9	140	6	-220	-317	-324	-331
Type VI	9	140	9	-329	-404	-408	-412

Due to the greater complexity of a prestressed concrete girder composite cross section, predicting the time-dependent behavior of these simple span bridges was much less straightforward than for the steel girder bridges. In the prestressed concrete girder models, the negative moment due to the upward camber of the girder counteracted the positive moments caused by the girder and deck self weights. The behavior of each system was further complicated by the time-dependent losses occurring at different rates in the girder and deck concretes of different ages. Therefore, the results of the prestressed concrete girder bridge parametric studies were much more dependent on the specific dimensions and characteristics of each model than in the steel girder bridges.

4.3.2.1 PCBT Girder Bridge Analyses

In all of the 33 simple span PCBT girder parametric studies, the entire depth of the bridge deck remained in compression at the end of the bridge service life. In each of these models except one, the compressive stresses in the bridge deck at the end of service were highest at the bottom of the deck, and became less compressive from the bottom to the top of the deck. In order to maintain compression throughout the depth of the concrete deck at midspan, at least 100 psi of initial post-tensioning in the precast panels was required. The initial compressive stress of 100 psi resulted in minimum residual compressive stresses ranging from 7 psi to 260 psi in the precast panel joints in the PCBT girder models. Figure 4.5 illustrates the relationship between the final stress at the middle of the concrete deck and the span length at the three different levels of initial post-tensioning in the simple span PCBT girder models.

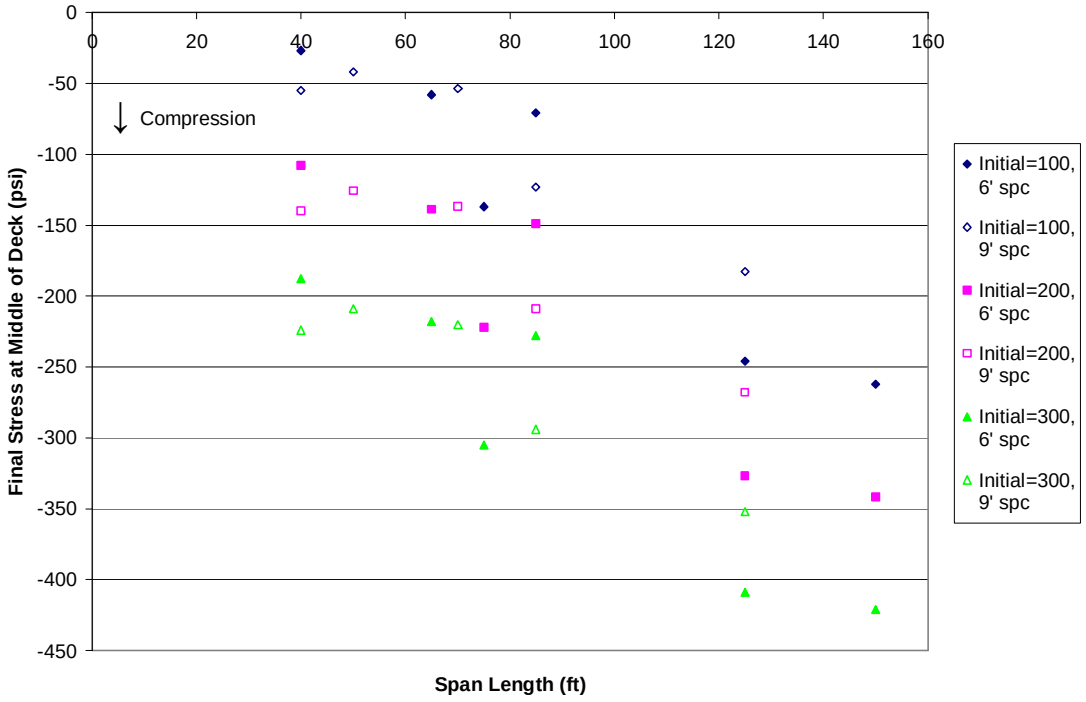

Figure 4.5: Final Deck Stress vs. Span Length for Simple Span PCBT Girder Models

Figure 4.5 shows a general trend of increasing residual compression in the concrete deck with increasing span length at each level of initial post-tensioning for both the 6 and 9 ft girder spacings. This behavior is the opposite of the trend observed in the simple span steel girder models, which involved decreasing residual compression in the concrete deck with increasing span length at each level of initial post-tensioning. While most of the concrete bridge decks in the simple span PCBT girder models experienced a net loss of compression from the time of post-tensioning to the end of service but still remained in compression, a few of the models with longer span lengths underwent an overall gain in compression during this time. Whereas the steel girders do not creep and shrink, the initial compression present in the concrete girders probably plays a role in helping the concrete girder bridge decks to lose a smaller amount of compression, or even gain some compression, by the end of service life. Figure 4.6 shows the net change in compressive stress at the middle of the deck for the simple span PCBT girder models.

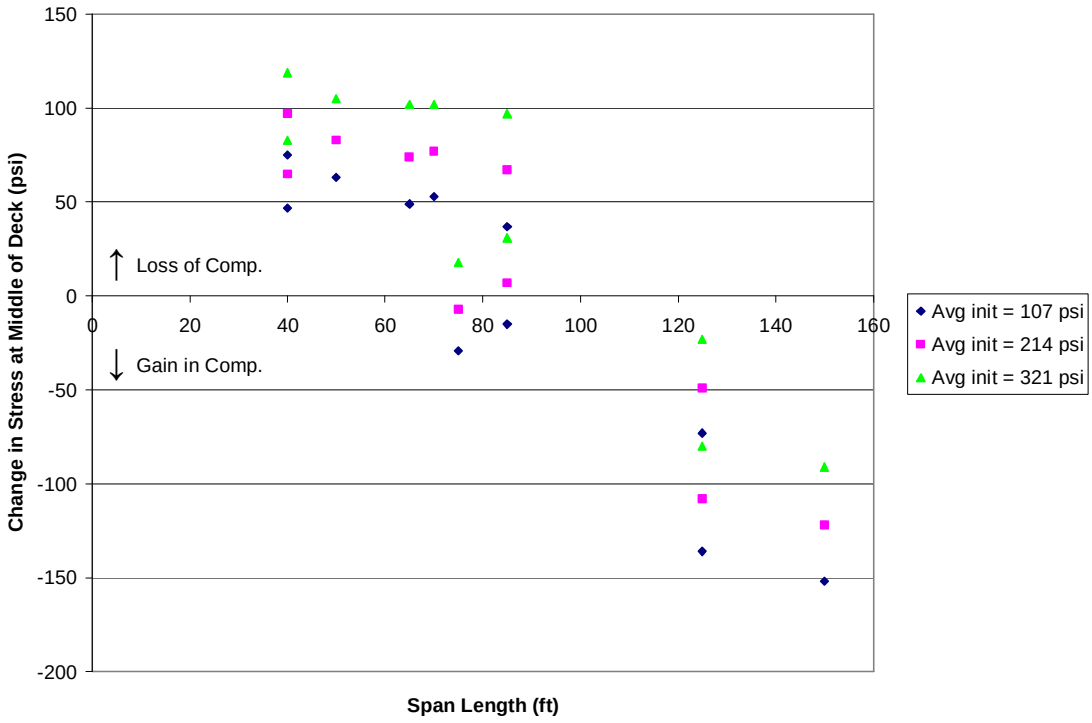

Figure 4.6: Net Change in Compression at Middle of Deck for PCBT Girder Models

4.3.2.2 AASHTO Girder Bridge Analyses

In the 36 simple span AASHTO girder parametric studies, the bridge decks again all remained in compression throughout their depths at the end of service life of each bridge model. In 20 of the parametric studies, the minimum residual compressive stress was located at the top of the concrete deck at midspan, while in the other 16 models the minimum residual compressive stress occurred at the bottom of the deck at midspan.

In order to maintain compression throughout the depth of the concrete deck at midspan, at least 100 psi of initial post-tensioning in the precast panels was required. The initial compressive stress of 100 psi resulted in minimum residual compressive stresses ranging from 85 psi to 321 psi in the precast deck panels in the PCBT girder models. Figure 4.7 illustrates the relationship between the final stress at the middle of the concrete deck and the span length at the three different levels of initial post-tensioning in the simple span AASHTO girder models.

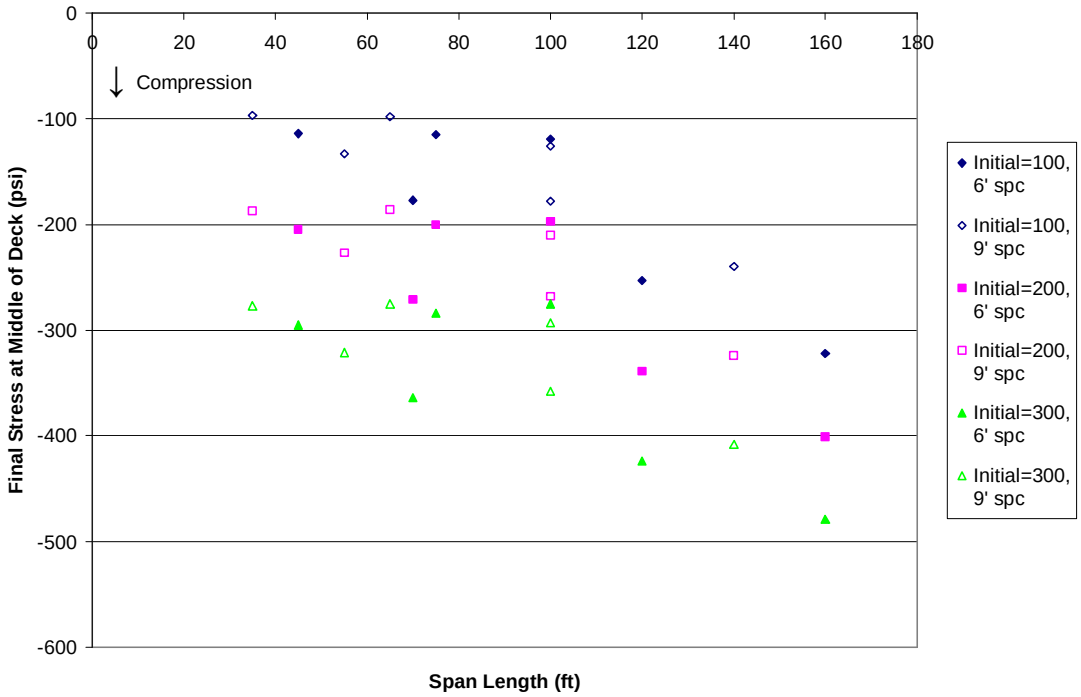

Figure 4.7: Final Deck Stress vs. Span Length for Simple Span AASHTO Girder Models

As observed for the PCBT girder models, Figure 4.7 illustrates a general trend of increasing residual compression in the concrete deck with increasing span length at each level of initial post-tensioning in the AASHTO girder models for both the 6 and 9 ft girder spacing. This time, only a few of the concrete bridge decks experienced a net loss of compression from the time of post-tensioning to the end of service but still remained in compression, while a majority of the models underwent an overall gain in compression during this time. Possible reasons for this behavior were addressed in the previous section. Figure 4.8 shows the net change in compressive stress at the middle of the deck for the simple span AASHTO girder models.

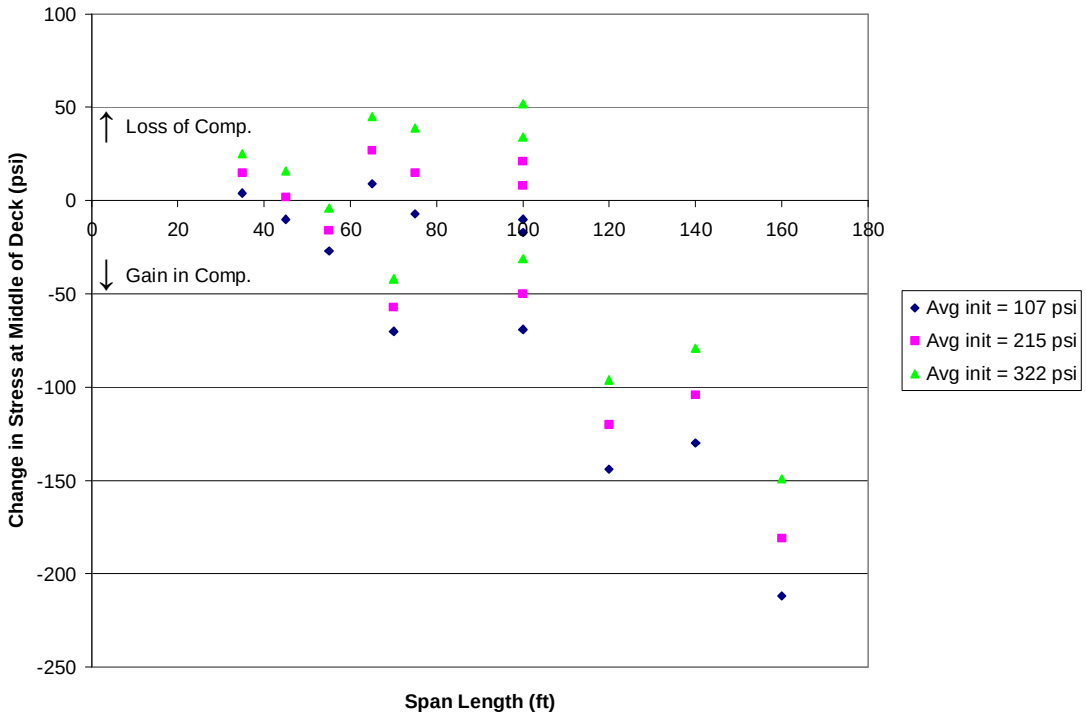

Figure 4.8: Net Change in Compression at Middle of Deck for AASHTO Girder Models

4.4 Continuous Span Models

4.4.1 Bridges with Steel Girders

The two and three span continuous models with steel girders exemplified behavior similar to the simple span steel girder models, but included much additional tension in the concrete deck due to negative moments caused by live loads and the restraint of downward deflection at the piers. Tables D.1 and D.2 in Appendix D show the results of the parametric studies for the two and three span continuous steel girder bridge models, respectively. The tables give the final stresses at the top of the concrete deck both with and without the tension due to live loads for each level of initial post-tensioning applied. All stresses given for the two and three span continuous bridges are located at the interior support(s), which was assumed to be the critical location because of the maximum negative moments created there by live loads and restraint moments. The results provided in these tables are illustrated graphically in Figures 4.9, 4.10, 4.11, and 4.12.

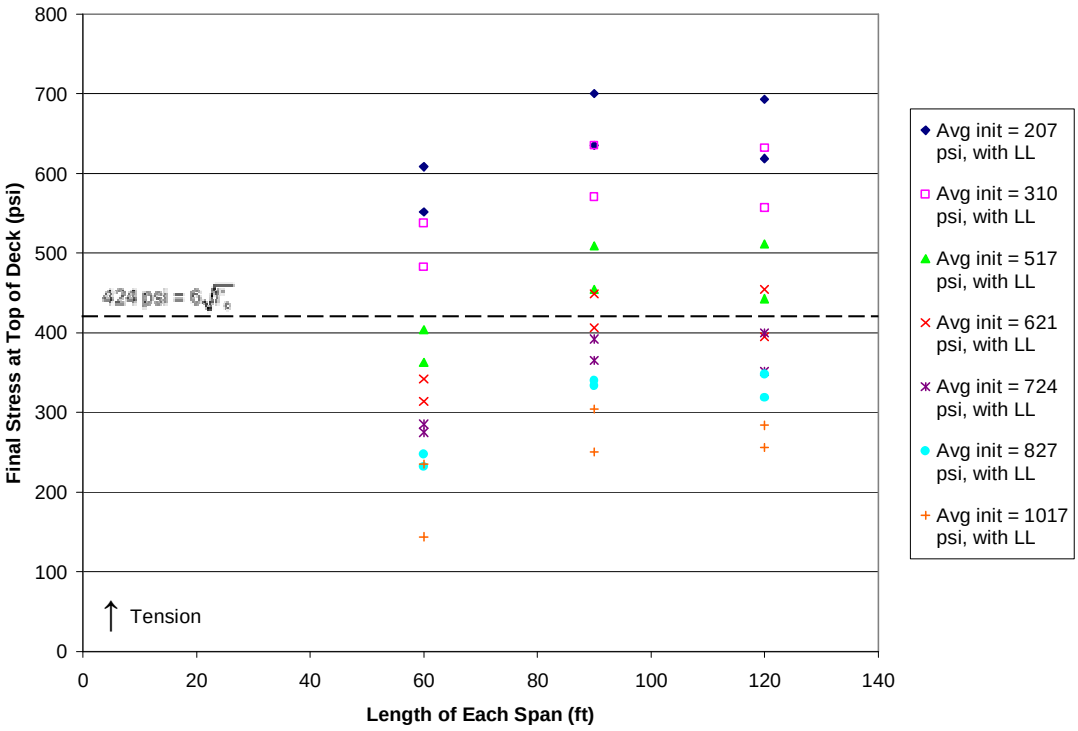

Figure 4.9: Final Stresses for Two-Span Continuous Steel Girder Bridges, Including Live Load

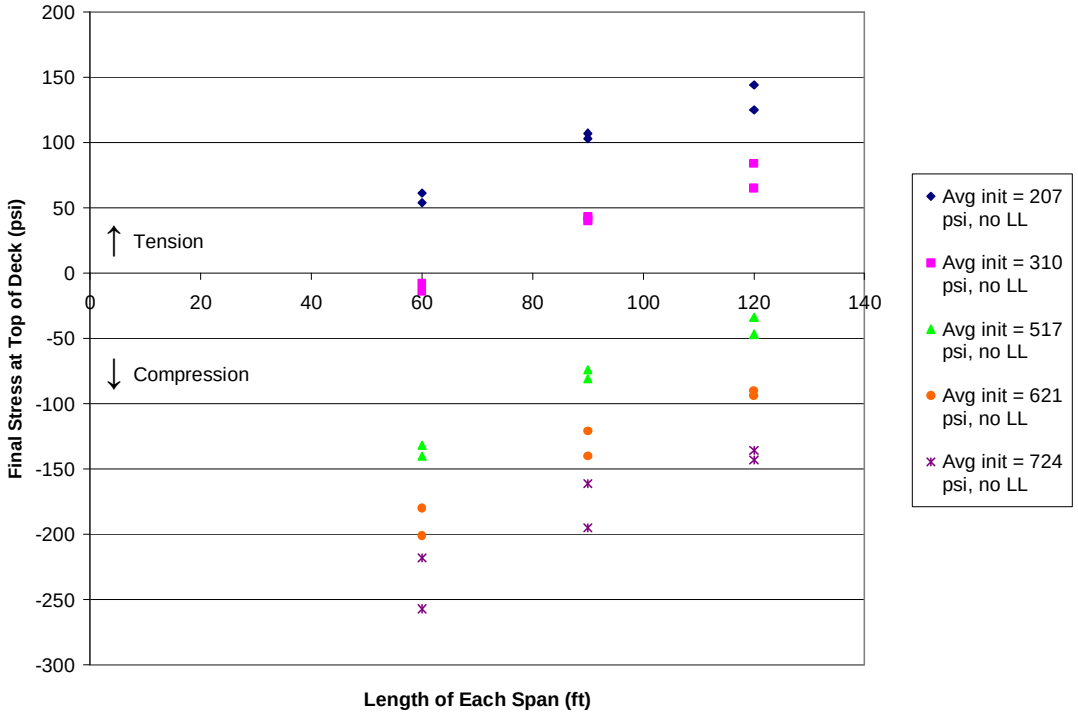

Figure 4.10: Final Stresses for Two-Span Continuous Steel Girder Bridges, Not Incl. Live Load

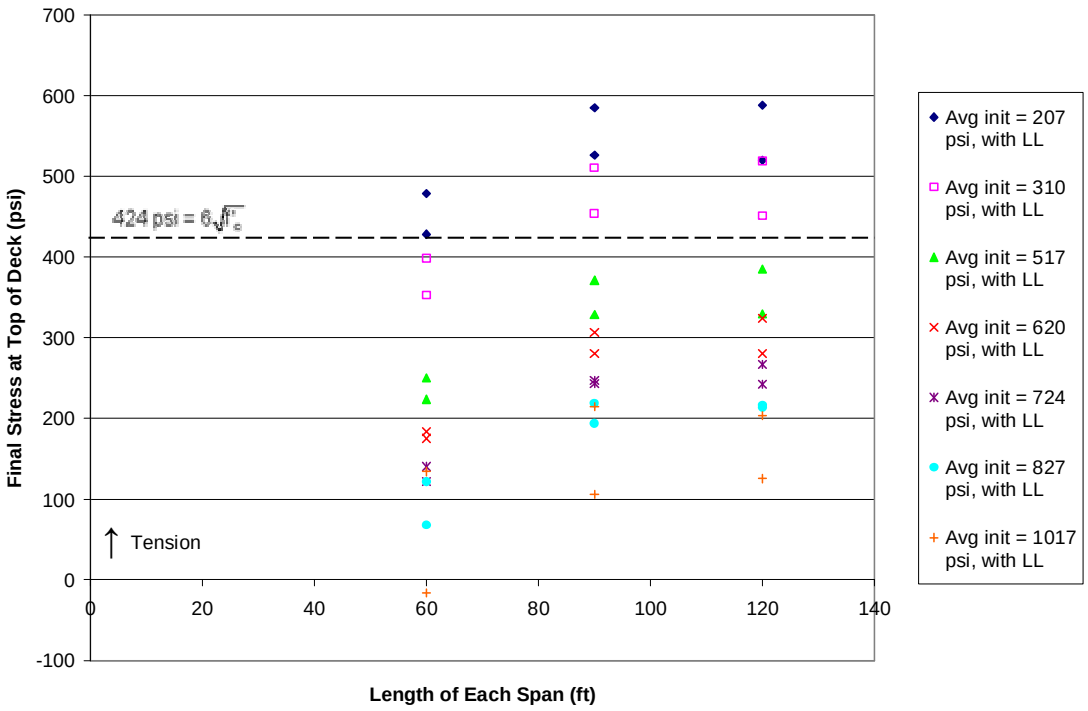

Figure 4.11: Final Stresses for Three-Span Continuous Steel Girder Bridges, Incl. Live Load

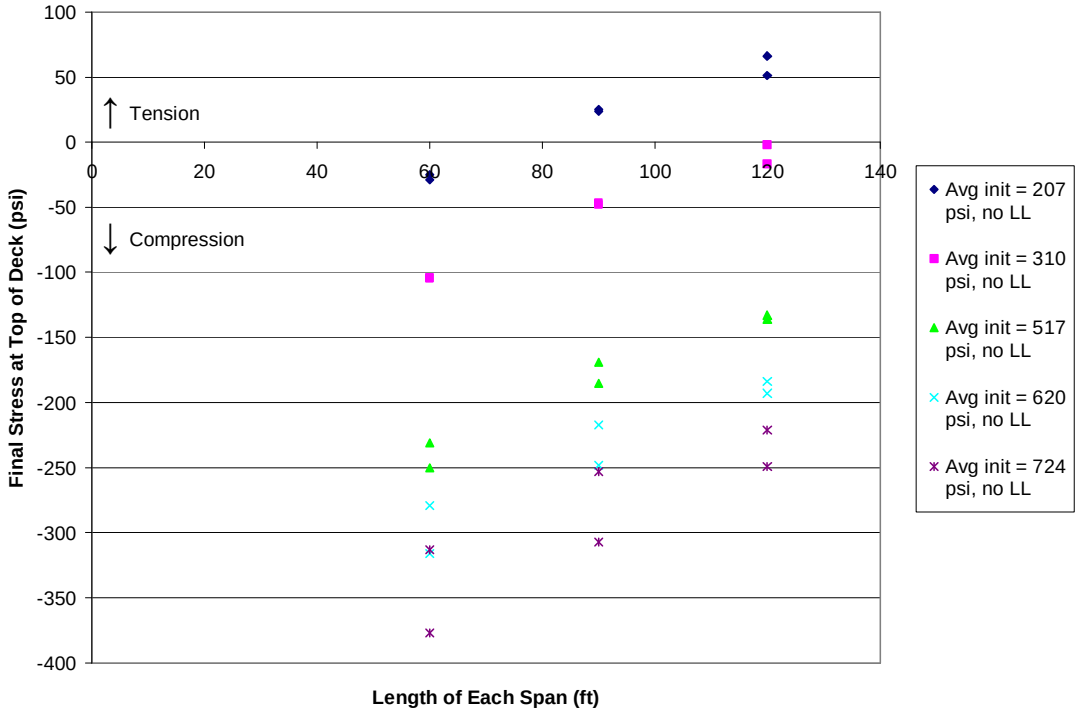

Figure 4.12: Final Stresses for Three-Span Continuous Steel Girder Bridges, Not Incl. Live Load

Figures 4.9 through 4.12 show the much larger losses of compression generated in the concrete decks of the two and three span continuous steel girder bridges than the losses which occurred in the simple span steel girder models. After comparing the respective two and three span graphs with and without the stress due to live loads, it is clear that the live loads contribute a significant portion of the tensile stress present in the concrete deck at the interior supports.

In order to further investigate the effect of live loads on the final stresses in the concrete deck, the live loads and corresponding deck stresses at a distance of 4 ft away from each interior support were calculated. While previous calculations were performed under the worst case assumption that a panel joint would be located directly over an interior support, these calculations incorporated the best case assumption that a typical 8 ft wide deck panel would be centered over each interior support, placing each of the adjacent panel joints 4 ft away from the interior support. The results of these analyses are given in Figures 4.13 and 4.14.

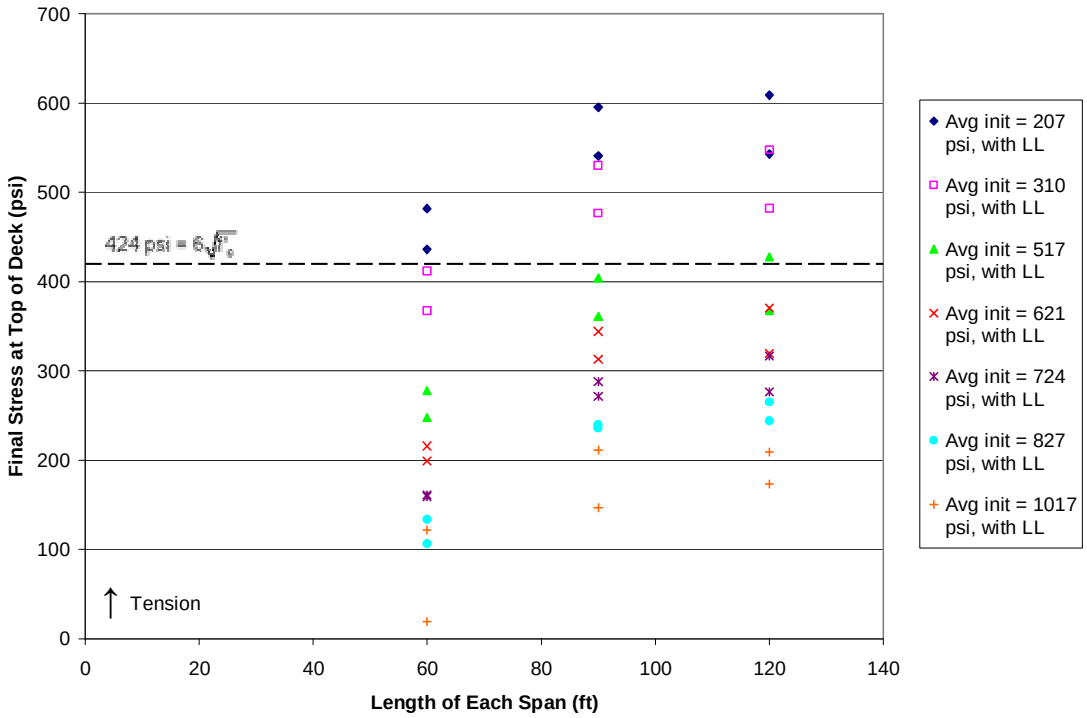

Figure 4.13: Final Stresses for Two-Span Continuous Steel Girder Bridges, 4 ft Away from Interior Support, Incl. Live Load

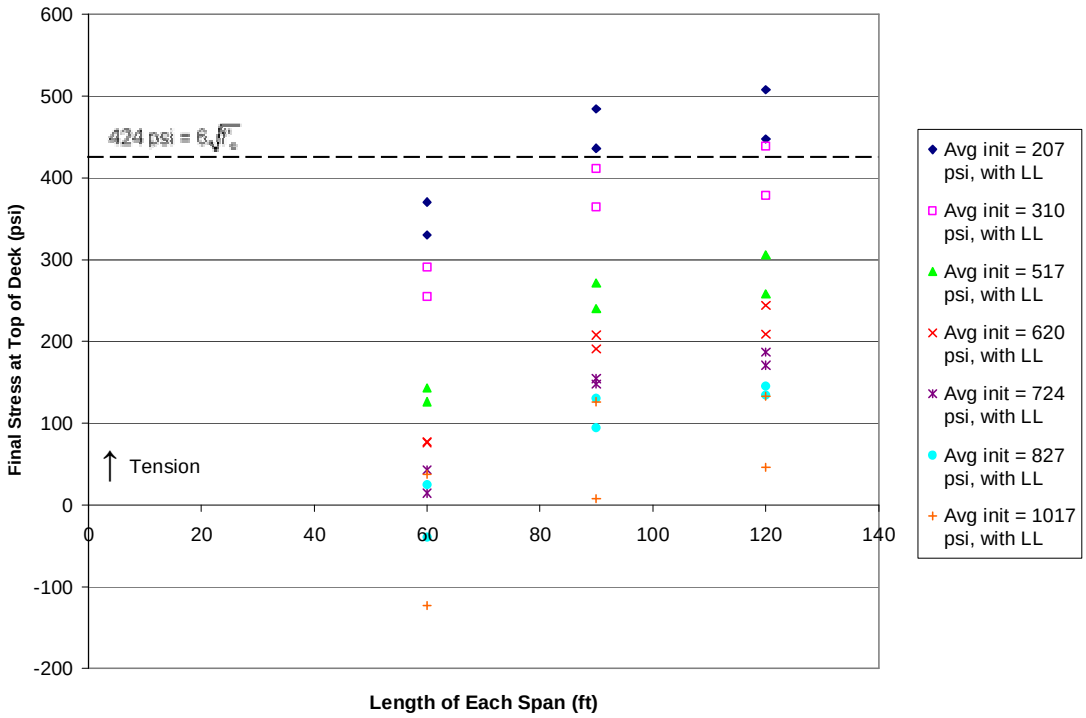

Figure 4.14: Final Stresses for Three-Span Continuous Steel Girder Bridges, 4 ft Away from Interior Supports, Incl. Live Load

The results given in Figures 4.13 and 4.14 indicate that the tension in the deck at a distance of 4 ft away from the interior supports is only reduced by about 100 psi. These findings verified the significance of the negative moment and corresponding tension in the deck produced by live loads, and the subsequent need for more initial post-tensioning than in the simple span steel girder bridges.

To provide reasonable recommendations for precast deck panel post-tensioning in the two and three span continuous steel girder models, the AASHTO LRFD limits regarding tensile stresses in concrete were incorporated. Table 5.9.4.2.2-1 in LRFD establishes a tension limit for the types of bridges considered in this research and "subjected to not worse than moderate corrosion conditions;" this limit is given in Equation 4.1:

$$\sigma_t = 0.19\sqrt{f'_c} \tag{4.1}$$

where:

f'_c is the concrete compressive strength in ksi.

Equation 4.1 is equivalent to $6\sqrt{f'_c}$ with f'_c in psi.

For the 5000 psi concrete panels used in this research, equation 4.1 produces a tensile stress limit of 425 psi. Based on the results illustrated in Figure 4.9 (the two span continuous system with live load), an initial compressive stress of about 650 psi must be provided in the precast concrete deck of a two span continuous steel girder bridge to prevent tensile stresses exceeding the limit 425 psi under time-dependent effects and live loads. For three span continuous steel girder bridges, Figure 4.11 shows that an initial compressive stress of about 500 psi must be provided in the precast concrete deck to prevent tensile stresses exceeding the limit of 425 psi under time-dependent effects and live loads. These initial compressive stresses are provided by longitudinal post-tensioning in the precast concrete deck. In addition to keeping the maximum deck stresses below the tensile limit, these initial levels of post-tensioning also keep the deck in compression under permanent loads and loads induced from time dependent effects in the concrete.

4.4.2 Bridges with Prestressed Concrete Girders

The two and three span continuous models with prestressed concrete girders behaved differently than the simple span concrete girder models, but were also less affected by the live loads than the continuous steel girder bridges. Tables E.1 and E.2 in Appendix E show the results of the parametric studies for the two and three span continuous prestressed concrete girder bridge models, respectively. Like the continuous steel girder results, the tables give the final stresses at the top of the concrete deck both with and without the tension due to live loads for each level of initial post-tensioning applied. Again, all stresses given for the two and three span continuous bridges are located at the interior support(s), which was assumed to be the critical location because of the maximum negative moments created there by live loads. Selected results from Tables E.1 and E.2 are summarized graphically in Figures 4.15 through 4.22 which follow. Additional figures which illustrate results for the two and three span continuous PCBT and AASHTO girder models are provided in Appendix E.

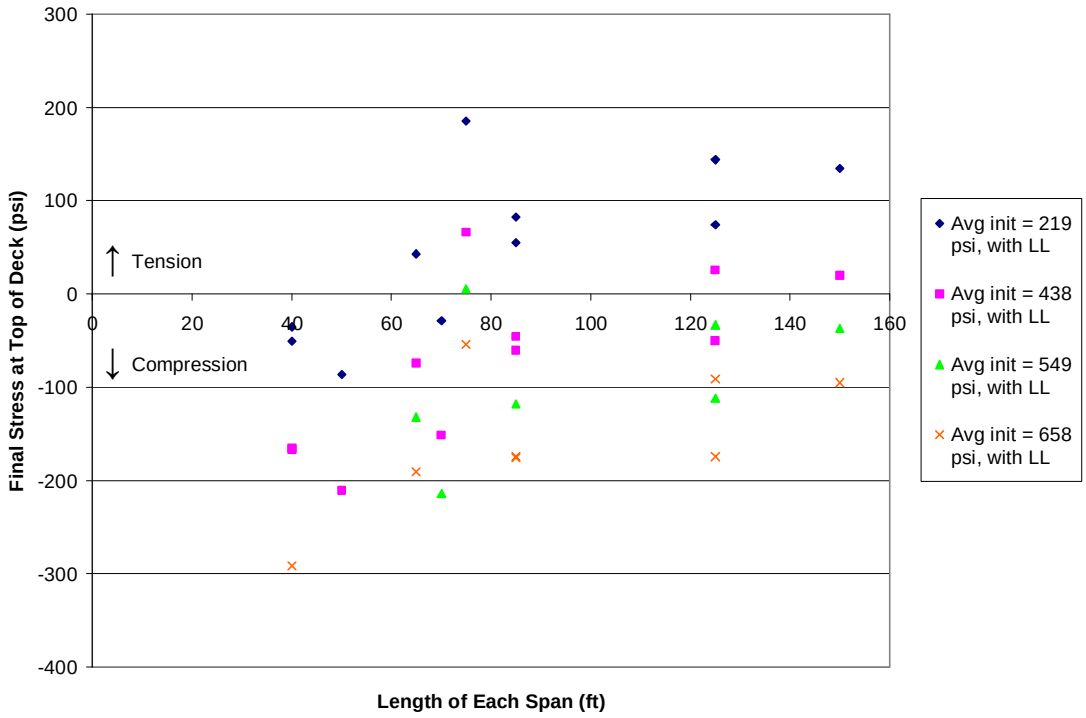

Figure 4.15: Final Stresses for Two-Span Continuous PCBT Girder Bridges, Incl. Live Load

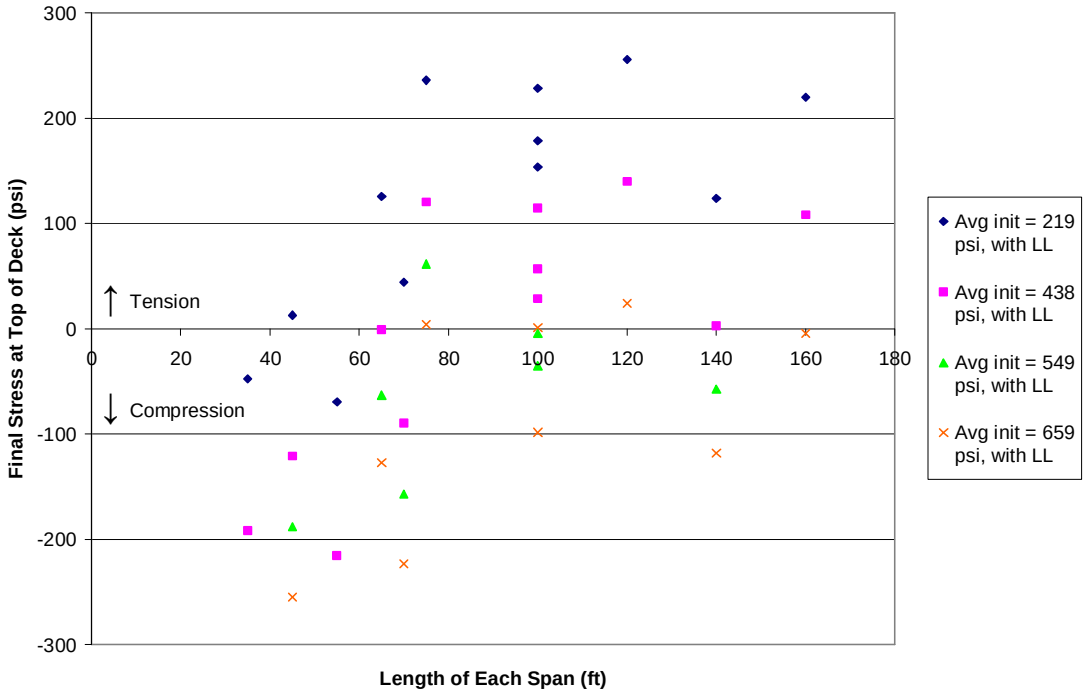

Figure 4.16: Final Stresses for Two-Span Continuous AASHTO Girder Bridges, Incl. Live Load

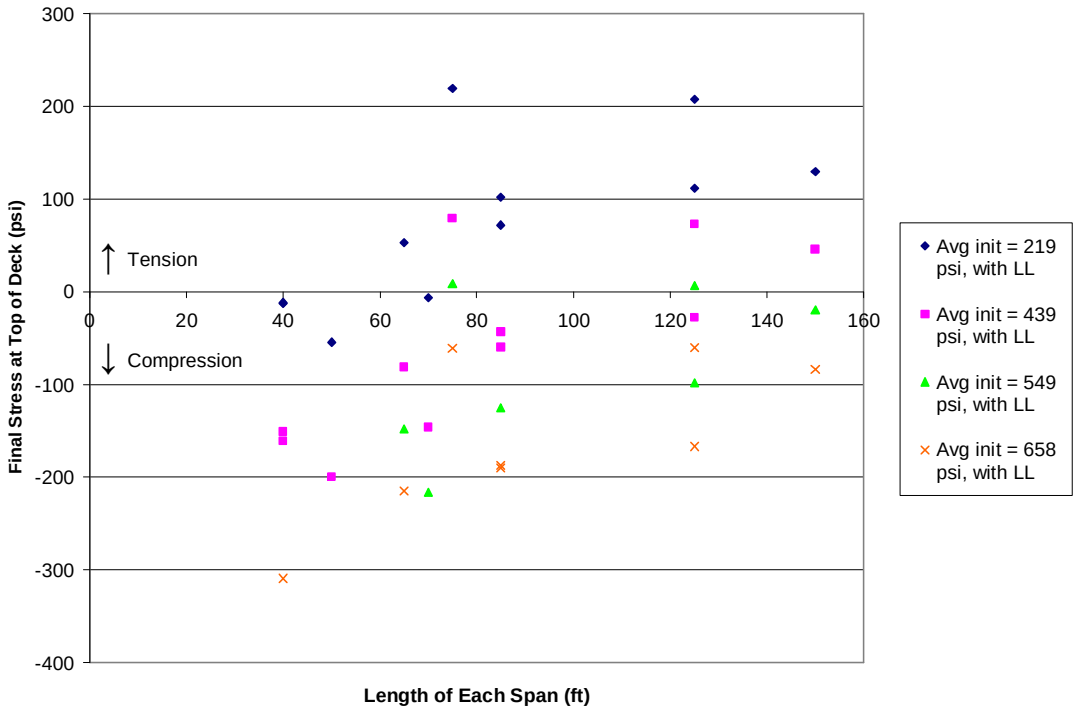

Figure 4.17: Final Stresses for Three-Span Continuous PCBT Girder Bridges, Incl. Live Load

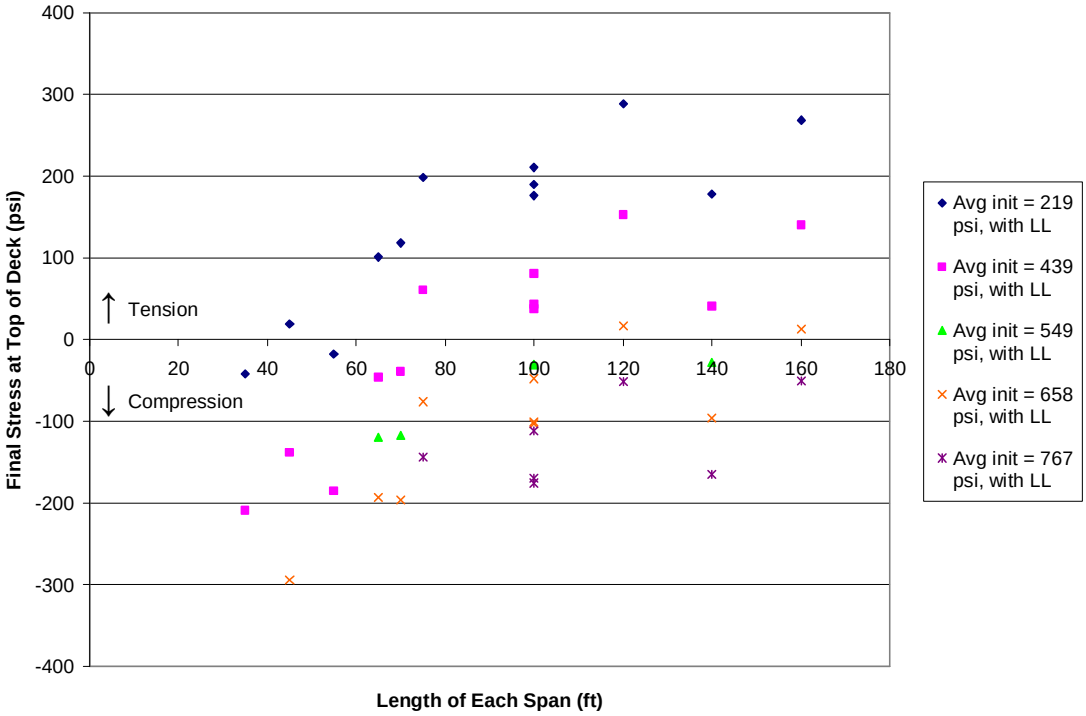

Figure 4.18: Final Stresses for Three-Span Cont. AASHTO Girder Bridges, Incl. Live Load

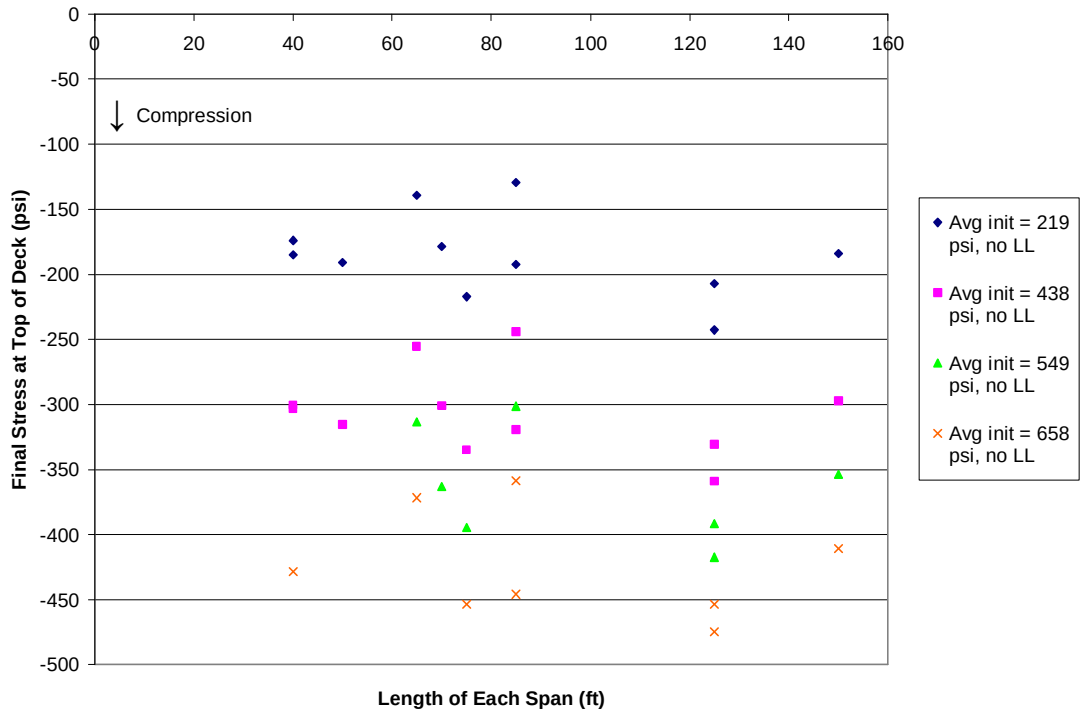

Figure 4.19: Final Stresses for Two-Span Continuous PCBT Girder Bridges, Not Incl. Live Load

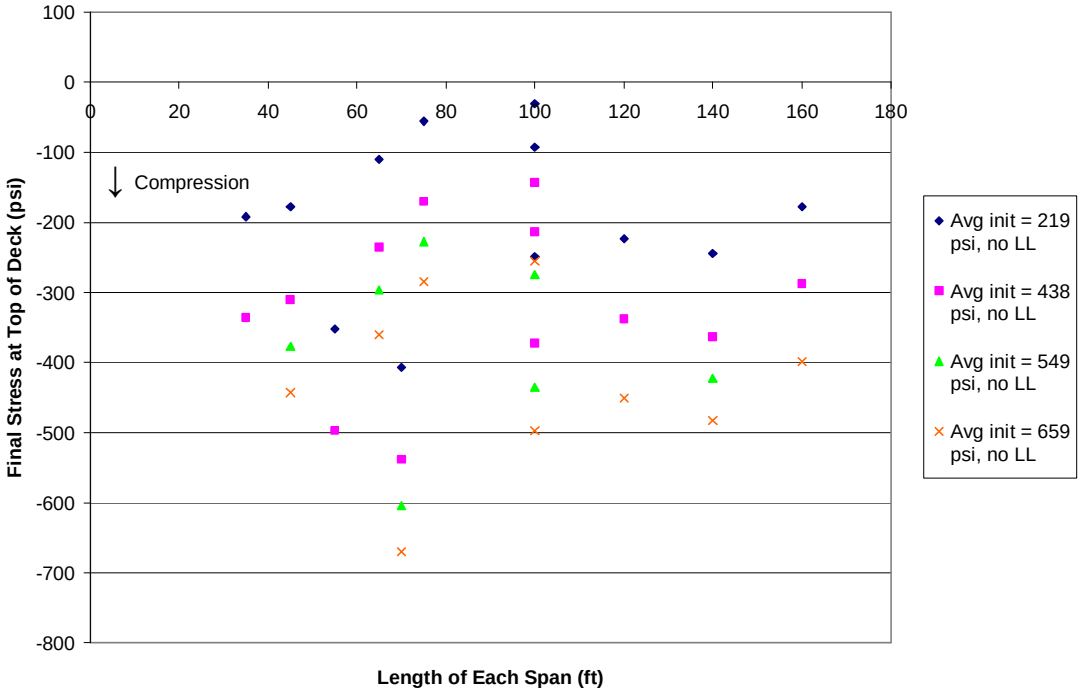

Figure 4.20: Final Stresses for Two-Span Cont. AASHTO Girder Bridges, Not Incl. Live Load

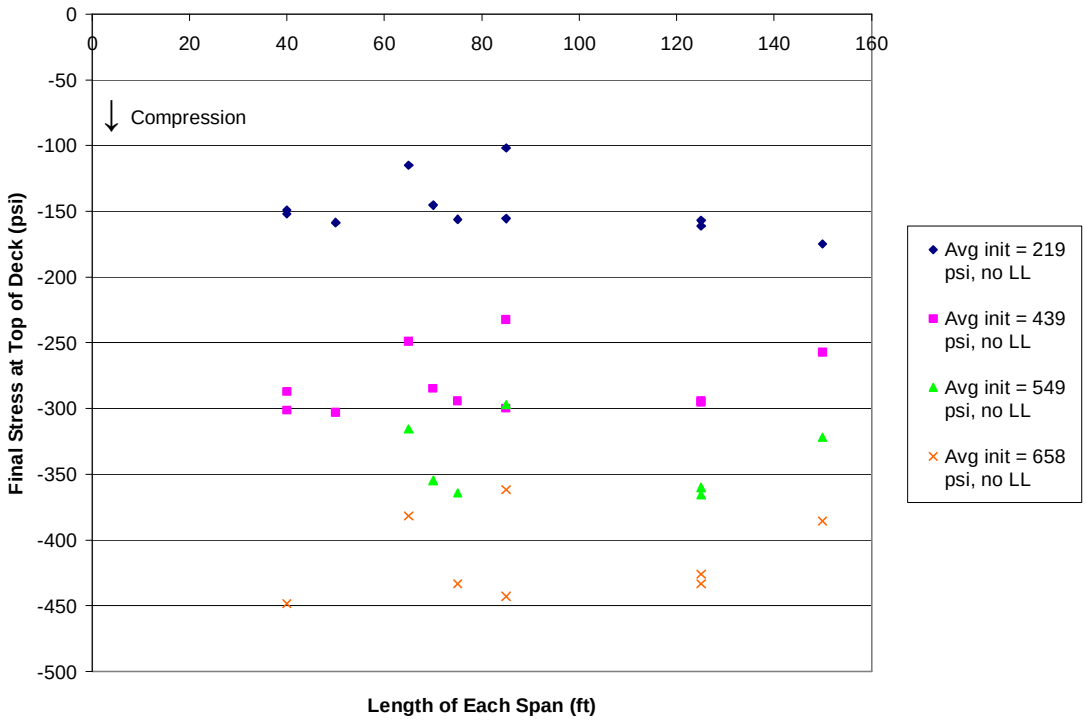

Figure 4.21: Final Stresses for Three-Span Cont. PCBT Girder Bridges, Not Incl. Live Load

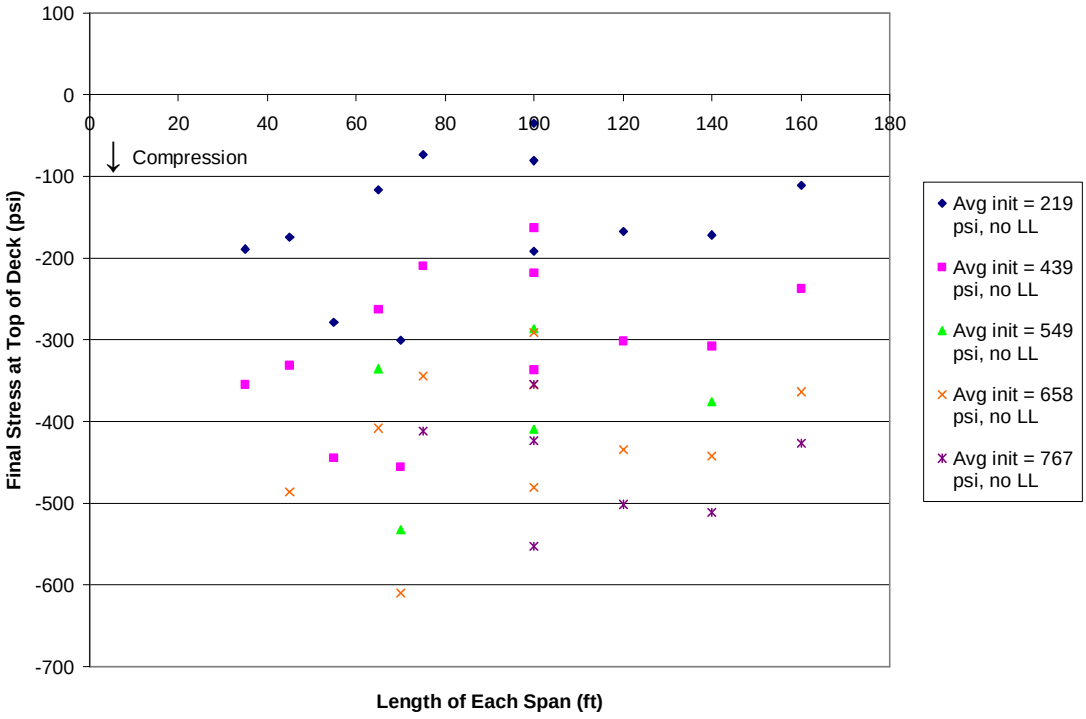

Figure 4.22: Final Stresses for Three-Span Cont. AASHTO Girder Bridges, Not Incl. Live Load

Unlike the continuous steel girder models, the maximum tensile stress in Figures 4.15-4.18 above is less than 300 psi. This result was obtained from the smallest applied initial compressive stress of about 220 psi. For this reason and for simplicity, Figures 4.15-4.18 do not depict results for models initially post-tensioned to levels greater than 767 psi. In two and three span continuous bridges with PCBT or AASHTO girders, only 200 psi of initial compression is needed to keep the precast concrete deck stresses well under the tensile stress limit of 425 psi after time-dependent effects and live loads are considered. In addition to keeping the maximum deck stresses below the tensile limit, these initial levels of post-tensioning also keep the deck in compression under permanent loads and loads induced from time dependent effects in the concrete. This preservation of compression in the deck is depicted in Figures 4.19-4.22 which do not include live loads.

4.5 Elaboration on Continuous Span Model Results

As stated in the previous sections, an initial compressive stress of 200 psi is recommended for the precast bridge decks in all of the PCBT and AASHTO girder bridges as well as the simple span steel girder bridges investigated in this research. This recommendation contrasts the initial compressive stresses of 650 psi and 500 psi recommended for the precast decks in the two and three span continuous steel girder bridges, respectively. The large difference in these recommendations may be better understood by examining two of the three components of stress which contribute to the total stress in the concrete deck at the interior supports. Tables D.1 and D.2 in Appendix D present the results of the two and three span continuous steel girder bridge parametric studies, while Tables E.1 through E.4 in Appendix E present the results of the two and three span continuous prestressed concrete girder bridge parametric studies. From these results, the stresses developed at the top of the concrete deck at the interior supports due to continuity and live loads are summarized in Table 4.7.

Table 4.7: Summary of Results of Continuous Bridge Parametric Studies

Type of Continuous Bridge and Girders	Approximate Range of Stress at Top of Deck over Interior Supports	
	Due to Force Redist. and Continuity (psi)	Due to Factored Live Load (psi)
2 Span Steel	200 to 400	450 to 600
3 Span Steel	100 to 300	450 to 600
2 Span PCBT	-200 to 50	100 to 400
3 Span PCBT	-200 to 50	100 to 400
2 Span AASHTO	-250 to 200	150 to 500
3 Span AASHTO	-200 to 150	200 to 450

Table 4.7 shows that the ranges of stresses due to both continuity and live loads are significantly higher for the two and three span continuous steel girder bridges than for the two and three span continuous prestressed concrete girder bridges. These differences may be partially attributed to the relative stiffnesses of the composite steel and composite concrete girder cross sections used in the parametric studies. While the steel girders were designed based on a span to depth ratio of 30, some of the prestressed concrete girders had a span to depth ratio significantly less than 30, as shown in Table 3.4. Therefore, some of the composite concrete girder cross sections were inherently stiffer than the composite steel girder cross sections, resulting in less tensile stresses over the interior supports in the continuous span concrete girder bridges compared to the continuous span steel girder bridges. These conditions should be kept in mind during interpretation of the design recommendations presented in the next chapter.

CHAPTER 5: CONCLUSIONS AND RECOMMENDATIONS

5.1 Summary

The research presented herein verifies the efficiency and practicality of using full-depth precast deck panel systems for new construction or rehabilitation of bridge decks. Casting of the concrete panels prior to their arrival at the bridge site eliminates many of the complications typically involved with a cast-in-place deck, and significantly reduces construction time and resulting traffic delays or detours.

To facilitate the implementation of these full-depth precast bridge deck systems, however, designers need an easy, straightforward method or guidelines for determining the amount of longitudinal post-tensioning required in the bridge deck in order to keep the transverse joints in compression. Prior to this research, a handful of recommendations for longitudinal post-tensioning in precast bridge decks were presented, but these suggestions were based on the results of at most a few laboratory tests or finite element model results. While these models were all limited to the use of steel girders, this research incorporates two different types of prestressed concrete girders as well as steel girders. In addition, the results of this research offer two different options for calculating the required amount of initial compression in a precast concrete bridge deck, which include 1) estimating the required initial compression from the general guidelines proposed, or 2) implementing the age-adjusted effective modulus method via the corresponding model developed and used to perform this research.

5.2 Conclusions

The parametric studies performed in this research indicated general trends of behavior for each of the four major groups of bridge models, which included both simple and continuous spans with either steel or prestressed concrete girders. In the simple span bridges, the steel girder models experienced greater overall losses of compression in their precast decks with increasing span length. This behavior was contrasted by the simple span prestressed concrete girder models, which demonstrated smaller net losses of (or even gains in) compression in their precast decks with increasing span lengths.

In the results of the two and three span continuous bridge model parametric studies, clear trends were more difficult to identify. Live loads had a significant affect on the losses of

compression and in some cases generated significant tensile stresses in the bridge decks, particularly in the continuous steel girder bridge models. The precast bridge decks in the continuous span steel girder models experienced much higher losses of initial compression than the precast decks in the continuous span prestressed concrete girder models. This outcome was partially attributed to the extra compressive forces provided by the prestressing as well as the creep and shrinkage occurring in both the girders and the deck in the concrete girder bridge models. Since the steel girder material was not creeping and shrinking like the concrete girders, the greater restraint of the concrete deck provided by the steel girders combined with the effect of live loads produced greater losses of compression in these precast bridge decks.

The precast decks in the continuous span steel girder bridge models without live load, like the corresponding simple span models, displayed greater losses of compression with increasing span lengths. When live load was included, however, these trends were not as clear. The precast decks in the continuous span concrete girder bridges, on the other hand, displayed results opposite of their simple span behavior. While the trends remained very unclear, the continuous concrete girder bridge decks seem to have experienced greater losses with increasing span lengths, whereas their simple span counterparts gained compression in the deck with increasing span lengths.

5.3 Design Recommendations

The results of this research indicate that the recommendations for initial longitudinal post-tensioning in precast concrete bridge deck panels need to be revised. In order to provide simple guidelines for use by designers, a single value of required initial post-tensioning was determined for each different type of bridge model investigated in this research. These guidelines are presented in Table 5.1.

Table 5.1: Recommended Values of Initial Post-Tensioning

Girder Type	Number of Spans	Required Initial P/T (psi)
Steel	1	200
	2	650
	3 or more	500
PCBT	1	200
	2	200
	3 or more	200
AASHTO	1	200
	2	200
	3 or more	200

As shown in Table 5.1, the recommendations for all of the three span continuous bridges were expanded to include three or more continuous spans. This modification was made based on the assumption that each additional span would theoretically provide more restraint against potential tension at the top of the deck over the interior supports, therefore reducing the successive amounts of initial compression required in the deck. This theory is already exemplified by the reduction from 650 psi to 500 psi of initial compression needed from two to three continuous steel girder spans.

As an alternative to the general guidelines provided in Table 5.1, the designer may also choose to implement the modeling procedure developed and used in this research to calculate a more specific initial compressive stress required in the precast deck of his or her bridge structure. This option may be productive when a given bridge cross section differs enough from the parametric studies performed in this research that the general guidelines provided here may be overly conservative or unconservative. As a second alternative to using the general guidelines provided, the designer may also be able to interpolate a more exact level of initial post-tensioning appropriate for his or her bridge configuration from the tables and graphs of results presented in this thesis.

5.4 Recommendations for Future Research

The results of this research inspire several topics for further study. First, since Mathcad is such a powerful tool, the models created for use in the parametric studies presented here could be easily implemented to investigate time-dependent effects in bridges with other types of steel or concrete girders, different span lengths, and/or various girder spacings. The studies of one,

two, and three span bridges conducted in this research could also be expanded to investigate bridges of four or more continuous spans. In addition, sensitivity analyses could be performed to examine the ways in which altering the aging coefficient or other material properties may affect the results of this research.

Another topic for additional study involves differing ages of precast concrete decks and girders. The behavior of a bridge which undergoes a deck replacement on existing precast concrete girders, for example, will be influenced by the minimal amount of creep and shrinkage occurring in the well aged concrete girders. As the concrete girders become very old, they will behave more like steel girders and provide more restraint due to the negligible amounts of creep and shrinkage occurring in the concrete. Minor modifications of the Mathcad models developed in this research would need to be made in order to account for precast concrete panels and prestressed concrete girders which are cast at significantly different times. Expansion of simple guidelines for post-tensioning precast concrete panels will promote the use of these panels in more newly constructed or rehabilitated bridge decks, thereby improving the quality and efficiency of transportation infrastructure everywhere.

REFERENCES

AASHTO (2004). *AASHTO LRFD Bridge Design Specifications, Third Edition with 2005 and 2006 Interims*. American Association of State Highway and Transportation Officials, Washington, D.C.

Bazant, Z. P. (1972). "Prediction of Concrete Creep Effects Using Age-Adjusted Effective Modulus Method." *ACI Journal*, 69, 212-217.

Brice, R. (2005). QConBridge, Washington State Department of Transportation Bridge and Structures Office.

Brockenbrough, R. and F. Merritt (2006). Structural Steel Designer's Handbook, Fourth Edition. McGraw-Hill, New York.

Dilger, W. H. (1982). "Creep Analysis of Prestressed Concrete Structures Using Creep-Transformed Section Properties." *PCI Journal*, 27(1), 98-117.

Dilger, W. (2005). "Time Dependent Effects in Concrete Structures." Draft Document, ACI Committee 209 – Creep and Shrinkage in Concrete.

England, G. L. and J. M. Illston (1965). "Methods of Calculating Stress in Concrete from a History of Measured Strain." *Civil Engineering and Public Works Review*, 60(705, 706, 707), 513-517, 692-694, 846-847.

Faber, O. (1927). "Plastic Yield, Shrinkage and Other Problems of Concrete and Their Effect on Design." *Proceedings, ICE Conference*, London.

Glanville, W. H. (1930). "Studies of Reinforced Concrete, III: The Creep and Flow of Concrete Under Load." Building Research Technical Paper No. 12, Department of Scientific and Industrial Research**,** London.

Issa, M. A., A. Idriss, I. Kaspar, and S. Khayyat (1995b). "Full Depth Precast and Precast, Prestressed Concrete Bridge Deck Panels." *PCI Journal*, 40(1), 59-80.

Issa, M. A., A. Yousif, and M. Issa (2000). "Experimental Behavior of Full-Depth Precast Concrete Panels for Bridge Rehabilitation." *ACI Structural Journal*, 97(3), 397-407.

Issa, M. A., A. Yousif, M. Issa, I. Kaspar, and S. Khayyat (1995a). "Field Performance of Full Depth Precast Concrete Panels in Bridge Deck Reconstruction." *PCI Journal*, 40(3), 82-107.

Issa, M. A., A. Yousif, M. Issa, I. Kaspar, and S. Khayyat (1998). "Analysis of Full Depth Precast Concrete Bridge Deck Panels." *PCI Journal*, 43(1), 74-85.

MacGregor, J. G., and J. K. Wight (2005). Reinforced Concrete: Mechanics and Design. Pearson Prentice Hall, Upper Saddle River, NJ.

McMillan, F. R. (1916). "Method of Designing Reinforced Concrete Slabs, discussion by A. C. Janni." *Transactions ASCE*, 80(1738).

Nielsen, L. F. (1970). "Kriechen des Betons." *Beton-und Stahlbetonbau*, 65, 272-275.

Nilson, A. H. (1987). Design of Prestressed Concrete. John Wiley & Sons, New York.

PCI (2005). Bridge Design Manual. Precast/Prestressed Concrete Institute, Chicago.

Rusch, H., D. Jungwirth, and H. Hilsdorf (1973). "Kritische Sichtung der Einflusse von Kriechen und Schwinden auf das Verhalten der Tragwerke." *Beton-und Stahlbetonbau* 68(3, 4, 5), 49-60, 76-86, 152-158.

Scholz, D.P. (2004). "Performance Criteria Recommendations for Mortars Used in Full Depth Precast Concrete Bridge Deck Panels." M.S. Thesis, Virginia Polytechnic Institute and State University, Blacksburg, Virginia.

Trost, H. (1967). "Implications of the Superposition Principle in Creep and Relaxation Problems for Concrete and Prestressed Concrete." *Beton-und Stahlbetonbau*, (10), 230-238, 261-269.

Virginia Department of Transportation (2006). "Volume V – Part 2: Design Aids – Typical Details." <http://www.vdot.virginia.gov/business/bridge-v5p2.asp> (April 25, 2007).

APPENDIX A

Variable Definitions

Variables used throughout the body of the thesis and the Mathcad models include:

a	=	distance between deck centroid and haunch centroid, in.
A_{atr}	=	age-adjusted transformed area of composite cross section, in^2
A_d	=	cross-sectional area of the effective deck, in^2
A_g	=	gross area of the girder, in^2
A_{gn}	=	net area of concrete girder, in^2
A_{gtr}	=	transformed area of girder concrete, in^2
A_h	=	cross-sectional area of the haunch, in^2
A_{psg}	=	total area of prestressing strands in girder, in^2
A_{pstr}	=	transformed area of girder prestressing strands, in^2
A_{ptd}	=	total area of post-tensioning strands in deck, in^2
A_{tr}	=	transformed area of the composite cross section, in^2
Ad_{atr}	=	age-adjusted transformed area of deck concrete, in^2
Ad_{tr}	=	transformed area of the deck, in^2
Ah_{atr}	=	age-adjusted transformed area of haunch concrete, in^2
Ah_{tr}	=	transformed area of the haunch, in^2
Aps_{atr}	=	in the steel girder models: age-adjusted transformed area of post-tensioning steel in the deck, in^2
Aps_{atr}	=	in the prestressed concrete girder models: age-adjusted transformed area of prestressing steel in the girder, in^2
Aps_g	=	total area of prestressing strands in the concrete girder, in^2
Aps_{tr}	=	in the steel girder models: transformed area of the deck post-tensioning steel, in^2
Aps_{tr}	=	in the prestressed concrete girder models: transformed area of the girder prestressing steel, in^2
Apt_{tr}	=	in the prestressed concrete girder models: transformed area of the deck post-tensioning steel, in^2

Apt_{atr} = in the prestressed concrete girder models: age-adjusted transformed area of post-tensioning steel in the deck, in^2

Apt_d = total area of post-tensioning in the deck, in^2

$Astr_d$ = area of each post-tensioning strand in the deck, in^2

$Astr_g$ = area of each prestressing strand in the concrete girder, in^2

b = distance between deck centroid and girder centroid, in.

c = distance between deck centroid and centroid of girder prestressing strands, in.

c_{atr} = centroid of age-adjusted transformed cross section, in.

c_g = centroid of the girder measured from the bottom, in.

c_{gn} = net centroid of concrete girder, in.

c_{gtr} = centroid of transformed girder cross section, in.

c_{tr} = centroid of the transformed composite cross section, in.

$depth_g$ = depth of the girder, in.

$depth_t$ = total depth of the composite section, in.

e_g = eccentricity of prestressing strands in the concrete girder, in.

e_{gA} = eccentricity of all strands at cross section denoted (here, cross section A), in.

e_{gn} = net eccentricity of prestressing strands in concrete girder, in.

e_{gtr} = eccentricity of prestressing strands in transformed girder cross section, in.

E_d = modulus of elasticity of the deck, ksi

E_{daatr} = age-adjusted modulus of elasticity of deck concrete, ksi

E_g = modulus of elasticity of the girder, ksi

E_h = modulus of elasticity of the haunch, ksi

E_{haatr} = age-adjusted modulus of elasticity of haunch concrete, ksi

E_{psg} = modulus of elasticity of girder prestressing strands, ksi

E_{ptd} = modulus of elasticity of deck post-tensioning strands, ksi

Eps_g = modulus of elasticity of prestressing strands in the concrete girder, ksi

Ept_d = modulus of elasticity of post-tensioning strands in the deck, ksi

f_{pj} = stress to which prestressing strands are jacked, ksi

$f_{pj\%}$ = percentage of the ultimate stress to which the girder prestressing strands are jacked, ksi

f_{pu} = ultimate strength of prestressing and post-tensioning strands, ksi

f_{py} = yield stress of prestressing and post-tensioning strands, ksi

fc_d = compressive strength of deck concrete, psi

fc_g = compressive strength of girder concrete, psi

fc_h = compressive strength of haunch material, psi

hum = relative humidity, percent

I_{atr} = moment of inertia of age-adjusted transformed composite cross section, in^4

I_d = moment of inertia of the effective deck, in^4

I_g = moment of inertia of the girder, in^4

I_{gn} = net moment of inertia of concrete girder, in^4

I_{gtr} = moment of inertia of transformed girder cross section, in^4

I_h = moment of inertia of the haunch, in^4

I_{tr} = moment of inertia of transformed composite cross section, in^4

K_L = factor indicating low relaxation strands

L_g = length of a single span, in.

M_{go} = initial moment in concrete girder, kip-in

M_{goc} = initial moment in concrete girder for composite phase, kip-in

M_{max} = maximum negative moment at interior support, kip-in

n = modular ratio of girder prestressing strand to girder concrete

n_{dg} = modular ratio of deck concrete to girder material

n_{dga} = modular ratio of age-adjusted deck concrete to girder material

n_{hg} = modular ratio of haunch concrete to girder material

n_{hga} = modular ratio of age-adjusted haunch concrete to girder material

n_{pg} = modular ratio of deck post-tensioning steel to girder material

n_{pga} = modular ratio of deck post-tensioning steel to girder material

num_{hp} = number of harped strands in the prestressed concrete girder

num_{st} = number of straight strands in the prestressed concrete girder

$numstr_{dpt}$ = number of post-tensioning strands in the deck

$numstr_g$ = number of prestressing strands in the concrete girder

N_{do} = initial force at centroid of deck, kips

N_{doc} = initial force at centroid of deck for composite phase, kips

N_{go} = initial force at centroid of concrete girder, kips

N_{goc} = initial force at centroid of concrete girder for composite phase, kips

$perim_d$ = perimeter of the effective deck (not including the thickness on either side), in.

$perim_g$ = perimeter of the concrete girder, in.

$perim_h$ = portion of the haunch perimeter open to the atmosphere in a composite section (twice the haunch thickness), in.

t_d = thickness of the deck, in.

t_{dcomp} = time that the deck is made composite with the girders relative to the age of the precast deck panel concrete, days

t_{dinf} = time considered as end of bridge service life, days

t_{dpt} = time that the deck is post-tensioned relative to the age of the precast deck panel concrete, days

t_{gcast} = time that the girder is cast, days

t_{gcomp} = time that the girder is made composite with the deck, days

t_{ginf} = time considered as end of bridge service life, days

t_h = thickness of the haunch, in.

t_{hcomp} = time that the haunch is placed (relative to the haunch material age), making the deck and girders composite, days

t_{hinf} = time considered as end of bridge service life, days

$topw_g$ = girder top flange width, in.

w_d = effective width of the deck (interior girder spacing), in.

w_h = width of the haunch, in.

x_A = location of cross section A: the ends of each span

x_B = location of cross section B: the ¼ and ¾ points of each span, in.

x_C = location of cross section C: midspan of each span, in.

x_{harp} = location of harping point for girder prestressing strands: 0.4*L from the end of each span, in.

y_d = centroid of the deck in the composite section measured from the bottom of the girder, in.

y_h = centroid of the haunch in the composite section measured from the bottom of the girder, in.

y_{ps} = in steel girder models: centroid of the deck post-tensioning in the composite section measured from the bottom of the girder, in.

y_{ps} = in prestressed concrete girder models: centroid of the girder prestressing strands measured from the bottom of the girder, in.

y_{psA} = centroid of all prestressing strands at cross section denoted (here, cross section A) measured from bottom of girder, in.

y_{pshpA} = centroid of harped strand group at cross section denoted (here, cross section A) measured from bottom of girder, in.

y_{psstA} = centroid of straight strand group at cross section denoted (here, cross section A) measured from bottom of girder, in.

χ = constant curvature of span, strain/inch

Δf_{pR} = change in stress due to relaxation in girder or deck strands over a given time interval

ΔM_d = change in moment in deck

ΔM_g = change in moment in girder

ΔM_h = change in moment in haunch

ΔN_d = change in force at centroid of deck

ΔN_g = change in force at centroid of girder

ΔN_h = change in force at centroid of haunch

ΔN_{psg} = change in force at centroid of prestress in girder

ΔN_{ptd} = change in force at centroid of post-tensioning in deck

$\Delta\chi$ = change in curvature

$\Delta\varepsilon_d$ = change in strain at centroid of deck

$\Delta\varepsilon_g$ = change in strain at centroid of girder

$\Delta\varepsilon_h$ = change in strain at centroid of haunch

$\Delta\varepsilon_{psg}$ = change in strain at centroid of prestress in girder

$\Delta\varepsilon_{ptd}$ = change in strain in post-tensioning strands in deck

ε_{shd} = shrinkage strain in deck concrete over a given time interval

ε_{shg} = shrinkage strain in girder concrete over a given time interval

ε_{shh} = shrinkage strain in haunch concrete over a given time interval

μ_d = aging coefficient for the deck

μ_g = aging coefficient for the girder concrete

μ_h = aging coefficient for the haunch

ϕ_d = creep coefficient for deck concrete over a given time interval

ϕ_g = creep coefficient for girder concrete over a given time interval

ϕ_h = creep coefficient for haunch concrete over a given time interval

APPENDIX B

Simple Span Bridge Model Details

Two examples of simple span Mathcad models are included in this appendix. The first is a 60 ft simple span bridge with W24x103 steel girders spaced at 6 ft, while the second is a 40 ft simple span bridge with PCBT-37 girders spaced at 6 ft.

ORIGIN := 1

Deck Panel Prestress Losses:
Precast Concrete Deck with Steel Girder, Simple Span
Parametric Study: W24x103, 6' spc., 60' span

Inputs (data to be entered is under blue headings)

a) Steel girder properties

Girder section properties - general

$A_g := 30.3$ $I_g := 3000$ $E_g := 29000$ $depth_g := 24.5$

$topw_g := 9$ $L_g := 60 \cdot 12$ $c_g := 12.25$

b) Concrete deck and post-tensioning strand properties

Deck section properties

$t_d := 8.5$ $w_d := 72$ $\mu_d := 0.7$ $fc_d := 5000$

Post tensioning strand properties

$numstr_{dpt} := 4$ $Astr_d := 0.153$ $Ept_d := 28500$ $f_{pu} := 270$ $K_{Lpr} := 45$

Deck time intervals

$t_{dpt} := 55$ $t_{dcomp} := 60$ $t_{dinf} := 10000$

Calculated properties - deck

$A_d := t_d \cdot w_d$ $I_d := \frac{w_d \cdot t_d^3}{12}$ $E_d := 57 \cdot \sqrt{fc_d}$ $perim_d := 2 \cdot w_d$ $A_{dws} := (t_d + 0.5) \cdot w_d$

$A_d = 612$ $I_d = 3685$ $E_d = 4031$ $perim_d = 144$ $A_{dws} = 648$

Calculated properties - P/T strand

$Apt_d := numstr_{dpt} \cdot Astr_d$ $f_{py} := 0.9 \cdot f_{pu}$

$Apt_d = 0.612$ $f_{py} = 243$

c) Haunch properties

Haunch section properties

$t_h := 1$ $\mu_h := 0.7$ $fc_h := fc_d$

Haunch time intervals

$t_{hcomp} := 0.75$ $t_{hinf} := t_{dinf}$

Calculated properties - haunch

$w_h := topw_g$ $A_h := t_h \cdot topw_g$ $I_h := \frac{w_h \cdot t_h^3}{12}$ $E_h := E_d$ $perim_h := 2 \cdot t_h$

$w_h = 9$ $A_h = 9$ $I_h = 0.75$ $E_h = 4031$ $perim_h = 2$

d) General properties

$hum := 70$

e) Composite section properties

$y_h := depth_g + \frac{t_h}{2}$ $y_d := depth_g + t_h + \frac{t_d}{2}$ $y_{ps} := y_d$ $depth_t := depth_g + t_h + t_d$

$y_h = 25$ $y_d = 29.75$ $y_{ps} = 29.75$ $depth_t = 34$

Creep and Shrinkage Models (from AASHTO LRFD 2006 Interims)

$$\text{CREEP}(fci, t1, t2, hum, area, perim) :=$$

$$ktd2 \leftarrow \frac{(t2 - t1)}{61 - \left(\frac{4 \cdot fci}{1000}\right) + (t2 - t1)}$$

$$kla \leftarrow t1^{-0.118}$$

$$khc \leftarrow 1.56 - (0.008 \cdot hum)$$

$$kvs \leftarrow \max\left[1.45 - 0.13 \cdot \left(\frac{area}{perim}\right), 0\right]$$

$$kf \leftarrow \frac{5}{1 + \frac{fci}{1000}}$$

$$creep \leftarrow 1.90 \cdot ktd2 \cdot kla \cdot kvs \cdot khc \cdot kf$$

$$creep$$

$$\text{SHRINKAGE}(fci, t1, t2, hum, area, perim) :=$$

$$ktd1 \leftarrow \frac{t1}{61 - \left(\frac{4 \cdot fci}{1000}\right) + t1}$$

$$ktd2 \leftarrow \frac{t2}{61 - \left(\frac{4 \cdot fci}{1000}\right) + t2}$$

$$khs \leftarrow 2 - (0.014 \cdot hum)$$

$$kvs \leftarrow \max\left[1.45 - 0.13 \cdot \left(\frac{area}{perim}\right), 0\right]$$

$$kf \leftarrow \frac{5}{1 + \frac{fci}{1000}}$$

$$shrink \leftarrow -480 \cdot 10^{-6} \cdot (ktd2 - ktd1) \cdot kvs \cdot khs \cdot kf$$

$$shrink$$

Sign Convention:
Tension = Lengthening = (+)
Compression = (-)

Outline of calculation steps for a steel girder with precast, post-tensioned deck panels

a) D/SG 1: Calculate redistribution of stresses in deck from post-tensioning to composite action

b) D/SG 2: Calculate redistribution of stresses in composite section from when it's made composite to any time in the future

a) D/SG 1: Calculate redistribution of stresses in deck from post-tensioning to composite action

Compute state of stress immediately following stressing - use average force in tendons

$P_{jack} := 0.80 \cdot f_{pu}\, numstr_{dpt} \cdot Astr_d$ $P_{jack} = 132.2$ kips

Consider seating losses....

Note: Post-tensioning tendons are straight so only have wobble losses --> k*l term

$\alpha := 0$ $\mu := 0$ $k := 0.0002$ per foot of length $\Delta S := \frac{3}{8}$ inch $len := \frac{L_g}{12}$ $len = 60$

$P_{dead} := P_{jack} \cdot e^{-(\mu \cdot \alpha + k \cdot len)}$ $P_{dead} = 130.6$ kips

$m := \frac{P_{jack} - P_{dead}}{len \cdot 12}$ $m = 0.00219$ kips/inch

$P_{SL} := \frac{\Delta S \cdot Apt_d \cdot Ept_d}{len \cdot 12}$ $P_{SL} = 9.084$ kips

$x_{AS} := \frac{\sqrt{\frac{\Delta S \cdot Apt_d \cdot Ept_d}{m}}}{12}$ $x_{AS} = 144.01$ feet

Note xAS is longer than the bridge...revise approach for finding Pavg

$area_{tris} := \frac{1}{2} \cdot \left(P_{jack} - P_{dead}\right) \cdot len \cdot 12 \cdot 2$ $area_{tris} = 1.14 \times 10^3$ kip-in

Given

$area_{tris} + x \cdot (len \cdot 12) = \Delta S \cdot Apt_d \cdot Ept_d$

$rh := \text{Find}(x) \rightarrow 7.5075508666443219600$ $rh = 7.508$ kips

$P_{sl} := rh + 2\cdot\left(P_{jack} - P_{dead}\right)$ $P_{sl} = 10.661$ kips

$P_{live} := P_{jack} - P_{sl}$ $P_{live} = 121.53$ kips

$P_{dead2} := P_{dead} - rh$ $P_{dead2} = 123.11$ kips

$P_{avg} := \frac{P_{live} + P_{dead2}}{2}$ $P_{avg} = 122.32$ kips

Initial state of internal equilibrium, assuming

1) No tendon eccentricity
2) Self-weight causes no significant stresses

$Nd_o + Nptd_o = 0$

$Nptd_o := P_{avg}$ $Nptd_o = 122.32$ kips $Nd_o := -Nptd_o$ $Nd_o = -122.32$ kips

Relaxation in deck post-tensioning strands from transfer to composite action

Average stress in tendons $f_{pt} := \frac{P_{avg}}{Apt_d}$ $f_{pt} = 199.87$

$t_i := t_{hcomp}$ $t := t_{dcomp} - t_{dpt}$

$t_i = 0.75$ $t = 5$

$\Delta f_{pR1} := \frac{-f_{pt}}{K_{Lpr}}\cdot\left(\frac{f_{pt}}{f_{py}} - 0.55\right)\cdot\frac{\log(24\cdot t)}{\log\left(24\cdot t_i\right)}$ $\Delta f_{pR1} = -2.005$

$\varepsilon sh_{d1} := SHRINKAGE\left(fc_d, t_{dpt}, t_{dcomp}, hum, A_d, perim_d\right)$ $\varepsilon sh_{d1} = -0.00000774$

$\phi_{d1} := CREEP\left(fc_d, t_{dpt}, t_{dcomp}, hum, A_d, perim_d\right)$ $\phi_{d1} = 0.096$

$$deqns1 := \begin{bmatrix} \frac{-\left(1 + \mu_d\cdot\phi_{d1}\right)}{A_d\cdot E_d} & 0 & 1 & 0 \\ 0 & -1 & 0 & Apt_d\cdot Ept_d \\ 1 & 1 & 0 & 0 \\ 0 & 0 & 1 & -1 \end{bmatrix} \qquad dvar1 := \begin{pmatrix} \Delta Nd_1 \\ \Delta Nptd_1 \\ \Delta\varepsilon d_1 \\ \Delta\varepsilon ptd_1 \end{pmatrix}$$

$$dans1 := \begin{pmatrix} \frac{Nd_o}{A_d \cdot E_d} \cdot \phi_{d1} + \varepsilon sh_{d1} \\ -\Delta f_{pR1} \cdot Apt_d \\ 0 \\ 0 \end{pmatrix}$$

$$dvalues1 := deqns1^{-1} \cdot dans1$$

$$dvalues1 = \begin{pmatrix} 1.4343626 \\ -1.4343626 \\ -0.0000119 \\ -0.0000119 \end{pmatrix}$$

$\Delta Nd_1 := dvalues1_1$ $\quad \Delta Nd_1 = 1.434$

$\Delta Nptd_1 := dvalues1_2$ $\quad \Delta Nptd_1 = -1.434$

$\Delta \varepsilon d_1 := dvalues1_3$ $\quad \Delta \varepsilon d_1 = -0.0000119$

$\Delta \varepsilon ptd_1 := dvalues1_4$ $\quad \Delta \varepsilon ptd_1 = -0.0000119$

deck should be losing compression --> +

PT strands should be losing tension --> -

b) D/SG 2: Calculate redistribution of stresses in composite section from when it's made composite to any time in the future

$\varepsilon sh_{h2} := SHRINKAGE(fc_h, t_{hcomp}, t_{hinf}, hum, A_h, perim_h)$ $\quad \varepsilon sh_{h2} = -0.000345$

$\phi_{h2} := CREEP(fc_h, t_{hcomp}, t_{hinf}, hum, A_h, perim_h)$ $\quad \phi_{h2} = 1.411$

$\varepsilon sh_{d2} := SHRINKAGE(fc_d, t_{dcomp}, t_{dinf}, hum, A_d, perim_d)$ $\quad \varepsilon sh_{d2} = -0.000147$

$\phi_{d2} := CREEP(fc_d, t_{dcomp}, t_{dinf}, hum, A_d, perim_d)$ $\quad \phi_{d2} = 0.873$

Need to establish all starting values based on results of previous stages: variables with subscript "oc" indicate starting values for composite stage

Initial moment at midspan of steel girder is due to self-weight only:

$w_g := A_g \cdot \frac{0.490}{12^3}$ $\quad w_g = 0.009$ kip/in

$$Mg_{self} := \frac{w_g \cdot L_g^{\,2}}{8} \qquad Mg_{self} = 556.76 \quad \text{kip-in}$$

Need to add deck weight moment to girder:

$$w_{dself} := A_{dws} \cdot \frac{0.150}{12^3} \qquad w_{dself} = 0.056 \quad \text{kip/in}$$

$$Md_{self} := \frac{w_{dself} \cdot L_g^{\,2}}{8} \qquad Md_{self} = 3645 \quad \text{kip-in}$$

Check deck weight moment...

Stresses in girder due to deck weight only:

$$\sigma_{top} := -\frac{Md_{self} \cdot (depth_g - c_g)}{I_g} \qquad \sigma_{bot} := \frac{Md_{self} \cdot c_g}{I_g}$$

all stress values in ksi, positive indicates tension

$\sigma_{top} = -14.88$ $\qquad$ $\sigma_{bot} = 14.88$

Strains in girder due to deck weight only:

$$\varepsilon_{top} := \frac{\sigma_{top}}{E_g} \cdot 10^6 \qquad \varepsilon_{bot} := \frac{\sigma_{bot}}{E_g} \cdot 10^6$$

all strain values in microstrain/inch

$\varepsilon_{top} = -513.2$ $\qquad$ $\varepsilon_{bot} = 513.2$

Moment in girder due to deck weight only (kip-in):

$$\phi_d := \frac{\varepsilon_{bot} - \varepsilon_{top}}{depth_g} \qquad \phi_d = 41.9$$

$$Mg_{fromdeck} := \phi_d \cdot 10^{-6} \cdot E_g \cdot I_g \qquad Mg_{fromdeck} = 3645$$

Revise starting values for composite analysis to include girder and deck weights (kips and in)

$$Mg_{oc} := Mg_{self} + Mg_{fromdeck} \qquad Mg_{oc} = 4201.76$$

$$Nd_{oc} := Nd_o + \Delta Nd_1 \qquad Nd_{oc} = -120.885$$

$$Nptd_{oc} := Nptd_o + \Delta Nptd_1 \qquad Nptd_{oc} = 120.885$$

$Nd_o = -122.319$

$Nptd_o = 122.319$

Relaxation in deck post-tensioning strands from composite action to end of service life

$f_{pt2} := Nptd_{oc}$ $\quad t := t_{dinf} - t_{dcomp}$ $\quad t_i := t_{dcomp}$

$t = 9940$ $\quad t_i = 60$

$$\Delta f_{pR2} := \frac{-f_{pt2}}{K_{Lpr}} \cdot \left(\frac{f_{pt2}}{f_{py}} - 0.55 \right) \cdot \frac{\log(24 \cdot t)}{\log(24 \cdot t_i)} \qquad \Delta f_{pR2} = 0.24$$

Calculations for system after it becomes composite

$$a := \frac{t_d}{2} + \frac{t_h}{2} \qquad b := \frac{t_d}{2} + t_h + (depth_g - c_g)$$

$a = 4.75$ $\quad b = 17.5$

$$coeff1 := \begin{bmatrix} 1 & 1 & 1 & 1 & 0 & 0 & 0 & 0 & 0 & 0 & 0 & 0 \\ 0 & a & b & 0 & 1 & 1 & 1 & 0 & 0 & 0 & 0 & 0 \\ 0 & 0 & 0 & 0 & 0 & 0 & 0 & 1 & 0 & 0 & -1 & 0 \\ 0 & 0 & 0 & 0 & 0 & 0 & 0 & 1 & -1 & 0 & 0 & a \\ 0 & 0 & 0 & 0 & 0 & 0 & 0 & 1 & 0 & -1 & 0 & b \\ \frac{-(1 + \mu_d \cdot \phi_{d2})}{A_d \cdot E_d} & 0 & 0 & 0 & 0 & 0 & 0 & 1 & 0 & 0 & 0 & 0 \\ 0 & 0 & \frac{-1}{A_g \cdot E_g} & 0 & 0 & 0 & 0 & 0 & 0 & 1 & 0 & 0 \\ 0 & \frac{-(1 + \mu_h \cdot \phi_{h2})}{A_h \cdot E_h} & 0 & 0 & 0 & 0 & 0 & 0 & 1 & 0 & 0 & 0 \end{bmatrix} \qquad vars12 := \begin{pmatrix} \Delta N_d \\ \Delta N_h \\ \Delta N_g \\ \Delta N_{ptd} \\ \Delta M_d \\ \Delta M_h \\ \Delta M_g \\ \Delta \varepsilon_d \\ \Delta \varepsilon_h \\ \Delta \varepsilon_g \\ \Delta \varepsilon_{ptd} \\ \Delta \chi \end{pmatrix}$$

$$coeff2 := \begin{bmatrix} 0 & 0 & 0 & -1 & 0 & 0 & 0 & 0 & 0 & 0 & Apt_d \cdot Ept_d & 0 \\ 0 & 0 & 0 & 0 & \frac{-(1 + \mu_d \cdot \phi_{d2})}{I_d \cdot E_d} & 0 & 0 & 0 & 0 & 0 & 0 & 1 \\ 0 & 0 & 0 & 0 & 0 & \frac{-(1 + \mu_h \cdot \phi_{h2})}{I_h \cdot E_h} & 0 & 0 & 0 & 0 & 0 & 1 \\ 0 & 0 & 0 & 0 & 0 & 0 & \frac{-1}{I_g \cdot E_g} & 0 & 0 & 0 & 0 & 1 \end{bmatrix}$$

coeffs := stack(coeff1, coeff2)

$$\text{coeffs} = \begin{pmatrix} 1 & 1 & 1 & 1 & 0 & 0 & 0 & 0 & 0 & 0 & 0 & \\ 0 & 4.75 & 17.5 & 0 & 1 & 1 & 1 & 0 & 0 & 0 & 0 & \\ 0 & 0 & 0 & 0 & 0 & 0 & 0 & 1 & 0 & 0 & -1 & \\ 0 & 0 & 0 & 0 & 0 & 0 & 0 & 1 & -1 & 0 & 0 & 4 \\ 0 & 0 & 0 & 0 & 0 & 0 & 0 & 1 & 0 & -1 & 0 & 1 \\ -0.0000007 & 0 & 0 & 0 & 0 & 0 & 0 & 1 & 0 & 0 & 0 & \\ 0 & 0 & -0.0000011 & 0 & 0 & 0 & 0 & 0 & 0 & 1 & 0 & \\ 0 & -0.0000548 & 0 & 0 & 0 & 0 & 0 & 0 & 1 & 0 & 0 & \\ 0 & 0 & 0 & -1 & 0 & 0 & 0 & 0 & 0 & 0 & 17442 & \\ 0 & 0 & 0 & 0 & -0.0000001 & 0 & 0 & 0 & 0 & 0 & 0 & \\ 0 & 0 & 0 & 0 & 0 & -0.0006576 & 0 & 0 & 0 & 0 & 0 & \\ 0 & 0 & 0 & 0 & 0 & 0 & -0 & 0 & 0 & 0 & 0 & \end{pmatrix}$$

$$\text{values12} := \begin{pmatrix} 0 \\ 0 \\ 0 \\ 0 \\ 0 \\ \frac{\text{Nd}_{oc}}{A_d \cdot E_d} \cdot \phi_{d2} + \varepsilon\text{sh}_{d2} \\ 0 \\ \varepsilon\text{sh}_{h2} \\ -\Delta f_{pR2} \cdot \text{Apt}_d \\ 0 \\ 0 \\ 0 \end{pmatrix} \qquad \text{values12} = \begin{pmatrix} 0 \\ 0 \\ 0 \\ 0 \\ 0 \\ -0.00019 \\ 0 \\ -0.00035 \\ -0.14705 \\ 0 \\ 0 \\ 0 \end{pmatrix}$$

$$\text{answers} := \text{coeffs}^{-1} \cdot \text{values12}$$

$$\text{answers} = \begin{pmatrix} 37.8626981 \\ 3.88202348 \\ -39.0102763 \\ -2.73444528 \\ 63.63738876 \\ 0.01049826 \\ 600.59233676 \\ -0.0001652 \\ -0.00013241 \\ -0.0000444 \\ -0.0001652 \\ 0.0000069 \end{pmatrix} \qquad \text{vars12} := \begin{pmatrix} \Delta N_d \\ \Delta N_h \\ \Delta N_g \\ \Delta N_{ptd} \\ \Delta M_d \\ \Delta M_h \\ \Delta M_g \\ \Delta \varepsilon_d \\ \Delta \varepsilon_h \\ \Delta \varepsilon_g \\ \Delta \varepsilon_{ptd} \\ \Delta \chi \end{pmatrix}$$

$Mg_f := Mg_{oc} + answers_7$ $\quad Mg_f = 4802.35$ kip-in

$Nd_f := Nd_{oc} + answers_1$ $\quad Nd_f = -83.02$ kips

$Nptd_f := Nptd_{oc} + answers_4$ $\quad Nptd_f = 118.15$ kips

$\chi_f := answers_{12}$ $\quad \chi_f = 6.9 \times 10^{-6}$ strain/inch

Define values for plot of strain throughout composite cross-section

$\Delta\varepsilon_d := answers_8$

$\Delta\varepsilon_h := answers_9$

$\Delta\varepsilon_g := answers_{10}$

$\Delta\varepsilon_{botg} := \Delta\varepsilon_g + \chi_f \cdot c_g$ $\quad \Delta\varepsilon_{botg} = 4.017 \times 10^{-5}$

$\Delta\varepsilon_{topg} := \Delta\varepsilon_g - \chi_f \cdot (depth_g - c_g)$ $\quad \Delta\varepsilon_{topg} = -1.29 \times 10^{-4}$

$\Delta\varepsilon_{both} := \Delta\varepsilon_h + \chi_f \cdot \frac{t_h}{2}$ $\quad \Delta\varepsilon_{both} = -1.29 \times 10^{-4}$

$\Delta\varepsilon_{toph} := \Delta\varepsilon_h - \chi_f \cdot \frac{t_h}{2}$ $\quad \Delta\varepsilon_{toph} = -1.359 \times 10^{-4}$

$\Delta\varepsilon_{botd} := \Delta\varepsilon_d + \chi_f \cdot \frac{t_d}{2}$ $\quad \Delta\varepsilon_{botd} = -1.359 \times 10^{-4}$

$\Delta\varepsilon_{topd} := \Delta\varepsilon_d - \chi_f \cdot \frac{t_d}{2}$ $\Delta\varepsilon_{topd} = -1.945 \times 10^{-4}$

$y_{botg} := 0$ $y_{botg} = 0$

$y_{topg} := depth_g$ $y_{topg} = 24.5$

$y_{both} := y_{topg}$ $y_{both} = 24.5$

$y_{toph} := y_{topg} + t_h$ $y_{toph} = 25.5$

$y_{botd} := depth_g + t_h$ $y_{botd} = 25.5$

$y_{topd} := depth_t$ $y_{topd} = 34$

$$microstrains := 10^6 \cdot \begin{pmatrix} \Delta\varepsilon_{topd} \\ \Delta\varepsilon_d \\ \Delta\varepsilon_{botd} \\ \Delta\varepsilon_h \\ \Delta\varepsilon_g \\ \Delta\varepsilon_{botg} \end{pmatrix} \qquad depth := \begin{pmatrix} y_{topd} \\ y_d \\ y_{botd} \\ y_h \\ c_g \\ y_{botg} \end{pmatrix}$$

$$microstrains = \begin{pmatrix} -194.5 \\ -165.2 \\ -135.9 \\ -132.4 \\ -44.4 \\ 40.2 \end{pmatrix} \qquad depth = \begin{pmatrix} 34 \\ 29.75 \\ 25.5 \\ 25 \\ 12.25 \\ 0 \end{pmatrix}$$

$$ms2 := \begin{pmatrix} microstrains_1 \\ 0 \end{pmatrix} \qquad depth2 := \begin{pmatrix} y_{topd} \\ y_{topd} \end{pmatrix}$$

$$ms2 = \begin{pmatrix} -194.544 \\ 0 \end{pmatrix} \qquad depth2 = \begin{pmatrix} 34 \\ 34 \end{pmatrix}$$

Graph of strains in composite section

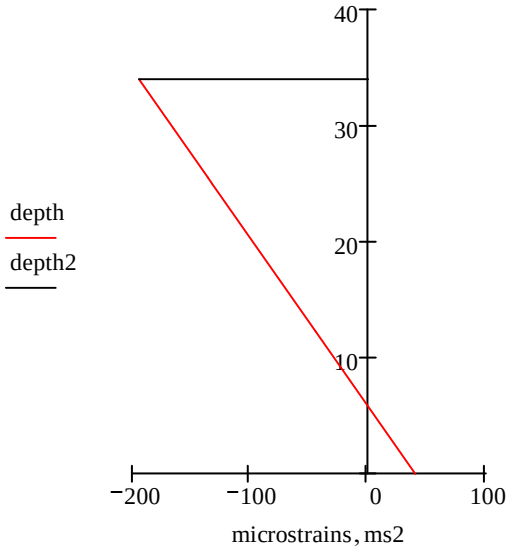

Define values for plot of stress throughout composite cross-section

Stresses in steel:

$$stress_g := \begin{pmatrix} \Delta\varepsilon_{topg} \cdot E_g \\ \Delta\varepsilon_g \cdot E_g \\ \Delta\varepsilon_{botg} \cdot E_g \end{pmatrix} \qquad stress_g = \begin{pmatrix} -3.74 \\ -1.287 \\ 1.165 \end{pmatrix} \qquad depths_g := \begin{pmatrix} y_{topg} \\ c_g \\ y_{botg} \end{pmatrix}$$

$\Delta N_d := answers_1$ $\quad \Delta N_d = 37.86$

$\Delta N_h := answers_2$ $\quad \Delta N_h = 3.882$

$\Delta M_d := answers_5$ $\quad \Delta M_d = 63.64$

$\Delta M_h := answers_6$ $\quad \Delta M_h = 0.0105$

$Nd_o = -122.319$

$Nd_{oc} = -120.885$

$Nd_f = -83.022$

Stresses in concrete:

$$stress_d := \begin{bmatrix} \frac{Nd_{oc} + \Delta N_d}{A_d} - \frac{\Delta M_d \cdot \left(\frac{t_d}{2}\right)}{I_d} \\ \frac{Nd_{oc} + \Delta N_d}{A_d} + 0 \\ \frac{Nd_{oc} + \Delta N_d}{A_d} + \frac{\Delta M_d \cdot \left(\frac{t_d}{2}\right)}{I_d} \end{bmatrix} \qquad stress_d = \begin{pmatrix} -0.209 \\ -0.136 \\ -0.062 \end{pmatrix} \qquad depths_d := \begin{pmatrix} y_{topd} \\ y_d \\ y_{botd} \end{pmatrix}$$

$$stress_h := \begin{bmatrix} \frac{\Delta N_h}{A_h} - \frac{\Delta M_h \cdot \left(\frac{t_h}{2}\right)}{I_h} \\ \frac{\Delta N_h}{A_h} + 0 \\ \frac{\Delta N_h}{A_h} + \frac{\Delta M_h \cdot \left(\frac{t_h}{2}\right)}{I_h} \end{bmatrix} \qquad stress_h = \begin{pmatrix} 0.424 \\ 0.431 \\ 0.438 \end{pmatrix} \qquad depths_h := \begin{pmatrix} y_{toph} \\ y_h \\ y_{both} \end{pmatrix}$$

$$depths_{hz1} := \begin{pmatrix} y_{topd} \\ y_{topd} \end{pmatrix} \qquad stress_{hz1} := \begin{pmatrix} stress_{d_1} \\ 0 \end{pmatrix}$$

$$depths_{hz2} := \begin{pmatrix} y_{botd} \\ y_{toph} \end{pmatrix} \qquad stress_{hz2} := \begin{pmatrix} stress_{d_3} \\ stress_{h_1} \end{pmatrix}$$

$$depths_{hz3} := \begin{pmatrix} y_{both} \\ y_{topg} \end{pmatrix} \qquad stress_{hz3} := \begin{pmatrix} stress_{h_3} \\ stress_{g_1} \end{pmatrix}$$

Graph of stresses in composite section (ksi)

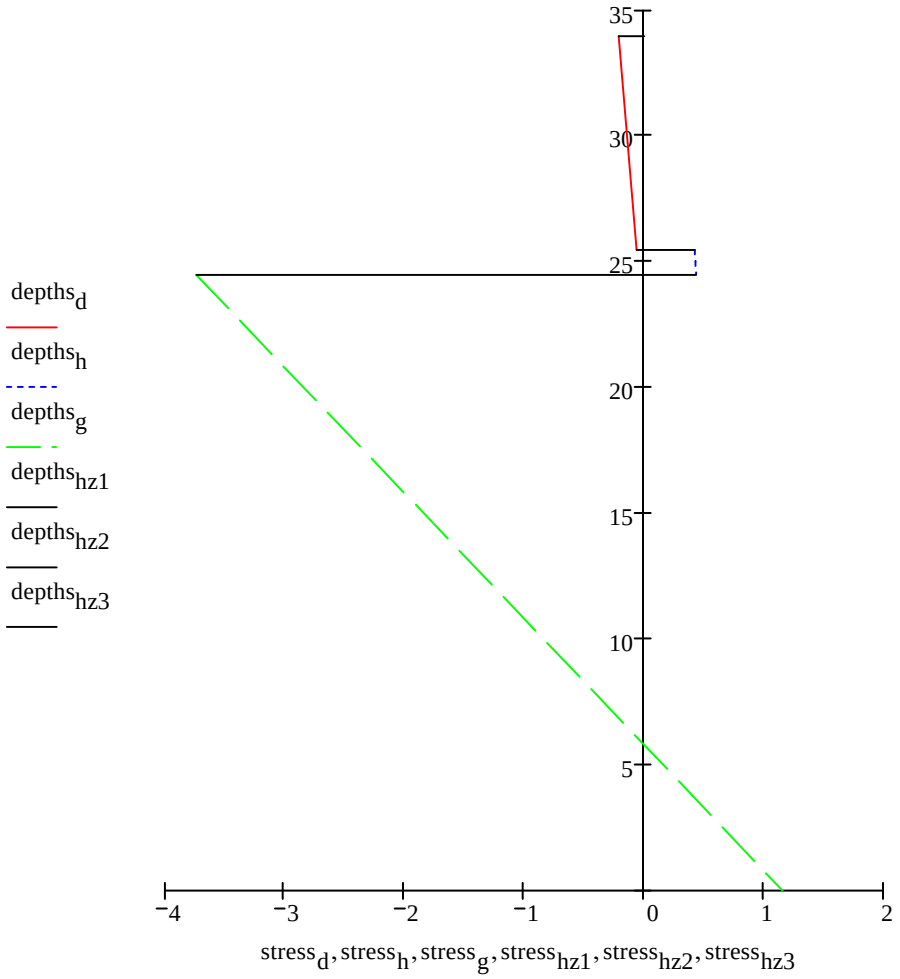

Conclusions for simple span with steel girder

Initial compression in deck (ksi)

$$\sigma simple_{initial} := \frac{Nd_o}{A_d}$$

$$\sigma simple_{initial} = -0.2 \quad \text{ksi}$$

Final compression at top, middle, & bottom of deck (ksi)

$$stress_d = \begin{pmatrix} -0.209 \\ -0.136 \\ -0.062 \end{pmatrix} \quad \text{ksi}$$

ORIGIN := 1

Deck Panel Prestress Losses:
Precast Concrete Deck with Concrete Girder, Simple Span
Parametric Study: PCBT-37, 6' spc., 40' span

Inputs (data to be entered is under blue headings)

a) Concrete girder and prestressing strand properties

Girder section properties - general

$depth_g := 37$ $topw_g := 47$ $perim_g := 203.65$ $L_g := 40 \cdot 12$

$c_g := 18.43$ $A_g := 690.7$ $I_g := 126000$

$fc_g := 7000$ $\mu_g := 0.7$

Girder prestressing strand properties

$numstr_g := 14$ $Astr_g := 0.153$ $Eps_g := 28500$ $K_{Lpr} := 45$

$f_{pu} := 270$ $y_{ps} := 2.25$ $f_{pj\%} := 0.75$

Girder time intervals

$t_{gcast} := 1$ $t_{gcomp} := 60$ $t_{ginf} := 10000$

Calculated properties - girder

$E_g := 57 \cdot \sqrt{fc_g}$

$E_g = 4769$

Calculated properties - P/S strand

$Aps_g := numstr_g \cdot Astr_g$ $e_g := c_g - y_{ps}$ $f_{pj} := f_{pj\%} \cdot f_{pu}$ $f_{py} := 0.9 \cdot f_{pu}$

$Aps_g = 2.14$ $e_g = 16.18$ $f_{pj} = 202.5$ $f_{py} = 243$

b) Concrete deck and post-tensioning strand properties

Deck section properties

$t_d := 8$ $w_d := 72$ $\mu_d := 0.7$ $fc_d := 5000$

Post tensioning strand properties

$numstr_{dpt} := 6$ $Astr_d := 0.153$ $Ept_d := 28500$

Deck time intervals

$t_{dpt} := 55$ $t_{dcomp} := t_{gcomp}$ $t_{dinf} := t_{ginf}$

Calculated properties - deck

$A_d := t_d \cdot w_d$ $I_d := \frac{w_d \cdot t_d^3}{12}$ $E_d := 57 \cdot \sqrt{fc_d}$ $perim_d := 2 \cdot w_d$ $A_{dws} := (t_d + 0.5) \cdot w_d$

$A_d = 576$ $I_d = 3072$ $E_d = 4031$ $perim_d = 144$ $A_{dws} = 612$

Calculated properties - P/T strand

$Apt_d := numstr_{dpt} \cdot Astr_d$

$Apt_d = 0.92$

c) Haunch properties

Haunch section properties

$t_h := 1$ $\mu_h := 0.7$ $fc_h := fc_d$

Haunch time intervals

$t_{hcomp} := 0.75$ $t_{hinf} := t_{ginf}$

Calculated properties - haunch

$w_h := topw_g$ $A_h := t_h \cdot topw_g$ $I_h := \frac{w_h \cdot t_h^3}{12}$ $E_h := E_d$ $perim_h := 2 \cdot t_h$

$w_h = 47$ $A_h = 47$ $I_h = 3.92$ $E_h = 4031$ $perim_h = 2$

d) General properties

$hum := 70$

$n := \frac{Eps_g}{E_g}$

e) Composite section properties

$y_h := depth_g + \frac{t_h}{2}$ $\quad y_h = 37.5$

$y_d := depth_g + t_h + \frac{t_d}{2}$ $\quad y_d = 42$

$depth_t := depth_g + t_h + t_d$ $\quad depth_t = 46$

Calculated net section properties - girder

$A_{gn} := A_g - Aps_g$ $\quad A_{gn} = 688.56$

$c_{gn} := \frac{A_g \cdot c_g - Aps_g \cdot y_{ps}}{A_{gn}}$ $\quad c_{gn} = 18.48$

$I_{gn} := I_g + A_g \cdot (c_{gn} - c_g)^2 - Aps_g \cdot (c_g - y_{ps})^2$ $\quad I_{gn} = 125440.99$

$e_{gn} := c_{gn} - y_{ps}$ $\quad e_{gn} = 16.23$

Calculated transformed section properties - girder

$A_{pstr} := Aps_g \cdot (n - 1)$ $\quad A_{pstr} = 10.66$

$A_{gtr} := A_g + A_{pstr}$ $\quad A_{gtr} = 701.36$

$c_{gtr} := \frac{A_g \cdot c_g + A_{pstr} \cdot y_{ps}}{A_g + A_{pstr}}$ $\quad c_{gtr} = 18.18$

$I_{gtr} := I_g + A_g \cdot (c_g - c_{gtr})^2 + A_{pstr} \cdot (c_{gtr} - y_{ps})^2$ $\quad I_{gtr} = 128748.01$

$e_{gtr} := c_{gtr} - y_{ps}$ $\quad e_{gtr} = 15.93$

Creep and Shrinkage Models (from AASHTO LRFD 2006 Interims)

$$\text{CREEP}(fci, t1, t2, hum, area, perim) := \left| \begin{array}{l} ktd2 \leftarrow \dfrac{(t2 - t1)}{61 - \left(\dfrac{4 \cdot fci}{1000}\right) + (t2 - t1)} \\ kla \leftarrow t1^{-0.118} \\ khc \leftarrow 1.56 - (0.008 \cdot hum) \\ kvs \leftarrow \max\left[1.45 - 0.13 \cdot \left(\dfrac{area}{perim}\right), 0\right] \\ kf \leftarrow \dfrac{5}{1 + \dfrac{fci}{1000}} \\ creep \leftarrow 1.90 \cdot ktd2 \cdot kla \cdot kvs \cdot khc \cdot kf \\ creep \end{array} \right.$$

$$\text{SHRINKAGE}(fci, t1, t2, hum, area, perim) := \left| \begin{array}{l} ktd1 \leftarrow \dfrac{t1}{61 - \left(\dfrac{4 \cdot fci}{1000}\right) + t1} \\ ktd2 \leftarrow \dfrac{t2}{61 - \left(\dfrac{4 \cdot fci}{1000}\right) + t2} \\ khs \leftarrow 2 - (0.014 \cdot hum) \\ kvs \leftarrow \max\left[1.45 - 0.13 \cdot \left(\dfrac{area}{perim}\right), 0\right] \\ kf \leftarrow \dfrac{5}{1 + \dfrac{fci}{1000}} \\ shrink \leftarrow -480 \cdot 10^{-6} \cdot (ktd2 - ktd1) \cdot kvs \cdot khs \cdot kf \\ shrink \end{array} \right.$$

Sign Convention:
Tension = Lengthening = (+)
Compression = (-)

Outline of calculation steps for a precast, prestressed girder with precast, post-tensioned deck panels

a) D/CG 1: Calculate redistribution of stresses in girder from transfer to composite action with deck

b) D/CG 2: Calculate redistribution of stresses in deck from post-tensioning to composite action with girder

c) D/CG 3: Calculate redistribution of stresses in composite section from when it's made composite to any time in the future

a) D/CG 1: Calculate redistribution of stresses in girder from transfer to composite action with deck

Moment at midspan due to girder self-weight only:

$w_g := A_g \cdot \frac{0.150}{12^3}$ $w_g = 0.06$ kips/inch

$Mg_{self} := \frac{w_g \cdot L_g^2}{8}$ $Mg_{self} = 1726.75$ k-in

Jacking force in prestressing strand:

$P_{jack} := f_{pj} \cdot Aps_g$ $P_{jack} = 433.75$ kips

Initial force in prestressing strand (jacking force minus ES losses):

$f_{cgp} := \frac{P_{jack}}{A_{gtr}} + \frac{P_{jack} \cdot e_{gtr}^2}{I_{gtr}} - \frac{Mg_{self} \cdot e_{gtr}}{I_{gtr}}$ $f_{cgp} = 1.26$ ksi

$P_i := P_{jack} - \left(n \cdot f_{cgp} \cdot Aps_g\right)$ $P_i = 417.62$ kips

$Nps_o := P_i$ $Nps_o = 417.6$ kips

Initial force in net concrete section is equal to initial force in prestressing strand:

$Ng_o := -Nps_o$ $Ng_o = -417.6$ kips

Sum moments about net centroid of girder to get initial moment at midspan:

$$-Mg_o + Mg_{self} - Nps_o \cdot e_{gn} = 0$$

$$Mg_o := Mg_{self} - Nps_o \cdot e_{gn} \qquad Mg_o = -5051.4 \text{ kip-in}$$

CHECK Mgo using a curvature approach...

$$\sigma_{top} := -\frac{P_{jack}}{A_{gtr}} + \frac{P_{jack} \cdot e_{gtr} \cdot (depth_g - c_{gtr})}{I_{gtr}} - \frac{Mg_{self} \cdot (depth_g - c_{gtr})}{I_{gtr}} \qquad \sigma_{top} = 0.14$$

$$\sigma_{bot} := -\frac{P_{jack}}{A_{gtr}} - \frac{P_{jack} \cdot e_{gtr} \cdot c_{gtr}}{I_{gtr}} + \frac{Mg_{self} \cdot c_{gtr}}{I_{gtr}} \qquad \sigma_{bot} = -1.35$$

$$\sigma_{cgs} := -\frac{P_{jack}}{A_{gtr}} - \frac{P_{jack} \cdot e_{gtr}^2}{I_{gtr}} + \frac{Mg_{self} \cdot e_{gtr}}{I_{gtr}} \qquad \sigma_{cgs} = -1.26$$

all stress values in ksi, compression

$$\varepsilon_{top} := \frac{\sigma_{top}}{E_g} \cdot 10^6 \qquad \varepsilon_{bot} := \frac{\sigma_{bot}}{E_g} \cdot 10^6 \qquad \varepsilon_{cgs} := \frac{\sigma_{cgs}}{E_g} \cdot 10^6$$

$$\varepsilon_{top} = 29.2 \qquad \varepsilon_{bot} = -283.2 \qquad \varepsilon_{cgs} = -264.2$$

all strain values in microstrain/inch

Initial force in strand:

$$P_{strand} := P_{jack} - \left(\left| \varepsilon_{cgs} \right| \cdot 10^{-6} \cdot Eps_g \cdot Aps_g \right) \qquad P_{strand} = 417.6 \text{ kips}$$

Initial force in concrete at net cg:

$$\sigma_{conc} := -\frac{P_{jack}}{A_{gtr}} + \frac{P_{jack} \cdot e_{gtr} \cdot (c_{gn} - c_{gtr})}{I_{gtr}} - \frac{Mg_{self} \cdot (c_{gn} - c_{gtr})}{I_{gtr}} \qquad \sigma_{conc} = -0.61$$

$$P_{conc} := \sigma_{conc} \cdot A_{gn} \qquad P_{conc} = -417.6 \text{ kips}$$

Moment in concrete:

$M = \phi \cdot E \cdot I \qquad \phi := \frac{\varepsilon_{bot} - \varepsilon_{top}}{depth_g} \qquad \phi = -8.44$

$M_{conc} := \phi \cdot 10^{-6} \cdot E_g \cdot I_{gn} \qquad M_{conc} = -5051.6 \quad \text{kip-in}$

Relaxation in girder prestressing strands from transfer to composite action

Average stress in tendons $f_{pt} := \frac{Nps_o}{Aps_g} \qquad f_{pt} = 194.97$

$t_i := t_{gcast} \qquad t := t_{gcomp}$

$t_i = 1 \qquad t = 60$

$\Delta f_{pR1} := \frac{-f_{pt}}{K_{Lpr}} \cdot \left(\frac{f_{pt}}{f_{py}} - 0.55 \right) \cdot \frac{\log(24 \cdot t)}{\log(24 \cdot t_i)} \qquad \Delta f_{pR1} = -2.5 \quad \text{ksi}$

Girder time interval 1: Girder shrinkage & creep from transfer to deck placement

$\varepsilon sh_{g1} := SHRINKAGE(fc_g, t_{gcast}, t_{gcomp}, hum, A_g, perim_g) \qquad \varepsilon sh_{g1} = -0.00019$

$\phi_{g1} := CREEP(fc_g, t_{gcast}, t_{gcomp}, hum, A_g, perim_g) \qquad \phi_{g1} = 0.77$

$$geqns1 := \begin{bmatrix} 1 & 1 & 0 & 0 & 0 & 0 \\ 0 & e_g & 1 & 0 & 0 & 0 \\ \frac{-(1 + \mu_g \cdot \phi_{g1})}{E_g \cdot A_{gn}} & 0 & 0 & 1 & 0 & 0 \\ 0 & -1 & 0 & 0 & Aps_g \cdot Eps_g & 0 \\ 0 & 0 & 0 & 1 & -1 & e_g \\ 0 & 0 & \frac{-(1 + \mu_g \cdot \phi_{g1})}{E_g \cdot I_{gn}} & 0 & 0 & 1 \end{bmatrix} \qquad gvar1 := \begin{pmatrix} \Delta Ng1 \\ \Delta Npsg1 \\ \Delta Mg1 \\ \Delta \varepsilon g1 \\ \Delta \varepsilon psg1 \\ \Delta \chi g1 \end{pmatrix}$$

$$gans1 := \begin{pmatrix} 0 \\ 0 \\ \frac{Ng_o}{E_g \cdot A_{gn}} \cdot \phi_{g1} + \varepsilon sh_{g1} \\ -\Delta f_{pR1} \cdot Aps_g \\ 0 \\ \frac{Mg_o}{E_g \cdot I_{gn}} \cdot \phi_{g1} \end{pmatrix}$$

Note: Ngo and Mgo both go in as negative values here

$$gvalues1 := geqns1^{-1} \cdot gans1$$

$$gvalues1 = \begin{pmatrix} 27.430574 \\ -27.430574 \\ 443.826692 \\ -0.000275 \\ -0.000362 \\ -0.000005 \end{pmatrix}$$

*Redistribution of stresses in girder from transfer to deck placement

$\Delta Ng_1 := gvalues1_1$ $\quad \Delta Ng_1 = 27.43$

$\Delta Npsg_1 := gvalues1_2$ $\quad \Delta Npsg_1 = -27.43$

$\Delta Mg_1 := gvalues1_3$ $\quad \Delta Mg_1 = 443.83$

$\Delta \varepsilon g_1 := gvalues1_4$ $\quad \Delta \varepsilon g_1 = -0.000275$

$\Delta \varepsilon psg_1 := gvalues1_5$ $\quad \Delta \varepsilon psg_1 = -0.000362$

$\Delta \chi g_1 := gvalues1_6$ $\quad \Delta \chi g_1 = -0.00000535$

b) D/CG 2: Calculate redistribution of stresses in deck from post-tensioning to composite action

Compute state of stress immediately following stressing - use average force in tendons

$P_{jack} := 0.80 \cdot f_{pu}\, numstr_{dpt} \cdot Astr_d$ $P_{jack} = 198.3$ kips

Consider seating losses....

Note: Post-tensioning tendons are straight so only have wobble losses --> k*l term

$\alpha := 0$ $\mu := 0$ $k := 0.0002$ per foot of length $\Delta S := \frac{3}{8}$ inch $len := \frac{L_g}{12}$ $len = 40$

$P_{dead} := P_{jack} \cdot e^{-(\mu \cdot \alpha + k \cdot len)}$ $P_{dead} = 196.7$ kips

$m := \frac{P_{jack} - P_{dead}}{len \cdot 12}$ $m = 0.00329$ kips/inch

$P_{SL} := \frac{\Delta S \cdot Apt_d \cdot Ept_d}{len \cdot 12}$ $P_{SL} = 20.44$ kips

$P_{live} := P_{jack} - P_{SL}$ $P_{live} = 177.85$ kips

$x_{AS} := \frac{\sqrt{\frac{\Delta S \cdot Apt_d \cdot Ept_d}{m}}}{12}$ $x_{AS} = 143.87$ feet

Note xAS is longer than the bridge...revise approach for finding Pavg

$area_{tris} := \frac{1}{2} \cdot (P_{jack} - P_{dead}) \cdot len \cdot 12 \cdot 2$ $area_{tris} = 758.39$ kip-in

Given

$area_{tris} + x \cdot (len \cdot 12) = \Delta S \cdot Apt_d \cdot Ept_d$

$rh := Find(x) \rightarrow 18.859868079211078270$ $rh = 18.86$ kips

$P_{sl} := rh + 2 \cdot (P_{jack} - P_{dead})$ $P_{SL} = 20.44$ kips

$P_{live} := P_{jack} - P_{sl}$ $P_{live} = 176.27$ kips

$P_{dead2} := P_{dead} - rh$ $P_{dead2} = 177.85$ kips

$P_{avg} := \frac{P_{live} + P_{dead2}}{2}$ $P_{avg} = 177.06$ kips

Initial state of internal equilibrium, assuming

1) No tendon eccentricity
2) Self-weight causes no significant stresses

$Nd_o + Nptd_o = 0$

$Nptd_o := P_{avg}$ $Nptd_o = 177.06$ kips $Nd_o := -Nptd_o$ $Nd_o = -177.06$ kips

Relaxation in deck post-tensioning strands from transfer to composite action

Average stress in tendons $f_{pt2} := \frac{P_{avg}}{Apt_d}$ $f_{pt2} = 192.87$

$t_i := t_{hcomp}$ $t := t_{dcomp} - t_{dpt}$

$t_i = 0.75$ $t = 5$

$\Delta f_{pR2} := \frac{-f_{pt2}}{K_{Lpr}} \cdot \left(\frac{f_{pt2}}{f_{py}} - 0.55 \right) \cdot \frac{\log(24 \cdot t)}{\log(24 \cdot t_i)}$ $\Delta f_{pR2} = -1.73$ ksi

$\varepsilon sh_{d2} := SHRINKAGE(fc_d, t_{dpt}, t_{dcomp}, hum, A_d, perim_d)$ $\varepsilon sh_{d2} = -0.00000802$

$\phi_{d2} := CREEP(fc_d, t_{dpt}, t_{dcomp}, hum, A_d, perim_d)$ $\phi_{d2} = 0.1$

$$deqns2 := \begin{bmatrix} \frac{-(1 + \mu_d \cdot \phi_{d2})}{A_d \cdot E_d} & 0 & 1 & 0 \\ 0 & -1 & 0 & Apt_d \cdot Ept_d \\ 1 & 1 & 0 & 0 \\ 0 & 0 & 1 & -1 \end{bmatrix} \qquad dvar2 := \begin{pmatrix} \Delta Nd2 \\ \Delta Nptd2 \\ \Delta \varepsilon d2 \\ \Delta \varepsilon ptd2 \end{pmatrix}$$

$$dans2 := \begin{pmatrix} \frac{Nd_o}{A_d \cdot E_d} \cdot \phi_{d2} + \varepsilon sh_{d2} \\ -\Delta f_{pR2} \cdot Apt_d \\ 0 \\ 0 \end{pmatrix} \qquad dvalues2 := deqns2^{-1} \cdot dans2 \qquad dvalues2 = \begin{pmatrix} 1.9734866 \\ -1.9734866 \\ -0.0000147 \\ -0.0000147 \end{pmatrix}$$

$\Delta Nd_2 := dvalues2_1$ $\Delta Nd_2 = 1.97$

$\Delta Nptd_2 := dvalues2_2$ $\Delta Nptd_2 = -1.97$

$\Delta \varepsilon d_2 := dvalues2_3$ $\Delta \varepsilon d_2 = -0.0000147$

$\Delta \varepsilon ptd_2 := dvalues2_4$ $\Delta \varepsilon ptd_2 = -0.0000147$

c) D/CG 3: Calculate redistribution of stresses in composite section from when it's made composite to any time in the future

$\varepsilon sh_{g3} := SHRINKAGE(fc_g, t_{gcomp}, t_{ginf}, hum, A_g, perim_g)$ $\varepsilon sh_{g3} = -0.000109$

$\phi_{g3} := CREEP(fc_g, t_{gcomp}, t_{ginf}, hum, A_g, perim_g)$ $\phi_{g3} = 0.74$

$\varepsilon sh_{h3} := SHRINKAGE(fc_h, t_{hcomp}, t_{hinf}, hum, A_h, perim_h)$ $\varepsilon sh_{h3} = 0$

$\phi_{h3} := CREEP(fc_h, t_{hcomp}, t_{hinf}, hum, A_h, perim_h)$ $\phi_{h3} = 0$

$\varepsilon sh_{d3} := SHRINKAGE(fc_d, t_{dcomp}, t_{dinf}, hum, A_d, perim_d)$ $\varepsilon sh_{d3} = -0.000152$

$\phi_{d3} := CREEP(fc_d, t_{dcomp}, t_{dinf}, hum, A_d, perim_d)$ $\phi_{d3} = 0.905$

Need to establish all starting values based on results of previous stages: variables with subscript "pr" (prime) indicate starting values for composite stage

$Mg_{opr} := Mg_o + \Delta Mg_1$ $Mg_{opr} = -4607.6$

$Ng_{opr} := Ng_o + \Delta Ng_1$ $Ng_{opr} = -390.2$

$Nps_{opr} := Nps_o + \Delta Npsg_1$ $Nps_{opr} = 390.2$

$Nd_{opr} := Nd_o + \Delta Nd_2$ $Nd_{opr} = -175.1$

$Nptd_{opr} := Nptd_o + \Delta Nptd_2$ $Nptd_{opr} = 175.1$

Need to add deck weight moment to girder

$w_{dself} := A_{dws} \cdot \frac{0.150}{12^3}$ $w_{dself} = 0.05$ kip/in

$$Md_{self} := \frac{w_{dself} \cdot L_g^{\,2}}{8} \qquad Md_{self} = 1530 \quad \text{kip-in}$$

Stresses in girder due to deck weight only:

$$\sigma_{top} := -\frac{Md_{self} \cdot (depth_g - c_{gtr})}{I_{gtr}} \qquad \sigma_{top} = -0.22$$

$$\sigma_{bot} := \frac{Md_{self} \cdot c_{gtr}}{I_{gtr}} \qquad \sigma_{bot} = 0.22$$

$$\sigma_{cgs} := \frac{Md_{self} \cdot (c_{gtr} - y_{ps})}{I_{gtr}} \qquad \sigma_{cgs} = 0.19$$

all stress values in ksi, positive indicates tension

$$\varepsilon_{top} := \frac{\sigma_{top}}{E_g} \cdot 10^6 \qquad \varepsilon_{bot} := \frac{\sigma_{bot}}{E_g} \cdot 10^6 \qquad \varepsilon_{cgs} := \frac{\sigma_{cgs}}{E_g} \cdot 10^6$$

$\varepsilon_{top} = -46.9$ $\varepsilon_{bot} = 45.3$ $\varepsilon_{cgs} = 39.7$

all strain values in microstrain/inch

Force in girder strands due to deck weight only (kips):

$$P_{strcomp} := \varepsilon_{cgs} \cdot 10^{-6} \cdot Eps_g \cdot Aps_g \qquad P_{strcomp} = 2.4 \quad \text{kips}$$

Force in girder concrete at net cg due to deck weight only (kips):

$$\sigma_{conc} := \frac{Md_{self} \cdot (c_{gtr} - c_{gn})}{I_{gtr}} \qquad \sigma_{conc} = -0.00352$$

$$P_{conccomp} := \sigma_{conc} \cdot A_{gn} \qquad P_{conccomp} = -2.4 \quad \text{kips}$$

Moment in girder concrete due to deck weight only (kip-in):

$$\phi_d := \frac{\varepsilon_{bot} - \varepsilon_{top}}{depth_g} \qquad \phi_d = 2.49$$

$$M_{gfromdeck} := \phi_d \cdot 10^{-6} \cdot E_g \cdot I_{gn} \qquad M_{gfromdeck} = 1490.7$$

Revise starting values for composite analysis to include deck weight

$Mg_{oc} := Mg_{opr} + M_{gfromdeck}$ $\quad Mg_{oc} = -3116.9$

$Ng_{oc} := Ng_{opr} + P_{conccomp}$ $\quad Ng_{oc} = -392.62$

$Nps_{oc} := Nps_{opr} + P_{strcomp}$ $\quad Nps_{oc} = 392.62$

$Nd_{oc} := Nd_{opr}$ $\quad Nd_{oc} = -175.08$

$Nptd_{oc} := Nptd_{opr}$ $\quad Nptd_{oc} = 175.08$

Relaxation in girder prestressing strands from composite action to end of service life

$f_{pt3} := \frac{Nps_{oc}}{Aps_g}$ $\quad f_{pt3} = 183.29$

$t_i := t_{gcomp}$ $\quad t := t_{ginf}$

$t_i = 60$ $\quad t = 10000$

$\Delta f_{pR3} := \frac{-f_{pt3}}{K_{Lpr}} \cdot \left(\frac{f_{pt3}}{f_{py}} - 0.55 \right) \cdot \frac{\log(24 \cdot t)}{\log(24 \cdot t_i)}$ $\quad \Delta f_{pR3} = -1.42$ ksi

Relaxation in deck post-tensioning strands from composite action to end of service life

$f_{pt4} := \frac{Nptd_{oc}}{Apt_d}$ $\quad f_{pt4} = 190.72$

$t_i := t_{dcomp}$ $\quad t := t_{dinf}$

$t_i = 60$ $\quad t = 10000$

$\Delta f_{pR4} := \frac{-f_{pt4}}{K_{Lpr}} \cdot \left(\frac{f_{pt4}}{f_{py}} - 0.55 \right) \cdot \frac{\log(24 \cdot t)}{\log(24 \cdot t_i)}$ $\quad \Delta f_{pR4} = -1.7$ ksi

Calculations for system after it becomes composite

$a := \frac{t_d}{2} + \frac{t_h}{2}$ $\quad b := \frac{t_d}{2} + t_h + (depth_g - c_{gtr})$ $\quad c := \frac{t_d}{2} + t_h + (depth_g - y_{ps})$

$a = 4.5$ $\quad b = 23.82$ $\quad c = 39.75$

$$\text{coeff1} := \begin{pmatrix} 1 & 1 & 1 & 1 & 1 & 0 & 0 & 0 & 0 & 0 & 0 & 0 & 0 & 0 \\ 0 & 0 & a & b & c & 1 & 1 & 1 & 0 & 0 & 0 & 0 & 0 & 0 \\ 0 & 0 & 0 & 0 & 0 & 0 & 0 & 0 & 1 & -1 & 0 & 0 & 0 & 0 \\ 0 & 0 & 0 & 0 & 0 & 0 & 0 & 0 & 1 & 0 & -1 & 0 & 0 & a \\ 0 & 0 & 0 & 0 & 0 & 0 & 0 & 0 & 1 & 0 & 0 & -1 & 0 & b \\ 0 & 0 & 0 & 0 & 0 & 0 & 0 & 0 & 1 & 0 & 0 & 0 & -1 & c \end{pmatrix}$$

$$\text{cf2} := \begin{bmatrix} \frac{-\left(1+\mu_d\cdot\phi_{d3}\right)}{E_d\cdot A_d} & 0 & 0 & 0 & 0 & 0 & 0 & 0 & 1 & 0 & 0 & 0 & 0 & 0 \\ 0 & 0 & 0 & 0 & 0 & \frac{-\left(1+\mu_d\cdot\phi_{d3}\right)}{E_d\cdot I_d} & 0 & 0 & 0 & 0 & 0 & 0 & 0 & 1 \\ 0 & 0 & 0 & \frac{-\left(1+\mu_g\cdot\phi_{g3}\right)}{E_g\cdot A_g} & 0 & 0 & 0 & 0 & 0 & 0 & 0 & 1 & 0 & 0 \\ 0 & 0 & 0 & 0 & 0 & 0 & 0 & \frac{-\left(1+\mu_g\cdot\phi_{g3}\right)}{E_g\cdot I_g} & 0 & 0 & 0 & 0 & 0 & 1 \\ 0 & -1 & 0 & 0 & 0 & 0 & 0 & 0 & 0 & \text{Apt}_d\cdot\text{Ept}_d & 0 & 0 & 0 & 0 \\ 0 & 0 & \frac{-\left(1+\mu_h\cdot\phi_{h3}\right)}{E_h\cdot A_h} & 0 & 0 & 0 & 0 & 0 & 0 & 0 & 1 & 0 & 0 & 0 \end{bmatrix}$$

$\text{coeff2} := \text{cf2}$ (Note: The matrix variable name above had to be shortened to fix the matrix on the page for printing purposes)

$$\text{coeff3} := \begin{bmatrix} 0 & 0 & 0 & 0 & -1 & 0 & 0 & 0 & 0 & 0 & 0 & \text{Aps}_g\cdot\text{Eps}_g & 0 \\ 0 & 0 & 0 & 0 & 0 & 0 & \frac{-\left(1+\mu_h\cdot\phi_{h3}\right)}{E_h\cdot I_h} & 0 & 0 & 0 & 0 & 0 & 0 & 1 \end{bmatrix}$$

$$\text{values14} := \begin{pmatrix} 0 \\ 0 \\ 0 \\ 0 \\ 0 \\ 0 \\ \frac{Nd_{oc}}{A_d \cdot E_d} \cdot \phi_{d3} + \varepsilon sh_{d3} \\ 0 \\ \frac{Ng_{oc}}{A_g \cdot E_g} \cdot \phi_{g3} + \varepsilon sh_{g3} \\ \frac{Mg_{oc}}{E_g \cdot I_g} \cdot \phi_{g3} \\ -\Delta f_{pR4} \cdot Apt_d \\ \varepsilon sh_{h3} \\ -\Delta f_{pR3} \cdot Aps_g \\ 0 \end{pmatrix} \qquad \text{values14} = \begin{pmatrix} 0 \\ 0 \\ 0 \\ 0 \\ 0 \\ 0 \\ -0.000221 \\ 0 \\ -0.000196 \\ -0.000004 \\ 1.556702 \\ 0 \\ 3.036427 \\ 0 \end{pmatrix} \qquad \text{unknowns14} := \begin{pmatrix} \Delta Nd \\ \Delta Nptd \\ \Delta Nh \\ \Delta Ng \\ \Delta Npsg \\ \Delta Md \\ \Delta Mh \\ \Delta Mg \\ \Delta \varepsilon d \\ \Delta \varepsilon ptd \\ \Delta \varepsilon h \\ \Delta \varepsilon g \\ \Delta \varepsilon psg \\ \Delta \chi \end{pmatrix}$$

$$\text{coeffs} := \text{stack}(\text{coeff1}, \text{coeff2}, \text{coeff3})$$

$$\text{coeffs} = \begin{pmatrix} 1 & 1 & 1 & 1 & 1 & 0 & 0 & 0 & 0 & 0 & 0 & 0 & 0 & 0 \\ 0 & 0 & 4.5 & 23.8159 & 39.75 & 1 & 1 & 1 & 0 & 0 & 0 & 0 & 0 & 0 \\ 0 & 0 & 0 & 0 & 0 & 0 & 0 & 0 & 1 & -1 & 0 & 0 & 0 & 0 \\ 0 & 0 & 0 & 0 & 0 & 0 & 0 & 0 & 1 & 0 & -1 & 0 & 0 & 4.5 \\ 0 & 0 & 0 & 0 & 0 & 0 & 0 & 0 & 1 & 0 & 0 & -1 & 0 & 23.8159 \\ 0 & 0 & 0 & 0 & 0 & 0 & 0 & 0 & 1 & 0 & 0 & 0 & -1 & 39.75 \\ -0 & 0 & 0 & 0 & 0 & 0 & 0 & 0 & 1 & 0 & 0 & 0 & 0 & 0 \\ 0 & 0 & 0 & 0 & 0 & -0 & 0 & 0 & 0 & 0 & 0 & 0 & 0 & 1 \\ 0 & 0 & 0 & -0 & 0 & 0 & 0 & 0 & 0 & 0 & 0 & 1 & 0 & 0 \\ 0 & 0 & 0 & 0 & 0 & 0 & 0 & -0 & 0 & 0 & 0 & 0 & 0 & 1 \\ 0 & -1 & 0 & 0 & 0 & 0 & 0 & 0 & 0 & 26163 & 0 & 0 & 0 & 0 \\ 0 & 0 & -0.00001 & 0 & 0 & 0 & 0 & 0 & 0 & 0 & 1 & 0 & 0 & 0 \\ 0 & 0 & 0 & 0 & -1 & 0 & 0 & 0 & 0 & 0 & 0 & 0 & 61047 & 0 \\ 0 & 0 & 0 & 0 & 0 & 0 & -0.00006 & 0 & 0 & 0 & 0 & 0 & 0 & 1 \end{pmatrix}$$

$$unknowns := coeffs^{-1} \cdot values14 \qquad unknowns = \begin{pmatrix} 66.73037071 \\ -6.10269459 \\ -33.89432117 \\ -10.3029355 \\ -16.43041945 \\ -8.70613926 \\ -0.01812849 \\ 1059.73152115 \\ -0.00017376 \\ -0.00017376 \\ -0.00017892 \\ -0.00020111 \\ -0.0002194 \\ -0.00000115 \end{pmatrix} \qquad unknowns14 := \begin{pmatrix} \Delta Nd \\ \Delta Nptd \\ \Delta Nh \\ \Delta Ng \\ \Delta Npsg \\ \Delta Md \\ \Delta Mh \\ \Delta Mg \\ \Delta \varepsilon d \\ \Delta \varepsilon ptd \\ \Delta \varepsilon h \\ \Delta \varepsilon g \\ \Delta \varepsilon psg \\ \Delta \chi \end{pmatrix}$$

$\chi_f := unknowns_{14}$ $\qquad \chi_f = -1.15 \times 10^{-6}$ train/inch

$Nd_f := Nd_{oc} + unknowns_1$ $\qquad Nd_f = -108.35$ kips

$Nptd_f := Nptd_{oc} + unknowns_2$ $\qquad Nptd_f = 168.98$ kips

Define values for plot of strain throughout composite cross-section

$\Delta\varepsilon_d := unknowns_9$ $\qquad \Delta\varepsilon_g := unknowns_{12}$

$\Delta\varepsilon_h := unknowns_{11}$

$\Delta\varepsilon_{botg} := \Delta\varepsilon_g + \chi_f \cdot c_g$ $\qquad \Delta\varepsilon_{botg} = -2.223 \times 10^{-4}$

$\Delta\varepsilon_{topg} := \Delta\varepsilon_g - \chi_f \cdot (depth_g - c_g)$ $\qquad \Delta\varepsilon_{topg} = -1.798 \times 10^{-4}$

$\Delta\varepsilon_{both} := \Delta\varepsilon_h + \chi_f \cdot \frac{t_h}{2}$ $\qquad \Delta\varepsilon_{both} = -1.795 \times 10^{-4}$

$\Delta\varepsilon_{toph} := \Delta\varepsilon_h - \chi_f \cdot \frac{t_h}{2}$ $\qquad \Delta\varepsilon_{toph} = -1.784 \times 10^{-4}$

$\Delta\varepsilon_{botd} := \Delta\varepsilon_d + \chi_f \cdot \frac{t_d}{2}$ $\quad \Delta\varepsilon_{botd} = -1.784 \times 10^{-4}$

$\Delta\varepsilon_{topd} := \Delta\varepsilon_d - \chi_f \cdot \frac{t_d}{2}$ $\quad \Delta\varepsilon_{topd} = -1.692 \times 10^{-4}$

$y_{botg} := 0$ $\quad y_{botg} = 0$

$y_{topg} := depth_g$ $\quad y_{topg} = 37$

$y_{both} := y_{topg}$ $\quad y_{both} = 37$

$y_{toph} := y_{topg} + t_h$ $\quad y_{toph} = 38$

$y_{botd} := depth_g + t_h$ $\quad y_{botd} = 38$

$y_{topd} := depth_t$ $\quad y_{topd} = 46$

$$microstrains := 10^6 \cdot \begin{pmatrix} \Delta\varepsilon_{topd} \\ \Delta\varepsilon_d \\ \Delta\varepsilon_{botd} \\ \Delta\varepsilon_h \\ \Delta\varepsilon_g \\ \Delta\varepsilon_{botg} \end{pmatrix} \qquad depth := \begin{pmatrix} y_{topd} \\ y_d \\ y_{botd} \\ y_h \\ c_g \\ y_{botg} \end{pmatrix}$$

$$microstrains = \begin{pmatrix} -169.2 \\ -173.8 \\ -178.4 \\ -178.9 \\ -201.1 \\ -222.3 \end{pmatrix} \qquad depth = \begin{pmatrix} 46 \\ 42 \\ 38 \\ 37.5 \\ 18.43 \\ 0 \end{pmatrix}$$

$$ms2 := \begin{pmatrix} microstrains_1 \\ 0 \end{pmatrix} \qquad depth2 := \begin{pmatrix} y_{topd} \\ y_{topd} \end{pmatrix}$$

$$ms2 = \begin{pmatrix} -169.16 \\ 0 \end{pmatrix} \qquad depth2 = \begin{pmatrix} 46 \\ 46 \end{pmatrix}$$

Graph of strains in composite section

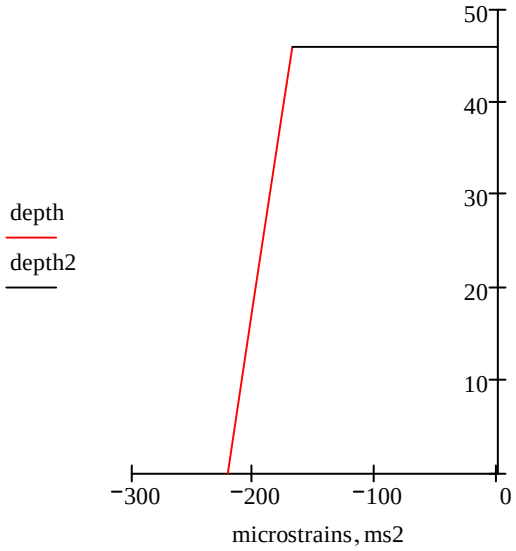

Define values for plot of stress throughout composite cross-section

$\Delta N_d := unknowns_1$ $\Delta N_d = 66.73$ $\Delta M_d := unknowns_6$ $\Delta M_d = -8.71$

$\Delta N_h := unknowns_3$ $\Delta N_h = -33.89$ $\Delta M_h := unknowns_7$ $\Delta M_h = -0.01813$

$\Delta N_g := unknowns_4$ $\Delta N_g = -10.3$ $\Delta M_g := unknowns_8$ $\Delta M_g = 1059.73$

Stresses in concrete:

$$stress_d := \begin{bmatrix} \frac{Nd_{oc} + \Delta N_d}{A_d} - \frac{\Delta M_d \cdot \left(\frac{t_d}{2}\right)}{I_d} \\ \frac{Nd_{oc} + \Delta N_d}{A_d} + 0 \\ \frac{Nd_{oc} + \Delta N_d}{A_d} + \frac{\Delta M_d \cdot \left(\frac{t_d}{2}\right)}{I_d} \end{bmatrix}$$

$$depths_d := \begin{pmatrix} y_{topd} \\ y_d \\ y_{botd} \end{pmatrix}$$

$$stress_d = \begin{pmatrix} -0.177 \\ -0.188 \\ -0.199 \end{pmatrix}$$

$$stress_h := \begin{bmatrix} \frac{\Delta N_h}{A_h} - \frac{\Delta M_h \cdot \left(\frac{t_h}{2}\right)}{I_h} \\ \frac{\Delta N_h}{A_h} + 0 \\ \frac{\Delta N_h}{A_h} + \frac{\Delta M_h \cdot \left(\frac{t_h}{2}\right)}{I_h} \end{bmatrix} \qquad depths_h := \begin{pmatrix} y_{toph} \\ y_h \\ y_{both} \end{pmatrix}$$

$$stress_h = \begin{pmatrix} -0.719 \\ -0.721 \\ -0.723 \end{pmatrix}$$

$$stress_g := \begin{bmatrix} \frac{Ng_{oc} + \Delta N_g}{A_g} - \frac{\Delta M_g \cdot (depth_g - c_g)}{I_g} - \frac{Mg_{oc} \cdot (depth_g - c_g)}{I_g} \\ \frac{Ng_{oc} + \Delta N_g}{A_g} + 0 \\ \frac{Ng_{oc} + \Delta N_g}{A_g} + \frac{\Delta M_g \cdot (c_g)}{I_g} + \frac{Mg_{oc} \cdot (depth_g - c_g)}{I_g} \end{bmatrix} \qquad depths_g := \begin{pmatrix} y_{topg} \\ c_g \\ y_{botg} \end{pmatrix}$$

$$stress_g = \begin{pmatrix} -0.28 \\ -0.583 \\ -0.888 \end{pmatrix}$$

$$depths_{hz1} := \begin{pmatrix} y_{topd} \\ y_{topd} \end{pmatrix} \qquad stress_{hz1} := \begin{pmatrix} stress_{d_1} \\ 0 \end{pmatrix}$$

$$depths_{hz2} := \begin{pmatrix} y_{botd} \\ y_{toph} \end{pmatrix} \qquad stress_{hz2} := \begin{pmatrix} stress_{d_3} \\ stress_{h_1} \end{pmatrix}$$

$$depths_{hz3} := \begin{pmatrix} y_{both} \\ y_{topg} \end{pmatrix} \qquad stress_{hz3} := \begin{pmatrix} stress_{h_3} \\ stress_{g_1} \end{pmatrix}$$

Graph of stresses in composite section (ksi)

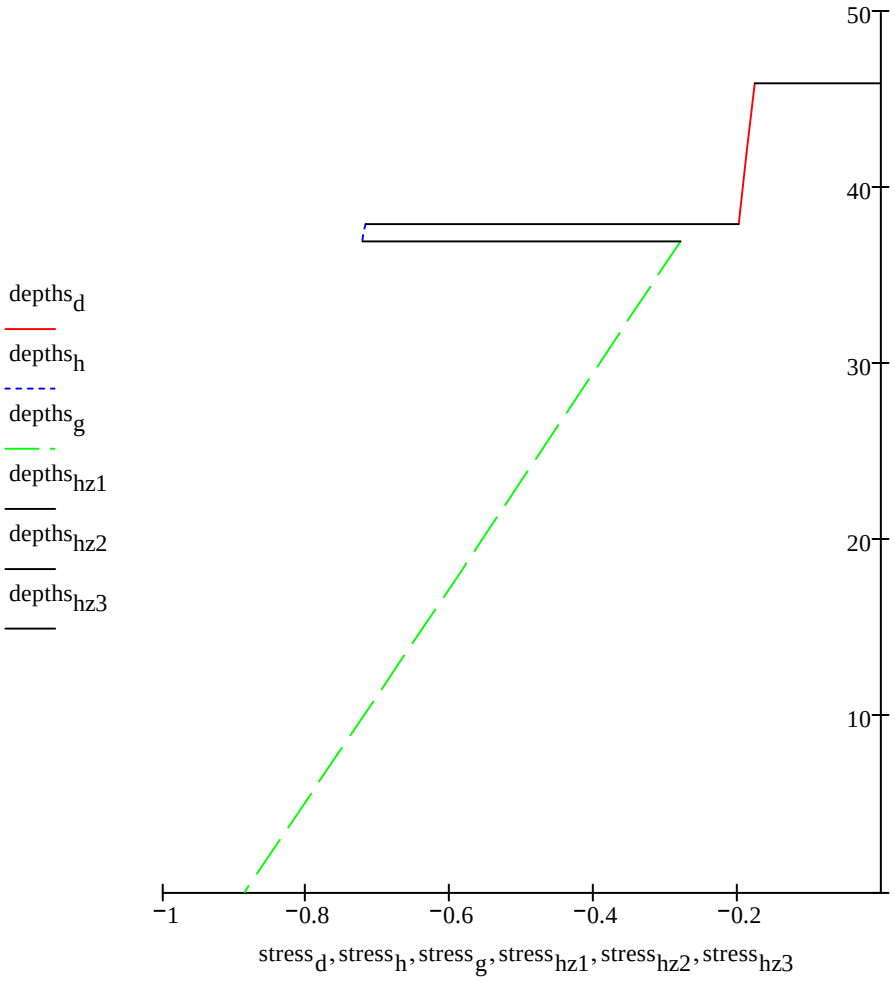

Conclusions for simple span with concrete girder

Initial compression in deck (ksi)

$$\sigma simple_{initial} := \frac{Nd_o}{A_d}$$

$$\sigma simple_{initial} = -0.307 \quad \text{ksi}$$

Final compression at top, middle, & bottom of deck (ksi)

$$stress_d = \begin{pmatrix} -0.177 \\ -0.188 \\ -0.199 \end{pmatrix} \quad \text{ksi}$$

APPENDIX C

Continuous Span Bridge Model Details

C.1: General Procedures

The equations for computing the live load distribution factors for moment in an interior girder were:

Interior girder, moment, two or more lanes loaded:

$$DFM_2 = 0.075 + \left[\left(\frac{S}{9.5} \right)^{0.6} \left(\frac{S}{L} \right)^{0.2} \left(\frac{K_g}{12Lt_s^3} \right)^{0.1} \right] \quad \text{(C.1)}$$

where:

$$K_g = n(I + Ae_g^2) \quad \text{(C.2)}$$

$$e_g = \frac{t_s}{2} + t_h + \frac{d}{2} \quad \text{(C.3)}$$

S = girder spacing, ft

L = span length, ft

t_s = slab thickness, in

n = modular ratio of girder material to deck concrete

A = area

t_h = haunch thickness, in

d = depth of girder, in

Interior girder, moment, one lane loaded:

$$DFM_1 = 0.06 + \left[\left(\frac{S}{14} \right)^{0.4} \left(\frac{S}{L} \right)^{0.3} \left(\frac{K_g}{12Lt_s^3} \right)^{0.1} \right] \quad \text{(C.4)}$$

Interior girder, moment, fatigue:

$$DFM_f = \frac{DFM_1}{m} \quad \text{(C.5)}$$

where:

m = multiple presence factor, which indicates the number of lanes loaded

The largest and therefore controlling one of these three distribution factors for moment was always the DFM_2, which was then used to factor the stress due to live loads in every bridge model.

C.2: Steel Girder Bridges

An example Mathcad model consisting of two continuous 90 ft spans of W36x232 steel girders at 9 ft spacing is provided at the end of this appendix.

C.3: Prestressed Concrete Girder Bridges

An example Mathcad model consisting of three continuous 100 ft spans of AASHTO Type IV prestressed concrete girders at 9 ft spacing is provided at the end of this appendix. Details regarding calculations performed in these models are provided in the following.

The straight strand layout for each prestressed concrete girder in the simple span models was established by filling in the available strand locations in each girder from the bottom up. The center of gravity of the prestressing strands was then calculated for the resulting strand layout in each girder.

The harped strand layout for each prestressed concrete girder in the continuous span analyses was designed using an iterative process in which the number and location of harped strands was adjusted based on allowable and actual stresses at the critical locations along each beam. The number of strands able to be held in each row of each girder type was accounted for in this procedure. The allowable stress limits were:

$$f_{ti} = \frac{3\sqrt{f'_{ci}}}{1000} \tag{C.6}$$

$$f_{ci} = \frac{-0.6 f'_{ci}}{1000} \tag{C.7}$$

where:

f_{ti} = allowable tensile stress, ksi

f'_{ci} = compressive strength of concrete in girder, psi

f_{ci} = allowable compressive stress, ksi

In general, the actual stresses at the supports and harping points were:

$$f_{ti} = \frac{-P_{jack}}{A_{tr}} + \frac{P_{jack} e_{tr} (d - c_{tr})}{I_{tr}} - \frac{M_o (d - c_{tr})}{I_{tr}} \quad \text{(C.8)}$$

$$f_{ci} = \frac{-P_{jack}}{A_{tr}} - \frac{P_{jack} e_{tr} c_{tr}}{I_{tr}} + \frac{M_o c_{tr}}{I_{tr}} \quad \text{(C.9)}$$

where:

f_{ti} = actual tensile stress, ksi

f_{ci} = actual compressive stress, ksi

P_{jack} = jacking force in strands, kips

A_{tr} = transformed area of girder at appropriate cross section, in^2

e_{tr} = transformed eccentricity of prestress at appropriate cross section, in.

d = depth of girder, in.

c_{tr} = centroid of transformed girder at appropriate cross section, in.

I_{tr} = moment of inertia of transformed girder at appropriate cross section, in^4

M_o = initial moment in the girder due to self weight, kip-in (equal to zero at supports)

Figure C.1 illustrates the general layout of each prestressed concrete girder, and Table C.1 provides the corresponding dimensions and strand centers of gravity obtained from the iterative design process explained above.

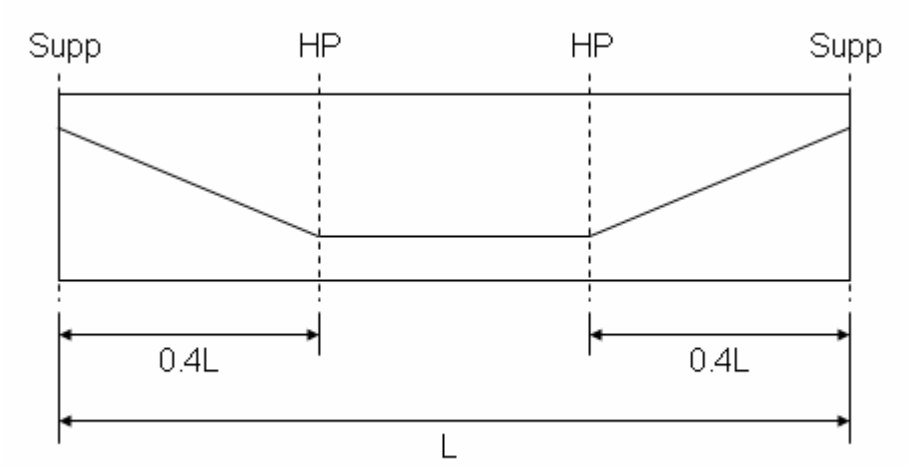

Figure C.1: Layout of each Prestressed Concrete Girder in a Continuous Span

Table C.1: Characteristics of Prestressed Concrete Girders with Harped Strands

Girder Type	Girder Spacing (ft)	Span Length (ft)	No. of ½ in. Dia. Strands	No. of Straight Strands	No. of Harped Strands	Strand cg at Supp (in from bot.)	Strand cg at HP (in from bot.)
PCBT-37	6	40	14	12	2	6.93	2.25
		75	28	24	4	7.64	3.25
	9	40	14	12	2	6.93	2.25
		-	-	-	-	-	-
PCBT-61	6	65	16	14	2	9.34	2.50
		125	50	44	6	10.82	5.21
	9	50	18	16	2	8.78	2.69
		85	28	24	4	11.07	3.25
PCBT-85	6	85	20	18	2	10.72	2.85
		150	50	42	8	16.53	5.21
	9	70	22	20	2	10.14	2.98
		125	44	38	6	14.72	4.52
AASHTO Type II (d = 36")	6	45	8	6	2	10.00	2.00
		70	28	24	4	8.29	4.86
	9	35	8	6	2	10.50	3.50
		55	24	20	4	9.33	5.67
AASHTO Type IV (d = 54")	6	75	16	12	4	14.50	2.50
		120	54	44	10	13.41	5.63
	9	65	18	14	4	13.33	2.67
		100	50	42	8	12.00	5.28
AASHTO Type VI (d = 72")	6	100	22	18	4	14.91	2.91
		160	76	64	12	16.21	7.68
	9	100	30	26	4	12.13	3.60
		140	76	64	12	16.21	7.68

Once the girder designs were complete, the time-dependent analyses were performed as in the concrete girder simple spans, but this time repeated three times for each section (A, B, and C) denoted along each span. The variables used to calculate section properties and other quantities throughout the continuous concrete girder bridge models are defined in Appendix A, with an additional "A," "B," or "C" to denote the cross section under consideration.

The next complication which was unique to the continuous concrete girder bridges involved finding the time-dependent stress induced at the interior support(s). Since these spans did not have the constant curvature of the spans with steel girders, the portion of the force method which required finding the deflection upon removal of the interior support(s) was much more complex. This deflection was found by applying the moment-area method to a graph of the changes in curvature from the D/CG 3 phase at each section along the continuous spans. The graph from the AASHTO Type IV example is shown in Figure C.2.

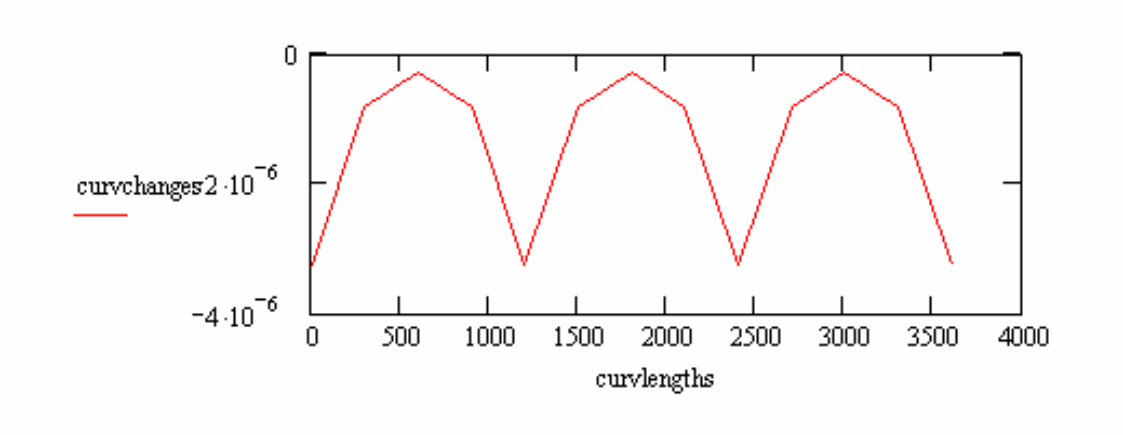

Figure C.2: Change in Curvature during Phase D/CG 3 vs. Length

In this case, the changes in curvature during the D/CG 3 time interval were all negative. However, in other instances, these changes were either all positive or both positive and negative. An Excel spreadsheet was created to expedite the moment-area calculations required to find the initial deflections for each two and three-span continuous concrete girder bridge model.

Following the computation of the initial deflection at the interior support(s), the steps to complete the force method as well as the rest of the models were identical to those described in the previous section for the continuous steel girder bridge models.

ORIGIN := 1

Deck Panel Prestress Losses:
Precast Concrete Deck with Steel Girder, 2 Cont. Spans
Parametric Study: W36x232, 9' spc., 90' span

Inputs (data to be entered is under blue headings)

a) Steel girder properties

Girder section properties - general

$A_g := 68.1$ $I_g := 15000$ $E_g := 29000$ $depth_g := 37.1$

$topw_g := 12.1$ $L_g := 90 \cdot 12$ $c_g := 18.55$

b) Concrete deck and post-tensioning strand properties

Deck section properties

$t_d := 8.5$ $w_d := 108$ $\mu_d := 0.7$ $fc_d := 5000$ $numspans := 2$

Post tensioning strand properties

$numstr_{dpt} := 9$ $Astr_d := 0.153$ $Ept_d := 28500$ $f_{pu} := 270$ $K_{Lpr} := 45$

Deck time intervals

$t_{dpt} := 55$ $t_{dcomp} := 60$ $t_{dinf} := 10000$

Calculated properties - deck

$A_d := t_d \cdot w_d$ $I_d := \frac{w_d \cdot t_d^3}{12}$ $E_d := 57 \cdot \sqrt{fc_d}$ $perim_d := 2 \cdot w_d$ $len := \frac{L_g}{12} \cdot numspans$

$A_d = 918$ $I_d = 5527$ $E_d = 4031$ $perim_d = 216$ $len = 180$

Calculated properties - P/T strand

$A_{dws} := (t_d + 0.5) \cdot w_d$

$Apt_d := numstr_{dpt} \cdot Astr_d$ $f_{py} := 0.9 \cdot f_{pu}$ $A_{dws} = 972$

$Apt_d = 1.377$ $f_{py} = 243$

c) Haunch properties

Haunch section properties

$t_h := 1$ $\mu_h := 0.7$ $fc_h := fc_d$

Haunch time intervals

$t_{hcomp} := 0.75$ $t_{hinf} := t_{dinf}$

Calculated properties - haunch

$w_h := topw_g$ $A_h := t_h \cdot topw_g$ $I_h := \frac{w_h \cdot t_h^3}{12}$ $E_h := E_d$ $perim_h := 2 \cdot t_h$

$w_h = 12.1$ $A_h = 12.1$ $I_h = 1.008$ $E_h = 4031$ $perim_h = 2$

d) General properties

$hum := 70$

e) Composite section properties

$y_h := depth_g + \frac{t_h}{2}$ $y_d := depth_g + t_h + \frac{t_d}{2}$ $y_{ps} := y_d$ $depth_t := depth_g + t_h + t_d$

$y_h = 37.6$ $y_d = 42.35$ $y_{ps} = 42.35$ $depth_t = 46.6$

Creep and Shrinkage Models (from AASHTO LRFD 2006 Interims)

$$\text{CREEP}(fci, t1, t2, hum, area, perim) := \left| \begin{array}{l} ktd2 \leftarrow \dfrac{(t2 - t1)}{61 - \left(\dfrac{4 \cdot fci}{1000}\right) + (t2 - t1)} \\ kla \leftarrow t1^{-0.118} \\ khc \leftarrow 1.56 - (0.008 \cdot hum) \\ kvs \leftarrow \max\left[1.45 - 0.13 \cdot \left(\dfrac{area}{perim}\right), 0\right] \\ kf \leftarrow \dfrac{5}{1 + \dfrac{fci}{1000}} \\ creep \leftarrow 1.90 \cdot ktd2 \cdot kla \cdot kvs \cdot khc \cdot kf \\ creep \end{array} \right.$$

$$\text{SHRINKAGE}(fci, t1, t2, hum, area, perim) := \left| \begin{array}{l} ktd1 \leftarrow \dfrac{t1}{61 - \left(\dfrac{4 \cdot fci}{1000}\right) + t1} \\ ktd2 \leftarrow \dfrac{t2}{61 - \left(\dfrac{4 \cdot fci}{1000}\right) + t2} \\ khs \leftarrow 2 - (0.014 \cdot hum) \\ kvs \leftarrow \max\left[1.45 - 0.13 \cdot \left(\dfrac{area}{perim}\right), 0\right] \\ kf \leftarrow \dfrac{5}{1 + \dfrac{fci}{1000}} \\ shrink \leftarrow -480 \cdot 10^{-6} \cdot (ktd2 - ktd1) \cdot kvs \cdot khs \cdot kf \\ shrink \end{array} \right.$$

Sign Convention:
Tension = Lengthening = (+)
Compression = (-)

Outline of calculation steps for a steel girder with precast, post-tensioned deck panels

a) D/SG 1: Calculate redistribution of stresses in deck from post-tensioning to composite action

b) D/SG 2: Calculate redistribution of stresses in composite section from when it's made composite to any time in the future

a) D/SG 1: Calculate redistribution of stresses in deck from post-tensioning to composite action

Compute state of stress immediately following stressing - use average force in tendons

$P_{jack} := 0.80 \cdot f_{pu}\, numstr_{dpt} \cdot Astr_d$ $P_{jack} = 297.4$ kips

Consider seating losses....

Note: Post-tensioning tendons are straight so only have wobble losses --> k*l term

$\alpha := 0$ $\mu := 0$ $k := 0.0002$ per foot of length $\Delta S := \frac{3}{8}$ inch $len = 180$

$P_{dead} := P_{jack} \cdot e^{-(\mu \cdot \alpha + k \cdot len)}$ $P_{dead} = 286.9$ kips

$m := \frac{P_{jack} - P_{dead}}{len \cdot 12}$ $m = 0.00487$ kips/inch

$x_{AS} := \frac{\sqrt{\frac{\Delta S \cdot Apt_d \cdot Ept_d}{m}}}{12}$ $x_{AS} = 144.88$ feet

Note xAS is NOT LONGER than the bridge...

$P_{SL} := 2 \cdot m \cdot x_{AS} \cdot 12$ $P_{SL} = 16.93$ kips

$P_{live} := P_{jack} - P_{SL}$ $P_{live} = 280.502$ kips

$P_{mid} := P_{jack} - \frac{P_{SL}}{2}$ $P_{mid} = 288.967$ kips

$P_{avg} := \frac{\left(\frac{P_{live} + P_{mid}}{2}\right) \cdot x_{AS} + \left(\frac{P_{mid} + P_{dead}}{2}\right) \cdot (len - x_{AS})}{len}$ $P_{avg} = 285.36$ kips

Initial state of internal equilibrium, assuming
1) No tendon eccentricity
2) Self-weight causes no significant stresses

$Nd_o + Nptd_o = 0$

$Nptd_o := P_{avg}$ $Nptd_o = 285.36$ kips $Nd_o := -Nptd_o$ $Nd_o = -285.36$ kips

Relaxation in deck post-tensioning strands from transfer to composite action

Average stress in tendons $f_{pt} := \frac{P_{avg}}{Apt_d}$ $f_{pt} = 207.23$

$t_i := t_{hcomp}$ $t := t_{dcomp} - t_{dpt}$

$t_i = 0.75$ $t = 5$

$\Delta f_{pR1} := \frac{-f_{pt}}{K_{Lpr}} \cdot \left(\frac{f_{pt}}{f_{py}} - 0.55 \right) \cdot \frac{\log(24 \cdot t)}{\log(24 \cdot t_i)}$ $\Delta f_{pR1} = -2.31$ ksi

$\varepsilon sh_{d1} := SHRINKAGE(fc_d, t_{dpt}, t_{dcomp}, hum, A_d, perim_d)$ $\varepsilon sh_{d1} = -0.00000774$

$\phi_{d1} := CREEP(fc_d, t_{dpt}, t_{dcomp}, hum, A_d, perim_d)$ $\phi_{d1} = 0.096$

$$deqns1 := \begin{bmatrix} \frac{-(1 + \mu_d \cdot \phi_{d1})}{A_d \cdot E_d} & 0 & 1 & 0 \\ 0 & -1 & 0 & Apt_d \cdot Ept_d \\ 1 & 1 & 0 & 0 \\ 0 & 0 & 1 & -1 \end{bmatrix} \qquad dvar1 := \begin{pmatrix} \Delta Nd_1 \\ \Delta Nptd_1 \\ \Delta \varepsilon d_1 \\ \Delta \varepsilon ptd_1 \end{pmatrix}$$

$$dans1 := \begin{pmatrix} \frac{Nd_o}{A_d \cdot E_d} \cdot \phi_{d1} + \varepsilon sh_{d1} \\ -\Delta f_{pR1} \cdot Apt_d \\ 0 \\ 0 \end{pmatrix}$$

$dvalues1 := deqns1^{-1} \cdot dans1$

$$dvalues1 = \begin{pmatrix} 3.7335124 \\ -3.7335124 \\ -0.0000141 \\ -0.0000141 \end{pmatrix}$$

$\Delta Nd_1 := dvalues1_1$ $\quad \Delta Nd_1 = 3.734$

$\Delta Nptd_1 := dvalues1_2$ $\quad \Delta Nptd_1 = -3.734$

$\Delta\varepsilon d_1 := dvalues1_3$ $\quad \Delta\varepsilon d_1 = -0.0000141$

$\Delta\varepsilon ptd_1 := dvalues1_4$ $\quad \Delta\varepsilon ptd_1 = -0.0000141$

deck should be losing compression --> +

PT strands should be losing tension --> -

b) D/SG 2: Calculate redistribution of stresses in composite section from when it's made composite to any time in the future

$\varepsilon sh_{h2} := SHRINKAGE(fc_h, t_{hcomp}, t_{hinf}, hum, A_h, perim_h)$ $\quad \varepsilon sh_{h2} = -0.000265$

$\phi_{h2} := CREEP(fc_h, t_{hcomp}, t_{hinf}, hum, A_h, perim_h)$ $\quad \phi_{h2} = 1.082$

$\varepsilon sh_{d2} := SHRINKAGE(fc_d, t_{dcomp}, t_{dinf}, hum, A_d, perim_d)$ $\quad \varepsilon sh_{d2} = -0.000147$

$\phi_{d2} := CREEP(fc_d, t_{dcomp}, t_{dinf}, hum, A_d, perim_d)$ $\quad \phi_{d2} = 0.873$

Need to establish all starting values based on results of previous stages: variables with subscript "oc" indicate starting values for composite stage

Initial moment at midspan of steel girder is due to self-weight only:

$w_g := A_g \cdot \frac{0.490}{12^3}$ $\quad w_g = 0.019$ kip/in

$Mg_{self} := \frac{w_g \cdot L_g^{\,2}}{8}$ $\quad Mg_{self} = 2815.51$ kip-in

Need to add deck weight moment to girder:

$w_{dself} := A_{dws} \cdot \frac{0.150}{12^3}$ $\quad w_{dself} = 0.084$ kip/in

$Md_{self} := \frac{w_{dself} \cdot L_g^2}{8}$ $Md_{self} = 12301.8$ kip-in

Check deck weight moment...

Stresses in girder due to deck weight only:

$\sigma_{top} := -\frac{Md_{self} \cdot (depth_g - c_g)}{I_g}$ $\sigma_{bot} := \frac{Md_{self} \cdot c_g}{I_g}$

all stress values in ksi, positive indicates tension

$\sigma_{top} = -15.21$ $\sigma_{bot} = 15.21$

Strains in girder due to deck weight only:

$\varepsilon_{top} := \frac{\sigma_{top}}{E_g} \cdot 10^6$ $\varepsilon_{bot} := \frac{\sigma_{bot}}{E_g} \cdot 10^6$

all strain values in microstrain/inch

$\varepsilon_{top} = -524.6$ $\varepsilon_{bot} = 524.6$

Moment in girder due to deck weight only (kip-in):

$\phi_d := \frac{\varepsilon_{bot} - \varepsilon_{top}}{depth_g}$ $\phi_d = 28.28$

$Mg_{fromdeck} := \phi_d \cdot 10^{-6} \cdot E_g \cdot I_g$ $Mg_{fromdeck} = 12301.9$

Revise starting values for composite analysis to include girder and deck weights (kips and in)

$Mg_{oc} := Mg_{self} + Mg_{fromdeck}$ $Mg_{oc} = 15117.38$

$Nd_o = -285.36$

$Nd_{oc} := Nd_o + \Delta Nd_1$ $Nd_{oc} = -281.627$

$Nptd_o = 285.36$

$Nptd_{oc} := Nptd_o + \Delta Nptd_1$ $Nptd_{oc} = 281.627$

Relaxation in deck post-tensioning strands from composite action to end of service life

$f_{pt2} := Nptd_{oc}$ $t := t_{dinf} - t_{dcomp}$ $t_i := t_{dcomp}$

$t = 9940$ $t_i = 60$

$$\Delta f_{pR2} := \frac{-f_{pt2}}{K_{Lpr}} \cdot \left(\frac{f_{pt2}}{f_{py}} - 0.55 \right) \cdot \frac{\log(24 \cdot t)}{\log\left(24 \cdot t_i\right)} \qquad \Delta f_{pR2} = -6.489 \ \text{ksi}$$

Calculations for system after it becomes composite

$$a := \frac{t_d}{2} + \frac{t_h}{2} \qquad b := \frac{t_d}{2} + t_h + \left(depth_g - c_g\right)$$

$$a = 4.75 \qquad b = 23.8$$

$$coeff1 := \begin{bmatrix} 1 & 1 & 1 & 1 & 0 & 0 & 0 & 0 & 0 & 0 & 0 \\ 0 & a & b & 0 & 1 & 1 & 1 & 0 & 0 & 0 & 0 \\ 0 & 0 & 0 & 0 & 0 & 0 & 0 & 1 & 0 & 0 & -1 \\ 0 & 0 & 0 & 0 & 0 & 0 & 0 & 1 & -1 & 0 & 0 \\ 0 & 0 & 0 & 0 & 0 & 0 & 0 & 1 & 0 & -1 & 0 \\ \frac{-\left(1 + \mu_d \cdot \phi_{d2}\right)}{A_d \cdot E_d} & 0 & 0 & 0 & 0 & 0 & 0 & 1 & 0 & 0 & 0 \\ 0 & 0 & \frac{-1}{A_g \cdot E_g} & 0 & 0 & 0 & 0 & 0 & 0 & 1 & 0 \\ 0 & \frac{-\left(1 + \mu_h \cdot \phi_{h2}\right)}{A_h \cdot E_h} & 0 & 0 & 0 & 0 & 0 & 0 & 1 & 0 & 0 \end{bmatrix} \qquad vars12 := \begin{pmatrix} \Delta N_d \\ \Delta N_h \\ \Delta N_g \\ \Delta N_{ptd} \\ \Delta M_d \\ \Delta M_h \\ \Delta M_g \\ \Delta \varepsilon_d \\ \Delta \varepsilon_h \\ \Delta \varepsilon_g \\ \Delta \varepsilon_{ptd} \\ \Delta \chi \end{pmatrix}$$

$$coeff2 := \begin{bmatrix} 0 & 0 & 0 & -1 & 0 & 0 & 0 & 0 & 0 & 0 & Apt_d \cdot Ept_d & 0 \\ 0 & 0 & 0 & 0 & \frac{-\left(1 + \mu_d \cdot \phi_{d2}\right)}{I_d \cdot E_d} & 0 & 0 & 0 & 0 & 0 & 0 & 1 \\ 0 & 0 & 0 & 0 & 0 & \frac{-\left(1 + \mu_h \cdot \phi_{h2}\right)}{I_h \cdot E_h} & 0 & 0 & 0 & 0 & 0 & 1 \\ 0 & 0 & 0 & 0 & 0 & 0 & \frac{-1}{I_g \cdot E_g} & 0 & 0 & 0 & 0 & 1 \end{bmatrix}$$

$$coeffs := stack(coeff1, coeff2)$$

$$\text{coeffs} = \begin{pmatrix} 1 & 1 & 1 & 1 & 0 & 0 & 0 & 0 & 0 & 0 & 0 & 0 \\ 0 & 4.75 & 23.8 & 0 & 1 & 1 & 1 & 0 & 0 & 0 & 0 & 0 \\ 0 & 0 & 0 & 0 & 0 & 0 & 0 & 1 & 0 & 0 & -1 & 0 \\ 0 & 0 & 0 & 0 & 0 & 0 & 0 & 1 & -1 & 0 & 0 & 4.75 \\ 0 & 0 & 0 & 0 & 0 & 0 & 0 & 1 & 0 & -1 & 0 & 23.8 \\ -0.0000004 & 0 & 0 & 0 & 0 & 0 & 0 & 1 & 0 & 0 & 0 & 0 \\ 0 & 0 & -0.0000005 & 0 & 0 & 0 & 0 & 0 & 0 & 1 & 0 & 0 \\ 0 & -0.000036 & 0 & 0 & 0 & 0 & 0 & 0 & 1 & 0 & 0 & 0 \\ 0 & 0 & 0 & -1 & 0 & 0 & 0 & 0 & 0 & 0 & 39244.5 & 0 \\ 0 & 0 & 0 & 0 & -0.0000001 & 0 & 0 & 0 & 0 & 0 & 0 & 1 \\ 0 & 0 & 0 & 0 & 0 & -0.0004325 & 0 & 0 & 0 & 0 & 0 & 1 \\ 0 & 0 & 0 & 0 & 0 & 0 & -0 & 0 & 0 & 0 & 0 & 1 \end{pmatrix}$$

$$\text{values12} := \begin{pmatrix} 0 \\ 0 \\ 0 \\ 0 \\ 0 \\ \frac{Nd_{oc}}{A_d \cdot E_d} \cdot \phi_{d2} + \varepsilon sh_{d2} \\ 0 \\ \varepsilon sh_{h2} \\ -\Delta f_{pR2} \cdot Apt_d \\ 0 \\ 0 \\ 0 \end{pmatrix} \qquad \text{values12} = \begin{pmatrix} 0 \\ 0 \\ 0 \\ 0 \\ 0 \\ -0.00021 \\ 0 \\ -0.00026 \\ 8.93529 \\ 0 \\ 0 \\ 0 \end{pmatrix}$$

$$\text{answers} := \text{coeffs}^{-1} \cdot \text{values12}$$

$$\text{answers} = \begin{pmatrix} 107.03098488 \\ 3.37072098 \\ -94.91282107 \\ -15.48888479 \\ 69.0993659 \\ 0.01155471 \\ 2173.80329612 \\ -0.00016699 \\ -0.00014326 \\ -0.00004806 \\ -0.00016699 \\ 0.000005 \end{pmatrix} \qquad \text{vars12} := \begin{pmatrix} \Delta N_d \\ \Delta N_h \\ \Delta N_g \\ \Delta N_{ptd} \\ \Delta M_d \\ \Delta M_h \\ \Delta M_g \\ \Delta \varepsilon_d \\ \Delta \varepsilon_h \\ \Delta \varepsilon_g \\ \Delta \varepsilon_{ptd} \\ \Delta \chi \end{pmatrix}$$

$Mg_f := Mg_{oc} + answers_7$ $\quad Mg_f = 17291.19$ kip-in

$Nd_f := Nd_{oc} + answers_1$ $\quad Nd_f = -174.6$ kips

$Nptd_f := Nptd_{oc} + answers_4$ $\quad Nptd_f = 266.14$ kips

$\chi_f := answers_{12}$ $\quad \chi_f = 5 \times 10^{-6}$ strain/inch

Define values for plot of strain throughout composite cross-section

$\Delta\varepsilon_d := answers_8$

$\Delta\varepsilon_h := answers_9$

$\Delta\varepsilon_g := answers_{10}$

$\Delta\varepsilon_{botg} := \Delta\varepsilon_g + \chi_f \cdot c_g$ $\quad \Delta\varepsilon_{botg} = 4.464 \times 10^{-5}$

$\Delta\varepsilon_{topg} := \Delta\varepsilon_g - \chi_f \cdot (depth_g - c_g)$ $\quad \Delta\varepsilon_{topg} = -1.408 \times 10^{-4}$

$\Delta\varepsilon_{both} := \Delta\varepsilon_h + \chi_f \cdot \frac{t_h}{2}$ $\quad \Delta\varepsilon_{both} = -1.408 \times 10^{-4}$

$\Delta\varepsilon_{toph} := \Delta\varepsilon_h - \chi_f \cdot \frac{t_h}{2}$ $\quad \Delta\varepsilon_{toph} = -1.458 \times 10^{-4}$

$\Delta\varepsilon_{botd} := \Delta\varepsilon_d + \chi_f \cdot \frac{t_d}{2}$ $\Delta\varepsilon_{botd} = -1.458 \times 10^{-4}$

$\Delta\varepsilon_{topd} := \Delta\varepsilon_d - \chi_f \cdot \frac{t_d}{2}$ $\Delta\varepsilon_{topd} = -1.882 \times 10^{-4}$

$y_{botg} := 0$ $y_{botg} = 0$

$y_{topg} := depth_g$ $y_{topg} = 37.1$

$y_{both} := y_{topg}$ $y_{both} = 37.1$

$y_{toph} := y_{topg} + t_h$ $y_{toph} = 38.1$

$y_{botd} := depth_g + t_h$ $y_{botd} = 38.1$

$y_{topd} := depth_t$ $y_{topd} = 46.6$

$$microstrains := 10^6 \cdot \begin{pmatrix} \Delta\varepsilon_{topd} \\ \Delta\varepsilon_d \\ \Delta\varepsilon_{botd} \\ \Delta\varepsilon_h \\ \Delta\varepsilon_g \\ \Delta\varepsilon_{botg} \end{pmatrix} \qquad depth := \begin{pmatrix} y_{topd} \\ y_d \\ y_{botd} \\ y_h \\ c_g \\ y_{botg} \end{pmatrix}$$

$$microstrains = \begin{pmatrix} -188.2 \\ -167 \\ -145.8 \\ -143.3 \\ -48.1 \\ 44.6 \end{pmatrix} \qquad depth = \begin{pmatrix} 46.6 \\ 42.35 \\ 38.1 \\ 37.6 \\ 18.55 \\ 0 \end{pmatrix}$$

$$ms2 := \begin{pmatrix} microstrains_1 \\ 0 \end{pmatrix} \qquad depth2 := \begin{pmatrix} y_{topd} \\ y_{topd} \end{pmatrix}$$

$$ms2 = \begin{pmatrix} -188.232 \\ 0 \end{pmatrix} \qquad depth2 = \begin{pmatrix} 46.6 \\ 46.6 \end{pmatrix}$$

Graph of strains in composite section

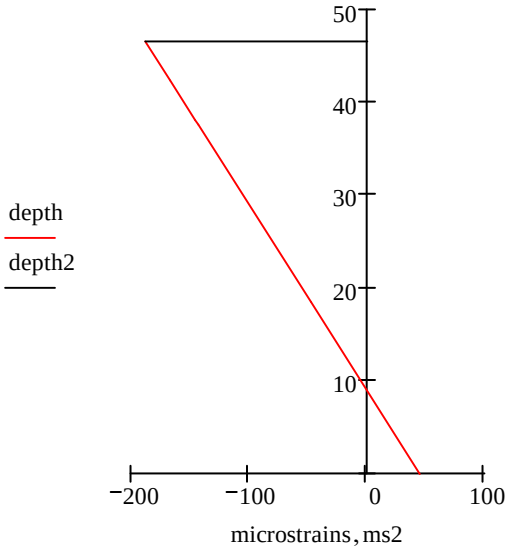

Define values for plot of stress throughout composite cross-section

Stresses in steel:

$$stress_g := \begin{pmatrix} \Delta\varepsilon_{topg} \cdot E_g \\ \Delta\varepsilon_g \cdot E_g \\ \Delta\varepsilon_{botg} \cdot E_g \end{pmatrix} \qquad stress_g = \begin{pmatrix} -4.082 \\ -1.394 \\ 1.295 \end{pmatrix} \qquad depths_g := \begin{pmatrix} y_{topg} \\ c_g \\ y_{botg} \end{pmatrix}$$

$\Delta N_d := answers_1$ $\quad \Delta N_d = 107.03$

$\Delta N_h := answers_2$ $\quad \Delta N_h = 3.371$

$\Delta M_d := answers_5$ $\quad \Delta M_d = 69.1$

$\Delta M_h := answers_6$ $\quad \Delta M_h = 0.01155$

$Nd_o = -285.36$

$Nd_{oc} = -281.627$

$Nd_f = -174.596$

Stresses in concrete:

$$stress_d := \begin{bmatrix} \dfrac{Nd_{oc} + \Delta N_d}{A_d} - \dfrac{\Delta M_d \cdot \left(\frac{t_d}{2}\right)}{I_d} \\ \dfrac{Nd_{oc} + \Delta N_d}{A_d} + 0 \\ \dfrac{Nd_{oc} + \Delta N_d}{A_d} + \dfrac{\Delta M_d \cdot \left(\frac{t_d}{2}\right)}{I_d} \end{bmatrix} \qquad stress_d = \begin{pmatrix} -0.243 \\ -0.19 \\ -0.137 \end{pmatrix} \qquad depths_d := \begin{pmatrix} y_{topd} \\ y_d \\ y_{botd} \end{pmatrix}$$

$$stress_h := \begin{bmatrix} \frac{\Delta N_h}{A_h} - \frac{\Delta M_h \cdot \left(\frac{t_h}{2}\right)}{I_h} \\ \frac{\Delta N_h}{A_h} + 0 \\ \frac{\Delta N_h}{A_h} + \frac{\Delta M_h \cdot \left(\frac{t_h}{2}\right)}{I_h} \end{bmatrix} \qquad stress_h = \begin{pmatrix} 0.273 \\ 0.279 \\ 0.284 \end{pmatrix} \qquad depths_h := \begin{pmatrix} y_{toph} \\ y_h \\ y_{both} \end{pmatrix}$$

$$depths_{hz1} := \begin{pmatrix} y_{topd} \\ y_{topd} \end{pmatrix} \qquad stress_{hz1} := \begin{pmatrix} stress_{d_1} \\ 0 \end{pmatrix}$$

$$depths_{hz2} := \begin{pmatrix} y_{botd} \\ y_{toph} \end{pmatrix} \qquad stress_{hz2} := \begin{pmatrix} stress_{d_3} \\ stress_{h_1} \end{pmatrix}$$

$$depths_{hz3} := \begin{pmatrix} y_{both} \\ y_{topg} \end{pmatrix} \qquad stress_{hz3} := \begin{pmatrix} stress_{h_3} \\ stress_{g_1} \end{pmatrix}$$

Graph of stresses in composite section (ksi)

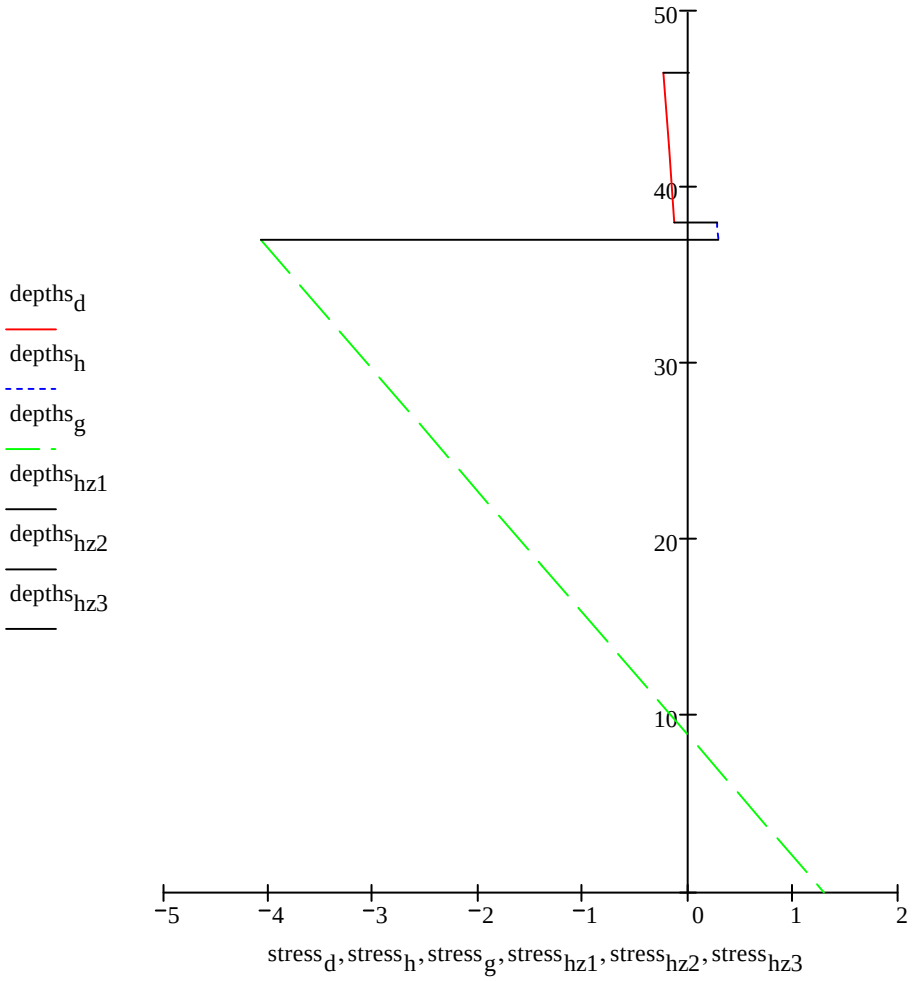

Conclusions for simple span with steel girder

Initial compression at top of deck (ksi)

$$\sigma simple_{initial} := \frac{Nd_o}{A_d}$$

$$\sigma simple_{initial} = -0.311 \quad \text{ksi}$$

Final compression at top, middle, & bottom of deck (ksi)

$$stress_d = \begin{pmatrix} -0.243 \\ -0.19 \\ -0.137 \end{pmatrix} \quad \text{ksi}$$

Add Continuity:
Precast Concrete Deck with Steel Girder, Two Continuous Spans

Find transformed section properties (regular and age adjusted) for composite section including haunch

$\phi_{dc} := \text{CREEP}(fc_d, t_{dcomp}, t_{dinf}, hum, A_d, perim_d)$ $\phi_{dc} = 0.873$

$\phi_{hc} := \text{CREEP}(fc_h, t_{hcomp}, t_{hinf}, hum, A_h, perim_h)$ $\phi_{hc} = 1.082$

Regular transformed section - for use with transient loads

Deck mod. ratio P/T mod. ratio Haunch mod. ratio

$n_{dg} := \frac{E_d}{E_g}$ $n_{pg} := \frac{Ept_d}{E_g}$ $n_{hg} := \frac{E_h}{E_g}$

$n_{dg} = 0.139$ $n_{pg} = 0.983$ $n_{hg} = 0.139$

$Ad_{tr} := n_{dg} \cdot A_d$ $Aps_{tr} := n_{pg} \cdot Apt_d$ $Ah_{tr} := n_{hg} \cdot A_h$

$Ad_{tr} = 127.586$ $Aps_{tr} = 1.353$ $Ah_{tr} = 1.682$

(areas transformed to steel equivalent of that in girder)

$A_{tr} := A_g + Aps_{tr} + Ad_{tr} + Ah_{tr}$ $A_{tr} = 198.7$

$c_{tr} := \frac{A_g \cdot c_g + Aps_{tr} \cdot y_{ps} + Ad_{tr} \cdot y_d + Ah_{tr} \cdot y_h}{A_{tr}}$ $c_{tr} = 34.15$

$I_{tr} := I_g + A_g \cdot (c_{tr} - c_g)^2 + Aps_{tr} \cdot (y_{ps} - c_{tr})^2 + I_d \cdot n_{dg} + Ad_{tr} \cdot (y_d - c_{tr})^2 + I_h \cdot n_{hg} + Ah_{tr} \cdot (y_h - c_{tr})^2$

$I_{tr} = 41031.1$

Age-adjusted transformed section - for use with permanent loads

$E_{daatr} := \frac{E_d}{1 + \mu_d \cdot \phi_{dc}}$ $E_{haatr} := \frac{E_h}{1 + \mu_h \cdot \phi_{hc}}$

$E_{daatr} = 2502$ $E_{haatr} = 2293$

Deck mod. ratio

$$n_{dga} := \frac{E_{daatr}}{E_g}$$

$n_{dga} = 0.0863$

P/T mod. ratio

$$n_{pga} := \frac{Ept_d}{E_g}$$

$n_{pga} = 0.983$

Haunch mod. ratio

$$n_{hga} := \frac{E_{haatr}}{E_g}$$

$n_{hga} = 0.079$

$Ad_{atr} := n_{dga} \cdot A_d$ $\quad Ad_{atr} = 79.193$

$Aps_{atr} := n_{pga} \cdot Apt_d$ $\quad Aps_{atr} = 1.353$

$Ah_{atr} := n_{hga} \cdot A_h$ $\quad Ah_{atr} = 0.957$

(areas transformed to steel equivalent of that in girder)

$A_{atr} := A_g + Aps_{atr} + Ad_{atr} + Ah_{atr}$ $\quad A_{atr} = 149.6$

$$c_{atr} := \frac{A_g \cdot c_g + Aps_{atr} \cdot y_{ps} + Ad_{atr} \cdot y_d + Ah_{atr} \cdot y_h}{A_{atr}} \qquad c_{atr} = 31.49$$

$$I_{atr1} := I_g + A_g \cdot (c_{atr} - c_g)^2 + Aps_{atr} \cdot (y_{ps} - c_{atr})^2 + I_d \cdot n_{dga} + Ad_{atr} \cdot (y_d - c_{atr})^2$$

$$I_{atr2} := I_h \cdot n_{hga} + Ah_{atr} \cdot (y_h - c_{atr})^2$$

$I_{atr} := I_{atr1} + I_{atr2}$ $\quad I_{atr} = 36415.1$

Midspan deflection (downward) due to constant curvature:

$$\Delta = \chi \cdot \frac{L^2}{8}$$

Midspan deflection (upward) due to restoring force P:

$$\Delta = \frac{P \cdot L^3}{48 \cdot E \cdot I}$$

Equate expressions for Δ and solve for P:

$$\chi \cdot \frac{L^2}{8} = \frac{P \cdot L^3}{48 \cdot E \cdot I}$$

Check variable values...

$E_g = 29000$ $I_{atr} = 36415.144$ $L_g = 1080$ $L_t := L_g \cdot 2$ $\chi_f = 4.997 \times 10^{-6}$

$L_t = 2160$

$$P := \frac{48 \cdot E_g \cdot I_{atr} \cdot \chi_f \cdot L_t^{\,2}}{8 \cdot L_t^{\,3}} \qquad P = 14.66 \text{ kips}$$

Maximum negative moment:

$$M_{max} := \frac{P \cdot L_t}{4} \qquad M_{max} = 7916 \text{ kip-in}$$

Stress at top fiber of composite section at middle support
(tensile due to negative M over middle support):

$$\sigma comp_M := \frac{M_{max} \cdot (depth_t - c_{atr})}{I_{atr}} \cdot n_{dga} \qquad \sigma comp_M = 0.28343 \text{ ksi}$$

Stress in top fiber due to force redistribution over time at midspan of a single span:

$$\sigma comp_{Fredist} := stress_{d_1} \qquad \sigma comp_{Fredist} = -0.243 \text{ ksi}$$

Obtain negative moment over middle support from QConBridge (ft-lbs):

$$M_{QCon} := 2.006 \cdot 10^6$$

$$M_{neg} := M_{QCon} \cdot \frac{12}{1000} \qquad M_{neg} = 24072 \text{ kip-in}$$

Stress at top of composite section due to live loads (tension):

$$\sigma comp_{LL} := \frac{|M_{neg}| \cdot (depth_t - c_{tr})}{I_{tr}} \cdot n_{dg} \qquad \sigma comp_{LL} = 1.015 \text{ ksi}$$

Factor LL using DFM and 0.8 Service III factor:

$e_g := \frac{t_d}{2} + t_h + \frac{depth_g}{2}$ $e_g = 23.8$ $n := \frac{E_g}{E_d}$ $n = 7.2$

$K_g := n\cdot\left[I_g + \left(A_g\cdot e_g^{\,2}\right)\right]$ $K_g = 385475.5$

$DFM_2 := 0.075 + \left[\left(\frac{\frac{w_d}{12}}{9.5}\right)^{0.6}\left(\frac{w_d}{L_g}\right)^{0.2}\left(\frac{K_g}{L_g\cdot t_d^{\,3}}\right)^{0.1}\right]$ $DFM_2 = 0.654$

$DFM_1 := 0.06 + \left[\left(\frac{\frac{w_d}{12}}{14}\right)^{0.4}\left(\frac{w_d}{L_g}\right)^{0.3}\left(\frac{K_g}{L_g\cdot t_d^{\,3}}\right)^{0.1}\right]$ $DFM_1 = 0.458$

$mp := 1$

$DFM_f := \frac{DFM_1}{mp}$ $DFM_f = 0.458$

$DFM := \max\left(DFM_2, DFM_1, DFM_f\right)$ $DFM = 0.654$

$\sigma comp_{LLf} := \sigma comp_{LL}\cdot DFM\cdot 0.8$ $\sigma comp_{LLf} = 0.531$ ksi - tension!!!

Conclusions for continuous span with steel girder

Initial compression in deck (ksi)

$\sigma comp_{initial} := \frac{Nd_o}{A_d}$

$\sigma comp_{initial} = -0.311$

Final stress in deck (ksi)

$\sigma comp_{final} := \sigma comp_{Fredist} + \sigma comp_M + \sigma comp_{LLf}$

$\sigma comp_{final} = 0.571$

ORIGIN := 1

Deck Panel Prestress Losses:
Precast Concrete Deck with Concrete Girder, 3 Cont. Spans
Parametric Study: AASHTO Type IV, 9' spc., 100' span

Inputs (data to be entered is under blue headings)

a) Concrete girder and prestressing strand properties

Girder section properties - general

$depth_g := 54$ $topw_g := 20$ $perim_g := 166.43$ $L_g := 100 \cdot 12$

$L_g = 1200$

$c_g := 24.73$ $A_g := 789$ $I_g := 260730$

$fc_g := 7000$ $\mu_g := 0.7$ numspans := 3

Prestressing strand properties

$numstr_g := 50$ $Astr_g := 0.153$ $Eps_g := 28500$ $K_{Lpr} := 45$

$f_{pu} := 270$ $f_{pj\%} := 0.75$

Girder time intervals

$t_{gcast} := 1$ $t_{gcomp} := 60$ $t_{ginf} := 10000$

Calculated properties - girder

$E_g := 57 \cdot \sqrt{fc_g}$ $L_t := L_g \cdot numspans$

$E_g = 4769$ $L_t = 3600$

Calculated properties - P/S strand

$Aps_g := numstr_g \cdot Astr_g$ $f_{pj} := f_{pj\%} \cdot f_{pu}$ $f_{py} := 0.9 \cdot f_{pu}$

$Aps_g = 7.65$ $f_{pj} = 202.5$ $f_{py} = 243$

b) Concrete deck and post-tensioning strand properties

Deck section properties

$t_d := 8$ $w_d := 108$ $\mu_d := 0.7$ $fc_d := 5000$

Post tensioning strand properties

$numstr_{dpt} := 12$ $Astr_d := 0.153$ $Ept_d := 28500$

Deck time intervals

$t_{dpt} := 55$ $t_{dcomp} := t_{gcomp}$ $t_{dinf} := t_{ginf}$

Calculated properties - deck

$A_d := t_d \cdot w_d$ $I_d := \frac{w_d \cdot t_d^3}{12}$ $E_d := 57 \cdot \sqrt{fc_d}$ $perim_d := 2 \cdot w_d$ $len := \frac{L_g}{12} \cdot numspans$

$A_d = 864$ $I_d = 4608$ $E_d = 4031$ $perim_d = 216$ $len = 300$

$A_{dws} := (t_d + 0.5) \cdot w_d$

$A_{dws} = 918$

Calculated properties - P/T strand

$Apt_d := numstr_{dpt} \cdot Astr_d$ $Apt_d = 1.84$

c) Haunch properties

Haunch section properties

$t_h := 1$ $\mu_h := 0.7$ $fc_h := fc_d$

Haunch time intervals

$t_{hcomp} := t_{gcomp}$ $t_{hinf} := t_{ginf}$

Calculated properties - haunch

$w_h := topw_g$ $A_h := t_h \cdot topw_g$ $I_h := \frac{w_h \cdot t_h^3}{12}$ $E_h := E_d$ $perim_h := 2 \cdot t_h$

$w_h = 20$ $A_h = 20$ $I_h = 1.67$ $E_h = 4031$ $perim_h = 2$

d) General properties

$hum := 70$ $\quad n := \frac{Eps_g}{E_g}$ $\quad n = 5.98$

e) Composite section properties

$y_h := depth_g + \frac{t_h}{2}$ $\quad y_d := depth_g + t_h + \frac{t_d}{2}$ $\quad y_{pt} := y_d$ $\quad depth_t := depth_g + t_h + t_d$

$y_h = 54.5$ $\quad y_d = 59$ $\quad y_{pt} = 59$ $\quad depth_t = 63$

f) Sections for analysis of continuous spans

$x_A := 0 \cdot L_g$ $\quad x_A = 0$

$x_B := 0.25 \cdot L_g$ $\quad x_B = 300$

$x_{harp} := 0.4 \cdot L_g$ $\quad x_{harp} = 480$

$x_C := 0.5 \cdot L_g$ $\quad x_C = 600$

$num_{hp} := 8$ $\quad num_{st} := 42$

At section A - support

$$y_{pshpA} := \frac{2 \cdot 52 + 2 \cdot 50 + 2 \cdot 48 + 2 \cdot 46}{num_{hp}} \qquad y_{pshpA} = 49$$

$$y_{psstA} := \frac{12 \cdot 2 + 10 \cdot 4 + 10 \cdot 6 + 8 \cdot 8 + 2 \cdot 10}{num_{st}} \qquad y_{psstA} = 4.95$$

$$y_{psA} := \frac{num_{hp} \cdot y_{pshpA} + num_{st} \cdot y_{psstA}}{numstr_g} \qquad y_{psA} = 12$$

$e_{gA} := c_g - y_{psA}$ $\quad e_{gA} = 12.73$

Calculated net section properties - girder

$A_{gn} := A_g - Aps_g$ $\quad A_{gn} = 781.35$

$Aps_{gst} := num_{st} \cdot Astr_g$ $\quad Aps_{gst} = 6.43$

$Aps_{ghp} := num_{hp} \cdot Astr_g$ $\quad Aps_{ghp} = 1.22$

$c_{gnA} := \frac{A_g \cdot c_g - Aps_g \cdot y_{psA}}{A_{gn}}$ $\quad c_{gnA} = 24.85$

$I_{gnA} := I_g + A_g \cdot (c_g - c_{gnA})^2 - Aps_{gst} \cdot (c_{gnA} - y_{psstA})^2 - Aps_{ghp} \cdot (c_{gnA} - y_{pshpA})^2$

$I_{gnA} = 257483.33$

$e_{gnA} := c_{gnA} - y_{psA}$ $\quad e_{gnA} = 12.85$

Calculated transformed section properties - girder

$A_{pstr} := Aps_g \cdot (n - 1)$ $\quad A_{pstr} = 38.07$

$A_{pstrst} := num_{st} \cdot Astr_g \cdot (n - 1)$ $\quad A_{pstrst} = 31.98$

$A_{pstrhp} := num_{hp} \cdot Astr_g \cdot (n - 1)$ $\quad A_{pstrhp} = 6.09$

$A_{gtr} := A_g + A_{pstr}$ $\quad A_{gtr} = 827.07$

$c_{gtrA} := \frac{A_g \cdot c_g + A_{pstr} \cdot y_{psA}}{A_g + A_{pstr}}$ $\quad c_{gtrA} = 24.14$

$I_{gtrA} := I_g + A_g \cdot (c_g - c_{gtrA})^2 + A_{pstrst} \cdot (c_{gtrA} - y_{psstA})^2 + A_{pstrhp} \cdot (c_{gtrA} - y_{pshpA})^2$

$I_{gtrA} = 276541.56$

$e_{gtrA} := c_{gtrA} - y_{psA}$ $\quad e_{gtrA} = 12.14$

At section B - between support and harping point - at 0.25*L

$y_{pshpB} := 22.75$ $y_{pshpB} = 22.75$

$y_{psstB} := y_{psstA}$ $y_{psstB} = 4.95$

$y_{psB} := \frac{num_{hp} \cdot y_{pshpB} + num_{st} \cdot y_{psstB}}{numstr_g}$ $y_{psB} = 7.8$

$e_{gB} := c_g - y_{psB}$ $e_{gB} = 16.93$

Calculated net section properties - girder

$A_{gn} = 781.35$

from above...

$Aps_{gst} = 6.43$

$Aps_{ghp} = 1.22$

$c_{gnB} := \frac{A_g \cdot c_g - Aps_g \cdot y_{psB}}{A_{gn}}$ $c_{gnB} = 24.9$

$I_{gnB} := I_g + A_g \cdot (c_g - c_{gnB})^2 - Aps_{gst} \cdot (c_{gnB} - y_{psstB})^2 - Aps_{ghp} \cdot (c_{gnB} - y_{pshpB})^2$

$I_{gnB} = 258190.18$

$e_{gnB} := c_{gnB} - y_{psB}$ $e_{gnB} = 17.1$

Calculated transformed section properties - girder

$A_{pstr} = 38.07$

(from above)

$A_{pstrst} = 31.98$

$A_{pstrhp} = 6.09$

$A_{gtr} = 827.07$

$c_{gtrB} := \frac{A_g \cdot c_g + A_{pstr} \cdot y_{psB}}{A_g + A_{pstr}}$ $c_{gtrB} = 23.95$

$$I_{gtrB} := I_g + A_g \cdot \left(c_g - c_{gtrB}\right)^2 + A_{pstrst} \cdot \left(c_{gtrB} - y_{psstB}\right)^2 + A_{pstrhp} \cdot \left(c_{gtrB} - y_{pshpB}\right)^2$$

$I_{gtrB} = 272759.49$

$e_{gtrB} := c_{gtrB} - y_{psB}$ $\quad e_{gtrB} = 16.15$

At section C - beyond harping point

$y_{pshpC} := 7$ $\quad y_{pshpC} = 7$

$y_{psstC} := y_{psstA}$ $\quad y_{psstC} = 4.95$

$$y_{psC} := \frac{num_{hp} \cdot y_{pshpC} + num_{st} \cdot y_{psstC}}{numstr_g}$$ $\quad y_{psC} = 5.28$

$e_{gC} := c_g - y_{psC}$ $\quad e_{gC} = 19.45$

Calculated net section properties - girder

$A_{gn} = 781.35$

from above...

$Aps_{gst} = 6.43$

$Aps_{ghp} = 1.22$

$$c_{gnC} := \frac{A_g \cdot c_g - Aps_g \cdot y_{psC}}{A_{gn}}$$ $\quad c_{gnC} = 24.92$

$$I_{gnC} := I_g + A_g \cdot \left(c_g - c_{gnC}\right)^2 - Aps_{gst} \cdot \left(c_{gnC} - y_{psstC}\right)^2 - Aps_{ghp} \cdot \left(c_{gnC} - y_{pshpC}\right)^2$$

$I_{gnC} = 257803.34$

$e_{gnC} := c_{gnC} - y_{psC}$ $\quad e_{gnC} = 19.64$

Calculated transformed section properties - girder

from above...

$A_{pstr} = 38.07$

$A_{pstrst} = 31.98$

$A_{pstrhp} = 6.09$

$A_{gtr} = 827.07$

$$c_{gtrC} := \frac{A_g \cdot c_g + A_{pstr} \cdot y_{psC}}{A_g + A_{pstr}} \qquad c_{gtrC} = 23.83$$

$$I_{gtrC} := I_g + A_g \cdot \left(c_g - c_{gtrC}\right)^2 + A_{pstrst} \cdot \left(c_{gtrC} - y_{psstC}\right)^2 + A_{pstrhp} \cdot \left(c_{gtrC} - y_{pshpC}\right)^2$$

$I_{gtrC} = 274489.64$

$$e_{gtrC} := c_{gtrC} - y_{psC} \qquad e_{gtrC} = 18.55$$

Creep and Shrinkage Models (from AASHTO LRFD 2006 Interims)

$$\text{CREEP}(fci, t1, t2, hum, area, perim) := \left| \begin{array}{l} ktd2 \leftarrow \dfrac{(t2 - t1)}{61 - \left(\dfrac{4 \cdot fci}{1000}\right) + (t2 - t1)} \\ kla \leftarrow t1^{-0.118} \\ khc \leftarrow 1.56 - (0.008 \cdot hum) \\ kvs \leftarrow \max\left[1.45 - 0.13 \cdot \left(\dfrac{area}{perim}\right), 0\right] \\ kf \leftarrow \dfrac{5}{1 + \dfrac{fci}{1000}} \\ creep \leftarrow 1.90 \cdot ktd2 \cdot kla \cdot kvs \cdot khc \cdot kf \\ creep \end{array} \right.$$

$$\text{SHRINKAGE}(fci, t1, t2, hum, area, perim) := \left| \begin{array}{l} ktd1 \leftarrow \dfrac{t1}{61 - \left(\dfrac{4 \cdot fci}{1000}\right) + t1} \\ ktd2 \leftarrow \dfrac{t2}{61 - \left(\dfrac{4 \cdot fci}{1000}\right) + t2} \\ khs \leftarrow 2 - (0.014 \cdot hum) \\ kvs \leftarrow \max\left[1.45 - 0.13 \cdot \left(\dfrac{area}{perim}\right), 0\right] \\ kf \leftarrow \dfrac{5}{1 + \dfrac{fci}{1000}} \\ shrink \leftarrow -480 \cdot 10^{-6} \cdot (ktd2 - ktd1) \cdot kvs \cdot khs \cdot kf \\ shrink \end{array} \right.$$

Sign Convention:
Tension = Lengthening = (+)
Compression = (-)

Outline of calculation steps for a precast, prestressed girder with precast, post-tensioned deck panels

a) D/CG 1: Calculate redistribution of stresses in girder from transfer to composite action with deck

b) D/CG 2: Calculate redistribution of stresses in deck from post-tensioning to composite action with girder

c) D/CG 3: Calculate redistribution of stresses in composite section from when it's made composite to any time in the future

a) D/CG 1: Calculate redistribution of stresses in girder from transfer to composite action with deck

Need to consider 3 different locations in girder

$x_A := 0 \cdot L_g$ $\quad x_A = 0$

$x_B := 0.25 \cdot L_g$ $\quad x_B = 300$

$x_{harp} := 0.4 \cdot L_g$ $\quad x_{harp} = 480$

$x_C := 0.5 \cdot L_g$ $\quad x_C = 600$

Girder self-weight:

$w_g := A_g \cdot \frac{0.150}{12^3}$ $\quad w_g = 0.068$ kips/inch

Moment at points A, B, and C due to girder self-weight only (girder is still simply supported):

$Mg_{selfA} := \frac{w_g \cdot x_A}{2} \cdot (L_g - x_A)$ $\quad Mg_{selfA} = 0$

$Mg_{selfB} := \frac{w_g \cdot x_B}{2} \cdot (L_g - x_B)$ $\quad Mg_{selfB} = 9246.09$

$Mg_{selfC} := \frac{w_g \cdot x_C}{2} \cdot (L_g - x_C)$ $\quad Mg_{selfC} = 12328.13$

Jacking force in prestressing strand:

$P_{jack} := f_{pj} \cdot Aps_g$ $\quad P_{jack} = 1549.13$ kips

Initial force in prestressing strand (jacking force minus ES losses):

$f_{cgpA} := \frac{P_{jack}}{A_{gtr}} + \frac{P_{jack} \cdot e_{gtrA}^2}{I_{gtrA}} - \frac{Mg_{selfA} \cdot e_{gtrA}}{I_{gtrA}}$ $\quad f_{cgpA} = 2.7$ ksi

$f_{cgpB} := \frac{P_{jack}}{A_{gtr}} + \frac{P_{jack} \cdot e_{gtrB}^2}{I_{gtrB}} - \frac{Mg_{selfB} \cdot e_{gtrB}}{I_{gtrB}}$ $\quad f_{cgpB} = 2.81$ ksi

$f_{cgpC} := \frac{P_{jack}}{A_{gtr}} + \frac{P_{jack} \cdot e_{gtrC}^2}{I_{gtrC}} - \frac{Mg_{selfC} \cdot e_{gtrC}}{I_{gtrC}}$ $\quad f_{cgpC} = 2.98$ ksi

$P_{iA} := P_{jack} - \left(n \cdot f_{cgpA} \cdot Aps_g\right)$ $\quad P_{iA} = 1425.73$ kips

$P_{iB} := P_{jack} - \left(n \cdot f_{cgpB} \cdot Aps_g\right)$ $\quad P_{iB} = 1420.8$ kips

$P_{iC} := P_{jack} - \left(n \cdot f_{cgpC} \cdot Aps_g\right)$ $\quad P_{iC} = 1412.76$ kips

$Nps_{oA} := P_{iA}$ $\quad Nps_{oA} = 1425.7$ kips

$Nps_{oB} := P_{iB}$ $\quad Nps_{oB} = 1420.8$ kips

$Nps_{oC} := P_{iC}$ $\quad Nps_{oC} = 1412.8$ kips

Initial force in net concrete section is equal to initial force in prestressing strand:

$Ng_{oA} := -Nps_{oA}$ $\quad Ng_{oA} = -1425.7$ kips

$Ng_{oB} := -Nps_{oB}$ $\quad Ng_{oB} = -1420.8$ kips

$Ng_{oC} := -Nps_{oC}$ $\quad Ng_{oC} = -1412.8$ kips

Sum moments about net centroid of girder to get initial moment at each location:

$$-Mg_o + Mg_{self} - Nps_o \cdot e_{gn} = 0$$

$Mg_{oA} := Mg_{selfA} - Nps_{oA} \cdot e_{gnA}$ $Mg_{oA} = -18327.2$ kip-in

$Mg_{oB} := Mg_{selfB} - Nps_{oB} \cdot e_{gnB}$ $Mg_{oB} = -15043.5$ kip-in

$Mg_{oC} := Mg_{selfC} - Nps_{oC} \cdot e_{gnC}$ $Mg_{oC} = -15419.2$ kip-in

Relaxation in girder prestressing strands from transfer to composite action

Average stress in tendons

$f_{ptA} := \frac{Nps_{oA}}{Aps_g}$ $f_{ptA} = 186.37$ $t_i := t_{gcast}$ $t := t_{gcomp}$

$t_i = 1$ $t = 60$

$\Delta f_{pR1A} := \frac{-f_{ptA}}{K_{Lpr}} \cdot \left(\frac{f_{ptA}}{f_{py}} - 0.55 \right) \cdot \frac{\log(24 \cdot t)}{\log(24 \cdot t_i)}$ $\Delta f_{pR1A} = -2.06$ ksi

$f_{ptB} := \frac{Nps_{oB}}{Aps_g}$ $f_{ptB} = 185.72$

$\Delta f_{pR1B} := \frac{-f_{ptB}}{K_{Lpr}} \cdot \left(\frac{f_{ptB}}{f_{py}} - 0.55 \right) \cdot \frac{\log(24 \cdot t)}{\log(24 \cdot t_i)}$ $\Delta f_{pR1B} = -2.02$ ksi

$f_{ptC} := \frac{Nps_{oC}}{Aps_g}$ $f_{ptC} = 184.68$

$\Delta f_{pR1C} := \frac{-f_{ptC}}{K_{Lpr}} \cdot \left(\frac{f_{ptC}}{f_{py}} - 0.55 \right) \cdot \frac{\log(24 \cdot t)}{\log(24 \cdot t_i)}$ $\Delta f_{pR1C} = -1.97$ ksi

Girder time interval 1: Girder shrinkage & creep from transfer to deck placement

Calculate at each point A B C

$\varepsilon sh_{g1} := \text{SHRINKAGE}\left(fc_g, t_{gcast}, t_{gcomp}, hum, A_g, perim_g\right)$ $\varepsilon sh_{g1} = -0.000157$

$\phi_{g1} := \text{CREEP}\left(fc_g, t_{gcast}, t_{gcomp}, hum, A_g, perim_g\right)$ $\phi_{g1} = 0.63$

Calcs at A

$$geqns1A := \begin{bmatrix} 1 & 1 & 0 & 0 & 0 & 0 \\ 0 & e_{gA} & 1 & 0 & 0 & 0 \\ \frac{-\left(1+\mu_g\cdot\phi_{g1}\right)}{E_g\cdot A_{gn}} & 0 & 0 & 1 & 0 & 0 \\ 0 & -1 & 0 & 0 & Aps_g\cdot Eps_g & 0 \\ 0 & 0 & 0 & 1 & -1 & e_{gA} \\ 0 & 0 & \frac{-\left(1+\mu_g\cdot\phi_{g1}\right)}{E_g\cdot I_{gnA}} & 0 & 0 & 1 \end{bmatrix} \qquad gvar1 := \begin{pmatrix} \Delta Ng1 \\ \Delta Npsg1 \\ \Delta Mg1 \\ \Delta\varepsilon g1 \\ \Delta\varepsilon psg1 \\ \Delta\chi g1 \end{pmatrix}$$

$$gans1A := \begin{pmatrix} 0 \\ 0 \\ \frac{Ng_{oA}}{E_g\cdot A_{gn}}\cdot\phi_{g1} + \varepsilon sh_{g1} \\ -\Delta f_{pR1A}\cdot Aps_g \\ 0 \\ \frac{Mg_{oA}}{E_g\cdot I_{gnA}}\cdot\phi_{g1} \end{pmatrix}$$

Note: Ngo and Mgo both go in as negative values here

$gvalues1A := geqns1A^{-1}\cdot gans1A$

$$gvalues1A = \begin{pmatrix} 114.772635 \\ -114.772635 \\ 1461.055646 \\ -0.000356 \\ -0.000454 \\ -0.000008 \end{pmatrix}$$

*Redistribution of stresses in girder from transfer to deck placement

$\Delta Ng_{1A} := gvalues1A_1$ $\Delta Ng_{1A} = 114.77$

$\Delta Npsg_{1A} := gvalues1A_2$ $\Delta Npsg_{1A} = -114.77$

$\Delta Mg_{1A} := gvalues1A_3$ $\Delta Mg_{1A} = 1461.06$

$\Delta \varepsilon g_{1A} := gvalues1A_4$ $\Delta \varepsilon g_{1A} = -0.000356$

$\Delta \varepsilon psg_{1A} := gvalues1A_5$ $\Delta \varepsilon psg_{1A} = -0.000454$

$\Delta \chi g_{1A} := gvalues1A_6$ $\Delta \chi g_{1A} = -0.00000776$

Calcs at B

$$geqns1B := \begin{bmatrix} 1 & 1 & 0 & 0 & 0 & 0 \\ 0 & e_{gB} & 1 & 0 & 0 & 0 \\ \frac{-\left(1+\mu_g\cdot\phi_{g1}\right)}{E_g\cdot A_{gn}} & 0 & 0 & 1 & 0 & 0 \\ 0 & -1 & 0 & 0 & Aps_g\cdot Eps_g & 0 \\ 0 & 0 & 0 & 1 & -1 & e_{gB} \\ 0 & 0 & \frac{-\left(1+\mu_g\cdot\phi_{g1}\right)}{E_g\cdot I_{gnB}} & 0 & 0 & 1 \end{bmatrix} \qquad gvar1 := \begin{pmatrix} \Delta Ng1 \\ \Delta Npsg1 \\ \Delta Mg1 \\ \Delta \varepsilon g1 \\ \Delta \varepsilon psg1 \\ \Delta \chi g1 \end{pmatrix}$$

$$gans1B := \begin{pmatrix} 0 \\ 0 \\ \frac{Ng_{oB}}{E_g\cdot A_{gn}}\cdot\phi_{g1} + \varepsilon sh_{g1} \\ -\Delta f_{pR1B}\cdot Aps_g \\ 0 \\ \frac{Mg_{oB}}{E_g\cdot I_{gnB}}\cdot\phi_{g1} \end{pmatrix}$$

Note: Ngo and Mgo both go in as negative values here

$gvalues1B := geqns1B^{-1}\cdot gans1B$

$$gvalues1B = \begin{pmatrix} 113.268785 \\ -113.268785 \\ 1917.640532 \\ -0.000355 \\ -0.000449 \\ -0.000006 \end{pmatrix}$$

*Redistribution of stresses in girder from transfer to deck placement

$\Delta Ng_{1B} := gvalues1B_1$ $\Delta Ng_{1B} = 113.27$

$\Delta Npsg_{1B} := gvalues1B_2$ $\Delta Npsg_{1B} = -113.27$

$\Delta Mg_{1B} := gvalues1B_3$ $\Delta Mg_{1B} = 1917.64$

$\Delta \varepsilon g_{1B} := gvalues1B_4$ $\Delta \varepsilon g_{1B} = -0.000355$

$\Delta \varepsilon psg_{1B} := gvalues1B_5$ $\Delta \varepsilon psg_{1B} = -0.000449$

$\Delta \chi g_{1B} := gvalues1B_6$ $\Delta \chi g_{1B} = -0.00000551$

Calcs at C

$$geqns1C := \begin{bmatrix} 1 & 1 & 0 & 0 & 0 & 0 \\ 0 & e_{gC} & 1 & 0 & 0 & 0 \\ \frac{-\left(1 + \mu_g \cdot \phi_{g1}\right)}{E_g \cdot A_{gn}} & 0 & 0 & 1 & 0 & 0 \\ 0 & -1 & 0 & 0 & Aps_g \cdot Eps_g & 0 \\ 0 & 0 & 0 & 1 & -1 & e_{gC} \\ 0 & 0 & \frac{-\left(1 + \mu_g \cdot \phi_{g1}\right)}{E_g \cdot I_{gnC}} & 0 & 0 & 1 \end{bmatrix} \qquad gvar1 := \begin{pmatrix} \Delta Ng1 \\ \Delta Npsg1 \\ \Delta Mg1 \\ \Delta \varepsilon g1 \\ \Delta \varepsilon psg1 \\ \Delta \chi g1 \end{pmatrix}$$

$$gans1C := \begin{pmatrix} 0 \\ 0 \\ \frac{Ng_{oC}}{E_g \cdot A_{gn}} \cdot \phi_{g1} + \varepsilon sh_{g1} \\ -\Delta f_{pR1C} \cdot Aps_g \\ 0 \\ \frac{Mg_{oC}}{E_g \cdot I_{gnC}} \cdot \phi_{g1} \end{pmatrix}$$

Note: Ngo and Mgo both go in as negative values here

$gvalues1C := geqns1C^{-1} \cdot gans1C$

$$gvalues1C = \begin{pmatrix} 114.763102 \\ -114.763102 \\ 2232.142326 \\ -0.000353 \\ -0.000457 \\ -0.000005 \end{pmatrix}$$

*Redistribution of stresses in girder from transfer to deck placement

$\Delta Ng_{1C} := gvalues1B_1$ $\Delta Ng_{1C} = 113.27$

$\Delta Npsg_{1C} := gvalues1B_2$ $\Delta Npsg_{1C} = -113.27$

$\Delta Mg_{1C} := gvalues1B_3$ $\Delta Mg_{1C} = 1917.64$

$\Delta \varepsilon g_{1C} := gvalues1B_4$ $\Delta \varepsilon g_{1C} = -0.000355$

$\Delta \varepsilon psg_{1C} := gvalues1B_5$ $\Delta \varepsilon psg_{1C} = -0.000449$

$\Delta \chi g_{1C} := gvalues1B_6$ $\Delta \chi g_{1C} = -0.00000551$

b) D/CG 2: Calculate redistribution of stresses in deck from post-tensioning to composite action

Compute state of stress immediately following stressing - use average force in tendons

$P_{jack} := 0.80 \cdot f_{pu} \, numstr_{dpt} \cdot Astr_d$ $P_{jack} = 396.6$ kips

Consider seating losses....

Note: Post-tensioning tendons are straight so only have wobble losses --> k*l term

$\alpha := 0$ $\mu := 0$ $k := 0.0002$ per foot of length $\Delta S := \frac{3}{8}$ inch $len = 300$

$P_{dead} := P_{jack} \cdot e^{-(\mu \cdot \alpha + k \cdot len)}$ $P_{dead} = 373.5$ kips

$m := \frac{P_{jack} - P_{dead}}{len \cdot 12}$ $m = 0.00642$ kips/inch

$x_{AS} := \frac{\sqrt{\frac{\Delta S \cdot Apt_d \cdot Ept_d}{m}}}{12}$ $x_{AS} = 145.74$ feet

Note xAS is SHORTER than the bridge...

$P_{SL} := 2 \cdot m \cdot x_{AS} \cdot 12$ $P_{SL} = 22.44$ kips

$P_{live} := P_{jack} - P_{SL}$ $P_{live} = 374.14$ kips

$P_{mid} := P_{jack} - \frac{P_{SL}}{2}$ $P_{mid} = 385.36$ kips

$$P_{avg} := \frac{\left(\frac{P_{live} + P_{mid}}{2}\right)\cdot x_{AS} + \left(\frac{P_{mid} + P_{dead}}{2}\right)\cdot\left(len - x_{AS}\right)}{len} \qquad P_{avg} = 379.58 \quad \text{kips}$$

Initial state of internal equilibrium, assuming

1) No tendon eccentricity
2) Self-weight causes no significant stresses

$$Nd_o + Nptd_o = 0$$

$$Nptd_o := P_{avg} \qquad Nptd_o = 379.58 \qquad Nd_o := -Nptd_o \qquad Nd_o = -379.58$$

Relaxation in deck post-tensioning strands from transfer to composite action

Average stress in tendons $\qquad f_{pt2} := \frac{P_{avg}}{Apt_d} \qquad f_{pt2} = 206.74$

$t_i := t_{hcomp} \qquad t := t_{dcomp} - t_{dpt}$

$t_i = 60 \qquad t = 5$

$$\Delta f_{pR2} := \frac{-f_{pt2}}{K_{Lpr}}\cdot\left(\frac{f_{pt2}}{f_{py}} - 0.55\right)\cdot\frac{\log(24\cdot t)}{\log\left(24\cdot t_i\right)} \qquad \Delta f_{pR2} = -0.91 \quad \text{ksi}$$

$$\varepsilon sh_{d2} := SHRINKAGE\left(fc_d, t_{dpt}, t_{dcomp}, hum, A_d, perim_d\right) \qquad \varepsilon sh_{d2} = -0.00000802$$

$$\phi_{d2} := CREEP\left(fc_d, t_{dpt}, t_{dcomp}, hum, A_d, perim_d\right) \qquad \phi_{d2} = 0.1$$

$$deqns2 := \begin{bmatrix} \frac{-\left(1 + \mu_d\cdot\phi_{d2}\right)}{A_d\cdot E_d} & 0 & 1 & 0 \\ 0 & -1 & 0 & Apt_d\cdot Ept_d \\ 1 & 1 & 0 & 0 \\ 0 & 0 & 1 & -1 \end{bmatrix} \qquad dvar2 := \begin{pmatrix} \Delta Nd2 \\ \Delta Nptd2 \\ \Delta\varepsilon d2 \\ \Delta\varepsilon ptd2 \end{pmatrix}$$

$$dans2 := \begin{pmatrix} \frac{Nd_o}{A_d \cdot E_d} \cdot \phi_{d2} + \varepsilon sh_{d2} \\ -\Delta f_{pR2} \cdot Aps_g \\ 0 \\ 0 \end{pmatrix} \qquad dvalues2 := deqns2^{-1} \cdot dans2 \qquad dvalues2 = \begin{pmatrix} 7.822326 \\ -7.822326 \\ -0.0000165 \\ -0.0000165 \end{pmatrix}$$

$\Delta Nd_2 := dvalues2_1$ $\quad \Delta Nd_2 = 7.82$

$\Delta Nptd_2 := dvalues2_2$ $\quad \Delta Nptd_2 = -7.82$

$\Delta \varepsilon d_2 := dvalues2_3$ $\quad \Delta \varepsilon d_2 = -0.0000165$

$\Delta \varepsilon ptd_2 := dvalues2_4$ $\quad \Delta \varepsilon ptd_2 = -0.0000165$

c) D/CG 3: Calculate redistribution of stresses in composite section from when it's made composite to any time in the future

$\varepsilon sh_{g3} := SHRINKAGE(fc_g, t_{gcomp}, t_{ginf}, hum, A_g, perim_g)$ $\quad \varepsilon sh_{g3} = -0.00009$

$\phi_{g3} := CREEP(fc_g, t_{gcomp}, t_{ginf}, hum, A_g, perim_g)$ $\quad \phi_{g3} = 0.61$

$\varepsilon sh_{h3} := SHRINKAGE(fc_h, t_{hcomp}, t_{hinf}, hum, A_h, perim_h)$ $\quad \varepsilon sh_{h3} = -0.000025$

$\phi_{h3} := CREEP(fc_h, t_{hcomp}, t_{hinf}, hum, A_h, perim_h)$ $\quad \phi_{h3} = 0.15$

$\varepsilon sh_{d3} := SHRINKAGE(fc_d, t_{dcomp}, t_{dinf}, hum, A_d, perim_d)$ $\quad \varepsilon sh_{d3} = -0.000152$

$\phi_{d3} := CREEP(fc_d, t_{dcomp}, t_{dinf}, hum, A_d, perim_d)$ $\quad \phi_{d3} = 0.9$

Need to establish all starting values based on results of previous stages: variables with subscript "pr" (prime) indicate starting values for composite stage

Calcs at A

$Mg_{oprA} := Mg_{oA} + \Delta Mg_{1A}$ $Mg_{oprA} = -16866.1$

$Ng_{oprA} := Ng_{oA} + \Delta Ng_{1A}$ $Ng_{oprA} = -1.3 \times 10^{3}$

$Nps_{oprA} := Nps_{oA} + \Delta Npsg_{1A}$ $Nps_{oprA} = 1.3 \times 10^{3}$

$Nd_{opr} := Nd_{o} + \Delta Nd_{2}$ $Nd_{opr} = -371.8$

$Nptd_{opr} := Nptd_{o} + \Delta Nptd_{2}$ $Nptd_{opr} = 371.8$

Need to add deck weight moment to girder

$wt_d := A_{dws} \cdot \frac{0.150}{12^3}$ $wt_d = 0.08$ kip/in

$Md_{selfA} := \frac{wt_d \cdot x_A}{2} \cdot \left(L_g - x_A\right)$ $Md_{selfA} = 0$ kip-in

Stresses in girder due to deck weight only:

$\sigma_{topA} := -\frac{Md_{selfA} \cdot \left(depth_g - c_{gtrA}\right)}{I_{gtrA}}$ $\sigma_{topA} = 0$

$\sigma_{botA} := \frac{Md_{selfA} \cdot c_{gtrA}}{I_{gtrA}}$ $\sigma_{botA} = 0$

$\sigma_{cgsA} := \frac{Md_{selfA} \cdot \left(c_{gtrA} - y_{psA}\right)}{I_{gtrA}}$ $\sigma_{cgsA} = 0$

all stress values in ksi, positive indicates tension

$\varepsilon_{topA} := \frac{\sigma_{topA}}{E_g} \cdot 10^6$ $\varepsilon_{topA} = 0$

$\varepsilon_{botA} := \frac{\sigma_{botA}}{E_g} \cdot 10^6$ $\varepsilon_{botA} = 0$

$\varepsilon_{cgsA} := \frac{\sigma_{cgsA}}{E_g} \cdot 10^6$ $\varepsilon_{cgsA} = 0$

all strain values in microstrain/inch

Force in girder strands due to deck weight only (kips):

$P_{strcompA} := \varepsilon_{cgsA} \cdot 10^{-6} \cdot Eps_g \cdot Aps_g$ $\quad P_{strcompA} = 0$ kips

Force in girder concrete at net cg due to deck weight only (kips):

$\sigma_{concA} := \frac{Md_{selfA} \cdot (c_{gtrA} - c_{gnA})}{I_{gtrA}}$ $\quad \sigma_{concA} = 0$

$P_{conccompA} := \sigma_{concA} \cdot A_{gn}$ $\quad P_{conccompA} = 0$ kips

Moment in girder concrete due to deck weight only (kip-in):

$\phi_{dA} := \frac{\varepsilon_{botA} - \varepsilon_{topA}}{depth_g}$ $\quad \phi_{dA} = 0$

$M_{gfromdeckA} := \phi_{dA} \cdot 10^{-6} \cdot E_g \cdot I_{gnA}$ $\quad M_{gfromdeckA} = 0$

Revise starting values for composite analysis to include deck weight

$Mg_{ocA} := Mg_{oprA} + M_{gfromdeckA}$ $\quad Mg_{ocA} = -16866.13$

$Ng_{ocA} := Ng_{oprA} + P_{conccompA}$ $\quad Ng_{ocA} = -1310.95$

$Nps_{ocA} := Nps_{oprA} + P_{strcompA}$ $\quad Nps_{ocA} = 1310.95$

$Nd_{oc} := Nd_{opr}$ $\quad Nd_{oc} = -371.76$

$Nptd_{oc} := Nptd_{opr}$ $\quad Nptd_{oc} = 371.76$

Relaxation in girder prestressing strands from composite action to end of service life

$f_{pt3A} := \frac{Nps_{ocA}}{Aps_g}$ $\quad f_{pt3A} = 171.37$

$t_i := t_{gcomp}$ $\quad t := t_{ginf}$

$t_i = 60$ $\quad t = 10000$

$\Delta f_{pR3A} := \frac{-f_{pt3A}}{K_{Lpr}} \cdot \left(\frac{f_{pt3A}}{f_{py}} - 0.55 \right) \cdot \frac{\log(24 \cdot t)}{\log(24 \cdot t_i)}$ $\quad \Delta f_{pR3A} = -1.01$ ksi

Relaxation in deck post-tensioning strands from composite action to end of service life

$f_{pt4} := \frac{Nptd_{oc}}{Apt_d}$ $f_{pt4} = 202.48$ $t_i := t_{dcomp}$ $t := t_{dinf}$

$t_i = 60$ $t = 10000$

$\Delta f_{pR4} := \frac{-f_{pt4}}{K_{Lpr}} \cdot \left(\frac{f_{pt4}}{f_{py}} - 0.55 \right) \cdot \frac{\log(24 \cdot t)}{\log(24 \cdot t_i)}$ $\Delta f_{pR4} = -2.17$ ksi

Calculations for system after it becomes composite

$a := \frac{t_d}{2} + \frac{t_h}{2}$ $b := \frac{t_d}{2} + t_h + (depth_g - c_{gtrA})$ $c := \frac{t_d}{2} + t_h + (depth_g - y_{psA})$

$a = 4.5$ $b = 34.86$ $c = 47$

$$coeff1A := \begin{pmatrix} 1 & 1 & 1 & 1 & 1 & 0 & 0 & 0 & 0 & 0 & 0 & 0 & 0 & 0 \\ 0 & 0 & a & b & c & 1 & 1 & 1 & 0 & 0 & 0 & 0 & 0 & 0 \\ 0 & 0 & 0 & 0 & 0 & 0 & 0 & 0 & 1 & -1 & 0 & 0 & 0 & 0 \\ 0 & 0 & 0 & 0 & 0 & 0 & 0 & 0 & 1 & 0 & -1 & 0 & 0 & a \\ 0 & 0 & 0 & 0 & 0 & 0 & 0 & 0 & 1 & 0 & 0 & -1 & 0 & b \\ 0 & 0 & 0 & 0 & 0 & 0 & 0 & 0 & 1 & 0 & 0 & 0 & -1 & c \end{pmatrix}$$

$$unknowns14 := \begin{pmatrix} \Delta Nd \\ \Delta Nptd \\ \Delta Nh \\ \Delta Ng \\ \Delta Npsg \\ \Delta Md \\ \Delta Mh \\ \Delta Mg \\ \Delta \varepsilon d \\ \Delta \varepsilon ptd \\ \Delta \varepsilon h \\ \Delta \varepsilon g \\ \Delta \varepsilon psg \\ \Delta \chi \end{pmatrix}$$

$$c2A := \begin{bmatrix} \frac{-(1+\mu_d\cdot\phi_{d3})}{E_d\cdot A_d} & 0 & 0 & 0 & 0 & 0 & 0 & 0 & 1 & 0 & 0 & 0 & 0 & 0 \\ 0 & 0 & 0 & 0 & 0 & \frac{-(1+\mu_d\cdot\phi_{d3})}{E_d\cdot I_d} & 0 & 0 & 0 & 0 & 0 & 0 & 0 & 1 \\ 0 & 0 & 0 & \frac{-(1+\mu_g\cdot\phi_{g3})}{E_g\cdot A_g} & 0 & 0 & 0 & 0 & 0 & 0 & 0 & 1 & 0 & 0 \\ 0 & 0 & 0 & 0 & 0 & 0 & 0 & \frac{-(1+\mu_g\cdot\phi_{g3})}{E_g\cdot I_g} & 0 & 0 & 0 & 0 & 0 & 1 \\ 0 & -1 & 0 & 0 & 0 & 0 & 0 & 0 & 0 & Apt_d\cdot Ept_d & 0 & 0 & 0 & 0 \\ 0 & 0 & \frac{-(1+\mu_h\cdot\phi_{h3})}{E_h\cdot A_h} & 0 & 0 & 0 & 0 & 0 & 0 & 0 & 1 & 0 & 0 & 0 \end{bmatrix}$$

coeff2A := c2A Note: Matrix variable name had to be shortened to fit on the page for printing purposes.

$$coeff3A := \begin{bmatrix} 0 & 0 & 0 & 0 & -1 & 0 & 0 & 0 & 0 & 0 & 0 & 0 & Aps_g\cdot Eps_g & 0 \\ 0 & 0 & 0 & 0 & 0 & 0 & \frac{-(1+\mu_h\cdot\phi_{h3})}{E_h\cdot I_h} & 0 & 0 & 0 & 0 & 0 & 0 & 1 \end{bmatrix}$$

$$values14A := \begin{pmatrix} 0 \\ 0 \\ 0 \\ 0 \\ 0 \\ 0 \\ \frac{Nd_{oc}}{A_d\cdot E_d}\cdot\phi_{d3} + \varepsilon sh_{d3} \\ 0 \\ \frac{Ng_{ocA}}{A_g\cdot E_g}\cdot\phi_{g3} + \varepsilon sh_{g3} \\ \frac{Mg_{ocA}}{E_g\cdot I_g}\cdot\phi_{g3} \\ -\Delta f_{pR4}\cdot Apt_d \\ \varepsilon sh_{h3} \\ -\Delta f_{pR3A}\cdot Aps_g \\ 0 \end{pmatrix} \qquad values14A = \begin{pmatrix} 0 \\ 0 \\ 0 \\ 0 \\ 0 \\ 0 \\ -0.000249 \\ 0 \\ -0.000302 \\ -0.000008 \\ 3.986228 \\ -0.000025 \\ 7.70257 \\ 0 \end{pmatrix}$$

coeffsA := stack(coeff1A, coeff2A, coeff3A)

$$\text{coeffsA} = \begin{pmatrix} 1 & 1 & 1 & 1 & 1 & 0 & 0 & 0 & 0 & 0 & 0 & 0 & 0 & 0 \\ 0 & 0 & 4.5 & 34.85592 & 47 & 1 & 1 & 1 & 0 & 0 & 0 & 0 & 0 & 0 \\ 0 & 0 & 0 & 0 & 0 & 0 & 0 & 0 & 1 & -1 & 0 & 0 & 0 & 0 \\ 0 & 0 & 0 & 0 & 0 & 0 & 0 & 0 & 1 & 0 & -1 & 0 & 0 & 4.5 \\ 0 & 0 & 0 & 0 & 0 & 0 & 0 & 0 & 1 & 0 & 0 & -1 & 0 & 34.85592 \\ 0 & 0 & 0 & 0 & 0 & 0 & 0 & 0 & 1 & 0 & 0 & 0 & -1 & 47 \\ -0 & 0 & 0 & 0 & 0 & 0 & 0 & 0 & 1 & 0 & 0 & 0 & 0 & 0 \\ 0 & 0 & 0 & 0 & 0 & -0 & 0 & 0 & 0 & 0 & 0 & 0 & 0 & 1 \\ 0 & 0 & 0 & -0 & 0 & 0 & 0 & 0 & 0 & 0 & 0 & 1 & 0 & 0 \\ 0 & 0 & 0 & 0 & 0 & 0 & 0 & -0 & 0 & 0 & 0 & 0 & 0 & 1 \\ 0 & -1 & 0 & 0 & 0 & 0 & 0 & 0 & 0 & 52326 & 0 & 0 & 0 & 0 \\ 0 & 0 & -0.00001 & 0 & 0 & 0 & 0 & 0 & 0 & 0 & 1 & 0 & 0 & 0 \\ 0 & 0 & 0 & 0 & -1 & 0 & 0 & 0 & 0 & 0 & 0 & 0 & 218025 & 0 \\ 0 & 0 & 0 & 0 & 0 & 0 & -0.00016 & 0 & 0 & 0 & 0 & 0 & 0 & 1 \end{pmatrix}$$

unknownsA := coeffsA^{-1} · values14A

$$\text{unknownsA} = \begin{pmatrix} 120.86844394 \\ -14.05173279 \\ -13.34111395 \\ -10.50398935 \\ -82.97160784 \\ -36.98755265 \\ -0.01982438 \\ 4362.83421947 \\ -0.00019236 \\ -0.00019236 \\ -0.000207 \\ -0.00030573 \\ -0.00034523 \\ -0.00000325 \end{pmatrix} \qquad \text{unknowns14A} := \begin{pmatrix} \Delta Nd \\ \Delta Nptd \\ \Delta Nh \\ \Delta Ng \\ \Delta Npsg \\ \Delta Md \\ \Delta Mh \\ \Delta Mg \\ \Delta \varepsilon d \\ \Delta \varepsilon ptd \\ \Delta \varepsilon h \\ \Delta \varepsilon g \\ \Delta \varepsilon psg \\ \Delta \chi \end{pmatrix}$$

$\Delta\chi_{finalA}$:= unknownsA$_{14}$ $\qquad \Delta\chi_{finalA} = -3.25 \times 10^{-6}$ strain/inch

$\chi_{finalA} := \Delta\chi g_{1A} + \Delta\chi_{finalA}$ $\qquad \chi_{finalA} = -1.1 \times 10^{-5}$

Conclusions for stresses at section A

$\Delta N_d := unknownsA_1$ $\Delta N_d = 120.87$

$\Delta N_h := unknownsA_3$ $\Delta N_h = -13.34$

$\Delta N_g := unknownsA_4$ $\Delta N_g = -10.5$

$\Delta M_d := unknownsA_6$ $\Delta M_d = -36.99$

$\Delta M_h := unknownsA_7$ $\Delta M_h = -0.01982$

$\Delta M_g := unknownsA_8$ $\Delta M_g = 4362.83$

$y_{botg} := 0$ $y_{botg} = 0$

$y_{topg} := depth_g$ $y_{topg} = 54$

$y_{both} := y_{topg}$ $y_{both} = 54$

$y_{toph} := y_{topg} + t_h$ $y_{toph} = 55$

$y_{botd} := depth_g + t_h$ $y_{botd} = 55$

$y_{topd} := depth_t$ $y_{topd} = 63$

Stresses in concrete:

$$stress_{dAf} := \begin{bmatrix} \frac{Nd_{oc} + \Delta N_d}{A_d} - \frac{\Delta M_d \cdot \left(\frac{t_d}{2}\right)}{I_d} \\ \frac{Nd_{oc} + \Delta N_d}{A_d} + 0 \\ \frac{Nd_{oc} + \Delta N_d}{A_d} + \frac{\Delta M_d \cdot \left(\frac{t_d}{2}\right)}{I_d} \end{bmatrix} \qquad stress_{dAf} = \begin{pmatrix} -0.26 \\ -0.29 \\ -0.32 \end{pmatrix} \qquad depths_d := \begin{pmatrix} y_{topd} \\ y_d \\ y_{botd} \end{pmatrix}$$

$$stress_{hAf} := \begin{bmatrix} \frac{\Delta N_h}{A_h} - \frac{\Delta M_h \cdot \left(\frac{t_h}{2}\right)}{I_h} \\ \frac{\Delta N_h}{A_h} + 0 \\ \frac{\Delta N_h}{A_h} + \frac{\Delta M_h \cdot \left(\frac{t_h}{2}\right)}{I_h} \end{bmatrix} \qquad stress_{hAf} = \begin{pmatrix} -0.661 \\ -0.667 \\ -0.673 \end{pmatrix} \qquad depths_h := \begin{pmatrix} y_{toph} \\ y_h \\ y_{both} \end{pmatrix}$$

$$stress_{gAf} := \begin{bmatrix} \frac{Ng_{oprA} + \Delta N_g}{A_g} - \frac{\Delta M_g \cdot (depth_g - c_g)}{I_g} - \frac{Mg_{oprA} \cdot (depth_g - c_g)}{I_g} \\ \frac{Ng_{oprA} + \Delta N_g}{A_g} + 0 \\ \frac{Ng_{oprA} + \Delta N_g}{A_g} + \frac{\Delta M_g \cdot (c_g)}{I_g} + \frac{Mg_{oprA} \cdot (depth_g - c_g)}{I_g} \end{bmatrix} \qquad depths_g := \begin{pmatrix} y_{topg} \\ c_g \\ y_{botg} \end{pmatrix}$$

$$stress_{gAf} = \begin{pmatrix} -0.271 \\ -1.675 \\ -3.154 \end{pmatrix}$$

$$depths_{hz1} := \begin{pmatrix} y_{topd} \\ y_{topd} \end{pmatrix} \qquad stress_{hz1} := \begin{pmatrix} stress_{dAf_1} \\ 0 \end{pmatrix}$$

$$depths_{hz2} := \begin{pmatrix} y_{botd} \\ y_{toph} \end{pmatrix} \qquad stress_{hz2} := \begin{pmatrix} stress_{dAf_3} \\ stress_{hAf_1} \end{pmatrix}$$

$$depths_{hz3} := \begin{pmatrix} y_{both} \\ y_{topg} \end{pmatrix} \qquad stress_{hz3} := \begin{pmatrix} stress_{hAf_3} \\ stress_{gAf_1} \end{pmatrix}$$

Graph of stresses in composite section (ksi)

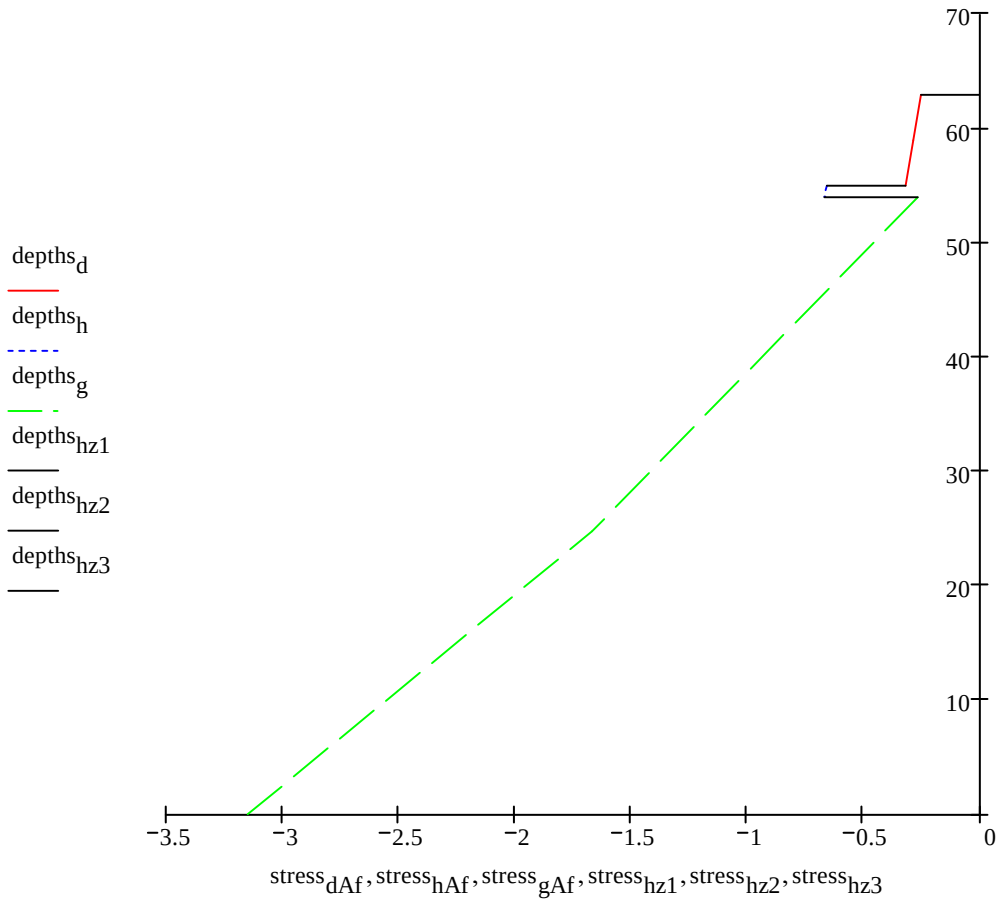

Calcs at B

$Mg_{oprB} := Mg_{oB} + \Delta Mg_{1B}$ $\quad Mg_{oprB} = -13125.8$

$Ng_{oprB} := Ng_{oB} + \Delta Ng_{1B}$ $\quad Ng_{oprB} = -1.3 \times 10^{3}$

$Nps_{oprB} := Nps_{oB} + \Delta Npsg_{1B}$ $\quad Nps_{oprB} = 1.3 \times 10^{3}$

Note Nd_{opr} and $Nptd_{opr}$ are same as above for A

Add deck weight moment to girder

$$Md_{selfB} := \frac{wt_d \cdot x_B}{2} \cdot \left(L_g - x_B\right) \qquad Md_{selfB} = 10757.813 \quad \text{kip-in}$$

Stresses in girder due to deck weight only:

$$\sigma_{topB} := -\frac{Md_{selfB} \cdot \left(depth_g - c_{gtrB}\right)}{I_{gtrB}} \qquad \sigma_{topB} = -1.19$$

$$\sigma_{botB} := \frac{Md_{selfB} \cdot c_{gtrB}}{I_{gtrB}} \qquad \sigma_{botB} = 0.94$$

$$\sigma_{cgsB} := \frac{Md_{selfB} \cdot \left(c_{gtrB} - y_{psB}\right)}{I_{gtrB}} \qquad \sigma_{cgsB} = 0.64$$

all stress values in ksi, positive indicates tension

$$\varepsilon_{topB} := \frac{\sigma_{topB}}{E_g} \cdot 10^6 \qquad \varepsilon_{botB} := \frac{\sigma_{botB}}{E_g} \cdot 10^6 \qquad \varepsilon_{cgsB} := \frac{\sigma_{cgsB}}{E_g} \cdot 10^6$$

$\varepsilon_{topB} = -248.5$ $\quad \varepsilon_{botB} = 198.1$ $\quad \varepsilon_{cgsB} = 133.6$

all strain values in microstrain/inch

Force in girder strands due to deck weight only (kips):

$$P_{strcompB} := \varepsilon_{cgsB} \cdot 10^{-6} \cdot Eps_g \cdot Aps_g \qquad P_{strcompB} = 29.1 \quad \text{kips}$$

Force in girder concrete at net cg due to deck weight only (kips):

$$\sigma_{concB} := \frac{Md_{selfB}\cdot\left(c_{gtrB} - c_{gnB}\right)}{I_{gtrB}} \qquad \sigma_{concB} = -0.03727$$

$$P_{conccompB} := \sigma_{concB}\cdot A_{gn} \qquad P_{conccompB} = -29.1 \text{ kips}$$

Moment in girder concrete due to deck weight only (kip-in):

$$\phi_{dB} := \frac{\varepsilon_{botB} - \varepsilon_{topB}}{depth_g} \qquad \phi_{dB} = 8.27$$

$$M_{gfromdeckB} := \phi_{dB}\cdot 10^{-6}\cdot E_g\cdot I_{gnB} \qquad M_{gfromdeckB} = 10183.2$$

Revise starting values for composite analysis to include deck weight

$$Mg_{ocB} := Mg_{oprB} + M_{gfromdeckB} \qquad Mg_{ocB} = -2942.65$$

$$Ng_{ocB} := Ng_{oprB} + P_{conccompB} \qquad Ng_{ocB} = -1336.65$$

$$Nps_{ocB} := Nps_{oprB} + P_{strcompB} \qquad Nps_{ocB} = 1336.65$$

Note Nd_{oc} and $Nptd_{oc}$ are same as above for A

Relaxation in girder prestressing strands from composite action to end of service life

$$f_{pt3B} := \frac{Nps_{ocB}}{Aps_g} \qquad f_{pt3B} = 174.73$$

$t_i := t_{gcomp}$ $\quad t := t_{ginf}$

$t_i = 60$ $\quad t = 10000$

$$\Delta f_{pR3B} := \frac{-f_{pt3B}}{K_{Lpr}}\cdot\left(\frac{f_{pt3B}}{f_{py}} - 0.55\right)\cdot\frac{\log(24\cdot t)}{\log\left(24\cdot t_i\right)} \qquad \Delta f_{pR3B} = -1.12 \text{ ksi}$$

Calculations for system after it becomes composite

$a := \frac{t_d}{2} + \frac{t_h}{2}$ $\quad b := \frac{t_d}{2} + t_h + \left(depth_g - c_{gtrB}\right)$ $\quad c := \frac{t_d}{2} + t_h + \left(depth_g - y_{psB}\right)$

$a = 4.5$ $\quad b = 35.05$ $\quad c = 51.2$

$$coeff1 := \begin{pmatrix} 1 & 1 & 1 & 1 & 1 & 0 & 0 & 0 & 0 & 0 & 0 & 0 & 0 \\ 0 & 0 & a & b & c & 1 & 1 & 1 & 0 & 0 & 0 & 0 & 0 \\ 0 & 0 & 0 & 0 & 0 & 0 & 0 & 0 & 1 & -1 & 0 & 0 & 0 \\ 0 & 0 & 0 & 0 & 0 & 0 & 0 & 0 & 1 & 0 & -1 & 0 & a \\ 0 & 0 & 0 & 0 & 0 & 0 & 0 & 0 & 1 & 0 & 0 & -1 & b \\ 0 & 0 & 0 & 0 & 0 & 0 & 0 & 0 & 1 & 0 & 0 & 0 & -1 \end{pmatrix} \qquad unknowns14 := \begin{pmatrix} \Delta Nd \\ \Delta Nptd \\ \Delta Nh \\ \Delta Ng \\ \Delta Npsg \\ \Delta Md \\ \Delta Mh \\ \Delta Mg \\ \Delta \varepsilon d \\ \Delta \varepsilon ptd \\ \Delta \varepsilon h \\ \Delta \varepsilon g \\ \Delta \varepsilon psg \\ \Delta \chi \end{pmatrix}$$

$$cf2 := \begin{bmatrix} \frac{-\left(1+\mu_d\cdot\phi_{d3}\right)}{E_d\cdot A_d} & 0 & 0 & 0 & 0 & 0 & 0 & 0 & 1 & 0 & 0 & 0 & 0 & 0 \\ 0 & 0 & 0 & 0 & 0 & \frac{-\left(1+\mu_d\cdot\phi_{d3}\right)}{E_d\cdot I_d} & 0 & 0 & 0 & 0 & 0 & 0 & 0 & 1 \\ 0 & 0 & 0 & \frac{-\left(1+\mu_g\cdot\phi_{g3}\right)}{E_g\cdot A_g} & 0 & 0 & 0 & 0 & 0 & 0 & 0 & 1 & 0 & 0 \\ 0 & 0 & 0 & 0 & 0 & 0 & 0 & \frac{-\left(1+\mu_g\cdot\phi_{g3}\right)}{E_g\cdot I_g} & 0 & 0 & 0 & 0 & 0 & 1 \\ 0 & -1 & 0 & 0 & 0 & 0 & 0 & 0 & 0 & Apt_d\cdot Ept_d & 0 & 0 & 0 & 0 \\ 0 & 0 & \frac{-\left(1+\mu_h\cdot\phi_{h3}\right)}{E_h\cdot A_h} & 0 & 0 & 0 & 0 & 0 & 0 & 0 & 1 & 0 & 0 & 0 \end{bmatrix}$$

$coeff2 := cf2$

$$\text{coeff3} := \begin{bmatrix} 0 & 0 & 0 & 0 & -1 & 0 & 0 & 0 & 0 & 0 & 0 & 0 & \text{Aps}_g \cdot \text{Eps}_g & 0 \\ 0 & 0 & 0 & 0 & 0 & 0 & \dfrac{-\left(1 + \mu_h \cdot \phi_{h3}\right)}{E_h \cdot I_h} & 0 & 0 & 0 & 0 & 0 & 0 & 1 \end{bmatrix}$$

$$\text{values14} := \begin{pmatrix} 0 \\ 0 \\ 0 \\ 0 \\ 0 \\ 0 \\ \dfrac{\text{Nd}_{oc}}{A_d \cdot E_d} \cdot \phi_{d3} + \varepsilon\text{sh}_{d3} \\ 0 \\ \dfrac{\text{Ng}_{ocB}}{A_g \cdot E_g} \cdot \phi_{g3} + \varepsilon\text{sh}_{g3} \\ \dfrac{\text{Mg}_{ocB}}{E_g \cdot I_g} \cdot \phi_{g3} \\ -\Delta f_{pR4} \cdot \text{Apt}_d \\ \varepsilon\text{sh}_{h3} \\ -\Delta f_{pR3B} \cdot \text{Aps}_g \\ 0 \end{pmatrix} \qquad \text{values14} = \begin{pmatrix} 0 \\ 0 \\ 0 \\ 0 \\ 0 \\ 0 \\ -0.000249 \\ 0 \\ -0.000306 \\ -0.000001 \\ 3.986228 \\ -0.000025 \\ 8.552952 \\ 0 \end{pmatrix}$$

coeffs := stack(coeff1, coeff2, coeff3)

$$\text{coeffs} = \begin{pmatrix} 1 & 1 & 1 & 1 & 1 & 0 & 0 & 0 & 0 & 0 & 0 & 0 & 0 & 0 \\ 0 & 0 & 4.5 & 35.04924 & 51.2 & 1 & 1 & 1 & 0 & 0 & 0 & 0 & 0 & 0 \\ 0 & 0 & 0 & 0 & 0 & 0 & 0 & 0 & 1 & -1 & 0 & 0 & 0 & 0 \\ 0 & 0 & 0 & 0 & 0 & 0 & 0 & 0 & 1 & 0 & -1 & 0 & 0 & 4.5 \\ 0 & 0 & 0 & 0 & 0 & 0 & 0 & 0 & 1 & 0 & 0 & -1 & 0 & 35.04924 \\ 0 & 0 & 0 & 0 & 0 & 0 & 0 & 0 & 1 & 0 & 0 & 0 & -1 & 51.2 \\ -0 & 0 & 0 & 0 & 0 & 0 & 0 & 0 & 1 & 0 & 0 & 0 & 0 & 0 \\ 0 & 0 & 0 & 0 & 0 & -0 & 0 & 0 & 0 & 0 & 0 & 0 & 0 & 1 \\ 0 & 0 & 0 & -0 & 0 & 0 & 0 & 0 & 0 & 0 & 0 & 1 & 0 & 0 \\ 0 & 0 & 0 & 0 & 0 & 0 & 0 & -0 & 0 & 0 & 0 & 0 & 0 & 1 \\ 0 & -1 & 0 & 0 & 0 & 0 & 0 & 0 & 0 & 52326 & 0 & 0 & 0 & 0 \\ 0 & 0 & -0.00001 & 0 & 0 & 0 & 0 & 0 & 0 & 0 & 1 & 0 & 0 & 0 \\ 0 & 0 & 0 & 0 & -1 & 0 & 0 & 0 & 0 & 0 & 0 & 0 & 218025 & 0 \\ 0 & 0 & 0 & 0 & 0 & 0 & -0.00016 & 0 & 0 & 0 & 0 & 0 & 0 & 1 \end{pmatrix}$$

unknowns := coeffs^{-1} · values14

$$\text{unknowns} = \begin{pmatrix} 13.32525119 \\ -16.69090279 \\ -16.23087844 \\ 90.28692796 \\ -70.69039792 \\ -9.37356302 \\ -0.00502399 \\ 537.27785883 \\ -0.0002428 \\ -0.0002428 \\ -0.00024651 \\ -0.00027169 \\ -0.000285 \\ -0.00000082 \end{pmatrix} \qquad \text{unknowns14} := \begin{pmatrix} \Delta Nd \\ \Delta Nptd \\ \Delta Nh \\ \Delta Ng \\ \Delta Npsg \\ \Delta Md \\ \Delta Mh \\ \Delta Mg \\ \Delta \varepsilon d \\ \Delta \varepsilon ptd \\ \Delta \varepsilon h \\ \Delta \varepsilon g \\ \Delta \varepsilon psg \\ \Delta \chi \end{pmatrix}$$

$\Delta\chi_{finalB} := \text{unknowns}_{14}$ $\quad \Delta\chi_{finalB} = -8.24 \times 10^{-7}$ strain/inch

$\chi_{finalB} := \Delta\chi g_{1B} + \Delta\chi_{finalB}$ $\quad \chi_{finalB} = -6.33 \times 10^{-6}$

Calcs at C

$Mg_{oprC} := Mg_{oC} + \Delta Mg_{1C}$ $\quad Mg_{oprC} = -13501.5$

$Ng_{oprC} := Ng_{oC} + \Delta Ng_{1C}$ $\quad Ng_{oprC} = -1.3 \times 10^{3}$

$Nps_{oprC} := Nps_{oC} + \Delta Npsg_{1C}$ $\quad Nps_{oprC} = 1.3 \times 10^{3}$

Note Nd_{opr} and $Nptd_{opr}$ are same as above for A

Add deck weight moment to girder

$$Md_{selfC} := \frac{wt_d \cdot x_C}{2} \cdot \left(L_g - x_C\right) \qquad Md_{selfC} = 14343.75 \text{ p-in}$$

Stresses in girder due to deck weight only:

$$\sigma_{topC} := -\frac{Md_{selfC} \cdot \left(depth_g - c_{gtrC}\right)}{I_{gtrC}} \qquad \sigma_{topC} = -1.58$$

$$\sigma_{botC} := \frac{Md_{selfC} \cdot c_{gtrC}}{I_{gtrC}} \qquad \sigma_{botC} = 1.25$$

$$\sigma_{cgsC} := \frac{Md_{selfC} \cdot \left(c_{gtrC} - y_{psC}\right)}{I_{gtrC}} \qquad \sigma_{cgsC} = 0.97$$

all stress values in ksi, positive indicates tension

$$\varepsilon_{topC} := \frac{\sigma_{topC}}{E_g} \cdot 10^6 \qquad \varepsilon_{botC} := \frac{\sigma_{botC}}{E_g} \cdot 10^6 \qquad \varepsilon_{cgsC} := \frac{\sigma_{cgsC}}{E_g} \cdot 10^6$$

$\varepsilon_{topC} = -330.5$ $\quad \varepsilon_{botC} = 261.2$ $\quad \varepsilon_{cgsC} = 203.3$

all strain values in microstrain/inch

Force in girder strands due to deck weight only (kips):

$P_{strcompC} := \varepsilon_{cgsC} \cdot 10^{-6} \cdot Eps_g \cdot Aps_g$ $P_{strcompC} = 44.3$ kips

Force in girder concrete at net cg due to deck weight only (kips):

$\sigma_{concC} := \frac{Md_{selfC} \cdot (c_{gtrC} - c_{gnC})}{I_{gtrC}}$ $\sigma_{concC} = -0.05673$

$P_{conccompC} := \sigma_{concC} \cdot A_{gn}$ $P_{conccompC} = -44.3$ kips

Moment in girder concrete due to deck weight only (kip-in):

$\phi_{dC} := \frac{\varepsilon_{botC} - \varepsilon_{topC}}{depth_g}$ $\phi_{dC} = 10.96$

$M_{gfromdeckC} := \phi_{dC} \cdot 10^{-6} \cdot E_g \cdot I_{gnC}$ $M_{gfromdeckC} = 13471.8$

Revise starting values for composite analysis to include deck weight

$Mg_{ocC} := Mg_{oprC} + M_{gfromdeckC}$ $Mg_{ocC} = -29.74$

$Ng_{ocC} := Ng_{oprC} + P_{conccompC}$ $Ng_{ocC} = -1343.82$

$Nps_{ocC} := Nps_{oprC} + P_{strcompC}$ $Nps_{ocC} = 1343.82$

Note Nd_{oc} and $Nptd_{oc}$ are same as above for A and B

Relaxation in girder prestressing strands from composite action to end of service life

$f_{pt3C} := \frac{Nps_{ocC}}{Aps_g}$ $f_{pt3C} = 175.66$

$t_i := t_{gcomp}$ $t := t_{ginf}$

$t_i = 60$ $t = 10000$

$\Delta f_{pR3C} := \frac{-f_{pt3C}}{K_{Lpr}} \cdot \left(\frac{f_{pt3C}}{f_{py}} - 0.55 \right) \cdot \frac{\log(24 \cdot t)}{\log(24 \cdot t_i)}$ $\Delta f_{pR3C} = -1.15$ ksi

Calculations for system after it becomes composite

$$a := \frac{t_d}{2} + \frac{t_h}{2} \qquad b := \frac{t_d}{2} + t_h + \left(depth_g - c_{gtrC}\right) \qquad c := \frac{t_d}{2} + t_h + \left(depth_g - y_{psC}\right)$$

$a = 4.5$ $b = 35.17$ $c = 53.72$

$$coeff1 := \begin{pmatrix} 1 & 1 & 1 & 1 & 1 & 0 & 0 & 0 & 0 & 0 & 0 & 0 & 0 \\ 0 & 0 & a & b & c & 1 & 1 & 1 & 0 & 0 & 0 & 0 & 0 \\ 0 & 0 & 0 & 0 & 0 & 0 & 0 & 0 & 1 & -1 & 0 & 0 & 0 \\ 0 & 0 & 0 & 0 & 0 & 0 & 0 & 0 & 1 & 0 & -1 & 0 & a \\ 0 & 0 & 0 & 0 & 0 & 0 & 0 & 0 & 1 & 0 & 0 & -1 & b \\ 0 & 0 & 0 & 0 & 0 & 0 & 0 & 0 & 1 & 0 & 0 & 0 & -1 & c \end{pmatrix}$$

$$unknowns14 := \begin{pmatrix} \Delta Nd \\ \Delta Nptd \\ \Delta Nh \\ \Delta Ng \\ \Delta Npsg \\ \Delta Md \\ \Delta Mh \\ \Delta Mg \\ \Delta \varepsilon d \\ \Delta \varepsilon ptd \\ \Delta \varepsilon h \\ \Delta \varepsilon g \\ \Delta \varepsilon psg \\ \Delta \chi \end{pmatrix}$$

$$cf2 := \begin{bmatrix} \frac{-\left(1+\mu_d\cdot\phi_{d3}\right)}{E_d\cdot A_d} & 0 & 0 & 0 & 0 & 0 & 0 & 0 & 1 & 0 & 0 & 0 & 0 & 0 \\ 0 & 0 & 0 & 0 & 0 & \frac{-\left(1+\mu_d\cdot\phi_{d3}\right)}{E_d\cdot I_d} & 0 & 0 & 0 & 0 & 0 & 0 & 0 & 1 \\ 0 & 0 & 0 & \frac{-\left(1+\mu_g\cdot\phi_{g3}\right)}{E_g\cdot A_g} & 0 & 0 & 0 & 0 & 0 & 0 & 0 & 1 & 0 & 0 \\ 0 & 0 & 0 & 0 & 0 & 0 & 0 & \frac{-\left(1+\mu_g\cdot\phi_{g3}\right)}{E_g\cdot I_g} & 0 & 0 & 0 & 0 & 0 & 1 \\ 0 & -1 & 0 & 0 & 0 & 0 & 0 & 0 & 0 & Apt_d\cdot Ept_d & 0 & 0 & 0 & 0 \\ 0 & 0 & \frac{-\left(1+\mu_h\cdot\phi_{h3}\right)}{E_h\cdot A_h} & 0 & 0 & 0 & 0 & 0 & 0 & 0 & 1 & 0 & 0 & 0 \end{bmatrix}$$

$$coeff2 := cf2$$

$$coeff3 := \begin{bmatrix} 0 & 0 & 0 & 0 & -1 & 0 & 0 & 0 & 0 & 0 & 0 & 0 & Aps_g\cdot Eps_g & 0 \\ 0 & 0 & 0 & 0 & 0 & 0 & \frac{-\left(1+\mu_h\cdot\phi_{h3}\right)}{E_h\cdot I_h} & 0 & 0 & 0 & 0 & 0 & 0 & 1 \end{bmatrix}$$

$$values14 := \begin{pmatrix} 0 \\ 0 \\ 0 \\ 0 \\ 0 \\ 0 \\ \frac{Nd_{oc}}{A_d\cdot E_d}\cdot\phi_{d3} + \varepsilon sh_{d3} \\ 0 \\ \frac{Ng_{ocC}}{A_g\cdot E_g}\cdot\phi_{g3} + \varepsilon sh_{g3} \\ \frac{Mg_{ocC}}{E_g\cdot I_g}\cdot\phi_{g3} \\ -\Delta f_{pR4}\cdot Apt_d \\ \varepsilon sh_{h3} \\ -\Delta f_{pR3C}\cdot Aps_g \\ 0 \end{pmatrix}$$

$$values14 = \begin{pmatrix} 0 \\ 0 \\ 0 \\ 0 \\ 0 \\ 0 \\ -0.000249 \\ 0 \\ -0.000307 \\ -0 \\ 3.986228 \\ -0.000025 \\ 8.795208 \\ 0 \end{pmatrix}$$

coeffs := stack(coeff1, coeff2, coeff3)

$$\text{coeffs} = \begin{pmatrix} 1 & 1 & 1 & 1 & 1 & 0 & 0 & 0 & 0 & 0 & 0 & 0 & 0 & 0 \\ 0 & 0 & 4.5 & 35.16523 & 53.72 & 1 & 1 & 1 & 0 & 0 & 0 & 0 & 0 & 0 \\ 0 & 0 & 0 & 0 & 0 & 0 & 0 & 0 & 1 & -1 & 0 & 0 & 0 & 0 \\ 0 & 0 & 0 & 0 & 0 & 0 & 0 & 0 & 1 & 0 & -1 & 0 & 0 & 4.5 \\ 0 & 0 & 0 & 0 & 0 & 0 & 0 & 0 & 1 & 0 & 0 & -1 & 0 & 35.16523 \\ 0 & 0 & 0 & 0 & 0 & 0 & 0 & 0 & 1 & 0 & 0 & 0 & -1 & 53.72 \\ -0 & 0 & 0 & 0 & 0 & 0 & 0 & 0 & 1 & 0 & 0 & 0 & 0 & 0 \\ 0 & 0 & 0 & 0 & 0 & -0 & 0 & 0 & 0 & 0 & 0 & 0 & 0 & 1 \\ 0 & 0 & 0 & -0 & 0 & 0 & 0 & 0 & 0 & 0 & 0 & 1 & 0 & 0 \\ 0 & 0 & 0 & 0 & 0 & 0 & 0 & -0 & 0 & 0 & 0 & 0 & 0 & 1 \\ 0 & -1 & 0 & 0 & 0 & 0 & 0 & 0 & 0 & 52326 & 0 & 0 & 0 & 0 \\ 0 & 0 & -0.00001 & 0 & 0 & 0 & 0 & 0 & 0 & 0 & 1 & 0 & 0 & 0 \\ 0 & 0 & 0 & 0 & -1 & 0 & 0 & 0 & 0 & 0 & 0 & 0 & 218025 & 0 \\ 0 & 0 & 0 & 0 & 0 & 0 & -0.00016 & 0 & 0 & 0 & 0 & 0 & 0 & 1 \end{pmatrix}$$

unknowns := coeffs^{-1} · values14

$$\text{unknowns} = \begin{pmatrix} -10.71801719 \\ -17.28093802 \\ -16.88119119 \\ 112.51704852 \\ -67.63690212 \\ -3.34687349 \\ -0.00179384 \\ -243.91909016 \\ -0.00025407 \\ -0.00025407 \\ -0.0002554 \\ -0.00026442 \\ -0.00026989 \\ -0.00000029 \end{pmatrix} \qquad \text{unknowns14} := \begin{pmatrix} \Delta Nd \\ \Delta Nptd \\ \Delta Nh \\ \Delta Ng \\ \Delta Npsg \\ \Delta Md \\ \Delta Mh \\ \Delta Mg \\ \Delta \varepsilon d \\ \Delta \varepsilon ptd \\ \Delta \varepsilon h \\ \Delta \varepsilon g \\ \Delta \varepsilon psg \\ \Delta \chi \end{pmatrix}$$

$\Delta\chi_{finalC} := \text{unknowns}_{14}$ $\quad \Delta\chi_{finalC} = -2.94 \times 10^{-7}$ strain/inch

$\chi_{finalC} := \Delta\chi g_{1C} + \Delta\chi_{finalC}$ $\quad \chi_{finalC} = -5.8 \times 10^{-6}$

Summary of Curvatures

1) Changes in curvature

$$\Delta\chi_{finalA} = -3.25 \times 10^{-6}$$

$$\Delta\chi_{finalB} = -8.24 \times 10^{-7}$$

$$\Delta\chi_{finalC} = -2.94 \times 10^{-7}$$

$$curvchanges := \begin{pmatrix} \Delta\chi_{finalA} \\ \Delta\chi_{finalB} \\ \Delta\chi_{finalC} \\ \Delta\chi_{finalB} \\ \Delta\chi_{finalA} \\ \Delta\chi_{finalA} \\ \Delta\chi_{finalB} \\ \Delta\chi_{finalC} \\ \Delta\chi_{finalB} \\ \Delta\chi_{finalA} \\ \Delta\chi_{finalA} \\ \Delta\chi_{finalB} \\ \Delta\chi_{finalC} \\ \Delta\chi_{finalB} \\ \Delta\chi_{finalA} \end{pmatrix} \quad curvchanges = \begin{pmatrix} -3.25 \times 10^{-6} \\ -8.24 \times 10^{-7} \\ -2.94 \times 10^{-7} \\ -8.24 \times 10^{-7} \\ -3.25 \times 10^{-6} \\ -3.25 \times 10^{-6} \\ -8.24 \times 10^{-7} \\ -2.94 \times 10^{-7} \\ -8.24 \times 10^{-7} \\ -3.25 \times 10^{-6} \\ -3.25 \times 10^{-6} \\ -8.24 \times 10^{-7} \\ -2.94 \times 10^{-7} \\ -8.24 \times 10^{-7} \\ -3.25 \times 10^{-6} \end{pmatrix}$$

$$\text{curvlengths} := \begin{pmatrix} x_A \\ x_B \\ x_C \\ L_g - x_B \\ L_g - x_A \\ L_g + x_A \\ L_g + x_B \\ L_g + x_C \\ 2\cdot L_g - x_B \\ 2\cdot L_g - x_A \\ 2\cdot L_g + x_A \\ 2\cdot L_g + x_B \\ 2\cdot L_g + x_C \\ 3\cdot L_g - x_B \\ 3\cdot L_g - x_A \end{pmatrix} \qquad \text{curvlengths} = \begin{pmatrix} 0 \\ 300 \\ 600 \\ 900 \\ 1200 \\ 1200 \\ 1500 \\ 1800 \\ 2100 \\ 2400 \\ 2400 \\ 2700 \\ 3000 \\ 3300 \\ 3600 \end{pmatrix}$$

Graph of changes in curvatures during last time interval

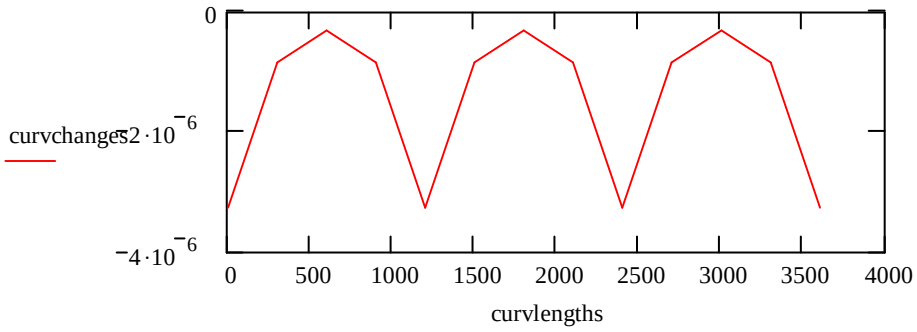

Sign conventions

Tension = lengthening = +

Compression @ top = + curvature and
+ moment

Add Continuity

Moment-area method to find deflection if middle support removed:

Need sum of areas times moment arms
Sum moments from left support
Units: strain/inch*inch*inch = inches

Equations for entire graph being **NEGATIVE** with 3 upside-down U's

$A_{t1} := \frac{1}{2} \cdot x_B \cdot \left| \Delta\chi_{finalA} - \Delta\chi_{finalB} \right|$ $\quad arm_{t1} := \frac{x_B}{3}$

$A_{t1} = 3.64 \times 10^{-4}$ $\quad arm_{t1} = 100$

$A_{r1} := x_B \cdot \left| \Delta\chi_{finalB} \right|$ $\quad arm_{r1} := \frac{x_B}{2}$

$A_{r1} = 2.47 \times 10^{-4}$ $\quad arm_{r1} = 150$

$A_{t2} := \frac{1}{2} \cdot (x_C - x_B) \cdot \left| \Delta\chi_{finalB} - \Delta\chi_{finalC} \right|$ $\quad arm_{t2} := x_B + \frac{(x_C - x_B)}{3}$

$A_{t2} = 7.95 \times 10^{-5}$ $\quad arm_{t2} = 400$

$A_{r2} := (x_C - x_B) \cdot \left| \Delta\chi_{finalC} \right|$ $\quad arm_{r2} := x_B + \frac{(x_C - x_B)}{2}$

$A_{r2} = 8.83 \times 10^{-5}$ $\quad arm_{r2} = 450$

$A_{t3} := A_{t2}$ $\quad arm_{t3} := x_C + \frac{2}{3} \cdot (x_C - x_B)$

$A_{t3} = 7.95 \times 10^{-5}$ $\quad arm_{t3} = 800$

$A_{r3} := A_{r2}$ $\quad arm_{r3} := x_C + \frac{(x_C - x_B)}{2}$

$A_{r3} = 8.83 \times 10^{-5}$ $\quad arm_{r3} = 750$

$A_{t4} := A_{t1}$ $\quad arm_{t4} := L_g - \frac{x_B}{3}$

$A_{t4} = 3.64 \times 10^{-4}$ $\quad arm_{t4} = 1100$

$A_{r4} := A_{r1}$ $\quad arm_{r4} := L_g - \frac{x_B}{2}$

$A_{r4} = 2.47 \times 10^{-4}$ $\quad arm_{r4} = 1050$

$A_{t5} := A_{t1}$ $\quad arm_{t5} := L_g + \frac{x_B}{3}$

$A_{t5} = 3.64 \times 10^{-4}$ $\quad arm_{t5} = 1300$

$A_{r5} := A_{r1}$ $\quad arm_{r5} := L_g + \frac{x_B}{2}$

$A_{r5} = 2.47 \times 10^{-4}$ $\quad arm_{r5} = 1350$

$A_{t6} := A_{t2}$ $\quad arm_{t6} := L_g + x_B + \frac{(x_C - x_B)}{3}$

$A_{t6} = 7.95 \times 10^{-5}$ $\quad arm_{t6} = 1600$

$A_{r6} := A_{r2}$ $\quad arm_{r6} := L_g + x_B + \frac{(x_C - x_B)}{2}$

$A_{r6} = 8.83 \times 10^{-5}$ $\quad arm_{r6} = 1650$

$\Delta_{mid1} := A_{t1} \cdot arm_{t1} + A_{r1} \cdot arm_{r1} + A_{t2} \cdot arm_{t2} + A_{r2} \cdot arm_{r2}$ $\quad \Delta_{mid1} = 0.145$

$\Delta_{mid2} := A_{t3} \cdot arm_{t3} + A_{r3} \cdot arm_{r3} + A_{t4} \cdot arm_{t4} + A_{r4} \cdot arm_{r4}$ $\quad \Delta_{mid2} = 0.7901$

$\Delta_{mid3} := A_{t5} \cdot arm_{t5} + A_{r5} \cdot arm_{r5} + A_{t6} \cdot arm_{t6} + A_{r6} \cdot arm_{r6}$ $\quad \Delta_{mid3} = 1.0802$

In this case, all areas are (-)

$\Delta_{middle} := \Delta_{mid1} + \Delta_{mid2} + \Delta_{mid3}$

$\Delta_{middle} = 2.0154$ inches

$\Delta_{thirdpt} := -(\Delta_{middle} - \Delta_{mid1})$

$\Delta_{thirdpt} = -1.8703$

$\Delta_{thirdpt} = \frac{P \cdot L^3}{28 \cdot E \cdot I}$

and solve for restoring force P
where
E = age adjusted E of girder
I = age adjusted transformed cross-section

Find transformed section properties (regular and age adjusted) for composite section including haunch

$\phi_{dc} := CREEP(fc_d, t_{dcomp}, t_{dinf}, hum, A_d, perim_d)$ $\phi_{dc} = 0.9$

$\phi_{hc} := CREEP(fc_h, t_{hcomp}, t_{hinf}, hum, A_h, perim_h)$ $\phi_{hc} = 0.15$

$\phi_{gc} := CREEP(fc_g, t_{gcomp}, t_{ginf}, hum, A_g, perim_g)$ $\phi_{gc} = 0.61$

Regular transformed section - for use with transient loads

Deck mod. ratio P/T mod. ratio Haunch mod. ratio P/S mod. ratio

$n_{dg} := \frac{E_d}{E_g}$ $n_{ptg} := \frac{Ept_d}{E_g}$ $n_{hg} := \frac{E_h}{E_g}$ $n_{psg} := \frac{Eps_g}{E_g}$

$n_{dg} = 0.845$ $n_{ptg} = 5.98$ $n_{hg} = 0.845$ $n_{psg} = 5.98$

$Ad_{tr} := n_{dg} \cdot A_d$ $Apt_{tr} := n_{ptg} \cdot Apt_d$ $Ah_{tr} := n_{hg} \cdot A_h$ $Aps_{tr} := n_{psg} \cdot Aps_g$

$Ad_{tr} = 730.21$ $Apt_{tr} = 10.97$ $Ah_{tr} = 16.9$ $Aps_{tr} = 45.72$

(areas transformed to concrete equivalent of that in girder)

AT SECTION A

$A_{tr} := A_g + Ad_{tr} + Apt_{tr} + Ah_{tr} + Aps_{tr}$ $A_{tr} = 1592.8$

$c_{tr} := \frac{A_g \cdot c_g + Ad_{tr} \cdot y_d + Apt_{tr} \cdot y_{pt} + Ah_{tr} \cdot y_h + Aps_{tr} \cdot y_{psA}}{A_{tr}}$ $c_{tr} = 40.63$

$I_{tr1} := I_g + A_g \cdot (c_{tr} - c_g)^2 + I_d \cdot n_{dg} + Ad_{tr} \cdot (y_d - c_{tr})^2 + Apt_{tr} \cdot (y_{pt} - c_{tr})^2$

$I_{tr2} := I_h \cdot n_{hg} + Ah_{tr} \cdot (y_h - c_{tr})^2 + Aps_{tr} \cdot (y_{psA} - c_{tr})^2$

$I_{tr} := I_{tr1} + I_{tr2}$ $I_{tr} = 754936.4$

Age-adjusted transformed section - for use with permanent loads

$$E_{daatr} := \frac{E_d}{1 + \mu_d \cdot \phi_{dc}} \qquad E_{haatr} := \frac{E_h}{1 + \mu_h \cdot \phi_{hc}} \qquad E_{gaatr} := \frac{E_g}{1 + \mu_g \cdot \phi_{gc}}$$

$E_{daatr} = 2468$ $E_{haatr} = 3657$ $E_{gaatr} = 3344$

Deck mod. ratio

$$n_{dga} := \frac{E_{daatr}}{E_{gaatr}}$$

$n_{dga} = 0.738$

P/T mod. ratio

$$n_{ptga} := \frac{Ept_d}{E_{gaatr}}$$

$n_{ptga} = 8.522$

Haunch mod. ratio

$$n_{hga} := \frac{E_{haatr}}{E_{gaatr}}$$

$n_{hga} = 1.094$

P/S mod. ratio

$$n_{psga} := \frac{Eps_g}{E_{gaatr}}$$

$n_{psga} = 8.522$

compare each element to girder mod. ratio

$$Ad_{atr} := n_{dga} \cdot A_d \qquad Apt_{atr} := n_{ptga} \cdot Apt_d \qquad Ah_{atr} := n_{hga} \cdot A_h \qquad Aps_{atr} := n_{psga} \cdot Aps_g$$

$Ad_{atr} = 637.6$ $Apt_{atr} = 15.65$ $Ah_{atr} = 21.87$ $Aps_{atr} = 65.2$

(areas transformed to age-adjusted concrete equivalent of that in girder)

AT SECTION A

$$A_{atr} := A_g + Ad_{atr} + Apt_{atr} + Ah_{atr} + Aps_{atr} \qquad A_{atr} = 1529.3 \text{ in}^2$$

$$c_{atr} := \frac{A_g \cdot c_g + Ad_{atr} \cdot y_d + Apt_{atr} \cdot y_{pt} + Ah_{atr} \cdot y_h + Aps_{atr} \cdot y_{psA}}{A_{atr}} \qquad c_{atr} = 39.25 \text{ in}$$

$$I_{atr1} := I_g + A_g \cdot (c_{atr} - c_g)^2 + I_d \cdot n_{dga} + Ad_{atr} \cdot (y_d - c_{atr})^2 + Apt_{atr} \cdot (y_{pt} - c_{atr})^2$$

$$I_{atr2} := I_h \cdot n_{hga} + Ah_{atr} \cdot (y_h - c_{atr})^2 + Aps_{atr} \cdot (y_{psA} - c_{atr})^2$$

$$I_{atr} := I_{atr1} + I_{atr2} \qquad I_{atr} = 738784.9 \text{ in}^4$$

Need force P to restore deflection at middle support to zero:

$$\Delta_{thirdpt} = \frac{P \cdot L^3}{28 \cdot E \cdot I} \qquad E_{gaatr} = 3344.13 \qquad I_{atr} = 738784.94 \qquad L_t = 3600$$

$$P := \frac{\Delta_{thirdpt} \cdot 28 \cdot E_{gaatr} \cdot I_{atr}}{L_t^3} \qquad P = -2.77 \quad \text{kips}$$

Maximum moment:

$$M_{max} := \frac{P \cdot L_t}{3} \qquad M_{max} = -3328 \quad \text{ip-in}$$

Stress at top fiber of composite section at middle support:

$$\sigma comp_M := \frac{M_{max} \cdot (depth_t - c_{atr})}{I_{atr}} \cdot n_{dga} \qquad \sigma comp_M = -0.0789 \quad \text{ksi}$$

Stress in top fiber due to force redistribution over time at midspan of a single span:

$$\sigma comp_{Fredist} := stress_{dAf_1} \qquad \sigma comp_{Fredist} = -0.258 \quad \text{ksi}$$

Obtain negative moment over middle support from QConBridge (ft-lbs):

$$M_{QCon} := 2180000$$

$$M_{neg} := M_{QCon} \cdot \frac{12}{1000} \qquad M_{neg} = 26160 \quad \text{kip-in}$$

Stress at top of composite section due to live loads (tension):

$$\sigma comp_{LL} := \frac{|M_{neg}| \cdot (depth_t - c_{tr})}{I_{tr}} \cdot n_{dg} \qquad \sigma comp_{LL} = 0.655 \quad \text{ksi}$$

Factor LL using DFM and 0.8 Service III factor:

$e_g := \frac{t_d}{2} + t_h + (depth_g - c_g)$ $e_g = 34.27$ $n := \frac{E_g}{E_d}$ $n = 1.18$

$K_g := n\cdot\left[I_g + \left(A_g\cdot e_g^{2}\right)\right]$ $K_g = 1404900.41$

$$DFM_2 := 0.075 + \left[\left(\frac{\frac{w_d}{12}}{9.5}\right)^{0.6}\left(\frac{w_d}{L_g}\right)^{0.2}\left(\frac{K_g}{L_g\cdot t_d^{3}}\right)^{0.1}\right] \qquad DFM_2 = 0.72$$

$$DFM_1 := 0.06 + \left[\left(\frac{\frac{w_d}{12}}{14}\right)^{0.4}\left(\frac{w_d}{L_g}\right)^{0.3}\left(\frac{K_g}{L_g\cdot t_d^{3}}\right)^{0.1}\right] \qquad DFM_1 = 0.5$$

$mp := 1$

$DFM_f := \frac{DFM_1}{mp}$ $DFM_f = 0.5$

$DFM := \max(DFM_2, DFM_1, DFM_f)$ $DFM = 0.725$

$\sigma comp_{LLf} := \sigma comp_{LL}\cdot DFM\cdot 0.8$ $\sigma comp_{LLf} = 0.38$ ksi

Final stress in deck (ksi)

$\sigma comp_{final} := \sigma comp_{Fredist} + \sigma comp_M + \sigma comp_{LLf}$

$\sigma comp_{final} = 0.043$

SUMMARY

Final stresses at section A (end of single beam)

Initial compression in deck (ksi)

$$stress_{dAi} := \frac{Nd_o}{A_d}$$

$stress_{dAi} = -0.439$ ksi

Compression at top, middle, & bottom of deck after SS analysis (ksi)

$$stress_{dAf} = \begin{pmatrix} -0.258 \\ -0.29 \\ -0.322 \end{pmatrix}$$ ksi

Final stress in deck (ksi)

$$\sigma comp_{final} := \sigma comp_{Fredist} + \sigma comp_{M} + \sigma comp_{LLf}$$

$\sigma comp_{final} = 0.043$

APPENDIX D

Results of Continuous Steel Girder Bridge Parametric Studies

Table D.1: Two Span Continuous Steel Girder Bridge Parametric Studies

Bridge Properties				Initial	Simple Span Analysis			Continuous Span Analysis				Results	
					Final Comp. in Deck			Tens. at Top of Deck					
Girder Type	Girder Spc. (ft)	Span Length (ft)	No. of Strands in Deck	Comp. in Deck (psi)	Top (psi)	Mid. (psi)	Bot. (psi)	Due to Force Redist. (psi)	Due to LL (psi)	DFM	Stress from Factored LL (psi)	Total Stress with LL (psi)	Total Stress without LL (psi)
W24x103	6	60	4	-206	-215	-141	-67	276	1416	0.483	547	608	61
W36x160	6	90	4	-207	-159	-109	-59	266	1559	0.476	594	701	107
PL 1, d=48	6	120	4	-207	-112	-76	-40	256	1448	0.474	549	693	144
W24x146	9	60	6	-206	-210	-138	-66	264	941	0.661	498	552	54
W36x232	9	90	6	-207	-157	-108	-59	260	1017	0.654	532	635	103
PL 2, d=50	9	120	6	-207	-118	-83	-48	243	955	0.646	494	619	125
W24x103	6	60	6	-309	-312	-230	-149	304	1413	0.483	546	538	-8
W36x160	6	90	6	-311	-250	-195	-140	293	1556	0.476	593	636	43
PL 1, d=48	6	120	6	-311	-199	-159	-120	283	1445	0.474	548	632	84
W24x146	9	60	9	-309	-302	-223	-144	288	939	0.661	497	483	-14
W36x232	9	90	9	-311	-243	-190	-137	283	1015	0.654	531	571	40
PL 2, d=50	9	120	9	-311	-201	-163	-125	266	952	0.646	492	557	65
W24x103	6	60	10	-515	-490	-395	-301	350	1408	0.483	544	404	-140
W36x160	6	90	10	-518	-419	-355	-291	338	1549	0.476	590	509	-81
PL 1, d=48	6	120	10	-518	-360	-314	-268	326	1438	0.474	545	511	-34
W24x146	9	60	15	-515	-448	-362	-275	316	935	0.661	494	362	-132
W36x232	9	90	15	-518	-385	-326	-268	311	1010	0.654	528	454	-74
PL 2, d=50	9	120	15	-518	-339	-297	-255	292	948	0.646	490	443	-47
W24x103	6	60	12	-618	-568	-469	-369	367	1405	0.483	543	342	-201
W36x160	6	90	12	-622	-494	-427	-360	354	1546	0.476	589	449	-140
PL 1, d=48	6	120	12	-622	-432	-384	-335	342	1435	0.474	544	454	-90
W24x146	9	60	18	-618	-496	-409	-322	316	934	0.661	494	314	-180
W36x232	9	90	18	-622	-432	-374	-315	311	1008	0.654	527	406	-121
PL 2, d=50	9	120	18	-622	-386	-344	-302	292	946	0.646	489	395	-94
W24x103	6	60	14	-721	-636	-533	-431	379	1403	0.483	542	285	-257
W36x160	6	90	14	-725	-560	-490	-421	365	1542	0.476	587	392	-195
PL 1, d=48	6	120	14	-725	-496	-446	-396	353	1431	0.474	543	400	-143
W24x146	9	60	21	-721	-522	-438	-354	304	932	0.661	493	275	-218
W36x232	9	90	21	-725	-460	-404	-347	299	1006	0.654	526	365	-161
PL 2, d=50	9	120	21	-725	-416	-376	-335	280	944	0.646	488	352	-136

Table D.1: Two Span Continuous Steel Girder Bridge Parametric Studies (continued)

Bridge Properties				Initial	Simple Span Analysis			Continuous Span Analysis				Results	
					Final Comp. in Deck			Tens. at Top of Deck					
Girder Type	Girder Spc. (ft)	Span Length (ft)	No. of Strands in Deck	Comp. in Deck (psi)	Top (psi)	Mid. (psi)	Bot. (psi)	Due to Force Redist. (psi)	Due to LL (psi)	DFM	Stress from Factored LL (psi)	Total Stress with LL (psi)	Total Stress without LL (psi)
W24x103	6	60	16	-824	-693	-589	-484	384	1400	0.483	541	232	-309
W36x160	6	90	16	-829	-616	-545	-475	370	1539	0.476	586	340	-246
PL 1, d=48	6	120	16	-829	-551	-500	-450	358	1428	0.474	541	348	-193
W24x146	9	60	24	-824	-522	-445	-368	278	930	0.661	492	248	-244
W36x232	9	90	24	-829	-465	-413	-362	273	1004	0.654	525	333	-192
PL 2, d=50	9	120	24	-829	-425	-388	-350	257	942	0.646	487	319	-168
W24x103	6	60	20	-1030	-766	-665	-564	371	1395	0.483	539	144	-395
W36x160	6	90	20	-1036	-691	-623	-555	358	1532	0.476	583	250	-333
PL 1, d=48	6	120	20	-1036	-629	-580	-531	346	1422	0.474	539	256	-283
W24x146	9	60	29	-996	-455	-400	-345	200	927	0.661	490	235	-255
W36x232	9	90	29	-1002	-414	-376	-339	195	1000	0.654	523	304	-219
PL 2, d=50	9	120	29	-1002	-385	-358	-331	184	938	0.646	485	284	-201
W24x103	6	60	24	-1236	-776	-687	-598	324	1390	0.483	537	85	-452
W36x160	6	90	24	-1243	-710	-650	-591	311	1526	0.476	581	182	-399
PL 1, d=48	6	120	24	-1243	-656	-613	-570	302	1415	0.474	537	183	-354
W24x146	9	60	36	-1236	-196	-196	-195	1	923	0.661	488	293	-195
W36x232	9	90	36	-1243	-192	-192	-192	-2	995	0.654	521	327	-194
PL 2, d=50	9	120	36	-1243	-192	-192	-192	-1	933	0.646	482	289	-193
W24x103	6	60	29	-1494	-680	-624	-567	205	1383	0.483	534	59	-475
W36x160	6	90	29	-1502	-638	-600	-562	196	1518	0.476	578	136	-442
PL 1, d=48	6	120	29	-1502	-604	-576	-549	191	1407	0.474	534	121	-413
W24x146	9	60	44	-1511	387	281	176	-376	919	0.661	486	497	11
W36x232	9	90	44	-1520	320	248	176	-377	989	0.654	517	460	-57
PL 2, d=50	9	120	44	-1520	265	213	161	-353	927	0.646	479	391	-88

Table D.2: Three Span Continuous Steel Girder Bridge Parametric Studies

Bridge Properties					Simple Span Analysis			Continuous Span Analysis				Results	
					Final Comp. in Deck			Tens. at Top of Deck					
Girder Type	Girder Spc. (ft)	Span Length (ft)	No. of Strands in Deck	Initial Comp. in Deck (psi)	Top (psi)	Mid. (psi)	Bot. (psi)	Due to Force Redist. (psi)	Due to LL (psi)	DFM	Stress from Factored LL (psi)	Total Stress with LL (psi)	Total Stress without LL (psi)
W24x103	6	60	4	-207	-216	-142	-68	191	1303	0.483	503	478	-25
W36x160	6	90	4	-207	-159	-109	-59	184	1470	0.476	560	585	25
PL 1, d=48	6	120	4	-206	-111	-75	-39	177	1376	0.474	522	588	66
W24x146	9	60	6	-207	-212	-139	-67	183	865	0.661	457	428	-29
W36x232	9	90	6	-207	-156	-108	-59	180	959	0.654	502	526	24
PL 2, d=50	9	120	6	-206	-117	-82	-47	168	907	0.646	469	520	51
W24x103	6	60	6	-311	-314	-232	-150	210	1300	0.483	502	398	-104
W36x160	6	90	6	-311	-250	-195	-140	202	1467	0.476	559	511	-48
PL 1, d=48	6	120	6	-309	-197	-158	-118	195	1373	0.474	521	519	-2
W24x146	9	60	9	-311	-303	-224	-146	199	864	0.661	457	353	-104
W36x232	9	90	9	-311	-243	-190	-137	196	957	0.654	501	454	-47
PL 2, d=50	9	120	9	-309	-200	-162	-124	183	905	0.646	468	451	-17
W24x103	6	60	10	-518	-493	-398	-303	243	1295	0.483	500	250	-250
W36x160	6	90	10	-518	-419	-355	-291	234	1460	0.476	556	371	-185
PL 1, d=48	6	120	10	-515	-358	-312	-266	225	1366	0.474	518	385	-133
W24x146	9	60	15	-518	-450	-363	-277	219	860	0.661	455	224	-231
W36x232	9	90	15	-518	-384	-326	-267	215	952	0.654	498	329	-169
PL 2, d=50	9	120	15	-515	-337	-295	-253	201	901	0.646	466	330	-136
W24x103	6	60	12	-622	-571	-471	-372	255	1293	0.483	500	184	-316
W36x160	6	90	12	-621	-493	-426	-359	245	1457	0.476	555	307	-248
PL 1, d=48	6	120	12	-618	-429	-381	-333	236	1363	0.474	517	324	-193
W24x146	9	60	18	-622	-498	-411	-324	219	859	0.661	454	175	-279
W36x232	9	90	18	-621	-432	-373	-315	215	950	0.654	497	280	-217
PL 2, d=50	9	120	18	-618	-385	-342	-300	201	899	0.646	465	281	-184
W24x103	6	60	14	-725	-639	-536	-433	262	1290	0.483	498	121	-377
W36x160	6	90	14	-725	-559	-490	-421	252	1454	0.476	554	247	-307
PL 1, d=48	6	120	14	-721	-493	-443	-394	244	1360	0.474	516	267	-249
W24x146	9	60	21	-725	-523	-440	-356	210	857	0.661	453	140	-313
W36x232	9	90	21	-725	-460	-404	-347	207	948	0.654	496	243	-253
PL 2, d=50	9	120	21	-721	-415	-374	-333	194	897	0.646	464	243	-221

Table D.2: Three Span Continuous Steel Girder Bridge Parametric Studies (continued)

Bridge Properties					Simple Span Analysis			Continuous Span Analysis				Results	
					Final Comp. in Deck			Tens. at Top of Deck					
Girder Type	Girder Spc. (ft)	Span Length (ft)	No. of Strands in Deck	Initial Comp. in Deck (psi)	Top (psi)	Mid. (psi)	Bot. (psi)	Due to Force Redist. (psi)	Due to LL (psi)	DFM	Stress from Factored LL (psi)	Total Stress with LL (psi)	Total Stress without LL (psi)
W24x103	6	60	16	-829	-696	-591	-487	266	1288	0.483	498	68	-430
W36x160	6	90	16	-828	-615	-545	-474	256	1451	0.476	553	194	-359
PL 1, d=48	6	120	16	-824	-548	-498	-447	247	1357	0.474	515	214	-301
W24x146	9	60	24	-829	-523	-446	-369	192	856	0.661	453	122	-331
W36x232	9	90	24	-828	-465	-413	-361	189	946	0.654	495	219	-276
PL 2, d=50	9	120	24	-824	-424	-386	-349	178	895	0.646	463	217	-246
W24x103	6	60	20	-1036	-769	-668	-566	257	1283	0.483	496	-16	-512
W36x160	6	90	20	-1035	-691	-623	-554	247	1444	0.476	550	106	-444
PL 1, d=48	6	120	20	-1030	-626	-577	-528	239	1351	0.474	512	125	-387
W24x146	9	60	29	-1002	-454	-400	-345	137	853	0.661	451	134	-317
W36x232	9	90	29	-1001	-414	-376	-339	135	943	0.654	493	214	-279
PL 2, d=50	9	120	29	-996	-385	-358	-331	128	891	0.646	460	203	-257
W24x103	6	60	24	-1243	-777	-689	-601	223	1278	0.483	494	-60	-554
W36x160	6	90	24	-1242	-710	-650	-590	215	1438	0.476	548	53	-495
PL 1, d=48	6	120	24	-1236	-654	-611	-568	209	1345	0.474	510	65	-445
W24x146	9	60	36	-1243	-191	-192	-192	-2	849	0.661	449	256	-193
W36x232	9	90	36	-1242	-192	-192	-193	-1	938	0.654	491	298	-193
PL 2, d=50	9	120	36	-1236	-195	-195	-195	2	887	0.646	458	265	-193
W24x103	6	60	29	-1502	-679	-623	-568	140	1272	0.483	492	-47	-539
W36x160	6	90	29	-1501	-638	-600	-562	136	1431	0.476	545	43	-502
PL 1, d=48	6	120	29	-1494	-604	-576	-548	134	1337	0.474	507	37	-470
W24x146	9	60	44	-1520	400	292	185	-266	845	0.661	447	581	134
W36x232	9	90	44	-1518	318	246	174	-259	933	0.654	488	547	59
PL 2, d=50	9	120	44	-1511	255	204	153	-238	881	0.646	455	472	17

APPENDIX E

Results of Continuous Prestressed Concrete Girder Bridge Parametric Studies

Table E.1: Two Span Continuous PCBT Girder Bridge Parametric Studies

Bridge Properties					Simple Span Analysis			Continuous Span Analysis					Results	
					Final Comp. in Deck				Tens. at Top of Deck					
Girder Type	Girder Spc. (ft)	Span Length (ft)	No. of Strands in Deck	Initial Comp. in Deck (psi)	Top (psi)	Mid. (psi)	Bot. (psi)	Curvature Changes	Due to Force Redist. (psi)	Due to LL (psi)	DFM	Stress from Factored LL (psi)	Total Stress with LL (psi)	Total Stress without LL (psi)
PCBT-37	6	40	4	-216	-63	-87	-110	all (-)	-122	261	0.643	134	-51	-185
PCBT-37	6	40	8	-432	-243	-257	-272	all (-)	-58	260	0.643	134	-167	-301
PCBT-37	6	75	4	-220	-16	-72	-127	all (-)	-201	922	0.546	403	186	-217
PCBT-37	6	75	8	-440	-200	-246	-291	all (-)	-135	918	0.546	401	66	-335
PCBT-37	6	75	10	-550	-292	-332	-373	all (-)	-103	916	0.546	400	6	-395
PCBT-37	6	75	12	-659	-383	-419	-455	some +/-	-71	914	0.546	399	-54	-454
PCBT-37	6	75	14	-769	-473	-504	-536	some +/-	-45	912	0.546	398	-120	-518
PCBT-37	9	40	6	-216	-98	-118	-137	all (-)	-76	201	0.861	138	-35	-174
PCBT-37	9	40	12	-432	-288	-297	-306	some +/-	-15	200	0.861	138	-166	-303
PCBT-37	9	40	18	-648	-476	-474	-473	all (+)	48	199	0.861	137	-291	-428
PCBT-61	6	65	4	-219	-58	-73	-89	all (-)	-81	365	0.624	182	43	-139
PCBT-61	6	65	8	-439	-229	-239	-249	some +/-	-26	363	0.624	181	-74	-255
PCBT-61	6	65	10	-548	-314	-322	-329	some +/-	1	363	0.624	181	-132	-313
PCBT-61	6	65	12	-658	-399	-404	-408	some +/-	27	362	0.624	181	-191	-372
PCBT-61	6	125	4	-220	20	-33	-86	all (-)	-263	919	0.526	387	144	-243
PCBT-61	6	125	8	-440	-153	-201	-248	all (-)	-206	914	0.526	385	26	-359
PCBT-61	6	125	10	-550	-239	-284	-329	all (-)	-178	913	0.526	384	-33	-417
PCBT-61	6	125	12	-660	-324	-367	-409	some +/-	-151	911	0.526	383	-91	-475
PCBT-61	9	50	6	-218	-84	-100	-116	all (-)	-107	146	0.897	105	-86	-191
PCBT-61	9	50	9	-327	-174	-187	-200	all (-)	-79	146	0.897	105	-148	-253
PCBT-61	9	50	12	-436	-264	-274	-284	all (-)	-52	146	0.897	105	-211	-316
PCBT-61	9	85	6	-220	-72	-99	-126	all (-)	-121	443	0.776	275	83	-193
PCBT-61	9	85	12	-440	-255	-276	-296	some +/-	-65	441	0.776	274	-46	-320
PCBT-61	9	85	18	-660	-436	-451	-465	some +/-	-10	438	0.776	272	-174	-446
PCBT-85	6	85	4	-220	-39	-53	-67	all (-)	-91	370	0.623	184	55	-130
PCBT-85	6	85	8	-440	-205	-215	-225	some +/-	-39	369	0.623	184	-60	-244
PCBT-85	6	85	10	-550	-287	-295	-303	some +/-	-14	368	0.623	183	-118	-301
PCBT-85	6	85	12	-660	-369	-375	-382	some +/-	10	367	0.623	183	-176	-359
PCBT-85	6	150	4	-220	-9	-42	-75	all (-)	-175	741	0.537	318	135	-184
PCBT-85	6	150	8	-439	-174	-204	-233	some +/-	-123	738	0.537	317	20	-297
PCBT-85	6	150	10	-549	-256	-284	-312	some +/-	-98	737	0.537	317	-37	-354
PCBT-85	6	150	12	-659	-338	-364	-390	some +/-	-73	735	0.537	316	-95	-411
PCBT-85	9	70	6	-220	-70	-83	-97	all (-)	-109	214	0.879	150	-28	-179
PCBT-85	9	70	12	-439	-245	-255	-264	all (-)	-56	213	0.879	150	-151	-301
PCBT-85	9	70	15	-549	-333	-340	-347	some +/-	-30	212	0.879	149	-214	-363
PCBT-85	9	125	6	-220	-47	-75	-103	all (-)	-160	469	0.750	281	74	-207
PCBT-85	9	125	12	-440	-224	-248	-271	all (-)	-107	467	0.750	280	-51	-331
PCBT-85	9	125	15	-550	-311	-333	-355	some +/-	-81	466	0.750	280	-112	-392
PCBT-85	9	125	18	-660	-399	-418	-438	some +/-	-55	465	0.750	279	-175	-454

Table E.2: Two Span Continuous AASHTO Girder Bridge Parametric Studies

Bridge Properties					Simple Span Analysis			Continuous Span Analysis					Results	
					Final Comp. in Deck				Tens. at Top of Deck					
Girder Type	Girder Spc. (ft)	Span Length (ft)	No. of Strands in Deck	Initial Comp. in Deck (psi)	Top (psi)	Mid. (psi)	Bot. (psi)	Curvature Changes	Due to Force Redist. (psi)	Due to LL (psi)	DFM	Stress from Factored LL (psi)	Total Stress with LL (psi)	Total Stress without LL (psi)
Type II	6	45	4	-217	-164	-174	-184	some +/-	-13	401	0.592	190	13	-177
Type II	6	45	8	-434	-366	-364	-362	all (+)	56	399	0.592	189	-121	-310
Type II	6	45	10	-542	-467	-459	-451	all (+)	90	398	0.592	188	-189	-377
Type II	6	45	12	-651	-566	-552	-539	all (+)	123	397	0.592	188	-255	-443
Type II	6	70	4	-220	-62	-144	-226	all (-)	-345	1068	0.528	451	44	-407
Type II	6	70	8	-439	-267	-337	-406	all (-)	-271	1062	0.528	449	-90	-538
Type II	6	70	10	-549	-369	-432	-496	all (-)	-235	1060	0.528	448	-157	-604
Type II	6	70	12	-659	-470	-528	-585	all (-)	-200	1057	0.528	446	-224	-670
Type II	9	35	6	-214	-176	-184	-192	all (-)	-16	213	0.847	144	-47	-192
Type II	9	35	9	-322	-278	-280	-282	some +/-	15	212	0.847	144	-120	-263
Type II	9	35	12	-429	-380	-376	-372	all (+)	45	212	0.847	144	-192	-336
Type II	9	55	6	-218	-111	-176	-241	all (-)	-241	472	0.749	283	-69	-352
Type II	9	55	9	-328	-216	-274	-333	all (-)	-209	471	0.749	282	-143	-425
Type II	9	55	12	-437	-320	-372	-425	all (-)	-177	470	0.749	282	-215	-497
Type IV	6	75	4	-220	-113	-117	-121	some +/-	57	621	0.587	292	236	-56
Type IV	6	75	8	-440	-295	-292	-289	all (+)	125	618	0.587	290	120	-170
Type IV	6	75	10	-550	-386	-379	-372	all (+)	158	616	0.587	289	62	-228
Type IV	6	75	12	-659	-476	-466	-455	all (+)	191	615	0.587	289	4	-285
Type IV	6	75	14	-769	-565	-552	-538	all (+)	224	613	0.587	288	-53	-341
Type IV	6	75	16	-879	-655	-638	-621	all (+)	256	612	0.587	287	-112	-399
Type IV	6	75	18	-989	-743	-723	-703	all (+)	288	610	0.587	286	-169	-456
Type IV	6	120	4	-220	-40	-85	-129	all (-)	-184	1153	0.520	480	256	-224
Type IV	6	120	6	-330	-132	-173	-213	all (-)	-149	1150	0.520	478	198	-281
Type IV	6	120	8	-440	-224	-261	-298	some +/-	-114	1148	0.520	478	140	-338
Type IV	6	120	12	-661	-405	-435	-465	some +/-	-46	1142	0.520	475	24	-451
Type IV	6	120	14	-771	-495	-522	-549	some +/-	-12	1139	0.520	474	-34	-507
Type IV	6	120	16	-881	-585	-608	-632	some +/-	21	1136	0.520	473	-92	-564
Type IV	6	120	18	-991	-674	-694	-714	some +/-	53	1134	0.520	472	-149	-621
Type IV	9	65	6	-219	-131	-136	-140	some +/-	21	362	0.814	236	125	-110
Type IV	9	65	9	-329	-226	-227	-228	some +/-	54	361	0.814	235	63	-172
Type IV	9	65	12	-439	-322	-319	-316	all (+)	87	360	0.814	234	-1	-235
Type IV	9	65	15	-548	-416	-410	-403	all (+)	119	359	0.814	234	-63	-297
Type IV	9	65	18	-658	-511	-500	-490	all (+)	151	358	0.814	233	-127	-360
Type IV	9	65	21	-767	-604	-590	-576	all (+)	182	357	0.814	232	-189	-422
Type IV	9	100	6	-220	-67	-107	-147	all (-)	-182	695	0.725	403	154	-249
Type IV	9	100	12	-441	-259	-291	-323	all (-)	-114	692	0.725	401	29	-373
Type IV	9	100	15	-551	-355	-383	-411	some +/-	-80	690	0.725	400	-35	-435
Type IV	9	100	18	-661	-450	-474	-499	some +/-	-47	688	0.725	399	-98	-497
Type IV	9	100	21	-771	-544	-565	-585	some +/-	-15	686	0.725	398	-161	-559
Type VI	6	100	4	-220	-45	-56	-67	some +/-	14	557	0.581	259	228	-31
Type VI	6	100	8	-441	-210	-216	-223	some +/-	67	555	0.581	258	114	-144
Type VI	6	100	12	-661	-373	-376	-378	some +/-	117	552	0.581	257	1	-256
Type VI	6	100	14	-771	-454	-455	-455	some +/-	143	551	0.581	256	-55	-312
Type VI	6	100	16	-881	-535	-534	-532	all (+)	168	550	0.581	256	-112	-367
Type VI	6	100	18	-991	-616	-612	-608	all (+)	192	549	0.581	255	-168	-424
Type VI	6	160	4	-219	31	-15	-61	all (-)	-208	963	0.515	397	220	-177
Type VI	6	160	8	-439	-133	-175	-217	some +/-	-155	960	0.515	396	108	-288
Type VI	6	160	12	-658	-297	-334	-372	some +/-	-102	956	0.515	394	-5	-399
Type VI	6	160	16	-878	-459	-493	-526	some +/-	-50	952	0.515	392	-117	-509
Type VI	9	100	6	-220	-55	-72	-88	some +/-	-38	437	0.776	271	179	-93
Type VI	9	100	12	-441	-231	-243	-254	some +/-	18	435	0.776	270	57	-214
Type VI	9	100	15	-551	-319	-328	-337	some +/-	45	434	0.776	269	-5	-274
Type VI	9	100	21	-771	-492	-497	-501	some +/-	98	432	0.776	268	-126	-395
Type VI	9	100	24	-881	-579	-581	-582	some +/-	124	431	0.776	268	-187	-455
Type VI	9	140	6	-220	-16	-59	-102	all (-)	-228	649	0.708	368	124	-244
Type VI	9	140	9	-330	-104	-144	-185	all (-)	-199	647	0.708	366	63	-303
Type VI	9	140	12	-440	-192	-230	-268	all (-)	-171	646	0.708	366	3	-363
Type VI	9	140	15	-550	-279	-315	-351	all (-)	-143	644	0.708	365	-57	-422
Type VI	9	140	18	-660	-367	-400	-433	some +/-	-115	643	0.708	364	-118	-482

Table E.3: Three Span Continuous PCBT Girder Bridge Parametric Studies

Bridge Properties					Simple Span Analysis			Continuous Span Analysis					Results	
					Final Comp. in Deck				Tens. at Top of Deck					
Girder Type	Girder Spc. (ft)	Span Length (ft)	No. of Strands in Deck	Initial Comp. in Deck (psi)	Top (psi)	Mid. (psi)	Bot. (psi)	Curvature Changes	Due to Force Redist. (psi)	Due to LL (psi)	DFM	Stress from Factored LL (psi)	Total Stress with LL (psi)	Total Stress without LL (psi)
PCBT-37	6	40	4	-219	-65	-89	-113	all (-)	-84	265	0.643	136	-13	-149
PCBT-37	6	40	8	-438	-248	-262	-276	all (-)	-39	264	0.643	136	-151	-287
PCBT-37	6	75	4	-220	-17	-72	-127	all (-)	-139	859	0.546	375	219	-156
PCBT-37	6	75	8	-440	-201	-247	-292	all (-)	-93	855	0.546	373	79	-294
PCBT-37	6	75	10	-551	-293	-333	-374	all (-)	-71	853	0.546	373	9	-364
PCBT-37	6	75	12	-661	-384	-420	-455	some +/-	-49	851	0.546	372	-61	-433
PCBT-37	6	75	14	-771	-474	-506	-537	some +/-	-27	849	0.546	371	-130	-501
PCBT-37	9	40	6	-219	-100	-120	-140	all (-)	-52	204	0.861	141	-11	-152
PCBT-37	9	40	12	-438	-293	-302	-311	some +/-	-8	203	0.861	140	-161	-301
PCBT-37	9	40	18	-657	-483	-482	-480	all (+)	35	202	0.861	139	-309	-448
PCBT-61	6	65	4	-220	-59	-74	-89	all (-)	-56	337	0.624	168	53	-115
PCBT-61	6	65	8	-441	-231	-241	-251	some +/-	-18	336	0.624	168	-81	-249
PCBT-61	6	65	10	-551	-316	-323	-331	some +/-	1	335	0.624	167	-148	-315
PCBT-61	6	65	12	-661	-401	-406	-411	some +/-	19	334	0.624	167	-215	-382
PCBT-61	6	125	4	-219	21	-33	-86	all (-)	-182	876	0.526	369	208	-161
PCBT-61	6	125	8	-437	-151	-199	-246	all (-)	-143	873	0.526	367	73	-294
PCBT-61	6	125	10	-547	-236	-281	-326	all (-)	-124	871	0.526	367	7	-360
PCBT-61	6	125	12	-656	-321	-364	-406	some +/-	-105	869	0.526	366	-60	-426
PCBT-61	6	125	14	-765	-406	-446	-485	some +/-	-86	867	0.526	365	-127	-492
PCBT-61	9	50	6	-220	-85	-101	-117	all (-)	-74	145	0.897	104	-54	-159
PCBT-61	9	50	12	-440	-268	-277	-287	all (-)	-35	144	0.897	103	-200	-303
PCBT-61	9	85	6	-220	-72	-99	-126	all (-)	-83	415	0.776	258	102	-155
PCBT-61	9	85	12	-440	-255	-276	-296	some +/-	-45	413	0.776	256	-43	-300
PCBT-61	9	85	18	-660	-436	-451	-465	some +/-	-7	412	0.776	256	-187	-443
PCBT-85	6	85	4	-220	-39	-53	-67	all (-)	-63	348	0.623	173	72	-102
PCBT-85	6	85	8	-440	-205	-215	-225	some +/-	-27	346	0.623	172	-60	-232
PCBT-85	6	85	10	-550	-287	-295	-303	some +/-	-10	345	0.623	172	-125	-297
PCBT-85	6	85	12	-660	-369	-375	-382	some +/-	7	345	0.623	172	-190	-362
PCBT-85	6	150	4	-218	-8	-41	-74	all (-)	-167	708	0.537	304	129	-175
PCBT-85	6	150	8	-435	-171	-201	-230	some +/-	-86	705	0.537	303	46	-257
PCBT-85	6	150	10	-544	-253	-280	-308	some +/-	-68	703	0.537	302	-19	-321
PCBT-85	6	150	12	-653	-334	-360	-386	some +/-	-51	702	0.537	302	-84	-385
PCBT-85	6	150	14	-761	-415	-439	-463	some +/-	-34	701	0.537	301	-148	-449
PCBT-85	9	70	6	-220	-70	-84	-97	all (-)	-75	198	0.879	139	-6	-145
PCBT-85	9	70	12	-441	-246	-256	-265	all (-)	-39	197	0.879	139	-146	-285
PCBT-85	9	70	15	-551	-334	-341	-349	some +/-	-21	197	0.879	139	-216	-355
PCBT-85	9	125	6	-219	-46	-74	-102	all (-)	-111	448	0.750	269	112	-157
PCBT-85	9	125	12	-437	-221	-245	-269	all (-)	-74	446	0.750	268	-28	-295
PCBT-85	9	125	15	-547	-309	-331	-352	some +/-	-56	445	0.750	267	-98	-365
PCBT-85	9	125	18	-656	-395	-415	-435	some +/-	-38	444	0.750	266	-167	-433

Table E.4: Three Span Continuous AASHTO Girder Bridge Parametric Studies

Bridge Properties					Simple Span Analysis			Continuous Span Analysis					Results	
					Final Comp. in Deck				Tens. at Top of Deck					
Girder Type	Girder Spc. (ft)	Span Length (ft)	No. of Strands in Deck	Initial Comp. in Deck (psi)	Top (psi)	Mid. (psi)	Bot. (psi)	Curvature Changes	Due to Force Redist. (psi)	Due to LL (psi)	DFM	Stress from Factored LL (psi)	Total Stress with LL (psi)	Total Stress without LL (psi)
Type II	6	45	4	-219	-166	-176	-186	some +/-	-9	409	0.592	194	19	-175
Type II	6	45	6	-329	-269	-273	-277	some +/-	16	408	0.592	193	-60	-253
Type II	6	45	8	-439	-371	-369	-366	all (+)	40	407	0.592	193	-138	-331
Type II	6	45	12	-658	-573	-559	-545	all (+)	87	405	0.592	192	-294	-486
Type II	6	70	4	-220	-62	-144	-226	all (-)	-238	991	0.528	419	118	-300
Type II	6	70	8	-441	-268	-338	-408	all (-)	-187	985	0.528	416	-39	-455
Type II	6	70	10	-551	-370	-434	-498	all (-)	-162	983	0.528	415	-117	-532
Type II	6	70	12	-661	-472	-529	-587	all (-)	-138	980	0.528	414	-196	-610
Type II	9	35	6	-218	-179	-187	-195	all (-)	-10	217	0.847	147	-42	-189
Type II	9	35	9	-327	-284	-285	-287	some +/-	11	216	0.847	146	-126	-273
Type II	9	35	12	-436	-387	-383	-378	all (+)	32	215	0.847	146	-209	-355
Type II	9	55	6	-220	-112	-177	-242	all (-)	-166	435	0.749	261	-18	-278
Type II	9	55	9	-330	-218	-276	-335	all (-)	-144	434	0.749	260	-102	-362
Type II	9	55	12	-440	-323	-375	-427	all (-)	-122	433	0.749	259	-185	-445
Type IV	6	75	4	-220	-113	-117	-121	some +/-	40	578	0.587	271	198	-73
Type IV	6	75	8	-440	-296	-293	-289	all (+)	87	575	0.587	270	61	-209
Type IV	6	75	12	-661	-477	-467	-456	all (+)	133	572	0.587	269	-76	-345
Type IV	6	75	14	-771	-567	-553	-539	all (+)	155	571	0.587	268	-144	-412
Type IV	6	75	16	-881	-656	-639	-622	all (+)	177	570	0.587	268	-211	-479
Type IV	6	120	4	-219	-40	-84	-128	all (-)	-127	1096	0.520	456	289	-167
Type IV	6	120	8	-438	-222	-259	-296	some +/-	-79	1091	0.520	454	152	-301
Type IV	6	120	12	-657	-402	-432	-463	some +/-	-32	1085	0.520	451	17	-434
Type IV	6	120	14	-766	-492	-519	-546	some +/-	-10	1082	0.520	450	-51	-502
Type IV	6	120	16	-876	-581	-604	-628	some +/-	13	1080	0.520	449	-118	-568
Type IV	9	65	6	-220	-131	-136	-141	some +/-	15	334	0.814	218	101	-117
Type IV	9	65	9	-330	-228	-229	-229	some +/-	38	333	0.814	217	26	-190
Type IV	9	65	12	-441	-323	-320	-317	all (+)	60	332	0.814	216	-46	-263
Type IV	9	65	15	-551	-418	-412	-405	all (+)	83	331	0.814	216	-120	-335
Type IV	9	65	18	-661	-513	-503	-492	all (+)	105	330	0.814	215	-193	-408
Type IV	9	100	6	-220	-66	-106	-146	all (-)	-126	659	0.725	382	190	-192
Type IV	9	100	12	-439	-258	-290	-322	all (-)	-79	655	0.725	380	43	-337
Type IV	9	100	15	-549	-353	-382	-410	some +/-	-56	653	0.725	379	-30	-409
Type IV	9	100	18	-659	-448	-473	-497	some +/-	-33	652	0.725	378	-103	-481
Type IV	9	100	21	-769	-542	-563	-584	some +/-	-11	650	0.725	377	-176	-553
Type VI	6	100	4	-220	-45	-56	-67	some +/-	10	528	0.581	245	210	-35
Type VI	6	100	8	-439	-209	-216	-222	some +/-	46	525	0.581	244	81	-163
Type VI	6	100	12	-659	-372	-374	-377	some +/-	81	523	0.581	243	-48	-291
Type VI	6	100	14	-769	-453	-453	-454	some +/-	99	522	0.581	243	-112	-355
Type VI	6	100	16	-879	-534	-532	-530	all (+)	116	521	0.581	242	-176	-418
Type VI	6	160	4	-217	33	-13	-60	all (-)	-144	921	0.515	379	268	-111
Type VI	6	160	8	-434	-130	-172	-214	some +/-	-107	917	0.515	378	140	-237
Type VI	6	160	12	-651	-292	-330	-367	some +/-	-72	914	0.515	377	13	-364
Type VI	6	160	14	-760	-373	-408	-444	some +/-	-54	912	0.515	376	-51	-427
Type VI	6	160	16	-868	-453	-486	-520	some +/-	-36	910	0.515	375	-114	-489
Type VI	6	160	18	-977	-533	-564	-596	some +/-	-19	908	0.515	374	-178	-552
Type VI	9	100	6	-220	-55	-71	-88	some +/-	-26	414	0.776	257	176	-81
Type VI	9	100	12	-439	-230	-242	-254	some +/-	12	412	0.776	256	38	-218
Type VI	9	100	15	-549	-317	-327	-336	some +/-	31	411	0.776	255	-31	-286
Type VI	9	100	18	-659	-404	-411	-418	some +/-	49	410	0.776	255	-100	-355
Type VI	9	100	21	-769	-491	-495	-499	some +/-	67	409	0.776	254	-170	-424
Type VI	9	140	6	-218	-14	-58	-101	all (-)	-158	618	0.708	350	178	-172
Type VI	9	140	12	-436	-189	-227	-265	all (-)	-119	615	0.708	348	41	-308
Type VI	9	140	15	-545	-276	-312	-347	all (-)	-100	613	0.708	347	-28	-376
Type VI	9	140	18	-654	-362	-396	-429	some +/-	-81	612	0.708	347	-96	-443
Type VI	9	140	21	-763	-449	-479	-510	some +/-	-62	610	0.708	346	-165	-511

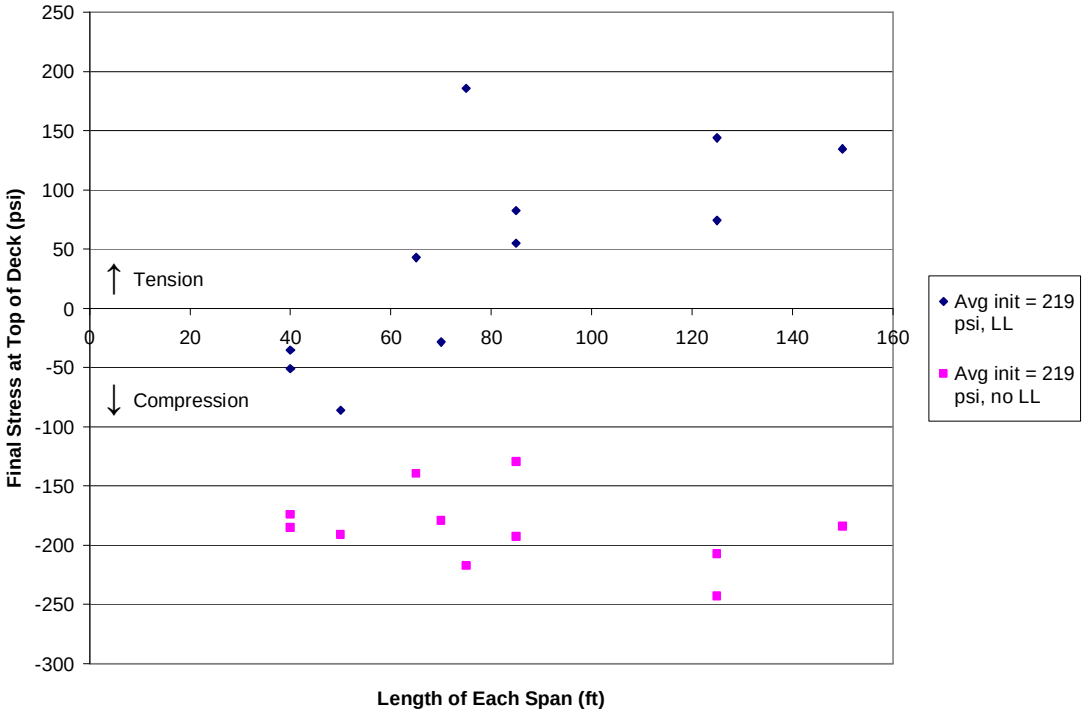

Figure E.1: Final Stresses for Two-Span Cont. PCBT Girder Bridges; Initial Comp. = 219 psi

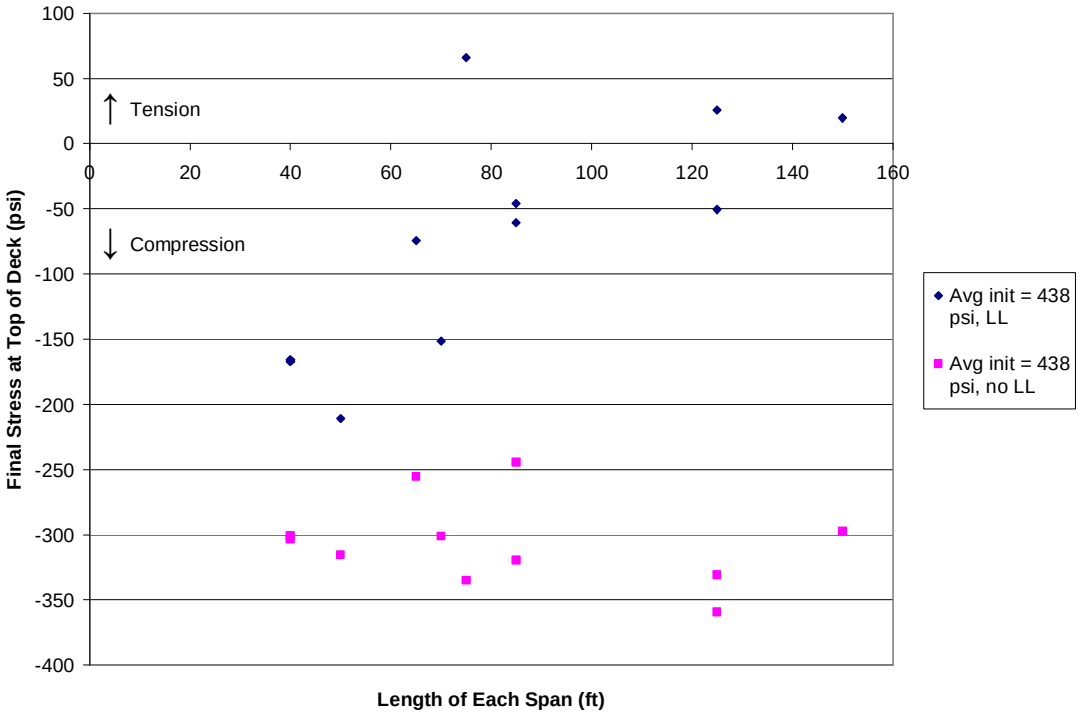

Figure E.2: Final Stresses for Two-Span Cont. PCBT Girder Bridges; Initial Comp. = 438 psi

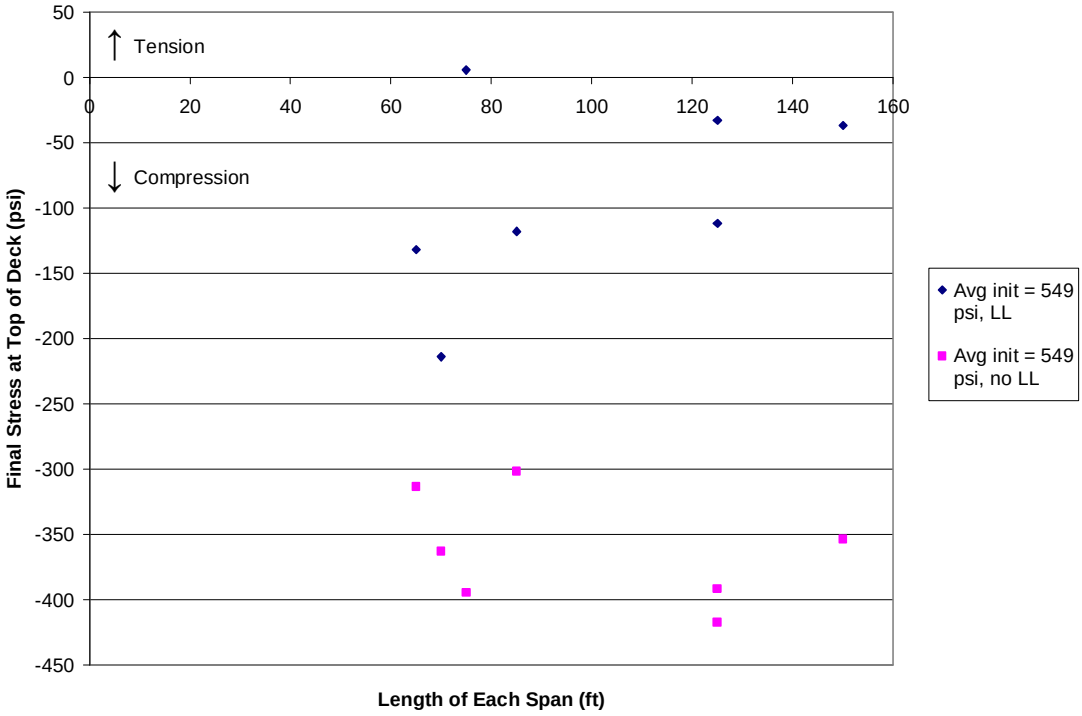

Figure E.3: Final Stresses for Two -Span Cont. PCBT Girder Bridges; Initial Comp. = 549 psi

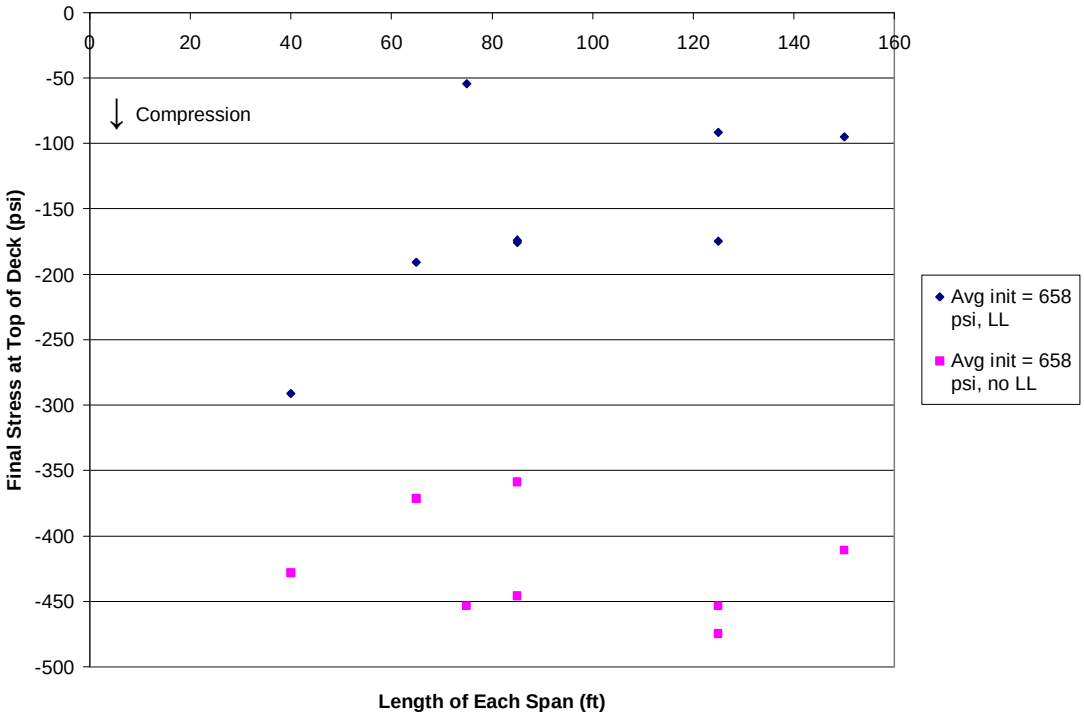

Figure E.4: Final Stresses for Two -Span Cont. PCBT Girder Bridges; Initial Comp. = 658 psi

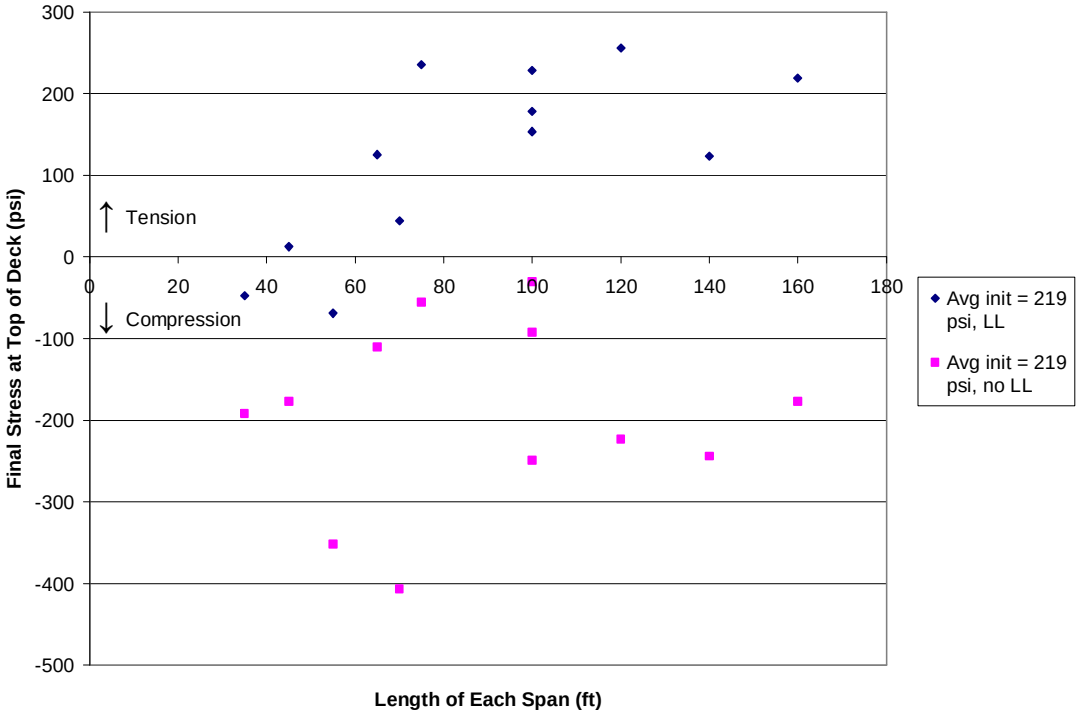

Figure E.5: Final Stresses for Two -Span Cont. AASHTO Girder Bridges; Init. Comp. = 219 psi

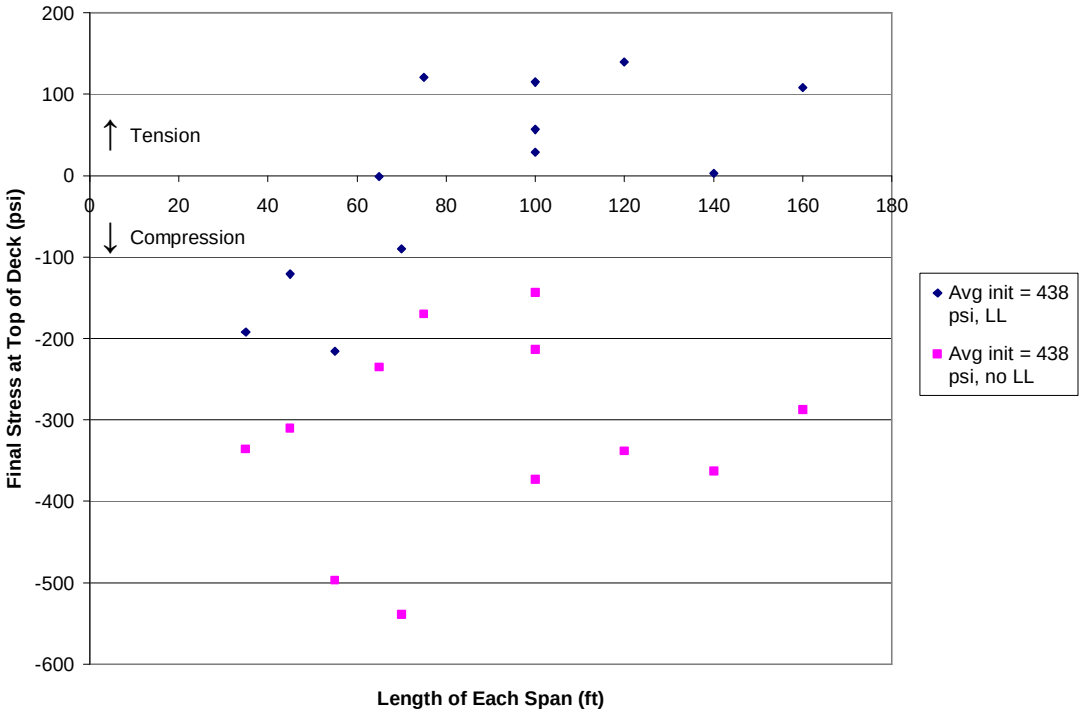

Figure E.6: Final Stresses for Two -Span Cont. AASHTO Girder Bridges; Init. Comp. = 438 psi

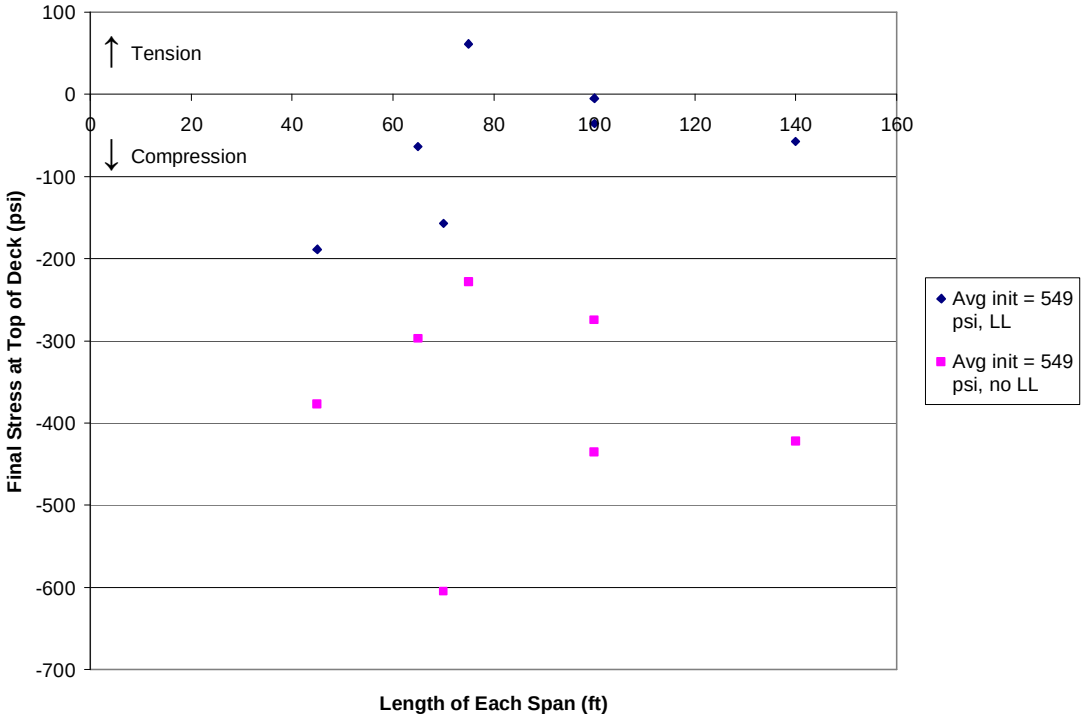

Figure E.7: Final Stresses for Two -Span Cont. AASHTO Girder Bridges; Init. Comp. = 549 psi

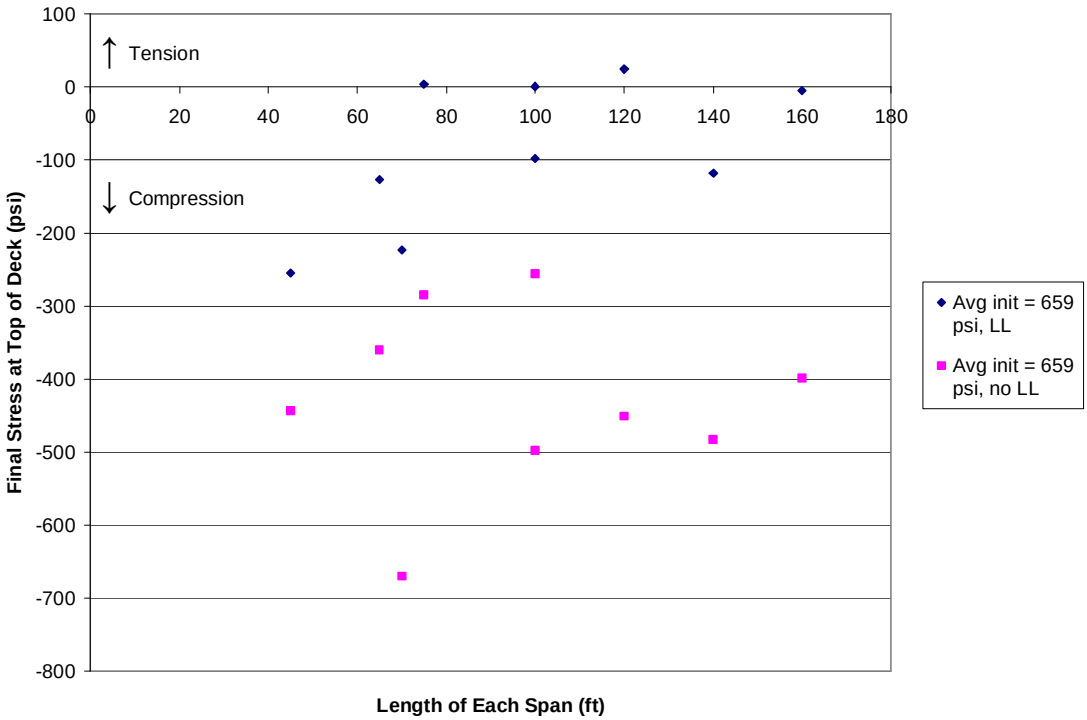

Figure E.8: Final Stresses for Two -Span Cont. AASHTO Girder Bridges; Init. Comp. = 659 psi

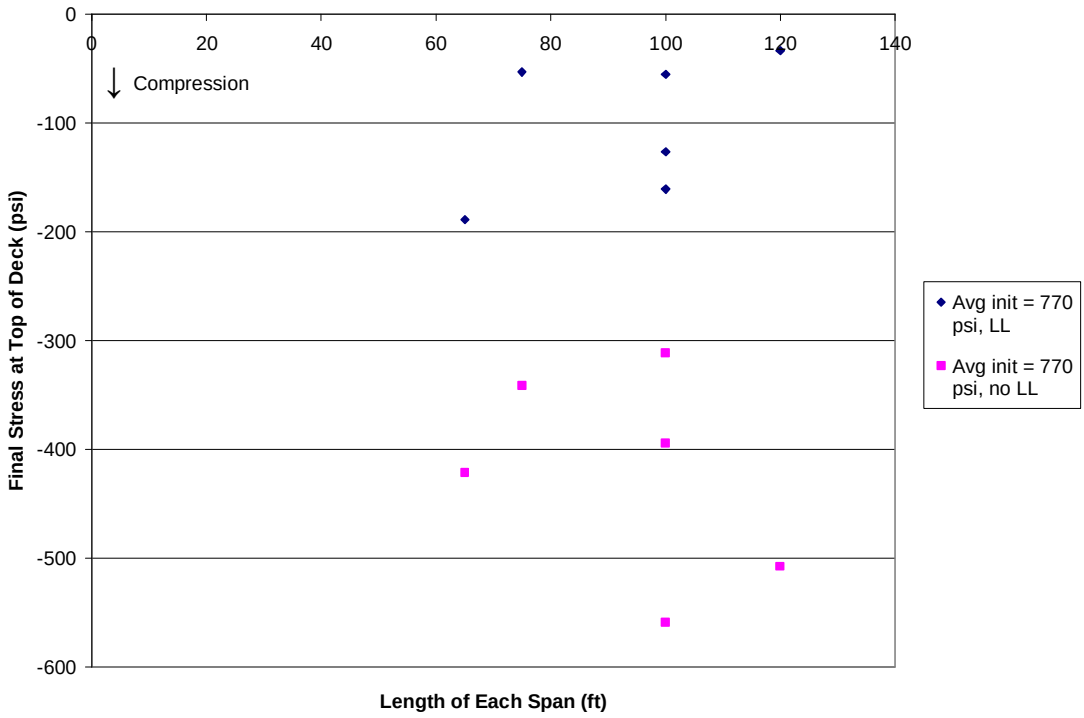

Figure E.9: Final Stresses for Two -Span Cont. AASHTO Girder Bridges; Init. Comp. = 770 psi

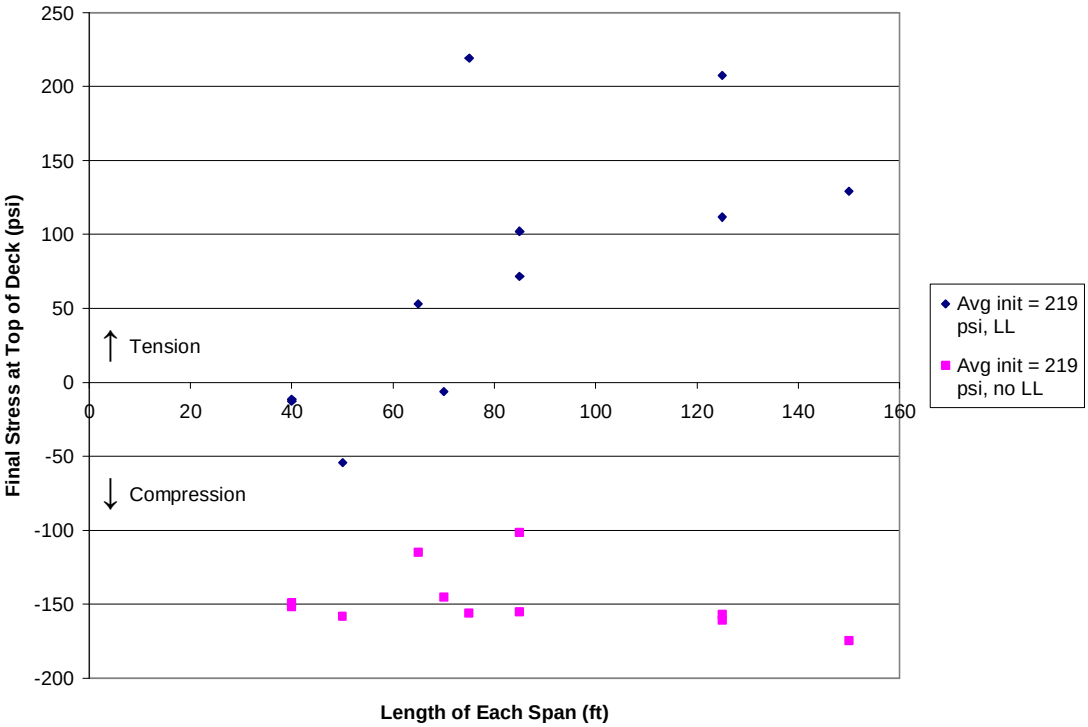

Figure E.10: Final Stresses for Three-Span Cont. PCBT Girder Bridges; Initial Comp. = 219 psi

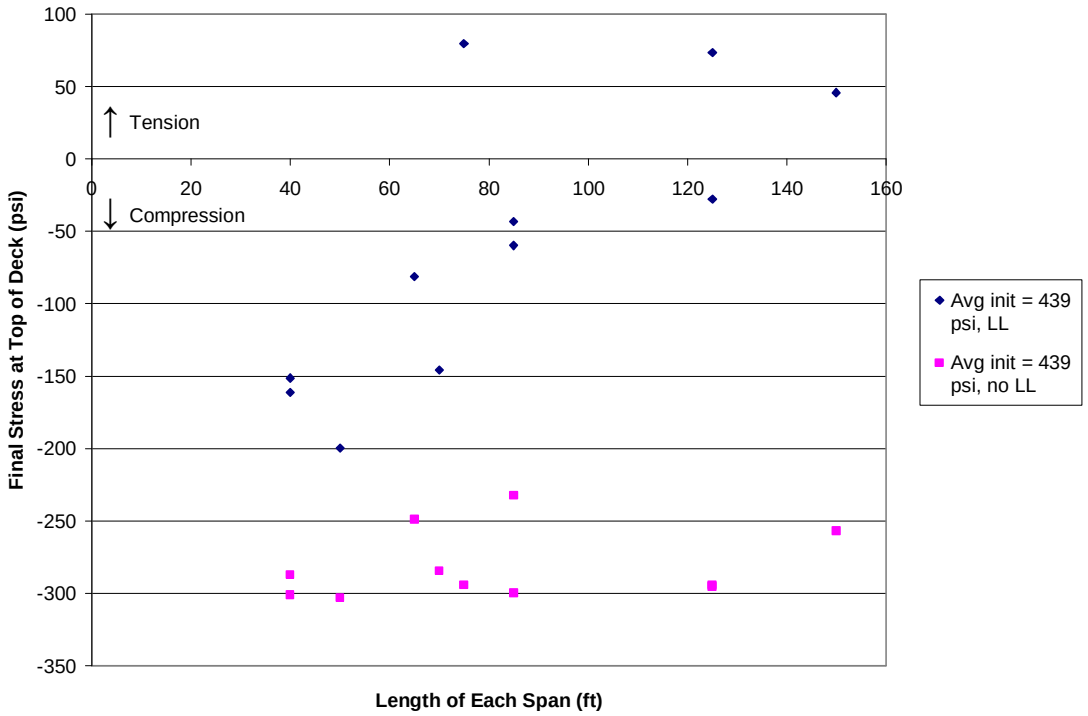

Figure E.11: Final Stresses for Three -Span Cont. PCBT Girder Bridges; Initial Comp. = 439 psi

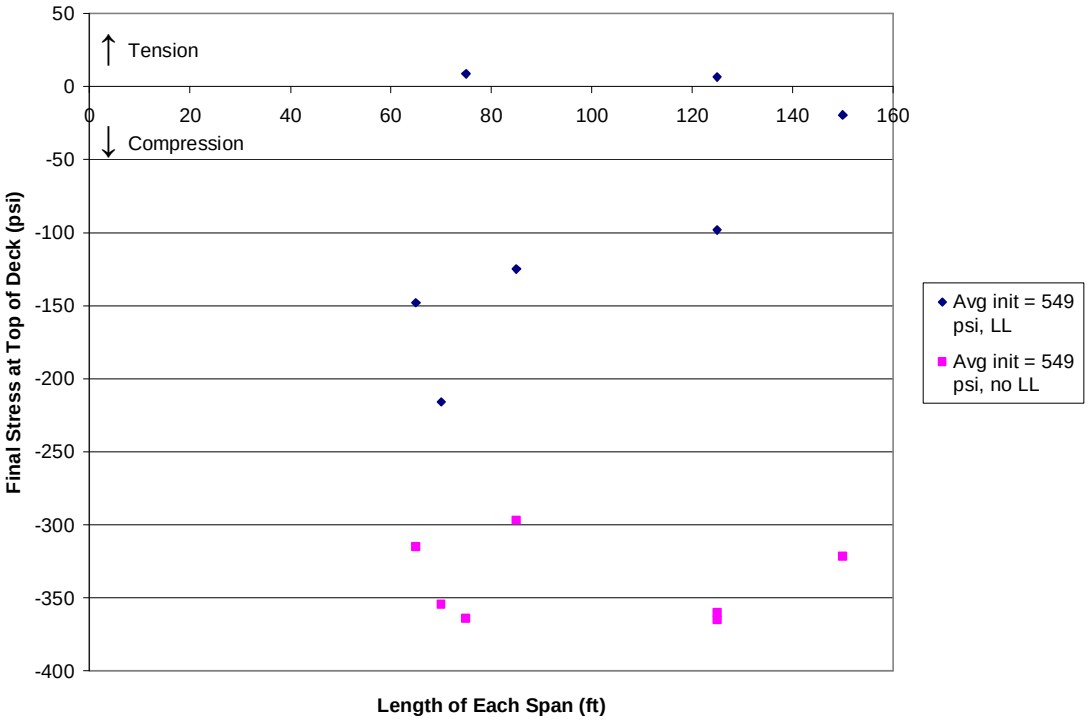

Figure E.12: Final Stresses for Three -Span Cont. PCBT Girder Bridges; Initial Comp. = 549 psi

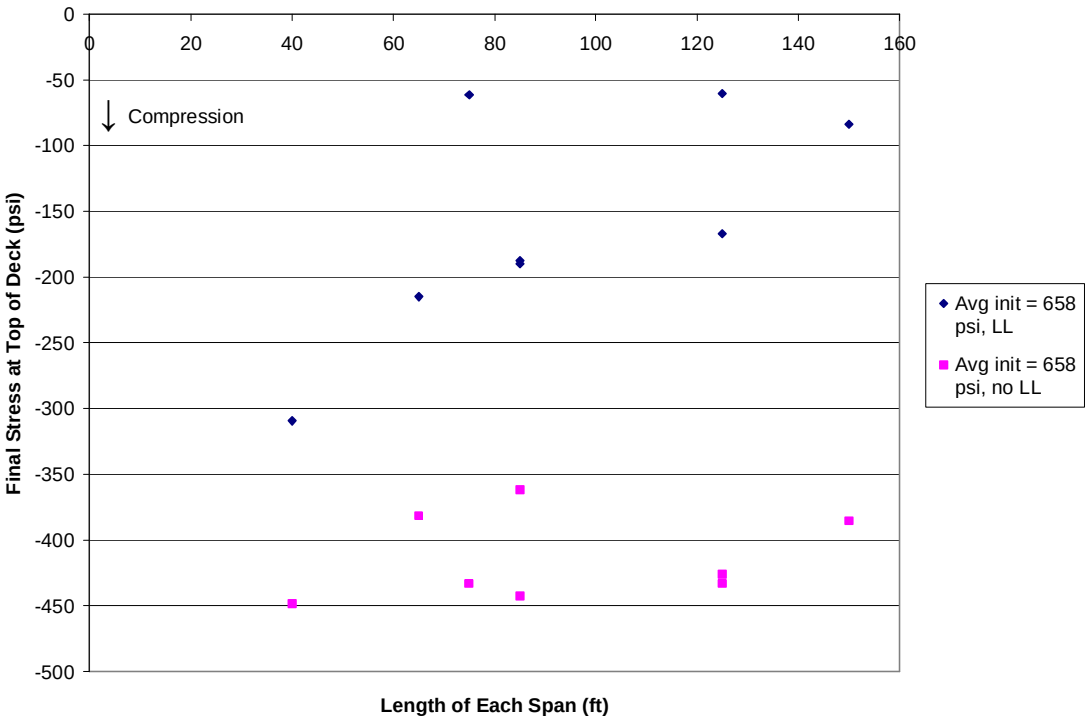

Figure E.13: Final Stresses for Three -Span Cont. PCBT Girder Bridges; Initial Comp. = 658 psi

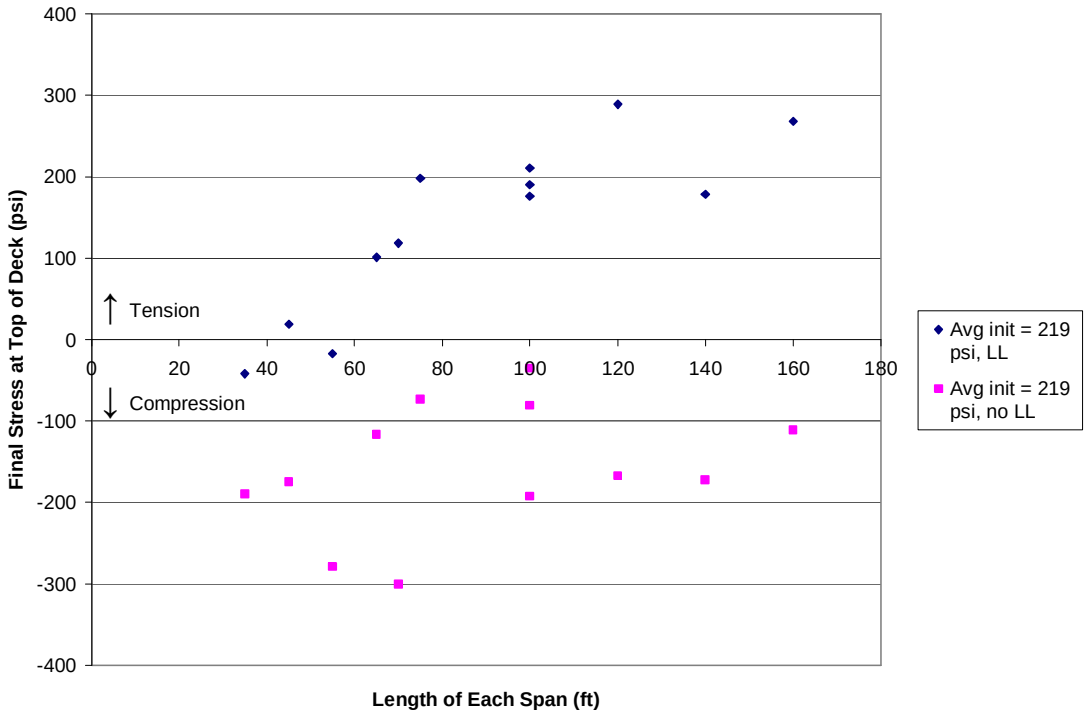

Figure E.14: Final Stresses for Three -Span Cont. AASHTO Bridges; Init. Comp. = 219 psi

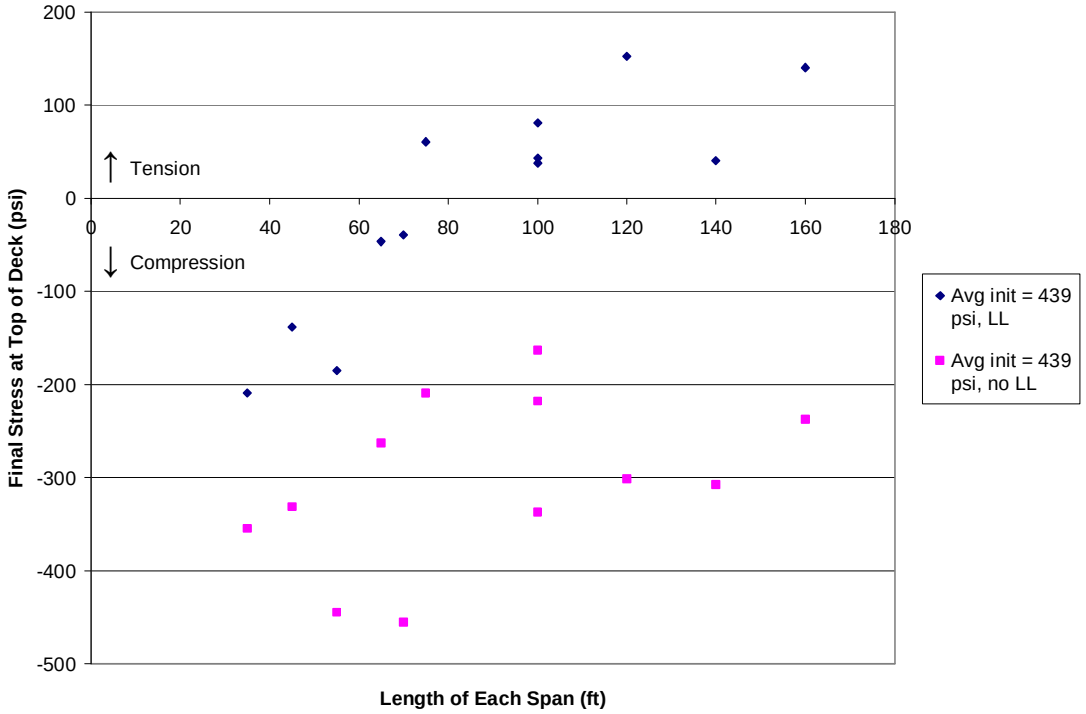

Figure E.15: Final Stresses for Three -Span Cont. AASHTO Bridges; Init. Comp. = 439 psi

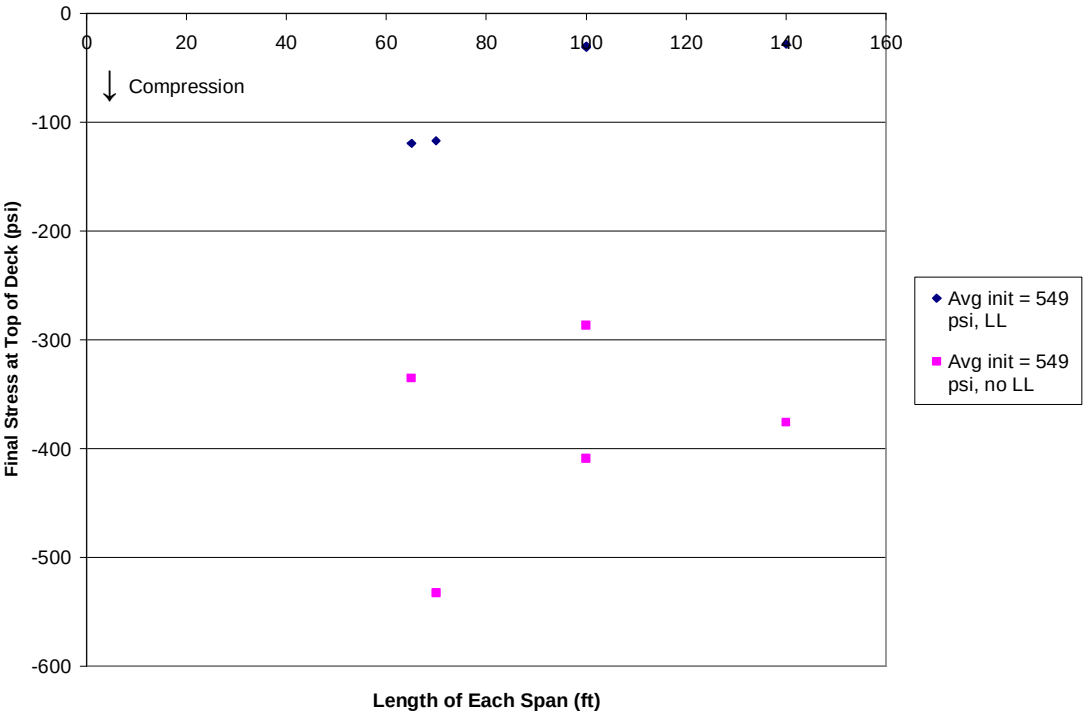

Figure E.16: Final Stresses for Three -Span Cont. AASHTO Bridges; Initial Comp. = 549 psi

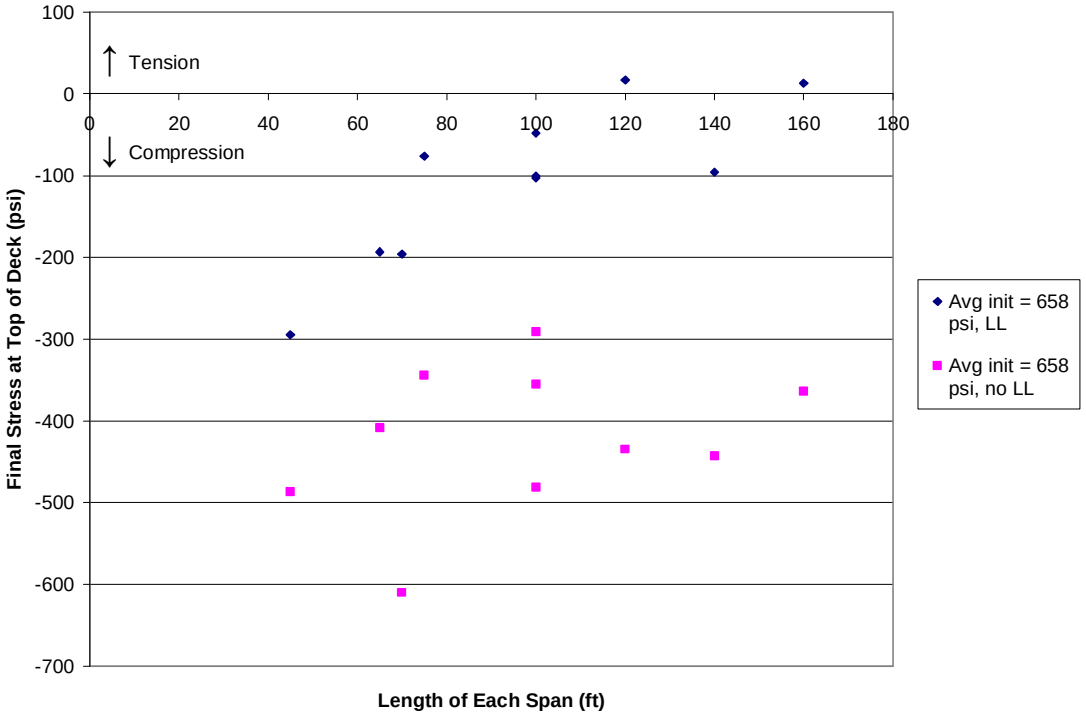

Figure E.17: Final Stresses for Three -Span Cont. AASHTO Bridges; Init. Comp. = 658 psi

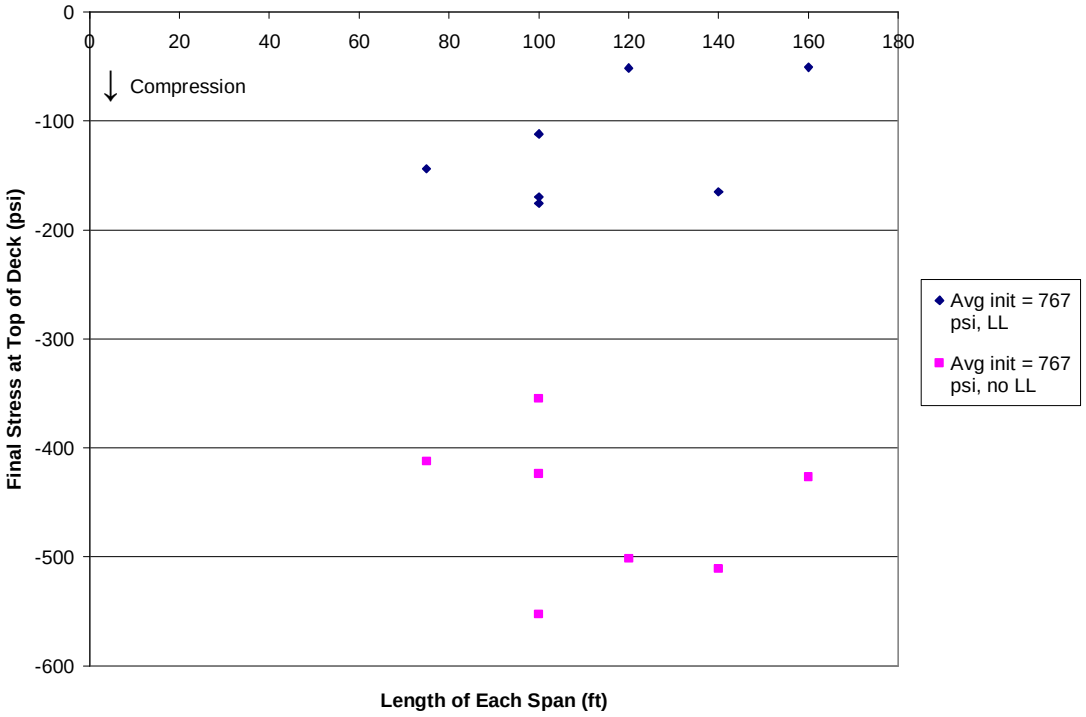

Figure E.18: Final Stresses for Three -Span Cont. AASHTO Bridges; Init. Comp. = 767 psi